NANOMATERIAL BASED SENSORS FOR THE DETERMINATION OF BIOMOLECULES AND DRUGS

Ph.D. THESIS

by

SAURABH KUMAR YADAV

DEPARTMENT OF CHEMISTRY
INDIAN INSTITUTE OF TECHNOLOGY ROORKEE
ROORKEE – 247667, INDIA
FEBRUARY, 2015

NANOMATERIAL BASED SENSORS FOR THE DETERMINATION OF BIOMOLECULES AND DRUGS

A THESIS

*Submitted in partial fulfilment of the
requirements for the award of the degree*

of

DOCTOR OF PHILOSOPHY
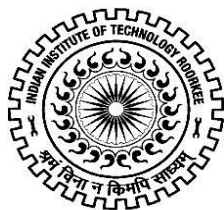
in

CHEMISTRY

by
SAURABH KUMAR YADAV

**DEPARTMENT OF CHEMISTRY
INDIAN INSTITUTE OF TECHNOLOGY ROORKEE
ROORKEE – 247667, INDIA
FEBRUARY, 2015**

INDIAN INSTITUTE OF TECHNOLOGY ROORKEE
ROORKEE

CANDIADATE'S DECLARATION

I hereby certify that the work which is being presented in the thesis entitled, **"NANOMATERIAL BASED SENSORS FOR THE DETERMINATION OF BIOMOLECULES AND DRUGS"** in partial fulfilment of the requirements for the award of the Degree of Doctor of Philosophy and submitted in the Department of Chemistry of the Indian Institute of Technology Roorkee, Roorkee is an authentic record of my own work carried out during a period from July, 2011 to February, 2015 under the supervision of Dr. R.N. Goyal, Professor, Department of Chemistry and Dr. D. Kaur, Professor, Department of Physics, Indian Institute of Technology Roorkee, Roorkee.

The matter presented in this thesis has not been submitted by me for the award of any other degree of this or any other institute.

(SAURABH KUMAR YADAV)

This is to certify that the above statement made by the candidate is correct to the best of our knowledge.

(D. Kaur)   (R.N. Goyal)

Supervisor   Supervisor

Dated:

ABSTRACT

Electrochemical investigation of biologically important compounds and drugs provide major challenges both from electro-mechanistic and analytical point of view. Electrochemistry at metal or carbon based electrode has emerged as an interesting area of analytical studies over the last few years, significantly changing the scope and sensitivity of electroanalytical methods. The field of nanoscience has blossomed over the last few decades, and the importance of nanotechnology has been increased due to the requirement of miniaturization in areas, such as computing, sensors, biomedical and many other applications. The advancements in these areas are depending largely due to the ability to synthesize nanoparticles of various materials, sizes and shapes, as well as to assemble them efficiently into complex architectures. Nanotechnology based electrochemical platform offers a promising tool for the attainment of multiple aims in biomolecular analysis. Nanomaterials prepared from metal, semiconductors and carbon or polymeric species have allured great attention due to their widespread applications in different areas of science. There has been a substantial progress in the construction of highly efficient nanomaterials based electrochemical sensors for the monitoring of biologically important molecules and pharmaceutical drugs. It is observed that the sensitive and selective detection of specific biomolecules and drugs is mandatory for elucidating the physiological processes as well as for early diagnosis and therapy of diseases. The recent upcoming of the new forms of nanomaterial/polymer composites have revolutionized the electrochemical research and brought many potential applications in nanoscience. Hybrid materials have enticed many researchers and opened a new dimension in the field of sensor fabrication due to their attractive electronic, optical, thermal and electro-catalytic properties over other conventional materials. These properties together with their nanometric size and high aspect ratio make them suitable for the electrochemical sensing of verities of organic compounds. Considering the significance of hybrid materials in the area of electrochemistry, in this thesis an attempt has been made to systematically utilize the different modification approaches employing nanomaterials, nanomaterial/polymer composites with a focus on the development of highly sensitive electrochemical sensors for the investigations of biomolecules and drugs. In a new perspective, aptamers which are small oligonucleic acids that specifically bind to the target molecules has also been explored. The advantages of aptamers are that they can be regenerated, highly stable to external factors, and do not require animal models for generation prepared through the SELEX (Systematic Evolution of Ligands by Exponential enrichment) process. The thesis is divided in six chapters.

The **first chapter** of the thesis is "General Introduction" which presents a compendious review of the pertinent work and highlights the importance of electrochemical studies in biological system along with its application in diverse areas. This chapter has an overview of conventional electrodes, types of nanomaterial and modification of electrodes using nanomaterials. This chapter also deals with the illustration of the methodology employed in the present investigation comprising some theoretical aspects of voltammetric techniques.

The **second chapter** of the thesis describes the application of gold nanoparticles decorated palladium for studying the electrochemical oxidation of dopamine which is one of the most important catecholamine that brain uses as the neurotransmitter as well as it is an important intermediate in the biosynthesis of other neurotransmitters of catecholamine family. Dopamine is also responsible for a variety of physiological functions like voluntary movement, ability to concentrate, feelings of pleasure, motivation and reward, gastrointestinal motility, pituitary hormone release, and higher cognitive processes. A stable layer of physisorbed gold nano particles at the surface of palladium has been used as a catalyst support. The modified sensor was characterized by field emission scanning electron microscopy (FE-SEM) and electrochemical impedance spectroscopy (EIS). The oxidation chemistry of dopamine has been investigated at bare and gold nanoparticle modified palladium sensor using cyclic and square wave voltammetry. The oxidation peak potential of dopamine shifted to lower values and peak current increased significantly, which is attributed to the electrocatalytic properties of nano gold modified palladium sensor. The peak potential of dopamine at pH 7.2 was 190 mV and 162 mV at bare and modified sensor respectively. The peak currents of dopamine were found to increase linearly with increase in the concentration of dopamine in the range 5–800 μM for bare and 0.5–1000 μM for nano gold modified palladium sensor respectively. The detection limit (3σ/b) and sensitivity were found to be 0.6 μM and 0.003 μA μM^{-1} for bare, 0.08 μM and 0.015 μA μM^{-1} for nano gold modified palladium respectively.

The **third chapter** of the thesis deals with the single-walled carbon nanotube (SWCNT) embedded poly 1,5-diaminonapthalene (p-DAN) modified pyrolytic graphite sensor for the determination of sulfacetamide (SFA). SFA is a synthetic, highly potent antibacterial agent that is widely used for the treatment of numerous dermatological diseases. The surface morphology of the modified sensor has been characterized by FE-SEM, which revealed a good dispersion of the carbon nanotube in polymer matrix of 1,5-diaminonapthalene. SFA was determined using square wave voltammetry in phosphate buffer of pH 7.2, which acted as supporting electrolyte during analysis. The modified sensor has been found to an effective catalytic response towards

the oxidation of SFA and excellent reproducibility and stability are observed. The peak current of SFA was found to be linearly dependent on the concentration of SFA in the concentration range 0.005–1.5 mM and detection limit and sensitivity of 0.11 µM (S/N=3) and 23.977 µA mM^{-1}, respectively were observed. The analytical utility of the method has also been explored by determining SFA in various pharmacological dosage forms. The results obtained from the voltammetry have also been validated by comparing the results with those obtained from HPLC. The proposed method is sensitive, simple, rapid and reliable and is useful for the routine analysis of SFA in pharmaceutical laboratories.
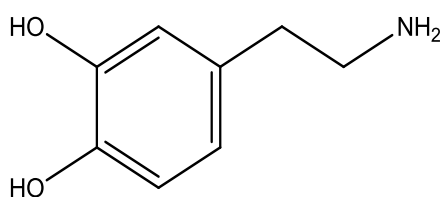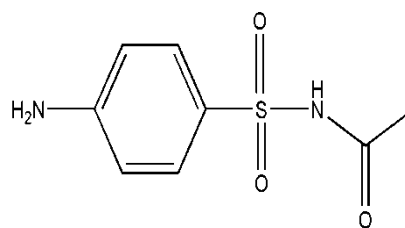
[Dopamine]   **[Sulfacetamide]**

In the **fourth chapter** of the thesis, the application of SWCNT for the modification of the surface of edge plane of pyrolytic graphite is presented. The electrochemical behavior of mometasone furoate (MF) has been studied at SWCNT modified pyrolytic graphite (MPG). The addition of cationic surfactant (cetyltrimethylammonium bromide, CTAB) was found to enhance the reduction current signal of MF, whereas, anionic (sodium dodecylsulfate, SDS) and non-ionic (Tween 60) surfactants exhibited opposite effect. Hence, detailed studies on the oxidation of mometasone are carried out in CTAB medium. A sensitive and selective electrochemical determination of MF by square wave voltammetry and cyclic voltammetry in phosphate buffer of pH 7.2 has been carried out in the presence of CTAB. The cathodic peak current showed a linear response for MF reduction in the concentration range 10–1000 µM. The effective surface area of the modified sensor was found to be 0.225 cm^2, The sensitivity and detection limit of MF were found to be 0.017 µA µM^{-1} and 1.23 µM, respectively were observed. The reduction site in MF has also been established by the separation and characterization of the product of reduction by ^{1}H NMR and FT-IR spectroscopic measurements and found to be carbonyl group at position 3. The developed method was successfully applied for the determination of MF in pharmaceutical preparations and in human urine.
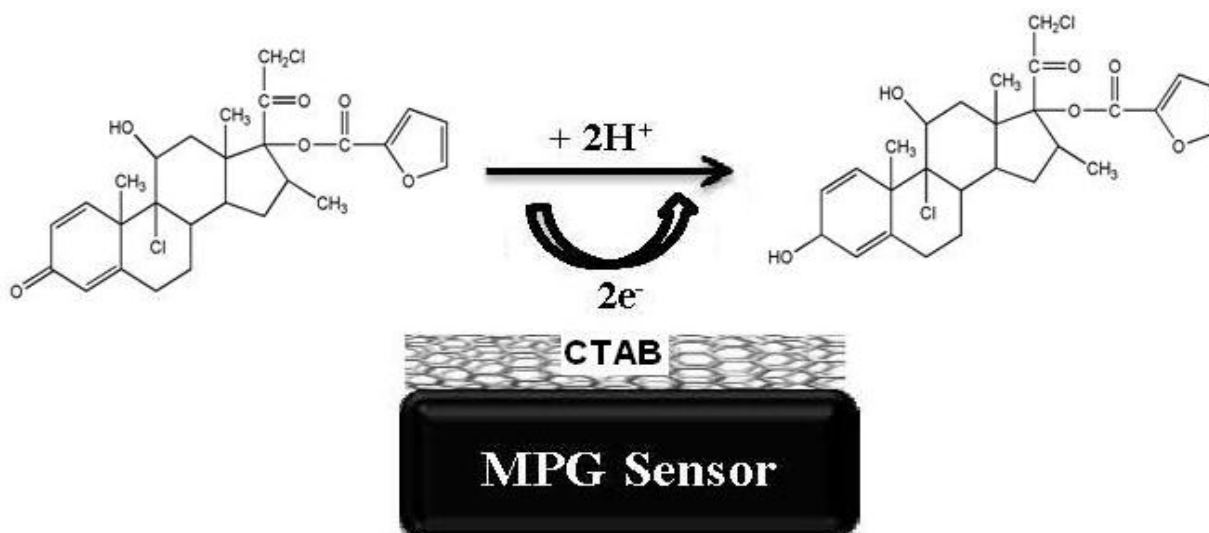
Tentative mechanism proposed for the reduction of MF

The **fifth chapter** of the thesis illustrates incorporation of gold nanoparticles onto the p-DAN coated pyrolytic graphite for the quantification of cefpodoxime proxetil (CP), which is a semi-synthetic beta-lactum antibiotic belonging to the third generation of cephalosporin group. The modified sensor was characterized by X-ray photoelectron spectroscopy (XPS) and FE-SEM. The sensor exhibited an effective catalytic response towards oxidation of CP with excellent reproducibility and stability. The peak current of CP was found to be linear in the range of 0.1–12 μM and detection limit and sensitivity of 39 nM (S/N=3) and 4.621 μA μM^{-1}, respectively, were observed. The method was successfully applied for the determination of CP in pharmaceutical formulations and human urine samples. The common metabolites present in human urine such as uric acid, ascorbic acid, xanthine and hypoxanthine did not interfere in the determination. A comparison of the results obtained by using developed method with high performance liquid chromatography (HPLC) indicated a good agreement. The method is simple, sensitive, rapid and precise and is useful for the routine determination of CP in pharmaceutical dosages and biological samples.

The last chapter of thesis (**chapter six)** describes the *in vitro* chloramphenicol detection in a *Haemophilus influenza* model using an aptamer-polymer based electrochemical biosensor. A sensitive and selective electrochemical biosensor for the determination of chloramphenicol (CAP) exploring its direct electron transfer processes in *in vitro* model and pharmaceutical samples. This biosensor exploits a selective binding of CAP with aptamer, immobilized onto the poly-(4-amino-3-hydroxynapthalene sulfonic acid) (p-AHNSA) modified edge plane pyrolytic graphite. The electrochemical reduction of CAP was observed in a well-defined peak.

A quartz crystal microbalance (QCM) study is performed to confirm the interaction between the polymer film and the aptamer. Cyclic voltammetry and square wave voltammetry were used to detect CAP. The *in vitro* CAP detection is performed using the bacterial strain of *Haemophilus influenza*. A significant accumulation of CAP by the drug sensitive *Haemophilus influenza* strain is observed for the first time in this study using a biosensor. Various parameters affecting the CAP detection in standard solution and in *in vitro* detection are optimized. The detection of CAP is linear in the range of 0.1–2500 nM with the detection limit and sensitivity of 0.02 nM and 0.102 μA nM^{-1}, respectively. CAP is also detected in the presence of other common antibiotics and proteins present in the real sample matrix, and negligible interference is observed.
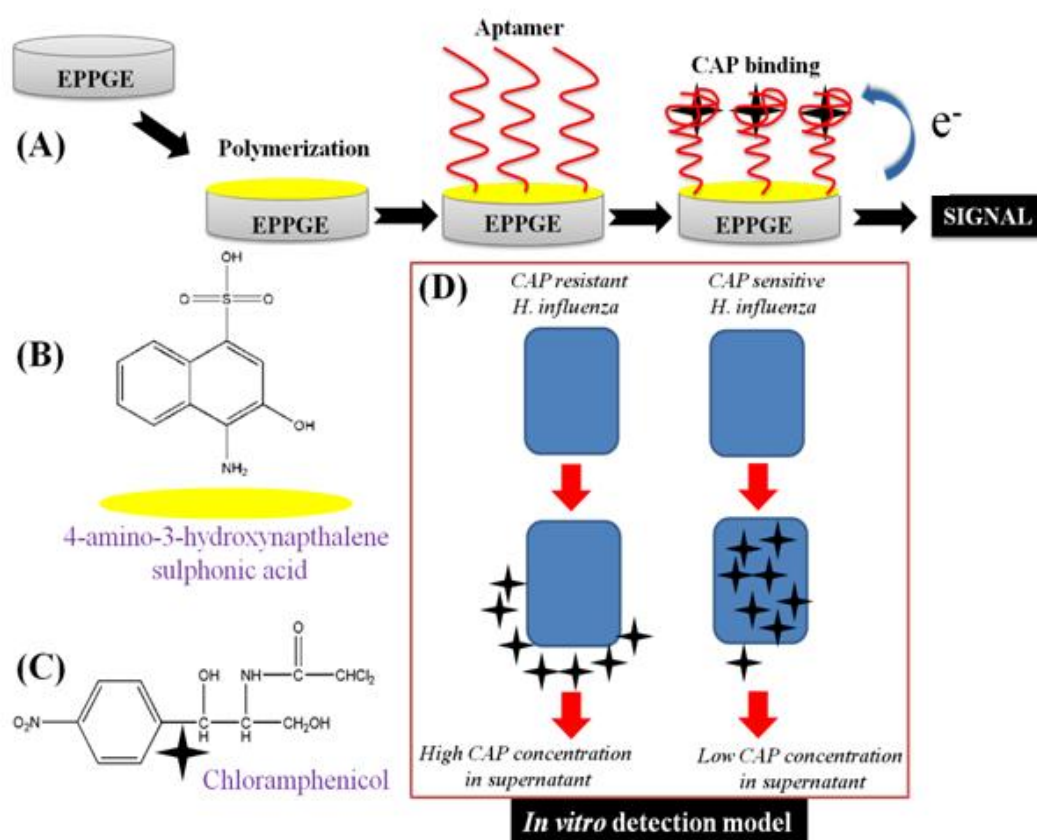
A representation of the biosensor fabrication and detection model used is presented.

ACKNOWLEDGEMENTS

I owe a deep sense of gratitude to the Almighty God whose devine light and warmth provided me the presevence, guidance, inperation, fath and strength to carry on even when the going got tough. It is because of his kind blessing that this work has reached from initial speculation to its fruitation. There are so many people that I have to thank and many of them are the ones I met here. These are the people who helped and supported me academically and mentally during my doctoral study.

First and foremost, I feel privileged to express my profound gratitude and sincere regards to my supervisor; **Dr. R.N. Goyal**, for his meticulous guidance, invigorating discussions, invaluable mentorship and constant encouragement throughout the course of my Ph.D. Working under his supervision was a confidence-building experience, whose wide experience, sharp intellect, incisive criticism, pertinent suggession, tireless interest, motivation and great efforts has unerringly steered the work on smooth and steady course. I humbly acknolge him for what I know today about the process of research and his assurance at the time of crisis would be remembered lifelong.

It gives me an immence pleasure in expressing deep sense of reverence to my mentor Prof. Davinder Kaur her valuable and scrupulous guidance, enthusiastic interest throughout my research work. Her affectionate treatment and magnaminity made it feasibile to bring the present work to conclusion. I am greatful to them for articulating this path and being a constant source of inspiration.

I sincerely thank to Indian Government especially to **Council of Scientific and Industrial Research, New Delhi** for providing me fellowship in the sponsored research project. It was a great opportunity to work in India's one of the leading Electrochemistry Lab and giving a sufficient grant for research work due to which I could pursue my doctoral programme without any mental or economic burden.

I owe my sincere gratitude to Indian Institute of Technology, Roorkee for bestowing me an honor to be a student of a prestigious institute. Prof. Anil Kumar; Head of the Department of Chemistry, is thankfully acknowledged for providing basic institute facilities and other required things.

A warm thank goes to the departmental staff, Shri A. Haq, and Madanpal for giving me a valuable support and patience for research.

comes. No words articulate to acknowledge the didactic guidance rendered by my loving parents. I owe my whole life to them.

The work could not have been completed without the moral support of my elder brothers Sandeep Kumar Yadav, Siddharath Yadav and Sister Shipra Yadav. I express the feelings of love to my sweet niece, Sanchi to whom I missed very much for months and years. I dedicate my Ph.D. thesis to my loving family.

Dated: **SAURABH KUMAR YADAV**

x

LIST OF PUBLICATIONS

1. **Saurabh K. Yadav**, Rosy, Munetaka Oyama, Rajendra N. Goyal, "A Biocompatible Nano Gold Modified Palladium Sensor for Determination of Dopamine in Biological Fluids", **Journal of the Electrochemical Society** 161(1) H41-H46 (2014).

2. **Saurabh K. Yadav**, Pravir K. Choubey, Bharati Agrawal, Rajendra N. Goyal, "Carbon nanotube embedded poly 1,5-diaminonapthalene modified pyrolytic graphite sensor for the determination of sulfacetamide in pharmaceutical formulations", **Talanta** 118 (2014) 96-103.

3. Rajendra N. Goyal, Davinder Kaur, Bharati Agrawal, **Saurabh Kumar Yadav**, "Electrochemical investigations of mometasone furoate, a topical corticosteroid, in micellar medium", **Journal of Electroanalytical Chemistry** 695 (2013) 17-23.

4. **Saurabh K. Yadav,** Bharati Agrawal, Rajendra N. Goyal, "AuNPs-poly-DAN modified pyrolytic graphite sensor for the determination of Cefpodoxime Proxetil in biological fluids", **Talanta** 108 (2013) 30–37.

5. **Saurabh K. Yadav**, Bharati Agrawal, Pranjal Chandra, Rajendra N. Goyal, "In vitro chloramphenicol detection in a *Haemophilus influenza* model using an aptamer-polymer based electrochemical biosensor", **Biosensors and Bioelectronics** 55 (2014) 337-342.

LIST OF CONFERENCES/ SCHOOL/ SYMPOSIA ATTENDED

1. A paper entitled "Facile voltammetric approach for the effective detection of propranlol" was presented in the conference organised by from March 27th to 29th, 2014, at Varanasi (India).

2. A paper entitled "A Biocompatible Nano Gold Modified Palladium Sensor for Determination of Dopamine in Biological Fluids" was presented in the international conference organised by Indian Society of Electro-analytical Chemistry (BARC, Mumbai) from February 20th to 25th, 2014, at Amritsar (India).

3. Partcipate in Symposium on modern trends in inorganic chemistry-XV (MTIC-XV) organised by from December 13rd to 16th, 2013 in department of chemistry IIT Roorkee (India)

4. A paper entitled "AuNPs-poly-DAN modified pyrolytic graphite sensor for the determination of Cefpodoxime Proxetil in biological fluids" was presented in the international conference organised by Indo-US Science and Techonology Forum from February 26th to 28th, 2013, at Varanasi (India).

5. A paper entitled "Electrochemical investigations of mometasone furoate, a topical corticosteroid, in micellar medium" was presented in the international conference organised by Indian Society of Electro-analytical Chemistry (BARC, Mumbai) from January 16th to 20th, 2013, at Ramoji Film City (Hyderabad, India).

6. Participated in Fifth BRNS-AEACI winter school on analytical chemistry organised by Association of environmental analytical chemistry of India (AEACI) from December 03rd to 10th, 2012 in the department of chemistry IIT Roorkee (India).

LIST OF ABBREVIATIONS

BAS	Bio Analytical System
PGE	Pyrolytic Graphite Electrode
EPPGE	Edge Plane Pyrolytic Graphite Electrode
BPPGE	Basal Plane Pyrolytic Graphite Electrode
GCE	Glassy Carbon Electrode
CNT	Carbon Nanotubes
SWCNT	Single Walled Carbon Nanotubes
MWCNT	Multi Walled Carbon Nanotubes
Ag/AgCl	Silver-Silver Chloride
CV	Cyclic Voltammetry
SWV	Square Wave Voltammetry
CPE	Controlled Potential Electrolysis
HPLC	High Performance Liquid Chromatography
FE-SEM	Field Emission Scanning Electron Microscopy
EDAX	Energy dispersive X-ray analysis
NMR	Nuclear Magnetic Resonance
FT-IR	Fourier Transform Infra-Red
E_p	Peak Potential
i_p	Peak Current
f	Square Wave Frequency
v	Scan Rate
δ	Chemical Shift

LOD	Limit of Detection
LOQ	Limit of Quantification
RSD	Relative Standard Deviation
NSAIDs	Non-Steroidal Anti Inflammatory Drugs
WADA	World Anti-Doping Agency
DMF	Dimethyl Formamide
SELEX	Systematic Evolution of Ligands by Exponential enrichment
EIS	Electrochemical Impedance Spectroscopy
p-DAN	poly 1,5-diaminonapthalene
SFA	Sulfacetamide
MF	Mometasone Furoate
CP	Cefpodoxime Proxetil
CAP	Chloramphenicol
p-AHNSA	poly-(4-amino-3-hydroxynapthalene sulfonic acid)
QCM	Quartz Crystal Microbalance

CONTENTS

Chapter 1

GENERAL INTRODUCTION

"Of all electrical phenomena electrolysis appears the most likely to furnish us with a real insight into the true nature of the electric current, because we find currents of ordinary matter and currents of electricity forming essential parts of same phenomenon".

James Clark Maxwell

The area of electrochemistry started as an exploration of fundamental forces at work in the universe-among them, the relationship between electricity and chemical change. The field of electrochemistry encompasses a huge array of various phenomenon (electrophoresis and corrosion), devices (batteries, fuel cells, electroanalytical sensors, and electrochromic displays), and technologies (electroplating and large scale production of elements). During last few decades, electrochemistry has become an area of electrochemical measurements on chemical systems for a variety of reasons, such as to analyze a solution for trace amount of metal ions or organic species, obtaining thermodynamics data about a reaction, generate intermediate ion or product during the electrochemical reaction and study its rate of decay or its spectroscopic properties [1-3].

Electrochemistry has acquired its present form during nearly two centuries of development. In the earliest stages of the development of electrochemistry, primary interest was devoted to the study of chemical transformations resulting from the flow of current through electrical cells. Emphasis on this stage was given to the qualitative observation of the various products obtained. Quantitative studies were pursued by Faraday, and in the year 1834 he demonstrated the famous law of electrochemical equivalence. The work of Faraday and law of diffusion proposed by A. Fick in the year 1855 really laid the foundations for the voltammetry and polarography. The first method based on mass transfer processes, that gained widespread attention, was that of Heyrovsky, who in 1922 discovered empirically the technique of polarography. Soon thereafter, in 1934, Ilkovic laid the theoretical ground work of this technique, from which many novel and important uses were emerged [4, 5].

The last few decades has seen an enormous growth in the field of analytical chemistry. A large number of new and increasingly complex materials have been developed and used for the surface modification purpose. The unrecognized or ignored constituents in the blood or urine posed more and more stringent demands for greater sensitivity, reliability, and speed to identify such constituents [6].

Electrochemical sensors have steadily gained importance during recent years in the qualitative and quantitative analysis of various compounds in human body fluids and drugs. It

1

has been proved in the recent years that electrochemical sensors provide indispensable, versatile and significant capabilities to extend and deepen the understanding of physico-chemical aspects of the biological changes undergoing in the living systems. Electrochemical sensors have demonstrated the potential to probe mechanism of biological reactions as the conditions normally employed for these techniques are more or less similar to biochemical reactions. As most of the biologically significant molecules, which are involved in the fundamental biological processes, are redox type, the study of their redox behavior provides insights about their metabolic fate [7-12].

In recent years application of several electrode modifiers such as nanomaterials, polymer, aptamer and their combination are playing an important role in the development of novel electrochemical sensors and biosensors. Due to the unique and attractive electrocatalytic properties of nanomaterials have been found to exhibit promising electroanalytical performances [13]. A wide variety of nanomaterials of different sizes, shapes and compositions at the 1-100 nm scale, are now easily available [14-17]. The special physical or chemical properties of nanomaterials have also been exploited to improve the suitability of sensors [18-20]. Conducting polymers have recently become one of the most exciting forefront fields in the surface modification [21]. A novel formulation on the conducting polymer is remarkably fruitful for the development of a chemical sensing device capable of detecting suitable analyte [22, 23]. Aptamer based electrochemical biosensors exhibited impressive signal amplifications and the use of nanomaterials and polymer further enhanced the electron transfer between the aptamer and the electrode [24-25]. Such hybrid materials have opened up new possibilities for tailoring the fundamental properties of the materials to reinforce considerably the useful properties of their components, and fulfill the requirement of the desired sensor. A brief description of various methodology, conventional electrodes, modified electrodes, surface modifiers (nanomaterials, polymer, and aptamer) and their utility for the application as sensors has been described in forthcoming sections.

1.1 A COMPENDIOUS OVERVIEW OF THE METHODOLOGY USED IN PRESENT INVESTIGATIONS

Electroanalytical methods are frequently used by analytical chemists for the study of fundamental studies of oxidation-reduction reactions in various media, adsorption process of surfaces, electron transfer mechanism of species and their quantitative determination. A brief description about the methodology employed in the present investigation comprising theoretical aspects of these techniques is summarized below:

1.1.1 Cyclic Voltammetry

Cyclic voltammetry (CV) is an important and widely used electroanalytical technique. CV is the first technique used to study oxidation/reduction reaction of a compound. It can also be used for the detection of reaction intermediates and the follow-up reactions of products formed at electrode [26]. In CV, the applied potential is swept in one direction and then in the reverse direction and the current is measured. A CV measurement may use one full cycle, a partial cycle, or even several cycles. During the CV, the current response of working electrode is excited by a triangular potential waveform such as that shown in **Fig 1.1**. The triangular waveform produces the forward and the reverse scan.
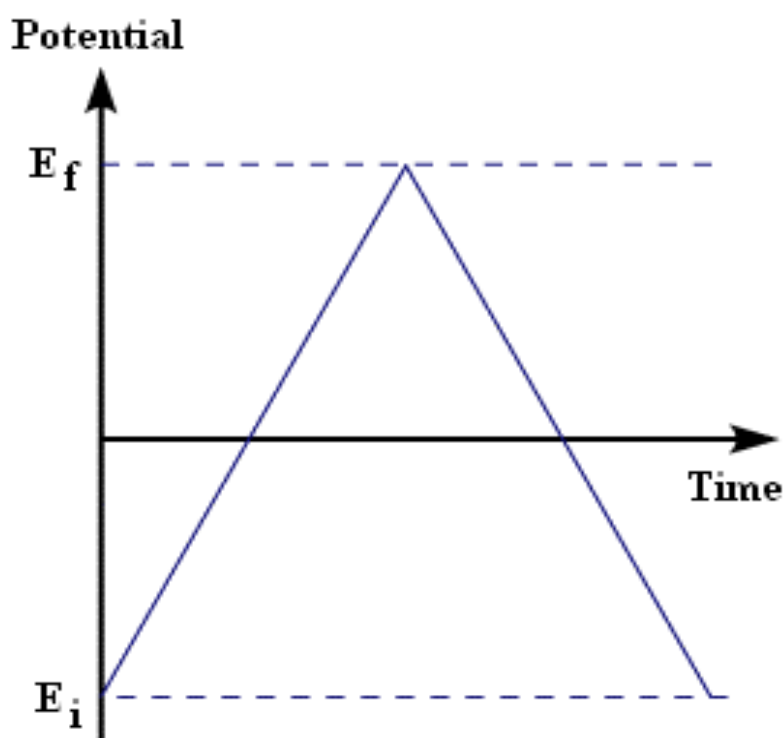
Fig. 1.1: A triangular potential waveform in CV

The important parameters of a cyclic voltammogram are the peak potentials (E_{pc}, E_{pa}) and peak currents (i_{pc}, i_{pa}) of cathodic and anodic peaks, respectively [**Fig. 1.2**]. For a reversible electrode reaction, anodic and cathodic peak currents are expected to be approximately equal in the magnitude. If the electron transfer rate in both forward and reverse scan is rapid, at 25ºC the reaction is defined as reversible and the peak separation is given by:

$\Delta E_p = [E_{pa} - E_{pc}] = 0.059/n$

3

Where, n represents the number of electron transferred. Practically it is difficult to achieve this value because of the potential drop caused by resistance between working and reference electrode and slow electron transfer kinetics results in ΔE_p exceeding from the ideal value of 0.059/n.
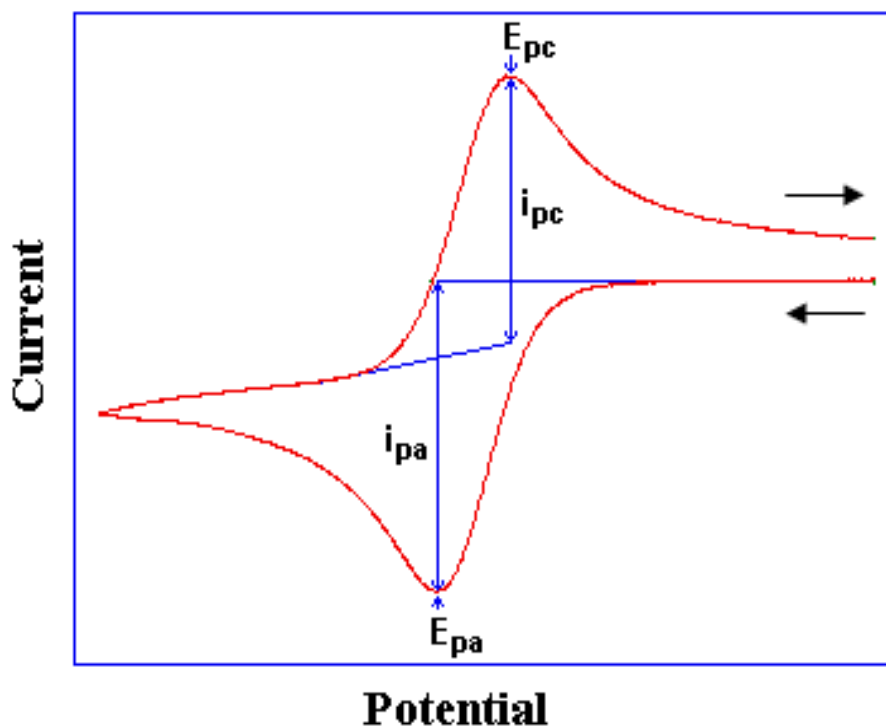
Fig. 1.2: A typical cyclic voltammogram for reversible redox system

The quantitative information in CV is obtained from peak current which is governed by the *Randles-Sevcik* equation (at 25°C):

$$i_p = (2.686 \times 10^5) \; n^{3/2} A \; D^{1/2} \; C_o v^{1/2}$$

where, i_p refers to the peak current (Ampere), A is the surface area of electrode (cm^2), D is the diffusion coefficient (cm^2 sec^{-1}), C_o is the concentration of analyte in mol cm^{-3} and v is the scan rate in Vs^{-1}. CV also offers a way of determining diffusion coefficient if other parameters of the above equation are known.

The major use of CV is to provide qualitative information about the electrochemical processes under various conditions. CV is widely employed as a first technique selected for the investigation of a system having electroactive species. CV reveals the redox behavior of biological molecules, organic and inorganic compounds with special emphasis on fundamental aspects of redox process, electron transfer reaction and understanding reaction intermediates.

This ability together with its variable time range and excellent sensitivity makes this technique the most versatile electrochemical technique. CV coupled with chromatographic, spectroscopic and several other techniques make it one of the most powerful tools for elucidating the complex redox mechanism of numerous biomolecules and drugs [27, 28].

1.1.2. Square Wave Voltammetry

Square wave voltammetry (SWV) is related to both pulse techniques and A.C. voltammetric techniques that offer the advantage of great speed and high sensitivity. It is somewhat similar to differential pulse voltammetry as the current response is a symmetric peak and that; there is effective discrimination against background charging currents. SWV was invented in 1969 by Ramaley and Krause [29]. Later, it was extensively developed by Osteryoung and coworkers [30, 31]. The potential wave used in SWV is shown in **Fig. 1.3**. The potential wave form for SWV consists of a square wave superimposed on a staircase wave form. It can also be viewed as a series of pulses alternating in direction (hence, the relation to both pulse and A.C. techniques). The current is sampled twice, once at the end of the forward pulse and again at the end of reverse pulse.

Square wave voltammograms can be obtained in less than 10 ms. The difference between forward current (i_{for}) and reverse current (i_{rev}) provides net current (Δi) which is proportional to the concentration of electroactive species. The differential current is plotted against potential measuring the oxidation or reduction of the species as a peak. Due to the negligible contribution of the charging current to the signal, detection limit can be achieved in the range in nano molar concentrations using SWV. Observation of the dimensional plot of the theoretical forward or reverse components is the main reason for the excellent sensitivity of the technique [32]. The precision of this analysis can be increased by averaging signal data from several square wave voltammetric scans. The ability to measure faradic current at the time when double layer charging current is negligible is primarily responsible for the success of SWV. The measurement speed coupled with signal averaging permits the experiment to be performed repetitively and increase signal to noise ratio. Such qualities of SWV make this technique very useful for the analysis of trace amount of drug compounds in their dosage forms and biological samples. In the present investigations, a bioanalytical system controlled via a computer (**Fig. 1.4**) by its own software was employed for the different voltammetric techniques for the electrochemical analysis of the selected compounds.
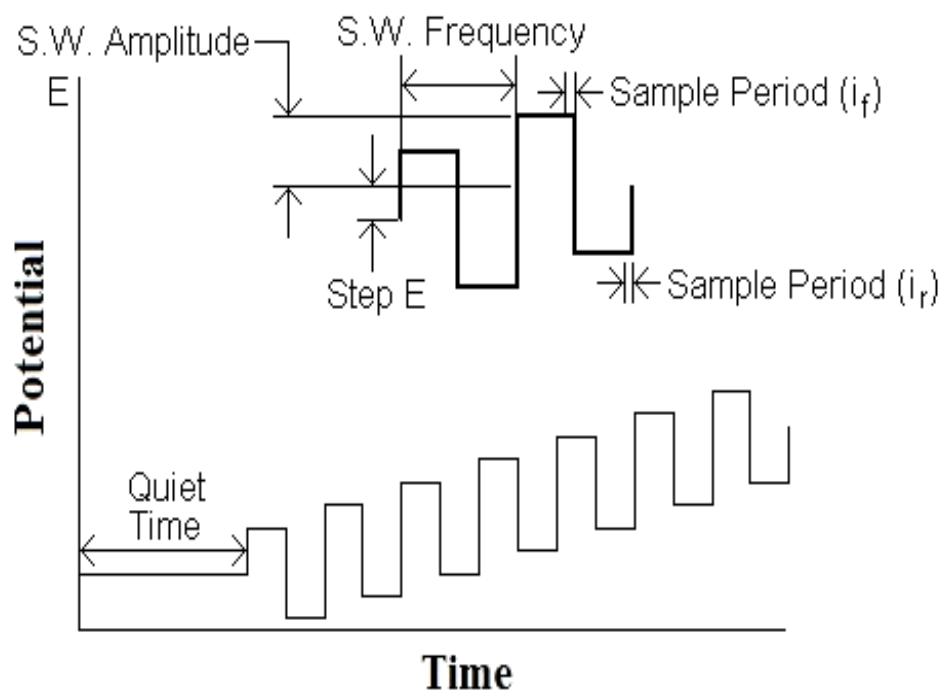
Fig. 1.3: Square wave potential sweep.

Fig. 1.4: Bioanlytical system used for electrochemical studies.

1.1.3 Controlled Potential Electrolysis

Controlled potential electrolysis (CPE) is a useful analysis technique, introduced by Haber, is based on the fundamental concepts expressed in the Faraday's laws [33]. Two simple and straight forward kinds of applications are carried out by CPE. The first one consists of synthesis of reaction product on a comparatively large scale, then identifying that product by any convenient technique. The other consists of integrating the current with respect to time during exhaustive controlled-potential electrolysis, calculating the number of electron from the ratio of the quantity of electricity consumed to the number of moles of starting material taken, and deducing the nature of the half-reaction. This information is helpful in the elucidation of the mechanism of electrode processes [34, 35]. The total charge passed during the CPE experiment is calculated by integrating the current and is related to the number of electrons transferred per molecule and the number of moles of the oxidized species initially present through Faraday's law:

$Q = nFN$

where,

Q = total charge passed during the experiment is calculated by the integration of current

n = number of electrons transferred per molecule

F = Faraday's constant

N = number of moles of species being electrolyzed

The electrolysis cell for CPE is entirely different to that used in voltammetry experiments. The rate of electrolysis significantly depends upon the area of working electrode, therefore, working (e.g., mercury pool, carbon sheet or a platinum gauze) and auxiliary (e.g., platinum coil or gauze) electrode with a large surface area is used in CPE. The solution is stirred to increase the rate of mass transport. The auxiliary electrode must be isolated from the working electrode to prevent species that are electrogenerated at the auxiliary electrode from interfering with electrolysis at the working electrode. The CPE is the most convenient method for synthetic purposes and the product obtained can be characterized by other techniques including NMR, UV-Vis and FT-IR techniques [36, 37].

1.2 CHROMATOGRAPHY

Chromatography is a separation technique that exploits the difference in partitioning behavior between a mobile phase and a stationary phase to separate the component in a mixture. The solute is distributed between two phases as a result of the molecular forces that exist between the solute molecules and those of two phases. The stronger the force between the solute molecules and those of the stationary phase, greater will be the amount of the solute held in the stationary phase under equilibrium conditions and vice versa. The solute can move through the chromatographic system while it is in the mobile phase. Solutes distributed preferentially in the mobile phase move more rapidly through the system than those distributed in the stationary phase. Thus, solute elute in order of increasing distribution coefficient with respect to the stationary phase [38-40]. Among the various chromatographic techniques available these days, HPLC has been used in the present studies.

1.2.1 High Performance Liquid Chromatography (HPLC)

High Performance Liquid Chromatography (HPLC) has become a valuable analytical tool due to its high sensitivity, selectivity and capability for individual and multi-elemental analysis [41-43]. The advances in the column technology and instrumentation have catalyzed the explosive growth in the field of HPLC. It is used to separate component of a mixture based on a variety of chemical interactions, usually of a non-covalent nature, between the analyte and the chromatographic column. Mixture of components injected into the column is eluted at different retention times (R_t) in the form of peaks. Each peak representing a different chemical species, can be collected as a separate purified component or can be simply detected to determine their presence or quantity. HPLC finds its application in biochemical analysis, analysis of human blood proteins and structural analysis of biomolecules [44-47]. It aims as a powerful clinical analytical tool in the field of pharmaceutical and pharmacological research [48].

1.3 WORKING ELECTRODES

The general information regarding the conventional electrodes, nanomaterials, modified electrodes and methodology used in the present investigations is being presented in the following sections:

1.3.1 Conventional Electrodes

The electrochemical experiment averse the fact that an electrode occupies a central place in an electrochemical procedure and turnout of various electrochemical techniques depends on the nature of electrodes used. Thus, selecting a proper material for the working electrode is the most important feature of an electrochemical investigation. The electrodes used in voltammetry take a variety of shapes and forms, often; it is small flat disk of a conductor that is press fitted into the rod of inert material. A vast variety of materials have found applications as working electrode. Available potential window, electrical conductivity, surface reproducibility, mechanical properties, cost, availability, toxicity, redox behavior of the target analyte and background current in the potential region under experimentation are the main features which need due consideration while selecting a suitable material to be used as working electrode. Generally, conventional working electrodes are based on mercury, noble metals, semiconductor or carbon. Each type of electrode has its advantages and disadvantages over others.

Mercury electrode has been widely used in voltammetry for several reasons such as relatively large negative potential range, many metal ions are reversibly reduced to amalgam at the surface of mercury electrode, high hydrogen over voltage, highly reproducible and smooth surface. Mercury electrode is liquid and it can take several forms. However, application of the mercury electrode is restricted now a day because it is easily oxidized. This property severally limits the range of anodic potential that can be used and also high charging current limits the sensitivity. In addition, due to toxic nature of mercury, its use in laboratory has been banned in almost all developed countries.

Metal electrodes include variety of electrodes such as gold, platinum, nickel, copper or silver. These metals have been used extensively as an electrode material, with each metal having its specific applications. Gold electrodes are inert and are commonly used for self-assembled monolayers or for stripping measurements of trace metals. Platinum electrodes are mostly applicable for fuel cells. Copper and nickel electrodes are commonly used in the detection of amino acids or carbohydrates, while silver electrodes are generally applied for the determination of cyanide or sulfur compounds. The last decade has seen the applications of palladium as electrode material for the analysis of biomolecules and drugs due to its unique mechanical and electrical properties [**Fig 1.5**]. Palladium exhibits chemical inertness and is conductive in nature. It is biocompatible and shows strong affinity towards the organic

9

molecules. It provides low background current and shows excellent stability and reproducibility during the experiments [49-53].

Fig. 1.5: Palladium electrode

Though, metal based electrodes satisfactorily overcome the disadvantage of mercury toxicity, but low hydrogen over voltage strictly limits the cathodic potential window. High background current is another disadvantage associated with these electrodes. Both these disadvantages can be circumvented by using carbon electrodes.

Carbon electrode is the most widely used working electrode in electroanalysis. Carbon surfaces are considered as an attractive material for electrochemical analysis as they can be synthesized in different forms (from powders to fibers, foams, fabrics and composites) and are found in the form of different allotropes (graphite, diamond, fullerene). Carbon electrode incorporates almost all the features of good electrode material like broad potential window, low background current, low cost, chemical inertness and suitability for various sensing and detection applications. Besides these, carbon based electrode has surface functional groups for chemical modification and controllable surface activity resulting from the pretreatment [54-57]. It is morphologically diverse; existing in a variety of forms suitable for electrochemical applications such as glassy carbon [58-61], graphite pastes [62], carbon films [63, 64], carbon fibers [65-68], and composites [69, 70]. In the present studies, edge plane pyrolytic graphite electrode (EPPGE) is used as working electrode. Pyrolytic graphite is a polycrystalline form of carbon with high degree of orientation and formed by pyrolysis (1900-2500ºC) of carbonaceous gas under low pressure. EPPGE are fabricated by taking a piece of high quality highly ordered pyrolytic graphite (HOPG) and cutting the desired electrode geometry such that the layers of graphite lie perpendicular to the surface **[Fig. 1.6]**. Surface defects occur in the form of steps exposing the edges of the graphite layers [71].
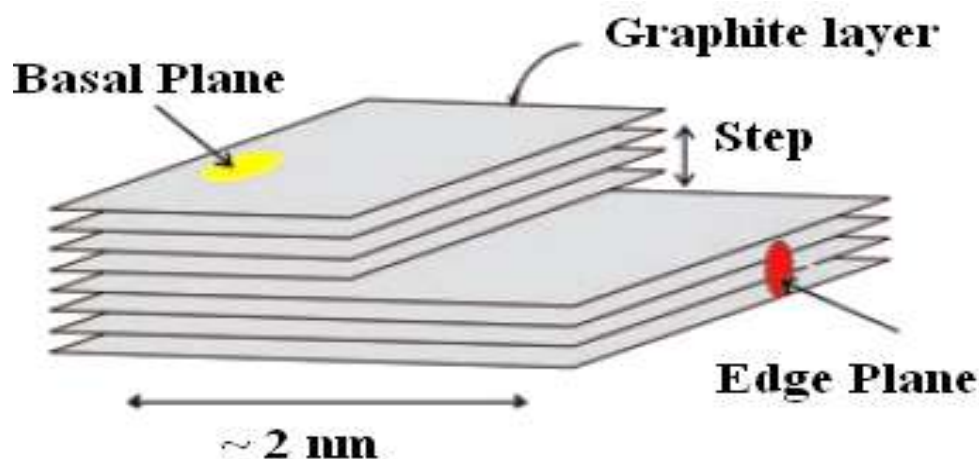
Fig. 1.6: Schematic representation of a crystal of highly ordered pyrolytic graphite surface.

Fig. 1.7: An edge plane pyrolytic graphite electrode used for voltammetric determinations.

PGE is most versatile electrode used in the electrochemical investigations due to its faster electrode kinetics and wide available potential window [72]. It has been used in the NADH oxidation [73], nitrogen dioxide sensing [74], reduction of chlorine [75], electrochemical investigation of hemoglobin and myoglobin [76], investigations of human adrenodoxin [77], detection of deoxyribonucleic acid [78], sensing of epinephrine [79] and electroanalytical chemistry of various small biological molecules [80]. Several PGE based biosensors [81, 82] and electrochemical atomic force microscopic studies [83, 84] of DNA immobilized onto PGE [85, 86] have been well documented in literature. In the present studies mainly PGE has been used as working electrode which is represented in **Fig. 1.7**.

1.3.2 Modified Electrodes

An active area of research in electrochemistry is the development of electrodes that are produced by chemical modification of various conducting substrates. Such electrode can, in principle, be tailored to accomplish various functions. Modification includes the presence of adsorbing substances with desired functionalities, covalent bonding of component to the surface, and coating of electrode with polymer films or film of other substances. Modified film can be prepared over working electrode by dip coating, spin coating, electrodeposition or covalent attachment, and adsorption or gel entrapment. The interdisciplinary trend of present day in sensor research makes it clear that the advancement in sensors is likely to be continued in future also and progress of this field will continue to be accelerated by advancement in other fields.

Nanotechnology is such an area, where recent advancement of technology has led to a substantial increase in understanding of the subject matter and basic phenomena influencing the properties of the matter. The nanomaterials or matrices with at least one of their dimensions ranging in scale from 1 to 100 nm, display unique physical and chemical features such as the quantum size effect, mini size effect, surface effect and macro-quantum tunnel effect. Through the different physico-chemical phenomena taking place at nanodimensions, the integration of nanotechnology approaches into sensors holds great promise for addressing the analytical needs of molecule detection. Novel functional nanomaterials, such as porous silicon, nanowire, carbon nanotubes, and nanoparticles modified sensors have been found to exert a profound influence on molecular detection. Nanoparticle study was initiated by Michael Faraday in 1847, where he discovered gold colloids. Ever since much work has been carried out mainly on metallic nanoparticles such as gold, silver iron, platinum, nickel, and copper. Among the different types of metal nanoparticles, gold is by far the most studied in the literature because gold at nanoscale manifests a number of interesting physico-chemical properties that have fascinated scientist of many disciplines including: material scientists, catalysts, biologists, surface and synthetic chemists and theoreticians since its discovery [87]. Fabrication of a sensor using nanoparticles has great concern with the methodology adopted for the attachment of nanomaterials to the electrode. There are several methods to fabricate nanomaterials on sensor surfaces, depending on the type of material and substrate. The slight change in the modification procedure of electrode, leads to different electrochemical and electrocatalytic characteristics of a sensor. Therefore, it is necessary to examine the behavior of different nano electrode materials as well as novel attachment approaches [88-90].

On the other hand, carbon nanoparticles which are member of nanocarbon materials have drawn a great attention for surface modification due to their high surface area, easiness of functionalization, and inexpensiveness [91, 92]. It has also been reported that carbon nanoparticles can change their electrical properties from semiconductor to metal, provided the particle size is less than 1 nm in diameter and their high elasticity is useful for protective or biocompatible coating purposes [93, 94]. The versatility, low cost and excellent electrocatalytic activity of carbon nanotubes (CNTs) have triggered their utilization in preparing electrochemically active surface for various electrochemical processes. CNTs are available in various form, among them, single walled carbon nanotubes (SWCNT) presents another most widely carbon based nanomaterial for the surface modification of electrodes. SWCNT has single layer cylinder extending from end to end with excellent uniformity in diameter (down to 7 nm). Metal impurities embedded in CNTs samples have been proposed as a potential reason for the high electrocatalytic activity for a wide range of compounds, such as neurotransmitters, NADH, hydrogen peroxide, ascorbic and uric acid, cytochrome C, hydrazines, hydrogen sulphide, amino acids, DNA etc [95, 96]. The CNT based lab-on-a chip system has been used for the determination of antithyroid drug [97]. It has been suggested that electrocatalytic properties originate from the ends of CNTs [98]. Liang and Zhuobin described direct electrochemistry of glucose oxidase at single-walled carbon nanotube modified gold electrode [99]. Zhao and Ju recently described the formation of a stable and uniform multilayer composed of multiwall carbon-nanotubes along with enzyme glucose oxidase on the surface of polyelectrolytes modified gold electrode [100]. The fabricated enzyme-nanotube-polyelectrolyte electrode system was used for the sensitive determination of glucose which has easily overcome the interference of ascorbic acid and uric acid [101]. Gooding and coworkers demonstrated, in a short communication, the advantages of bamboo-like nanotubes for electrochemical biosensor applications [102]. From last several years our laboratory is actively involved in using carbon nanotubes for the modification of electrode surface and a variety of biomolecules have been detected in urine and serum.

Besides the nanomaterials conducting polymers have been extensively used for the surface modification, due to the conjugated π-electron backbones. They are drawing great deal of attention in the fabrication of electrochemical sensors. Their electronic, structural and optical properties with easy synthesis and good stability have been the driving force for the voltammetric determination of several biologically important compounds [103, 104]. Polymer/nanoparticle hybrid material lays on the large improvements in the mechanical, electrical, and thermal properties [105]. Pumera et al. fabricated and characterized carbon

nanotube epoxy composites for electrochemical sensing [106]. The prepared composite electrode showed more robustness when compared with carbon nanotube paste electrode and teflon composite electrode [107]. An epoxy casted electrode was also fabricated and found to have low background current, which makes it suitable for future sensor applications. Zheng's research group demonstrated the electrochemical behaviour of rutin at single-walled nanotube modified gold electrode and also described indirect determination of hemoglobin at the modified electrode [108]. Many papers are published every year describing the application of polymer modified electrodes for analytical purposes; however, actual implementation requires a rigorous evaluation covering electronic aspects also [109]. Today it is very evident that nano science and nanotechnology offers novel hybrid materials and methods that may significantly improve the peak current in electroanalytical methods. The new materials will probably bring great advances in fields such as medical research to improve the quality of health as well as other applications concerned with the interest of the society. However, the present day research interest towards nanotechnology is driven by desirable properties offered by nanomaterials. The ease of fabrication and functionalization of nanoparticles makes them very useful for the development of the modified electrodes for the specific detection of molecules with biological interest. Such modified electrodes have potential applications in electroanalytical chemistry because the signal-to-background ratio observed can be several orders of magnitudes higher than at a conventional electrode, resulting in a detection limit that can be orders of magnitude lower. A wide range of newly introduced nanomaterials are expected to expand the realm of nanomaterial-based electrochemical sensors.

Nanomaterial modified electrodes have also been explored for the electrochemical reduction or oxidation of various steroids for their detection in various complex matrices. However, in case of steroids less sensitivity, selectivity, and electrode fouling is observed. To overcome these problems, in the last few years, several methods based on immunosensor, peptide sensor, aptamer sensor, enzyme based sensor have been developed. These methods were more selective and sensitive for the detection of various steroids. Additionally, multienzyme functionalized mesoporous silica nanoparticles, graphene, etc. based sensors reported for steroids determination were found to be highly sensitive. Immunosensors are ligand-based biosensors and the fundamental basis of determination is the specificity of the molecular recognition of antigens by antibodies to form a stable complex. The principle used for detection by immunosensors can be electrochemical, optical, or microgravimetric [110]. Recently, an electrochemical immunosensor has been reported by Ojeda et al. for the rapid and sensitive detection of estradiol [111]. In this study a disposable screen printed electrode was

modified with p-aminobenzoic acid followed by covalent binding of streptavidin. Then the immobilization of biotinylated anti-estradiol was carried out for the determination of estradiol using competitive immunoassay. The signal was obtained through peroxidase-labeled estradiol by measuring the amperometric response at −0.2 V using hydroquinone as redox mediator. The detection limit of the immunosensor was impressive; however, this modified sensor was not selective as structurally related compounds and other hormones could not be distinguished and exhibited significant interference. Moreover, the electrode surface was nonconducting in nature, which drastically affected the sensitivity for the steroid determination. A dual electrochemical immunosensor for the multiplexed determination of adrenocorticotropin and cortisol has also been reported in literature [112]. The sensor involved use of screen-printed carbon electrode, which was modified with aminophenylboronic acid. The corresponding adrenocorticotropin and cortisol antibodies were immobilized on the sensor. Competitive immunoassays involved biotinylated adrenocorticotropin and alkaline phosphatase labeled streptavidin, or alkaline phosphatase labeled cortisol. The affinity reactions were monitored by using differential pulse voltammetry. However, it was noticed that the method had a disadvantage due to the nonconducting nature of the electrode preparation and the requirement of multistep preparation. Additionally screen printed electrodes in general are not user friendly. They possess short electrode life time and exhibit poor inter electrode reproducibility and hence, limit the applications. Thus, in a recent study a nanoconducting immunosensor surface was developed and applied for the electrochemical determination of progesterone using enzymatic reaction [113]. A significantly lower detection limit of 0.08 ng mL^{-1} compared to previously reported methods was observed, indicating thereby that the determination of steroids using a nanoconducting surface coupled with enzymatic or nonenzymatic catalytic reaction may allow their detection at significant low levels.

Thus, electrodes modification is emerging as a powerful platform for the direct detection of biological and chemical species. In view of the interesting properties exhibited by nanomaterials, it was considered worthwhile to prepare nanomaterial based sensors for the determination of biologically important compounds and drugs.

1.3.3 Modification Used In The Present Thesis

An increased attention has been paid for the modification of electrodes using nanomaterials, polymers and hybrid materials due to their excellent structural, mechanical and electrical properties. Since the discovery of nanomaterials, many papers have reported the use of nanomaterials as electrode modifier for the determination of variety of compounds. In the

present work gold nano particles, carbon nanotubes, conducting polymers and aptamers are used for the surface modification. The electrochemical sensors and biosensors thus, prepared are used for the determination of biomolecules and drugs. The important information on various modifications used in the present thesis is given below.

1.3.3.1 AuNPs modified electrodes

Nanoparticles of noble metals, especially gold nanoparticles (AuNPs), have received great interest in the last two decades due to their attractive electronic, optical, and thermal properties as well as catalytic properties. The potential applications of AuNPs in the fields of physics, chemistry, biology, medicine, and material science and their different interdisciplinary fields have been demonstrated. In biosensor research, AuNPs has attracted more attention because of their good biological compatibility, excellent conducting capability and high surface-to-volume ratio. In recent years, several research papers have been published using AuNPs for electrochemical applications. AuNPs modified carbon ionic liquid electrode was used for the investigation of a flavonoid; rutin which serves as an antitumor, antioxidant and anti-inflammatory agent. Modified electrode showed the increase of peak current and decrease of peak potential as compared to the bare. This behaviour is attributed to the catalytic activity of gold nano particles [114]. AuNPs/TiO$_2$ composite modified electrode was constructed by Milsom *et al.* to study the electrochemical behaviour of nitric oxide [115]. AuNPs have been widely applied in the study of direct electron transfer (DET) of some redox proteins. For instance, Li *et al.* reported DET immobilized hemoglobin and surfactant protected AuNPs modified glassy carbon electrode. The hemoglobin immobilized on colloidal AuNPs showed a quasi-reversible redox couple at about - 0.256 V and - 0.206 V in phosphate buffer [116]. Another application of DET was reported by Frasca *et al.* in which they showed direct electron transfer of human sulfite oxidase enzyme immobilized on AuNPs modified electrode. These nano particles were covalently bonded to acid treated gold electrode, where this enzyme was absorbed and an increased interfacial electron transfer and electro-catalysis was obtained [117]. Bare gold electrode has also been extensively used for the quantification of metals in water samples [118]. A large number of biomolecules have been studied using AuNPs as enhancing materials, such as glucose [119], dopamine and serotonin [120], norepinephrine [121], epinephrine [122], ascorbic acid [123] etc. A substantial fraction of the work presented in this thesis illustrates application of the AuNPs modified palladium sensor, AuNPs -polymer network modified edge-plane pyrolytic graphite sensor for electroanalytical determination of different biomolecules and drugs with elaborate discussion on their electrochemical aspects.

1.3.3.2 CNT modified electrodes

The turn of the last decade has seen the development of carbon nanotubes based nanomaterials, for the signal amplification in electrochemical sensors. Construction of efficient CNT modified electrochemical sensors is a very promising tool in promoting the electron transfer reactions of biologically important biomolecules and various pharmaceutical drugs. Carbon nanotubes are broadly classified as single-wall carbon nanotubes (SWCNT) and multi-walled carbon nanotubes (MWCNT) [124-126]. SWCNT possess a cylindrical nanostructure formed by rolling up a single graphite sheet into a tube (**Fig 1.8**). As SWCNT exhibits higher ratios of surface area to volume, hence SWCNT modified electrochemical interfaces provide effective larger electrochemically active area in comparison to unmodified surface and therefore probably lead to higher detection sensitivity for target molecules. SWCNT can thus be viewed as molecular wires with every carbon atom on the surface. On the other hand, MWCNT comprises of an array of such nanotubes that are concentrically nested like rings of a tree trunk. SWCNT are constructed of a single sheet of graphite of diameter 0.4-2 nm, while MWCNT consists of multiple concentric graphite cylinders of increasing diameter of 2-100 nm. The interlayer spacing between the layers in MWCNT is close to that of interlayer distance in graphite (0.36 nm). SWCNT are less resistant to chemical attack, whereas MWCNT are more resistant to chemical attack. The first utilization of CNT in electrochemistry was reported in 1996 by Britto *et al.* [127], who used a paste of nanotubes with bromoform as binder. The paste was filled into a glass tube and used as a working electrode to study the redox reactions of dopamine. At nanotubes modified electrode the oxidation of dopamine occurred at low potential with a faster rate than found using other catalytic surfaces. Britto's pioneering study explained some unique features of carbon nanotubes and spawned several other methods for the fabrication of sensors using these nanotubes. Carbon nanotubes doped with overoxidized pyrrole molecules have been used as composite for surface modification for the determination of drugs [128, 129]. A substantial fraction of the work presented in this thesis illustrates application of the SWCNT, SWCNT-polymer network modified edge-plane pyrolytic graphite electrode for electroanalytical determination of different biomolecules and drugs with detailed discussion on their electrochemical panoramas.
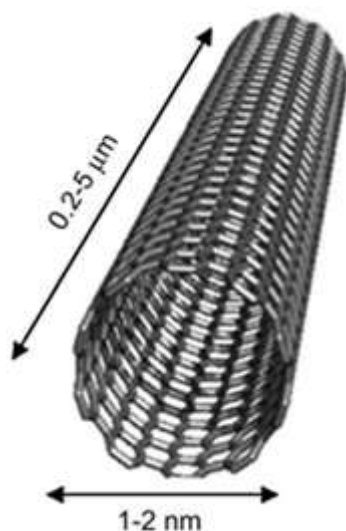
Fig. 1.8: Schematic representation of single-wall carbon nanotubes.

1.3.3.3 Polymer modified electrodes

The first highly-conductive polymer was synthesised by Shirakawa, Heeger and MacDiarmid in 1977. After this discovery, a variety of conductive polymers came along as an attractive field of study in scientific and industrial researches. Conducting polymers (CP) are termed as "synthetic metals" due to their excellent electric, electronic, magnetic and optical properties inherent to the metals. Hence, CP have been considered as a promising tool in various research areas, such as light-emitting diodes, drug release systems, electrochromic devices, solar cells, and electrochemical sensors. The conductivity of CP is assigned to the delocalization of π-bonded electrons over the polymeric backbone [130]. The use of CP such as polypyrrole, polythiophene, polydiaminonapthalene and polyaniline for the modification of electrode surface is increasing due to their wide electrochemical window, high conductivity and good stability. These polymers are considered as one of the promising conductive polymeric materials due to the ease of synthesis and low cost in comparison to other conducting polymers [131, 132]. The excellent adhesive property and dense structure polymer films obtained by electrochemical synthesis are of great advantage and can effectively respond to the specific chemical or biological species and are also very useful for solid-phase applications [133, 134]. Nanostructurization of CPs and their composites has emerged as a new area of research and development and is unveiling a new class of smart materials for the use in modern and future technologies. The great mechanical properties of CNT make them the filler material of choice for composite reinforcement [135]. The interaction between carbon nanotubes surface and polymer backbone is through π-π stacking interaction, which may cause a large net-stabilized

structure [136, 137]. Nanostructured nickel hydroxide modified electrodes have been used for the determination of isoniazid [138]. Polymer-gold nanoparticles hybrid materials are prepared by engrafting gold nanoparticles into the matrix of conducting polymer structures. They provide interesting properties from both the size effects of the gold nanoparticles as well as the exceptional properties of the polymers, which allow stacking of the particles and increase their stabilization [139]. Such type of interaction may offer significant advantages in several applications including microelectronics, sensing and energy systems. An attempt has been made in this work to utilize conducting polymer for the modification of the surface of pyrolytic graphite to determine sulfacetamide, cefpodoxime proxetil and chloramphenicol.

1.3.3.4 Aptamer modified electrode

Aptamers are small oligonucleic acids that specifically bind to the target molecule have attracted attention in the last decade. The reason for using aptamers are that they can be regenerated, highly stable to external factors, and does not require animal models for generation [140]. Kim et al. selected DNA aptamers that specifically bind to 17β-estradiol through, the SELEX (Systematic Evolution of Ligands by Exponential enrichment) process from a random ssDNA [141]. The DNA aptamer was immobilized on the surface of gold electrode through the avidin–biotin interaction. The oxidation potential values were then measured using cyclic voltammetry and square wave voltammetry to evaluate the chemical binding to aptamer. It was noticed that when 17β-estradiol interacted with the DNA aptamer, the current signal decreased due to the electron flow produced by a redox reaction between ferrocyanide and ferricyanide. The aptamer sensor in this case was found to be more sensitive than previous studies designed for chemical sensing. Thus, it was concluded that it is advantageous to use aptamers for the determination of various steroids. Most of the methods reported so far for determination of steroids required enzyme tagging, due to which an additional step is needed. In addition, enzyme tagged secondary antibodies can easily denature at unfavourable temperature or pH. Thus, some more advancement is needed in biomolecules determination to avoid enzyme tagging. In a new perspective, a label free impedance method is also attempted for the determination of estrogen using the estrogen receptor biosensor [142]. The electrochemical impedance spectroscopy is a label free technique and has been widely applied for the biomolecules detection in recent years [143]. The impedance method relied on the detection of change in electrode surface resistance in the presence of $K_3Fe(CN)_6/K_4Fe(CN)_6$ redox indicator. This is a quite promising approach and can be easily applied for other steroids

detection, however, the detection can be further significantly improved using a conducting polymer–nanomaterials composites [144, 145] in place of the simple gold plate electrode.

1.4 ANALYTES OF INTEREST

The biomolecules are essential substances for all living beings due to their active participation in several physiological processes. A minute change in their concentration may lead to several physical or mental disorders resulting in severe health problems. In last few decades the use of pharmaceutical drugs to prevent various diseases has gained much attention. It is suggested that these drugs should be prescribed in a controlled way. The overdose of these drugs may cause several side effects on human body. The misuse of many drugs (steroids etc.) to enhance the performance at the site of competitive games has also become an increasing problem. With the ongoing advancement in biomedical technology, drugs have become more potent, more effective and more dangerous. Therefore, ultrasensitive and selective detection of biomolecules and pharmaceutical drugs including doping agents is highly desirable.

Neurotransmitters are endogenous brain chemicals that are released from the presynaptic nerve terminal of neurons and transmit signals across a synapse from one neuron to another 'target' neuron. They can affect concentration, mood, sleep and weight and in imbalance form may cause adverse symptoms. **Dopamine** is one of the most important catecholamine that brain uses as the neurotransmitter as well as it is an important intermediate in the biosynthesis of two other neurotransmitters of catecholamine family, epinephrine and norepinephrine. The brain deals with several distinct dopamine systems, one of which plays a major role in reward-motivated behaviour. In such cases an increased level of dopamine in the brain is observed, and a variety of addictive drugs have been found to increase dopamine neuronal activity. Other brain dopamine systems are involved in motor control and in controlling the release of several other important hormones. Due to the direct involvement of dopamine in the series of functions, it plays a vital role in human behaviour and thus changes in its level or disturbances in its transmission has been implicated in a number of disorders associated with central nervous system like Parkinson's disease [146], schizophrenia and psychosis [147, 148]. The precursor of dopamine such as L-DOPA (3,4-dihydroxyphenylalanine) and carbidopa, a drug that inhibits aromatic L-aminoacid decarboxylase, have been studied by voltammetry and a high sensitivity was observed [149]. Because of several physiological functions of neurotransmitters, they have been determined in human urine and plasma using highly sensitive electrode. Gold nano particles decorated

palladium electrode was used for the determination of dopamine, a well-known neurotransmitter, in this thesis.

Antibiotics, also known as antibacterial, are most frequently prescribed medications that are used to destroy or kill the bacteria. Different types of antibiotics affect different bacteria in a different way. **Sulfacetamide** is a sulfonamide antibiotic which shows broad spectrum antimicrobial activity against a wide range of bacteria. It is most commonly used in the treatment of pityriasis versicolor [150] and rosacea [151]. It also has anti-inflammatory properties, when used to treat blepharitis or conjunctivitis. Overdose of this drug may lead to several side effects such as nausea, diarrhea, local irritation and contact dermatitis [152]. The effects and side effects of sulfacetamide on human health triggered our interest to detect this drug in human biological samples. Hence, we determined this drug using polymer/carbon nanotubes modified electrode based on its electrochemical oxidation. **Cefpodoxime** (CP) is a third-generation cephalosporin antibiotic. The broad spectrum of activity of third-generation cephalosporins against both Gram-positive and Gram-negative bacteria renders them an excellent choice as 'first line' or 'blind' therapy, especially for situations in which penicillin-resistant organisms may be present [153]. CP is used orally for the treatment of mild to moderate respiratory tract infections, gonorrhoea and urinary tract infections and also in the treatment of skin infections, acute media otitis, pharyngitis and tonsillitis [154, 155]. The overdose of CP is associated with nausea, vomiting, flatulence, oral candidiasis, epigastria distress and diarrhea [156]. Hence, this drug is determined using polymer/gold nano particles modified electrode.

Chloramphenicol (CAP) is a synthetic, broad spectrum antibiotic, which inhibits the activity of both Gram-positive and Gram-negative bacteria. It slows growth of bacteria by preventing them from producing important proteins that they need to survive [157]. CAP has been considered as a prototypical broad-spectrum antibiotic, alongside the tetracycline. CAP is less expensive than other antibiotics and is easy to manufacture, hence, it is frequently used as an antibiotic of choice in the developing world. The common side effects of CAP are headache, mental confusion, fever, rash, diarrhea, and optic atrophy. CAP also causes Gray syndrome and serious, fatal blood dyscrasias [158]. Thus, keeping in consideration the efficacy of this antibiotic, a need was felt to develop a sensitive and rapid assay for the detection of CAP.

Another compound selected for the study belongs to the steroid family. Corticosteroids are man-made chemicals that closely resemble the hormones produced by adrenal cortex of vertebrates. Glucocorticoids such as cortisol control the metabolism of carbohydrate, fat and

protein and act as anti-inflammatory by preventing phospholipid release, decreasing eosinophil action and a number of other mechanisms. Topical corticosteroids are used for the localized treatment of skin from various inflammatory skin disorders. One of the important topical corticosteroids is **Mometasone furoate (MF),** which is used as antipyretic, anti-inflammatory and vasoconstrictive agent [159]. The clinical effectiveness of MF has been assigned to its vasoconstrictive, anti-inflammatory, immunosuppressive and anti-proliferative properties [160]. The overdose of MF absorbed into bloodstream has been reported to cause a group of symptoms called Cushing's syndrome which exhibits acne, depression, high blood pressure, muscle weakness and paranoia [161]. Thus, it is highly desirable to develop a method to determine its concentration in various biological samples. Therefore, an attempt has been made to detect this drug using SWCNT modified pyrolytic graphite based on its reduction. A probable mechanism for the reduction has also been suggested.

1.5 SUBJECT MATTER OF THE THESIS

Detection of biomolecules of physiological importance and pharmaceutical drugs in human body fluids has always been a topic of considerable significance as it gives a big support in bio-analytical research field. Several methods have been reported for detecting these molecules. Most of the methods are based on the fact that these biomolecules and drugs are found in human system in micro or nano molar range; hence, it is usually difficult to achieve a very low detection limit using electrochemical methods. However, nanomaterials modified sensors fulfill this task very effectively, which can be attributed to their high sensitivity and low over potential. Hence, in this dissertation attempts have been made to modify the surface of electrodes by the use of nano structured substances. The modified surfaces have been characterized by scanning electron microscopy (SEM) and electrochemical impedance spectroscopy (EIS). The detection of a variety of biologically important molecules and drugs has been carried out. It is believed that the modified electrochemical sensors continue to be an important aspect of biomedical sensor development. The whole work has been systematically organized in six chapters in order to clearly present the results of investigations.

Chapter 1   Introduction.

Chapter 2   Determination of dopamine using nano gold modified palladium sensor.

Chapter 3   Carbon nanotube embedded polymer modified sensor for the determination of sulfacetamide.

Chapter 4   Electrochemical determination of mometasone furoate in micellar medium.

Chapter 5   AuNPs-poly-DAN modified pyrolytic graphite sensor for the determination of Cefpodoxime Proxetil in biological fluids.

Chapter 6   *In vitro* chloramphenicol detection in a *Haemophilus influenza* model using an aptamer-polymer based electrochemical biosensor.

Chapter 2

Determination of dopamine using nano gold modified palladium sensor
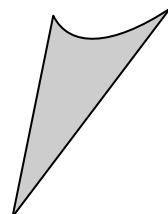
2.1 INTRODUCTION

Nano sized particles of noble metals have received great interests of scientists and become one of the most exciting cutting edge fields in chemistry [162]. Excellent conductivity, good biological compatibility, high stability, large surface-to-volume ratio, tremendous catalytic activity and control over electrode microenvironment render gold nanoparticles excellent scaffolds for the fabrication of sensor [163, 164]. In recent years, noble metals have attracted the interest of scientific community involved in the electrode development. Platinum group metals have been widely used in electrochemistry due to their excellent electrical conductivity, wide potential window, high mechanical strength and chemical inertness, low background current, suitability for various sensing and detection applications [165]. Palladium has been widely used as catalyst in hetroaromatic couplings during microwave irradiation [166]. Its application in the construction of modified electrodes, which are utilized as sensors, has attracted attention. It has strong adsorption behavior towards hydrogen, electrocatalytic activity against organic molecules and high resistance to corrosion [167].

Dopamine **(I)**, is one of the most important catecholamine that brain uses as the neurotransmitter as well as it is an important intermediate in the biosynthesis of two other neurotransmitters of catecholamine family, epinephrine and norepinephrine [168]. Dopamine is responsible for a variety of physiological functions like voluntary movement, ability to concentrate, feelings of pleasure, motivation and reward, gastrointestinal motility, pituitary hormone release, and higher cognitive processes [169]. Moreover, it is crucially involved in the renal, hormonal, and cardiovascular systems [170]. Due to direct involvement of dopamine in the series of functions it plays a vital role in human behavior and thus changes in its level or disturbances in its transmission have been implicated in a number of disorders associated with central nervous system like Parkinson's disease [146], schizophrenia and psychosis [147-149]. Therefore, the determination of dopamine concentration is essential for efficient diagnosis of these degenerative diseases and for the study of physiological mechanisms. Thus, it is very necessary to design sensitive, selective, and reliable sensors for the direct determination of dopamine. A number of investigations have been conducted for the determination of dopamine by various methods such as HPLC, fluorimetry, titrimetry, spectrophotometry, and immunological methods, but these methods hold several limitations like low sensitivity, requirement of sample pretreatment and time consuming processing [171]. Since, dopamine is electrochemically active thus, electroanalytical methods are usually employed for the detection of dopamine due to simplicity and ease in preparation of sensors which, leads to fast detection,

appreciable stability and impressive reproducibility. Several voltammetric attempts have also been made for the determination of dopamine in pharmaceuticals and biological fluids utilizing different electrodes [172, 173]. To the best of our knowledge, no study has reported the voltammetric determination of dopamine by using nano gold modified palladium sensor. Thus, in the present work, we have described initially the preparation of nano gold modified palladium electrode as a new sensor in the electrocatalysis and determination of dopamine in an aqueous buffered solution. The analytical performance of the modified sensor in quantification of dopamine in the biological fluids has also been evaluated.
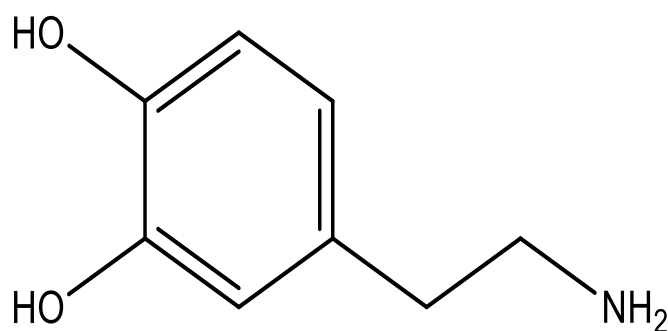
(I)

2.2 EXPERIMENTAL

2.2.1 Instrumentation

The electrochemical techniques were executed using Bioanalytical system (BAS, West Lafayette, USA) Epsilon EC-USB voltammetric analyzer, equipped with a conventional three electrode glass cell. Platinum wire was used as counter electrode, Ag/AgCl (3 M NaCl) as reference electrode (BAS Model MF-2052 RB-5B), and Palladium (Pd) electrode (0D-0.6 mm^2, 1.6 mm^2, BAS, USA) as working electrode. The pH of the buffer solutions was measured by using digital pH meter (Eutech Instruments, Model pH 700). Characterization of the electrode surface was accomplished using field emission scanning electron microscopy (FE-SEM; Zeiss ultra plus 55). Electrochemical impedance spectroscopy was performed using Versastat 3 galvanostat (PAR USA).

2.2.2 Chemicals and reagents

Dopamine, $HAuCl_4$, tri-sodium citrate and $NaBH_4$ were obtained from Sigma Aldrich, USA. Phosphate buffers of different pH were prepared using analytical grade chemicals (NaH_2PO_4, Na_2HPO_4 and H_3PO_4) by following the method of Christian and Purdy [174]. All other reagents and solvents used during the experiment were of analytical grade.

2.2.3 Fabrication of nano gold modified palladium (AuNP/Pd) sensor from bare palladium (B/Pd)

Prior to modification of electrode, its surface was polished with a paste of alumina (grade I) and zinc oxide using micro cloth pads until a mirror like finish was obtained. For modification, nano gold seeds were prepared. According to the procedure previously reported [175], 20 mL aqueous solution containing 0.25 mM $HAuCl_4$ and 0.25 mM tri-sodium citrate was prepared and to this solution 0.6 mL of ice cold 0.1 M $NaBH_4$ solution was added all at once with continuous stirring. Immediately after adding $NaBH_4$, solution turned pink indicating formation of nano gold seeds. Palladium electrode was then immersed into the solution containing nano gold seeds for 2 hrs in order to allow the physisorption of gold nanoparticle on the palladium surface. After 2 hrs, electrode was taken out and the surface of the electrode was washed with double distilled water [176]. The surface morphology of the bare and AuNP/Pd sensor was studied by FE-SEM and is presented in **Fig. 2.1.** The physisorption of nano gold onto the Pd surface was clearly observed in the AuNP/Pd.
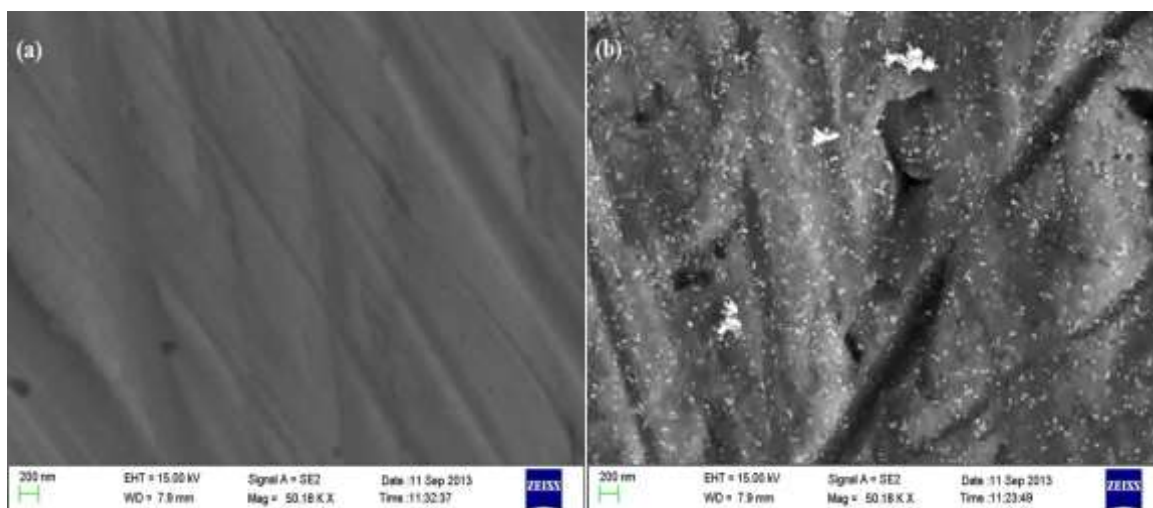
Fig. 2.1: Typical FE-SEM images observed for (a) bare and (b) AuNP/Pd surfaces.

2.2.4 Analytical procedure

Stock solution of dopamine (2 mM) was prepared by dissolving the required amount in double distilled water. The solutions for voltammetric procedures were prepared by adding required volume of the stock solution into a glass cell containing 2 mL of phosphate buffer and final volume was made to 4 mL using double distilled water. The blank was estimated by using a solution of 2 mL double distilled water and equal volume of phosphate buffer solution ($\mu = 1$ M). Voltammograms were then recorded under optimized parameters. Optimized square wave voltammetric parameters used were: initial (E): 0 mV, final (E): 600 mV, square wave amplitude (E_{sw}): 25 mV, potential step (E): 4 mV, square wave frequency (f): 15 Hz. All the potentials reported were with respect to Ag/AgCl electrode at an ambient temperature of 25 $\pm$ 2°C.

2.2.5 Analysis of biological samples

The human plasma samples and urine samples from healthy persons, obtained with the consent of the person from the hospital of I.I.T. Roorkee were diluted 1:1 with buffer of pH 7.2 and analyzed by voltammetric procedure.

2.3 RESULTS AND DISCUSSION

2.3.1 Comparison of bare and AuNP/Pd sensor

The effective surface area of bare and AuNP/Pd sensors was calculated by recording cyclic voltammograms of 2 mM $K_3[Fe(CN)_6]$ in presence of 0.1 M KCl at different scan rates. A well-defined redox couple of Fe^{3+}/Fe^{2+} were observed at both the sensors. A comparison of cyclic voltammograms corresponding to Fe^{3+}/Fe^{2+} system at bare and AuNP/Pd is presented in **Fig. 2.2.** The surface area is calculated by using the relation:

$$i_p = 2.69 \times 10^5 \, An^{3/2}D^{1/2}C_o v^{1/2}$$

where, i_p refers to the peak current in Ampere and A is the surface area of electrode in cm^2. For Fe^{3+}/Fe^{2+}, n = 1, diffusion coefficient D = 7.6×10^{-6} $cm^2 s^{-1}$, C_o is the concentration of $K_3[Fe(CN)_6]$ in mole cm^{-3} and v is the scan rate in Vs^{-1}. The slope of i_p versus $v^{1/2}$ plot was then used to calculate the surface area of bare and AuNP/Pd sensors, and was found to be 0.0808 cm^2 and 0.161 cm^2, respectively. Thus, it was concluded that the effective working area of AuNP/Pd sensor was ~2 times greater than bare sensor.
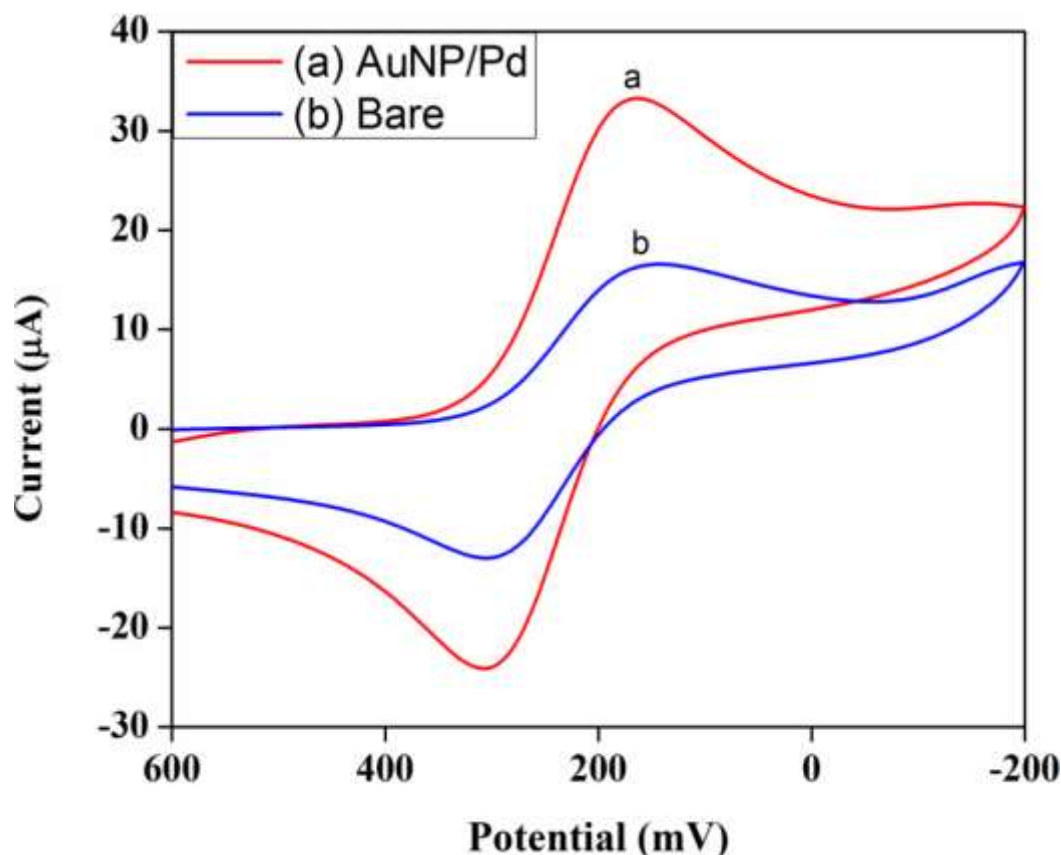
Fig. 2.2: A comparison of cyclic voltammograms of 1mM K$_3$[Fe(CN)$_6$] observed in 0.1 M KCl at (a) AuNP/Pd and (b) bare sensor.

The square wave voltammograms were recorded for 200 µM of dopamine at bare and AuNP/Pd sensors as shown in **Fig. 2.3.** The voltammetric response clearly showed an increase in current by ~ 4.5 times at AuNP/Pd in comparison to the response at bare sensor. Hence, the AuNP/Pd sensor was employed for the detection of dopamine. The oxidation of dopamine at bare sensor shows a weak signal at 190 mV, whereas AuNP/Pd sensor exhibits oxidation peak at 162 mV with an increase in peak current. This substantial increase in peak current together with shifting of peak potential to less positive values clearly demonstrates that the AuNP/Pd sensor exhibits excellent electrocatalytic properties towards oxidation of DA. Hence, detailed electrochemical studies of DA were carried out using square wave voltammetry.

The modified sensor not only showed enhanced peak current and large surface area in comparison to the unmodified sensor, modification of the nano gold also eliminated the problem of fouling by virtue of which the sensor exhibited larger working range.
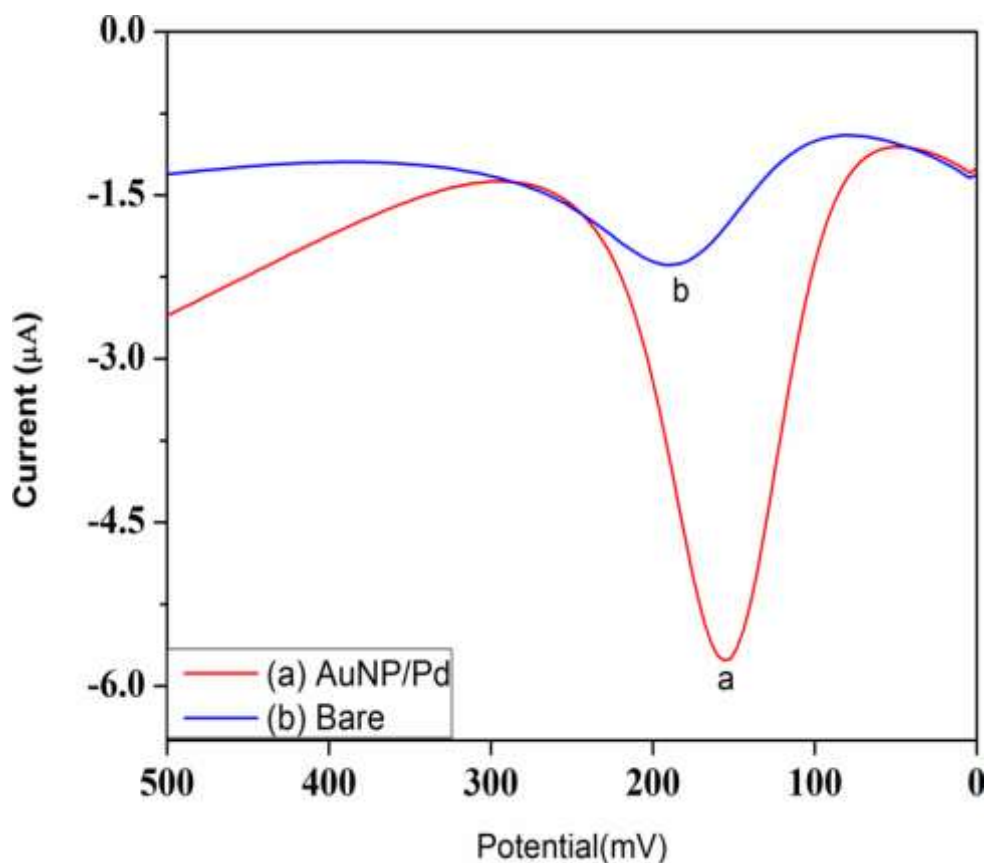
Fig. 2.3: Typical square wave voltammograms of 200 μM DA observed at (a) AuNP/Pd and (b) bare sensors at pH 7.2.

2.3.2 Electrochemical Impedance Spectroscopy (EIS)

EIS was carried out to investigate the impedance changes that occurred at electrode surface on modification. **Fig. 2.4** demonstrates the result of EIS at bare and AuNP/Pd sensors in presence of equal volumes (2 mL) of 10 mM $K_3[Fe(CN)_6]$ and 1M KCl. The data was approximated using Randle's circuit. According to the Randle's circuit, charge transfer resistance (R_{CT}) is parallel to double layer capacitance (C_{dl}) and this parallel combination results in a semicircular portion in Z_{img} versus Z_{real} plot. The diameter of this semicircle is equal to R_{CT}. From **Fig. 2.4**, it can be seen that the nano gold modification results in substantial decrease in R_{CT}. The value of R_{CT} obtained at bare sensor (4596 Ω) is much higher in comparison to 3095 Ω at AuNP/Pd sensor. This decrease in R_{CT} symbolizes that nano gold modification facilitates the redox process of $[Fe(CN)_6]^{3-}/ [Fe(CN)_6]^{4-}$ at the surface of AuNP/Pd sensor. From the observed results it can be concluded that the modification occurred successfully and had an influence on the electrochemical processes occurring on the surface of the modified sensor.
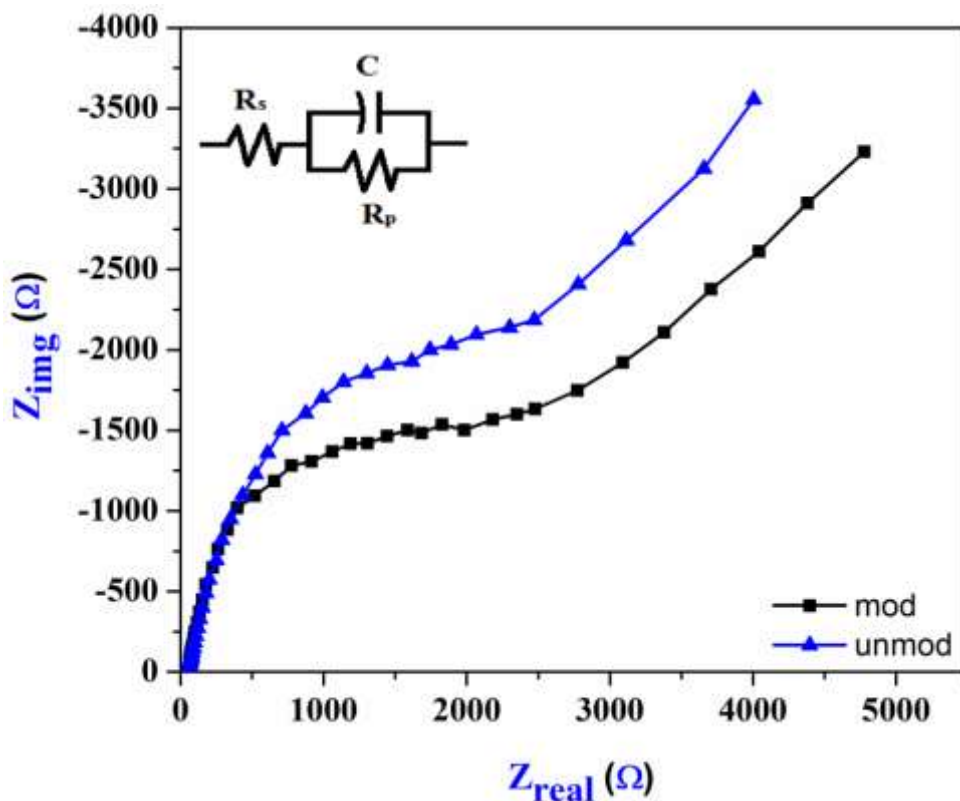
Fig. 2.4: EIS plots observed corresponding to bare and AuNP/Pd sensors.

2.3.3 Effect of square wave frequency

The effect of square wave frequency on peak current of DA was investigated in the frequency range 5-50 Hz. The peak current of DA increases with an increase in square wave frequency and was found to be linearly dependent on the square root of square wave frequency. Such a behavior indicates that the oxidation process of dopamine at the electrode surface is diffusion controlled [177]. The plot of i_p versus $f^{1/2}$ was found to be linear (**Fig 2.5 (a)**) and the dependence can be represented by the equation:

$$i_p = 1.2944\, f^{1/2} + 0.1789$$

having correlation coefficient of 0.9802. The diffusion controlled nature of the oxidation process was further confirmed using cyclic voltammetry. The effect of scan rate (v) on the peak current (i_p) of DA was evaluated in the range of 5-250 mV s^{-1}. A plot of log i_p versus log v was a straight line (**Fig 2.5 (b)**), which can be expressed by the relation:

$$\log (i_p) = 0.3036 \log (v) - 0.3151$$

having correlation coefficient of 0.9739. A slope < 0.50 for log i_p versus log v plot showed that oxidation of DA at AuNP/Pd occurred via diffusion controlled process [178]. Moreover,

31

electrode passivation was not observed during the whole experiment which also demonstrated the fact that the oxidation of DA occurred by virtue of diffusion controlled process.
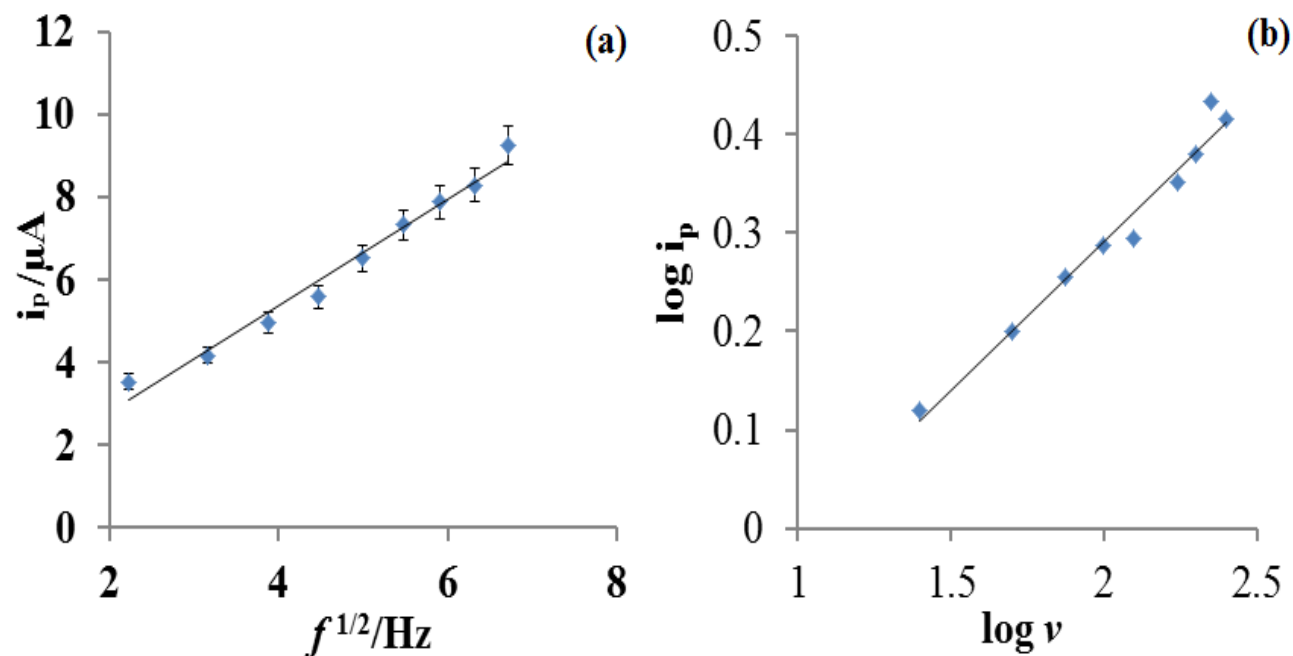
Fig. 2.5: Dependence of (a) i_p versus square root of square wave frequency ($f^{1/2}$) and (b) log (i_p) versus log (v) for DA.

2.3.4 Effect of pH

The pH of the solution affects the peak potential significantly; hence the effect of pH on the oxidation peak potential of DA was studied in the pH range 2.4–10.0 using square wave voltammetry. The peak potential varies linearly with pH and is shifted to less positive potentials with increase in pH as shown in **Fig. 2.6.** The dependence of the peak potential on pH can be expressed by the relation:

E_p (pH 2.4 - 10.0) = [-55.87 pH + 572.7] vs. Ag/AgCl (R^2 = 0.9981)

The slope of ~56 mV/pH suggests that equal number of protons and electrons are involved in the oxidation process of DA [179]. This conclusion also supported the previously reported mechanism of DA oxidation which involved a two electron two proton change [180].
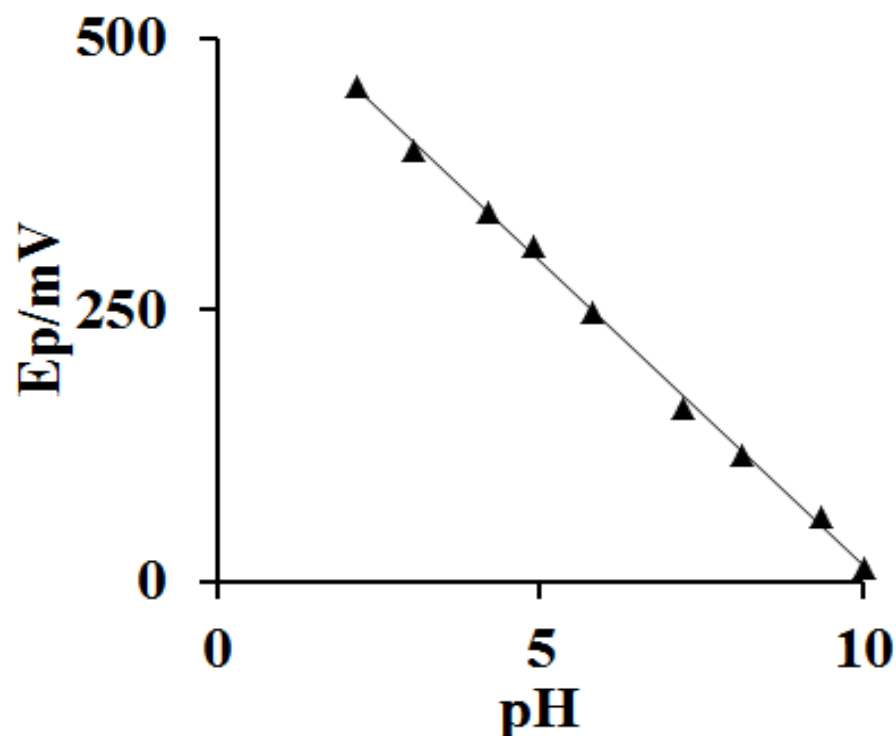
Fig. 2.6: Observed effect of pH on E$_p$ of DA.

2.3.5 Effect of concentration

To study the effect of concentration of DA on the peak current, square wave voltammograms were recorded for various concentrations (**Fig. 2.7A**). At each concentration at least three repetitive measurements were taken and the values were plotted as error bars in the **Fig. 2.7B**. It was observed that the peak current increases with an increase in DA concentration and a linear relationship between peak current and concentration can be demonstrated using following linear regression equation:

i_p (μA) = 0.015 C (μM) + 0.5181

The correlation coefficient for the equation was 0.987 and the sensitivity of the proposed method was found to be 0.015 μA μM^{-1}. The detection limit is calculated according to the formula 3σ/b, where σ is the standard deviation of the blank and b is the slope of the calibration curve, and is found to be 0.08 μM (S/N = 3).
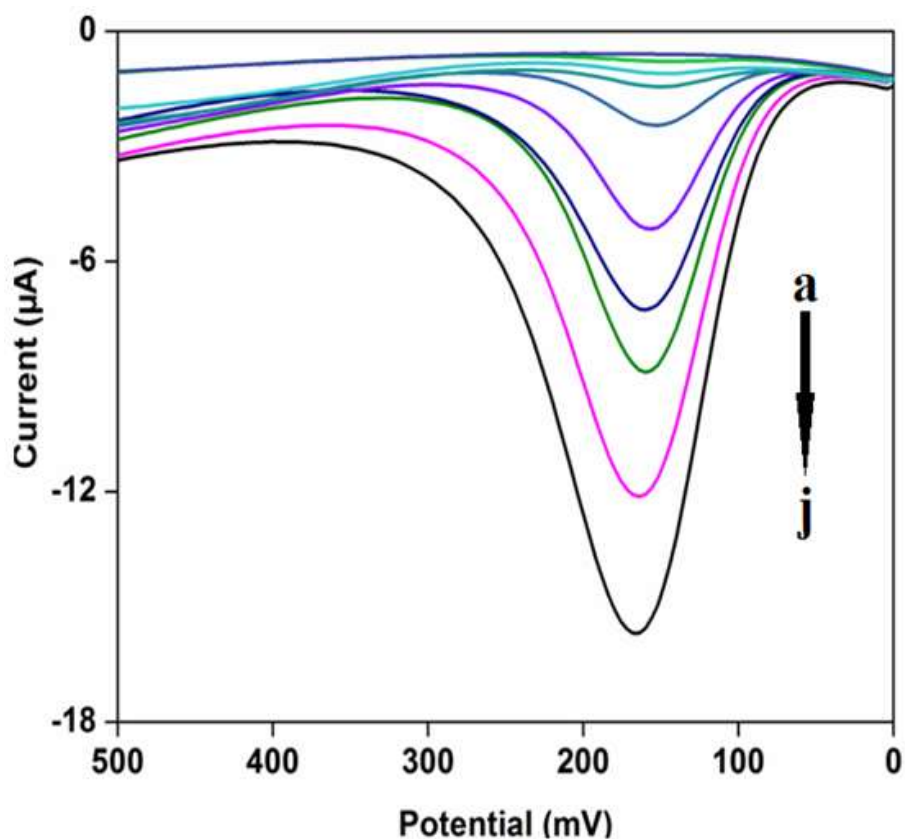
Fig. 2.7A: Square wave voltammograms of DA observed at different concentrations (a) = blank; (b) = 0.5; (c) = 5; (d) = 50; (e) = 100; (f) = 200; (g) = 400; (h) = 600; (i) = 800; and (j) 1000 μM.
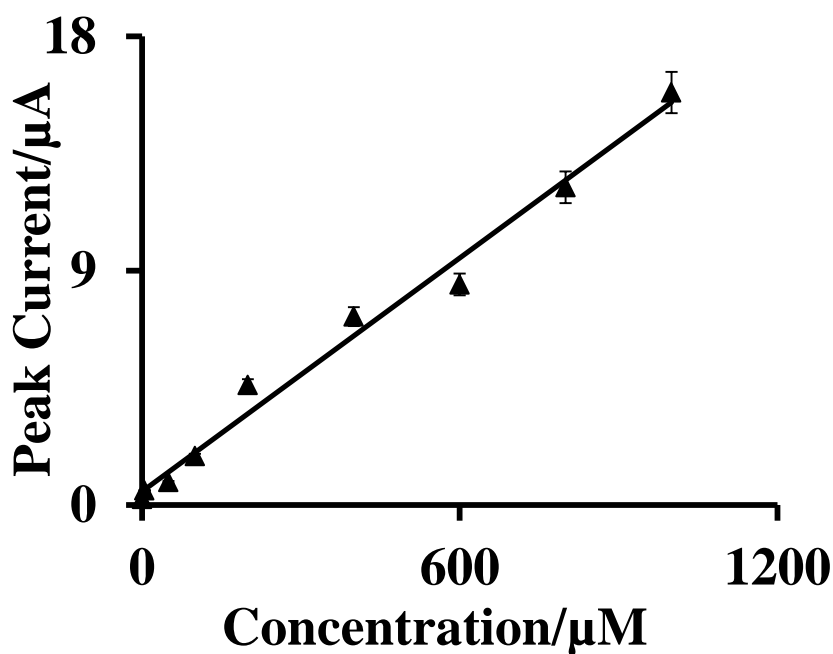
Fig. 2.7B: Calibration curve of peak current versus DA concentration observed at AuNP/Pd sensor.

2.3.6 Specificity

Specificity is an important characteristic of a sensor, which determines whether target species at a given concentration can be analyzed accurately by the proposed sensor or not. The specificity of the optimized procedure for the assay of DA was investigated by observing any interference from endogenous substances, which are usually present in complex matrices like urine, plasma and other biological fluids. A systematic study was carried out in order to check the interference of uric acid and serotonin (5-HT) using both the unmodified as well as nano gold modified Pd sensor **(Fig. 2.8)**. Under optimized experimental conditions, the effect of interferent concentration on the oxidation of 200 μM dopamine was evaluated. From **Fig. 2.9**, it can be seen that determination of DA using the AuNP/Pd sensor can be achieved even in presence of large concentration of interfering metabolites. Thus, the proposed sensor can be successfully employed for the determination of dopamine in biological fluids.
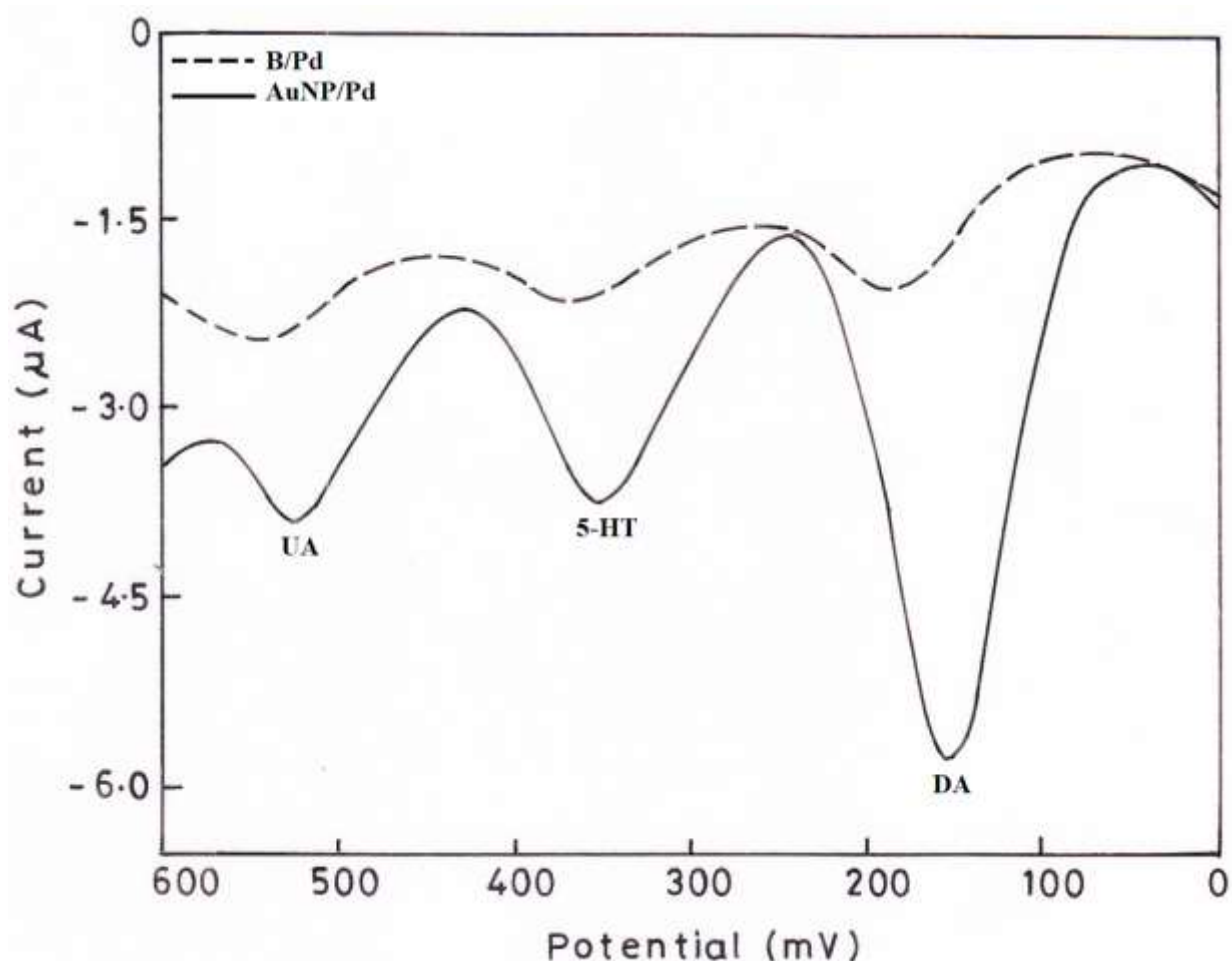
Fig. 2.8: Comparison of square wave voltammograms of DA in presence of UA and 5-HT as interferents on AuNP/Pd and Bare/Pd.
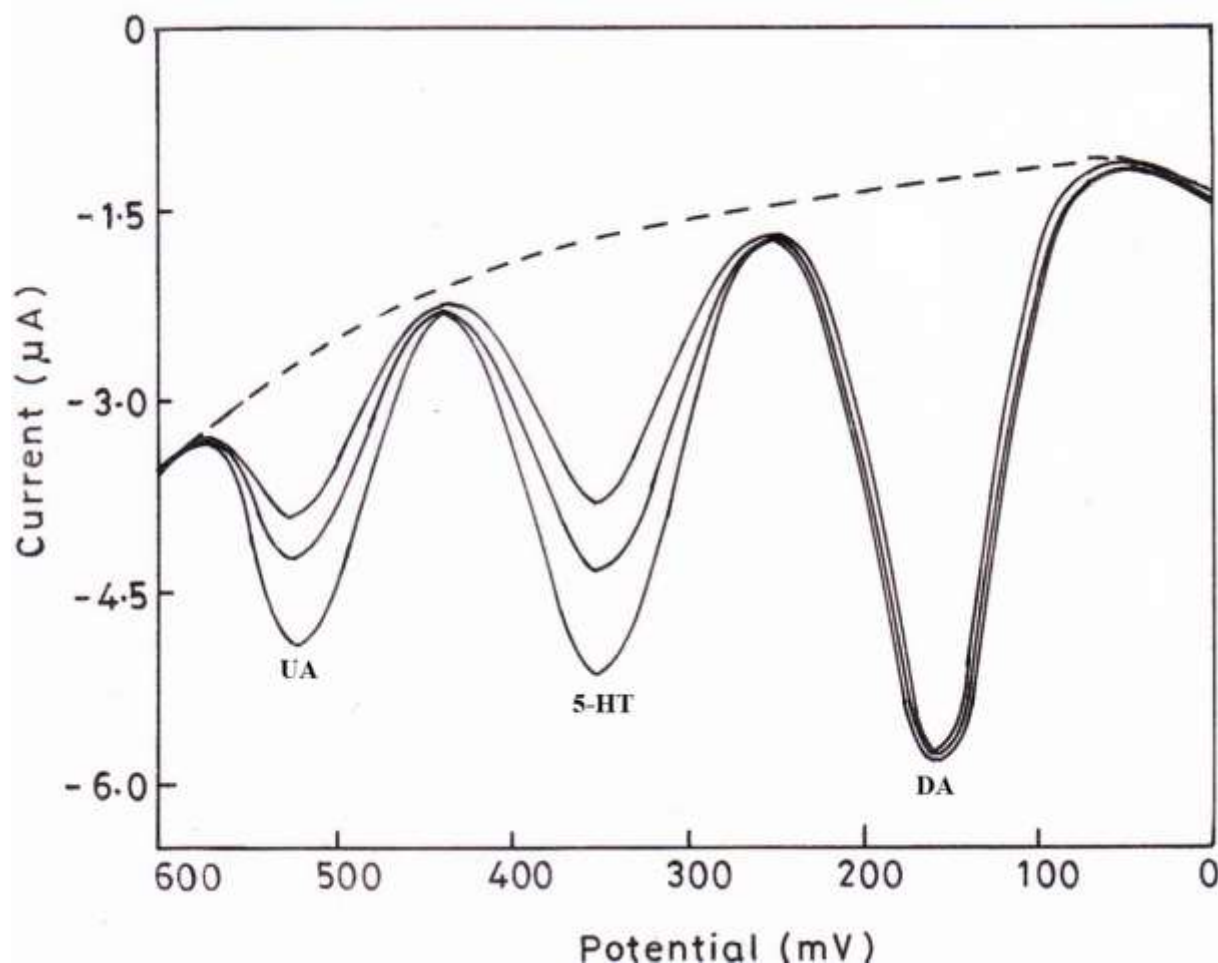
Fig. 2.9: Square wave voltammograms representing the interference study for DA in presence of increasing concentrations UA and 5-HT on AuNP/Pd.

2.3.7 Stability and reproducibility of the sensor

To evaluate the long-term stability of the AuNP/Pd sensor, square wave voltammograms were recorded for 200 µM dopamine over a period of 15 days. The modified sensor was stored in the air at room temperature and was daily used just after rinsing it with double distilled water. Only a minimal deviation in i_p was observed with a relative standard deviation (RSD) of about 3.84%. This data reveals that AuNP/Pd sensor exhibits good stability.

The reproducibility of the sensor has also been investigated. To monitor the intraday reproducibility of the sensor, repetitive determinations of DA were carried out with 200 µM dopamine at pH 7.2. The results of six consecutive measurements showed a RSD of 1.86%, indicating thereby that the results were reproducible. Further, inter-day precision was investigated by recording the square wave voltammograms daily using the identical 200 µM dopamine at the modified sensor for seven days. The RSD corresponding to these current

36

measurements was found to be 2.57 %. Therefore, this can be inferred that the proposed sensor possesses acceptable stability and also showed appreciable reproducibility.

2.3.8 Analytical applications

2.3.8.1 Pharmaceutical formulations

In order to demonstrate the practical applicability of the present methodology, the analysis of pharmaceutical samples was successfully performed under the optimized experimental conditions. Different pharmaceutical samples containing DA, named Dopalim (Ancalima Lifesciences Limited), Dopaa (Aaa Pharmaceuticals Pvt. Ltd), Dopasys (Symperlife), Osdop (Oscar Remedies Pvt. Ltd) were purchased from the local market of Roorkee. The pharmaceutical samples were diluted with buffer to bring DA concentration in the linear working range. Concentration of dopamine in the various pharmaceutical preparations was then ascertained using the AuNP/Pd sensor. The results are summarized in **Table 2.1** and clearly show that the content for all assay falls within the labeled amount, indicating the applicability of the proposed sensor towards detection of dopamine in pharmaceutical formulations.

Table 2.1: Determination of dopamine in pharmaceutical formulations using AuNP/Pd sensor.

Sample	Stated content (mg)	Determined content[a] (mg)	Error (%)
Dopaa	200	202.15	1.07
Dopalim	200	196.72	-1.64
Dopasys	200	197.26	-1.37
Osdop	50	48.37	-3.2

[a]The R.S.D. value for determination was less than 2.57% for n = 3.

2.3.8.2 Recovery test

In order to demonstrate the accuracy of the present methodology, attempts were made to obtain the blood and urine samples from the patients undergoing treatment with dopamine. However, due to the major use of this compound as a lifesaving drug, no urine or plasma samples could be obtained in spite of our best efforts. An attempt to determine DA in plasma

sample of normal person was then made, however, no peak corresponding to DA was observed in 1:1 buffer diluted samples as the concentration of DA in plasma of normal person is reported in the range 10^{-10} to 10^{-12} M [181]. A typical voltammogram of the plasma sample is shown in **Fig. 2.10**. In the potential range 0 to 600 mV, no peak was observed in the plasma samples indicating thereby that the common metabolites present in plasma did not oxidize in this potential range and hence did not interfere in the DA determination at AuNP/Pd sensor. Therefore, recovery experiments were carried out by the standard addition method in plasma. Recovery experiments following same methodology were also carried out in urine samples of healthy volunteers. The results observed are listed in **Table 2.2**. The recovery of dopamine was found to be in the range from 99.11 % to 101.42 % in the case of human blood plasma and from 97.93 % to 102.15 % in the case of urine samples. Thus, it is quite evident that the recovery data lie in the acceptable range and the sensor can be used for such determinations.
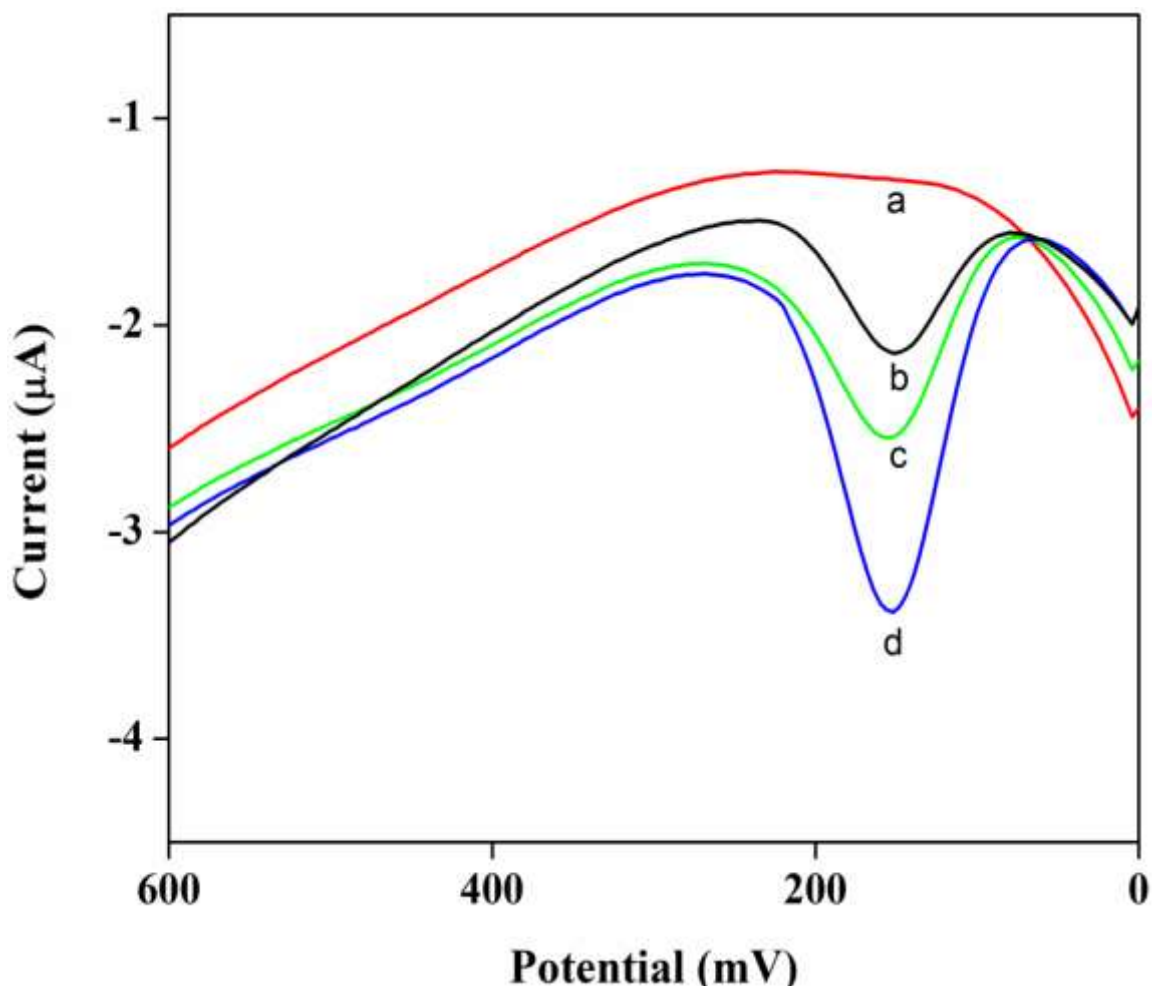
Fig. 2.10: Square wave voltammograms observed for the recovery of DA in plasma samples. Curve (a) is the plasma sample after 1:1 dilution with buffer and (b) to (d) after addition of DA.

Table 2.2: Observed recovery of DA in human plasma and urine samples at AuNP/Pd sensor.

Sample		Plasma		Urine	
	Added (µM)	Found (µM)[a]	Recovery (%)	Found (µM)[a]	Recovery (%)
Sample 1	40	40.17	100.42	40.28	100.7
	60	60.82	101.36	60.55	100.9
	80	81.36	101.7	79.86	99.82
Sample 2	40	40.32	100.8	39.34	98.35
	60	59.47	99.11	58.76	97.93
	80	80.97	101.21	81.72	102.15

[a]The R.S.D. value for the determination was less than 2.32% and 2.83% for plasma and urine respectively for n = 3.

Table 2.3: Comparison of detection limit of DA reported during recent years at different electrodes

Electrode	Linear range (µM)	LOD (nM)	Reference
CPE/GNS	2.0-1000	85	[182]
CeO$_2$/Au/GCE	10-500	56	[183]
ZnO/CPE	0.2-1300	80	[184]
TiO$_2$-GR/4-ABSA/GCE	1–400	100	[185]
PEDOT/PDA/Pt	1.5-50	650	[186]
PyC	17-270	1400	[187]
Graphene/AuNP/GCE	5-1000	1860	[188]
AuNP/Pd	0.5-1000	80	This work

CPE/GNS- carbon paste electrode/graphene nanosheets, CeO$_2$/Au/GCE- cerium oxide/gold/glassy carbon electrode, TiO$_2$-GR/4-ABSA/GCE- Titanium oxide/graphene/4-aminobenzenesulfonic acid, ZnO/CPE- zinc oxide/carbon paste electrode, PEDOT/PDA/Pt- poly(3,4-ethylenedioxythiophene)/polydopamine/platinum, PyC- pyrolytic carbon, Graphene/AuNP/GCE- Graphene/goldnanoparticle/ glassy carbon electrode.

2.4   CONCLUSIONS

The purpose of the present investigation was to develop a simple and robust sensor for the easy and rapid determination of DA using a biocompatible electrode. The present studies clearly demonstrate that AuNP/Pd sensor gives a better response in comparison to the bare palladium. The AuNP/Pd sensor exhibits catalytic activity towards the oxidation of DA, which results in an increased current response accompanied with a shift of the oxidation potential to less positive values. The AuNP/Pd sensor showed a stable and reproducible response. The proposed sensor was employed for the determination of dopamine content in various pharmaceutical formulations and was found to be satisfactory as the amount determined matched with their labeled quantity. Though, the detection limit of DA at AuNP/Pd was 80 nM and higher than the concentration of DA in human serum sample, however, the sensor can be effectively used in the cases where DA levels significantly increased. Also, the detection limit of the AuNP/Pd sensor was lower or comparable than sensor reported during last few years as shown in **Table 2.3**. The application of the developed protocol for recovery of DA in human urine and plasma samples has also been demonstrated. The results thus obtained, supports the use of AuNP/Pd sensor for sensing DA in biological samples.

CHAPTER 3

Carbon nanotube embedded polymer modified sensor for the determination of sulfacetamide
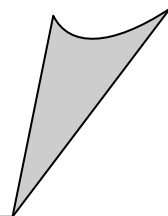
3.1 INTRODUCTION

Sulfonamides, commonly known as sulfa drugs, are benzenoid amino compounds derived from the parent molecule sulfanilic acid that acts as bacteriostatics by inhibiting the formation of dihydrofolic acid, which is essential for the development of bacterial cells [189]. Sulfonamides are most widely prescribed antimicrobial agents to cure human and veterinary infections due to their low cost and capability for remedy of various bacterial infections [190].

Sulfacetamide (SFA, **Structure I**), an important member of sulfonamide group is a synthetic antibacterial agent, employed for the treatment of numerous dermatological aberrations [152]. SFA is a highly potent drug and its sodium salt is effective in curing of conjunctivitis [191], pityriasis versicolor [192] and acne [193]. The combination of sodium sulfacetamide with sulfur has been found to provide adjunctive effect for the treatment of rosacea armamentarium due to its dual uses as topical therapy and therapeutic cleansers [151]. It is suggested that SFA in combination with sulfathiazole may be used for healing of T-47D breast cancer cells [194]. In addition to its various uses as medicines, SFA has many side-effects including rashes on skin, fever, vasculitis, anaphylaxis, cutaneous drug reaction, fixed drug eruption and hypersensitivity reactions like erythema and Stevens-Johnson syndrome [152]. SFA has also been found to cause toxic epidermal necrolysis, which is a more severe form of Stevens-Johnson syndrome [195].

The extensive clinical applications and side-effects of SFA render it necessary to develop a highly sensitive, fast and reliable approach to determine SFA in pharmaceutical formulations. Owing to concerns over the analytical determination of SFA, several methods have been developed for the analysis of SFA employing various techniques. Jen et al. reported the use of high performance liquid chromatography (HPLC) method to determine several sulfonamides in highly complex swine waste water [196]. The Gas chromatography-mass spectrometric (GC-MS) method was utilized to analyze six sulfonamides in animal tissues [197]. Other kinds of detection such as spectrophotometric determination [198, 199], photochemically induced fluorescence [200], flow injection analysis with fluorimetric [201] or chemiluminescence detection [202] and FT-IR spectroscopy have also been employed [203]. Other separation techniques, e.g. capillary zone electrophoresis with amperometric [204] or spectrophotometric detection [205, 206], micellar electro kinetic capillary chromatography [207, 208] and gas chromatography with atomic-emission detector were also used [209]. Nevertheless, most of these techniques often suffer from several disadvantages regarding to the cost, complex sample preparation due to tedious extraction and separation steps, use of various

organic solvents and long analysis time, which make them practically unhelpful in routine analysis. However, electroanalytical methods have attracted much attention of researchers towards the monitoring of drugs and biomolecules, owing to their low cost, ease of instrumentation, high sensitivity and selectivity and possibility of analysis without complicated sample pretreatment [210]. In the last decade although, there are several reports available concerning the electrochemical properties of sulfonamides using different types of electrodes [211-216], but very few electroanalytical methods have been developed for the determination of SFA due to the problem associated with electrode surface fouling. Fogg et al. have determined SFA by cathodic stripping voltammetry using hanging mercury drop electrode [217], but this method is not much beneficial due to the environmental toxicity of mercury.

In the present chapter we explored the use of carbon nanotube (CNT) embedded conductive polymer composite coated surface for the anodic analysis of SFA and to the best of our knowledge such type of sensor has not been used till now. Carbon nanotubes possess exceptional mechanical, thermal and electrical properties with their very high aspect ratio (length to diameter ratio > 1000), hence they are considered as an ideal additives for the formation of conductive network within a polymer matrix [218, 219]. By now, several papers have reported certain aspects of mechanical enhancement of polymer system by the incorporation of CNT [220]. This composite has been found to exhibit unique properties due to the electronic interaction between two components; therefore many applications have been reported, such as capacitors, actuators, electrodes, schottky diodes and organic light emitting diodes [221]. Both nanotubes and conductive polymer possess conjugated π-electron system and interaction is likely to occur through π-π stacking [222, 223]. It is well reported that properties of CNT/polymer composite strongly depend on the extent of CNT dispersion in monomer solution, hence insufficient dispersion of CNT is established as a diminishing factor for the composite's physical properties. Poor dispersion of CNT is due to their strong agglomeration tendency which is caused by intermolecular Vander Waals interactions and entanglement between them [138]. Sonication is the most ubiquitous method as it is associated with cavitation forces which results in localized heating followed by separating nanotube from each other. However, intense mixing of CNT can induce breakage of CNT that drives to poor electrical properties in the nano composite. In most cases mild sonication conditions (low power, short time) in the presence of an appropriate solvent allows agglomerates to be separated from each other due to some degree of interaction between CNT and solvent and this results in disaggregation [224].

Poly 1,5-diaminonapthalene (p-DAN), which has received an increasing interest due to its unique electroconductive, electroactive and electrocatalytic properties [133], is selected in the present study for embedding CNT. The carbon nanotube/conductive p-DAN composite was prepared by electro-polymerization of monomer (DAN) in the presence of suspended nanotube (in ethanol) at the edge plane surface of pyrolytic graphite (EPPG).The composite film was found to exhibit effective catalytic response towards the electro-oxidation of SFA. The developed method is simple, sensitive, low cost and free from requirement of sample pretreatment and is successfully applied for the determination of SFA in pharmaceutical formulations. Moreover, the results obtained from electrochemical sensing of SFA in pharmaceuticals have been successfully validated using HPLC.
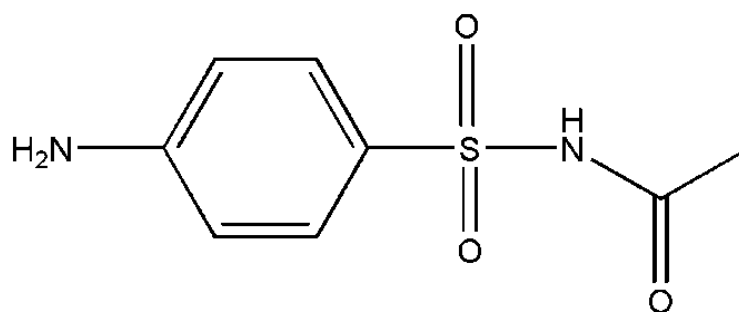
(I)

3.2 EXPERIMENTAL

3.2.1 Chemicals and reagents

Sulfacetamide was purchased from Sigma Aldrich, USA and used without further purification. Single walled carbon nanotube (SWCNT) of purity > 98% were obtained from Bucky, USA. Pyrolytic graphite pieces were obtained from Pfizer, USA as a gift. Perchloric acid, potassium chloride, potassium ferricyanide and 1,5-diaminonapthalene were purchased from Sigma Aldrich, USA. All the chemicals used to prepare phosphate buffers in the pH range 2.4-11.0 were obtained from E. Merck (India) Ltd., Mumbai. Phosphate buffers were prepared according to the method reported by Christian and Purdy [174]. The ionic strength was maintained at 1.00 M during all the study. All the reagents used were of analytical grade and double distilled water was used throughout the experiments.

3.2.2 Instrumentation

All electrochemical measurements were carried out with the help of computer controlled model (Epsilon-EC USB, ver. 2.00.71) electrochemical work station at room temperature. The electrochemical cell set-up included Ag/AgCl (saturated 1 M KCl, CH Instruments) as reference electrode, platinum wire as counter electrode and EPPG as working electrode. Field emission scanning electron microscopy (FE-SEM, JEOL-JSM 7400) instrument was used to study the surface morphology of bare and modified sensors. HPLC studies were performed using Shimadzu (LC-2010 HT) instrument equipped with C-18 reverse phase column. A mixture of acetonitrile and water (ratio of 20:80) was used at a flow rate of 1 mLmin^{-1} and the absorbance of eluent was monitored at 254 nm. The AC impedance of the modified sensor was measured using a potentiostat/galvanostat (PAR, model; versastat 3) linked to a personal computer.

3.2.3 Fabrication of SWCNT/p-DAN composite film covered pyrolytic graphite

The pyrolytic graphite sensor was prepared according to the previously reported method [225]. A piece of pyrolytic graphite was fixed into one end of the hollow glass tube with araldite adhesive so that its edge plan side is exposed. The glass tube was then kept undisturbed for about 24 h, at room temperature, so that adhesive becomes hard and holds the graphite piece tightly. The glass tube was rubbed on an emery paper till the surface of edge plane of graphite was exposed. The glass tube was then filled with mercury and the contact was made by means of copper wire.

The SWCNT/polymer composite film was grown using an electrochemical method in which SWCNT and polymer are simultaneously deposited on the edge plane surface of pyrolytic graphite sensor. First, purified SWCNT (2.5 mg) was dispersed in 5 mL ethanol under ultrasonic agitation for 20 min to achieve well dispersed suspension. 10 mM solution of monomer 1,5-DAN was prepared in 1 M HClO$_4$. Then, suspended SWCNT was mixed with monomer solution and solvent (ethanol) was evaporated by mild heating. The fabrication process used was as reported by Silva et al. [226]. Prior to the fabrication, the EPPG was first cleaned by rubbing it on an emery paper and dried under nitrogen flow. Then, electrochemical polymerization of 1,5-DAN monomer was carried out using cyclic voltammetry (CV); the potential range was varied from –0.1 V up to +1.0 V at a scan rate of 0.1V s^{-1}. The SWCNT/p-DAN composite film was produced by sweeping continuously for 50 cycles.

3.2.4 Experimental procedure

The stock solution of sulfacetamide (2 mM) was prepared by dissolving the required amount of the compound in double distilled water. In order to prepare desired concentration of SFA, required amount of this solution was added to the cell containing 2 mL of buffer and total volume was made to 4 mL using double distilled water. Blank experiment was run in presence of buffer and water. Solutions were purged with high purity nitrogen for 15 min to remove oxygen before recording each voltammogram. Phosphate buffer of pH 7.2 was used as supporting electrolyte during the experiments. The optimized operating conditions for square wave voltammetry (SWV) were set with initial potential at 500 mV, final potential 1200 mV, square wave frequency 15 Hz, square wave amplitude 25 mV and potential step 4 mV. The surface of the modified sensor was cleaned after each run using time base technique by applying a constant potential (-100 mV) for 60 s in buffer.

3.3 RESULTS AND DISCUSSION

3.3.1 Electrochemical synthesis of polymer nano composite thin film

Electrochemical polymerization of 1,5-DAN was carried out using cyclic voltammetry in the presence of SWCNT. **Fig. 3.1** shows successive cyclic voltammograms recorded during the growth of SWCNT/p-DAN composite film at the surface of EPPG. The initial scan to positive potentials gives an oxidation peak corresponding to the oxidation of monomer at 665 mV. One cathodic peak is obtained at 475 mV in the reverse sweep. The peak current of the oxidation peak decreases, whereas, the reduction peak increases with increasing potential cycles. In the second scan, two additional anodic peaks are obtained at 311 mV and 505 mV and one cathodic peak at 145 mV. These peaks were absent in the first cycle. The current of anodic and cathodic peaks increases with the time which reflects the growth of polymer film. In addition, simultaneously the incorporation of SWCNT in polymer matrix provides the nano structured composite frame work to enhance electrocatalytic property of the sensor [227].
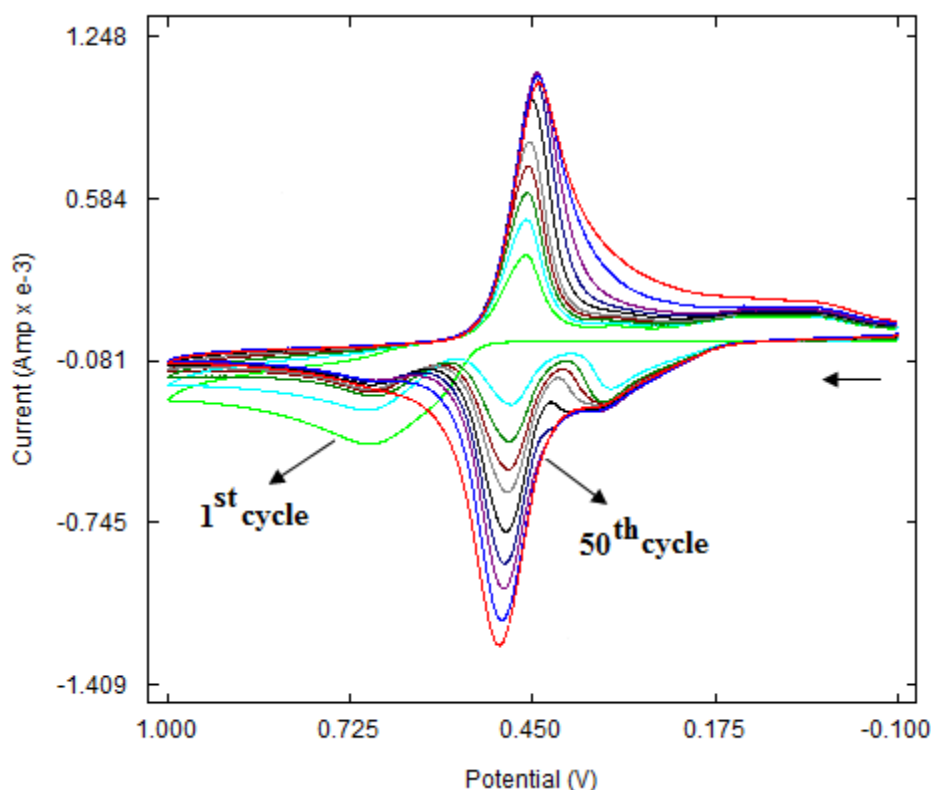
Fig. 3.1: A series of cyclic voltammograms recorded during fifty consecutive potential cycles between -0.1 to 1.0 V in 10 mM 1,5-diaminonaphthalene and 1 M HClO$_4$ at a scan rate 100 mV s^{-1} using EPPGE

3.3.2 Effect of number of cycles during the growth of thin film

In order to check the effect of number of polymerization cycles upon the deposition of polymer nano composite thin film on the EPPG surface, electropolymerization of 1,5-DAN in presence of nanotube was carried out by varying the number of cycles ranging from 20 to 50. It was observed that on increasing the number of cycles, more nanotube was found to embed into the polymeric structure. This was confirmed by the characterization of thin films with the help of FE-SEM analysis. Before characterization, SWCNT/p-DAN composite film was first rinsed with double distilled water and then with ethanol. **Fig. 3.2** compares the SEM images of bare EPPG (a), p-DAN modified EPPG (b) and SWCNT/p-DAN composite modified EPPG after 30th (c) and 50th (d) polymerization cycle. A clear surface can be seen at bare EPPG (a) and sponge like structure is observed in case of p-DAN. From the comparison of SEM micrographs of image (c) and image (d), it can be clearly seen that the nanotubes are more effectively embedded in polymer structure after 50th cycle in comparison to 30th cycle. It is indicated that the embedment of nanotube in polymer framework is an important issue for interfacial bonding

between polymer and nanotube, which provides a surface with high surface area and good conductivity.
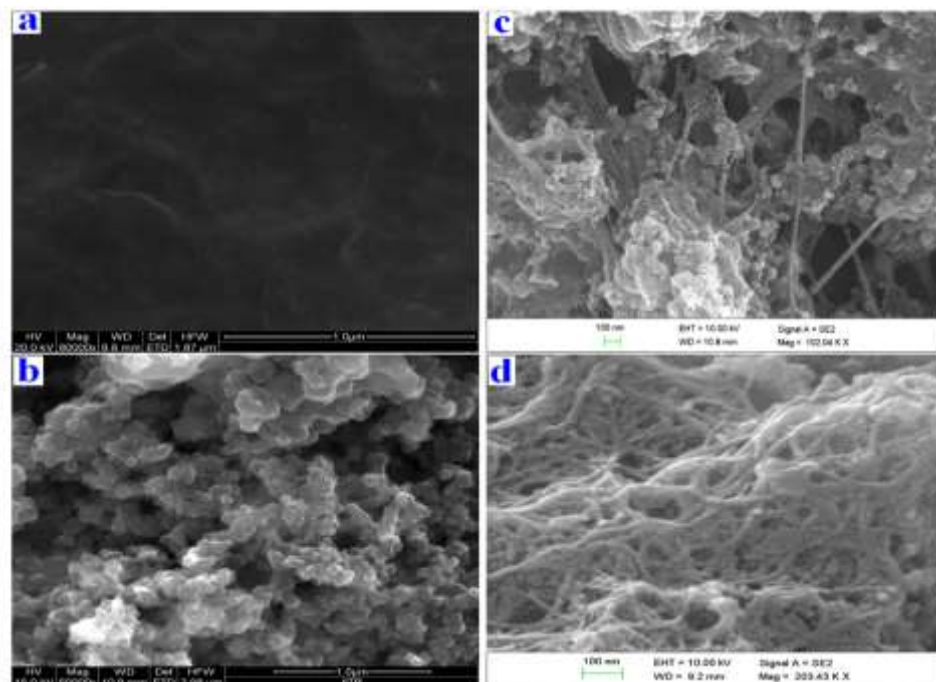
Fig. 3.2: FE-SEM images of (a) bare EPPG, (b) p-DAN/EPPG and SWCNT/p-DAN/EPPG after 30th (c) and 50th (d) polymerization cycle.

3.3.3 Electrochemical reactivity in terms of surface area

Impact of modification on electrode surface area was calculated by recording cyclic voltammograms of 1 mM $K_3Fe(CN)_6$ at different scan rates using 0.1 M KCl as supporting electrolyte at unmodified EPPG, p-DAN/EPPG and SWCNT/p-DAN modified EPPG. A redox couple was observed due to the Fe^{+3}/Fe^{+2} conversions at unmodified and modified pyrolytic graphite. It was noticed that in case of SWCNT/p-DAN modified EPPG, an increase in peak current for Fe^{+3}/Fe^{+2} system was dependent on number of cycles used during polymerization**.** **Fig. 3.3** clearly shows that the peak current for Fe^{+3}/Fe^{+2} system increases from 20 cycles to 50 cycles and then became constant at higher number of cycles. Thus, polymerization of 1,5-DAN at the pyrolytic graphite surface was carried out for 50 cycles and used in further studies.

At unmodified pyrolytic graphite surface high peak-to-peak separation (ΔE_p=0.165, peak a) and low value of peak current were observed for Fe^{3+}/Fe^{2+} of redox couple. In comparison to unmodified surface, polymer modified surface exhibited lower peak separations (ΔE_p=0.145, peak b) and higher peak current. The best results were obtained for SWCNT/p-DAN modified EPPG with lowest peak-to-peak separation (ΔE_p=0.120 V, peak d; 50th cycle)

and highest peak current showing the enhancement in the reversibility of Fe^{3+}/Fe^{2+} of redox couple on embedment of nanotube in polymer matrix, as depicted in **Fig. 3.3.** The peak current for a reversible process follows the relation:

$$i_p = 0.4463 \; (F^3/RT)^{1/2} An^{3/2} D^{1/2} C_0 v^{1/2}$$

where i_p refers to the peak current (Ampere), F is Faraday's constant (96,485 C mol^{-1}), R is the universal gas constant (8.314 J $mol^{-1}K^{-1}$), T is the absolute temperature (298 K), A is the surface area of electrode (cm^2), n = 1 for $K_3Fe(CN)_6$, D is diffusion coefficient (7.6 × 10^{-6} cm^2s^{-1}), v is scan rate (Vs^{-1}) and C_0 is the concentration of $K_3Fe(CN)_6$ in mol cm^{-3}. The surface area was calculated from the slopes of i_p versus $v^{1/2}$ plots and found as 0.084 cm^2, 0.297 cm^2 and 0.679 cm^2 for the unmodified, p-DAN modified EPPG and SWCNT/p-DAN modified EPPG, respectively, exhibiting significant improvement in surface area after modification with polymer and nanotube.
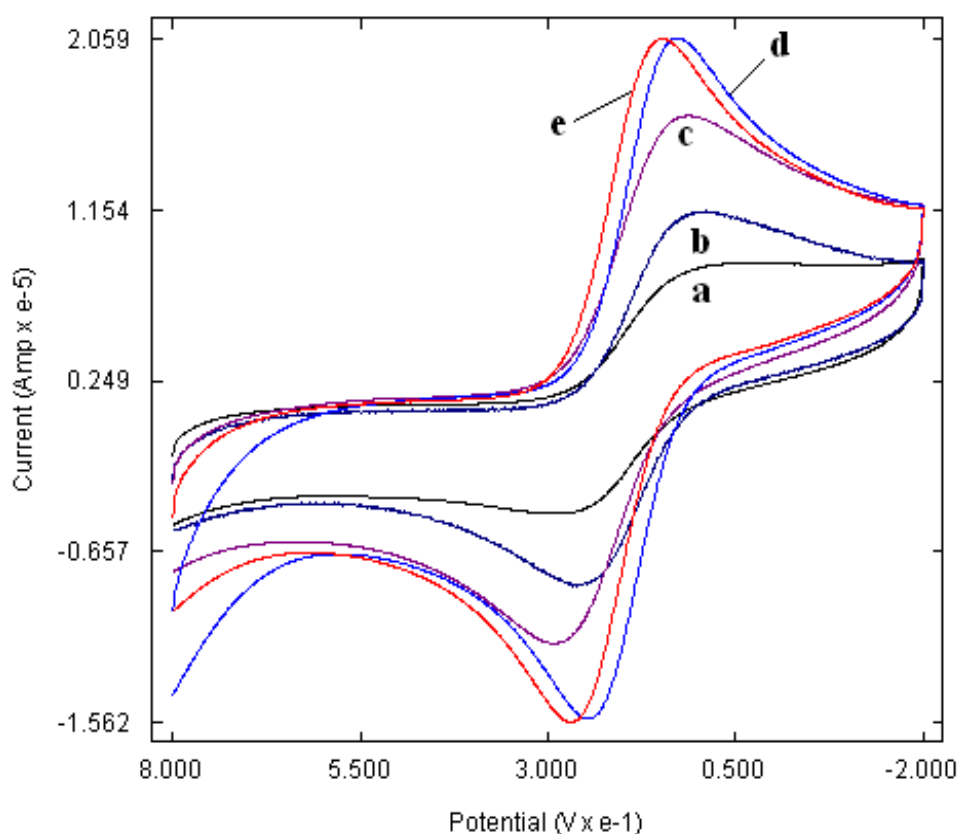
Fig. 3.3: Comparison of cyclic voltammograms of 1 mM K_3 [Fe(CN)$_6$] in 0.1 M KCl at (a) bare EPPG, (b) polymer modified EPPG and SWCNT/p-DAN/EPPG during 30th cycle (c), 50th cycle (d) and 70th cycle (e).

The feature of modified sensor was also probed using electrochemical impedance spectroscopy over the frequency range 0.1-10^5 Hz at 10 points per decade in 5 mM solution of $K_3Fe(CN)_6$. **Fig. 3.4** shows a Nyquist plot obtained for bare EPPG, p-DAN/EPPG and SWCNT/p-DAN/EPPG. The charge transfer resistances for bare EPPG, p-DAN/EPPG and SWCNT/p-DAN/EPPG were 3518 Ω, 854 Ω and 353 Ω, respectively. A semicircle showing the maximum resistance was obtained for unmodified EPPG. In the case of modified sensors, significant decrease in resistance was observed. The SWCNT/p-DAN/EPPG exhibited lowest resistance, which may be attributed to the unique characteristics of polymer and CNT, such as good electrical conductivity, high surface area and high chemical stability. This indicates the capability of polymer nano composite to facilitate the electron transfer at the surface of sensor [228].
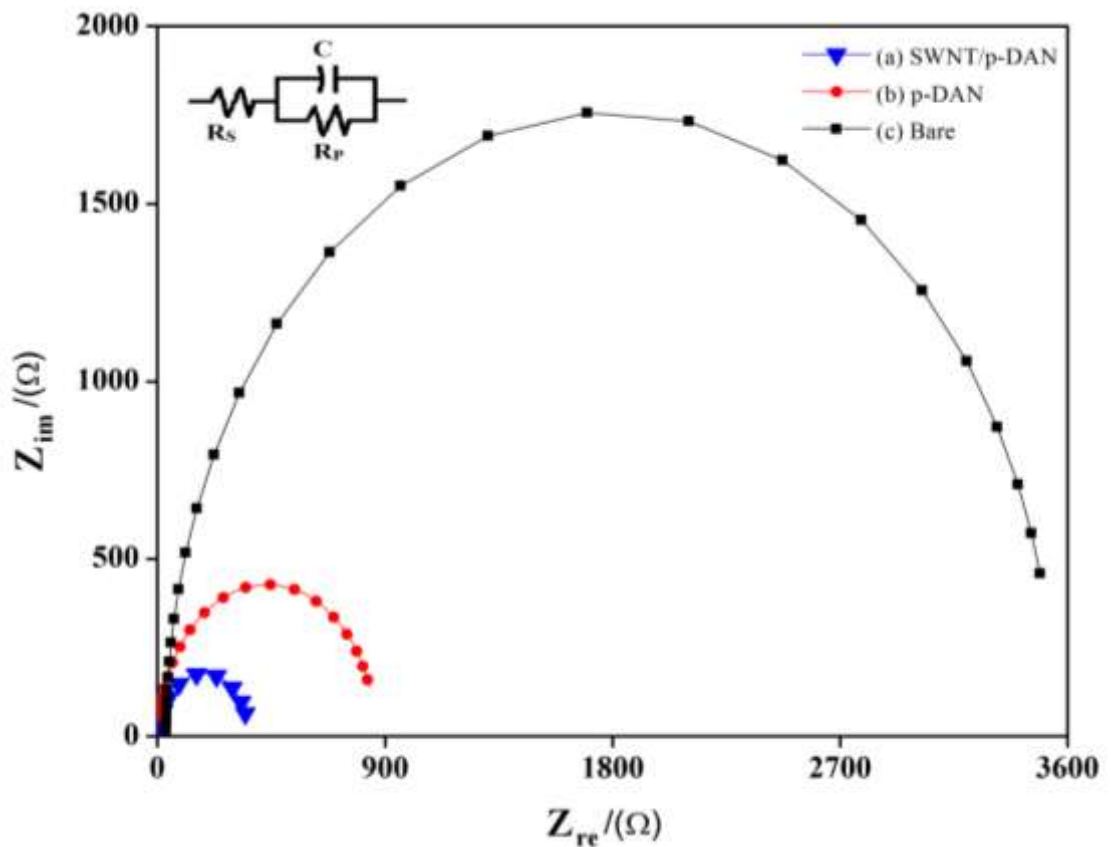
Fig. 3.4: The impedance changes of different modified pyrolytic graphite sensor. SWCNT/p-DAN modified pyrolytic graphite sensor (a), p-DAN modified pyrolytic graphite sensor (b) and bare pyrolytic graphite sensor (c). Electrolyte composition of EIS measurement: 5.0 mM $K_3Fe(CN)_6$/$K_4Fe(CN)_6$ and 100 mM KCl. Frequency range: 0.1–10^5 Hz.

3.3.4 Cyclic voltammetry

Cyclic voltammograms were recorded for 1 mM sulfacetamide at SWCNT/p-DAN modified EPPG at pH 7.2 using a sweep rate of 0.1 Vs^{-1} as shown in **Fig. 3.5**. A well-defined peak at (E_p) ~900 mV (I_a) was observed, when the sweep was initiated in the positive direction. In the reverse sweep two cathodic peaks II_a and II_b were noticed. These cathodic peaks formed a quasi-reversible couples with peaks $II_{a'}$ and $II_{b'}$, respectively, on the second sweep in the positive direction. Cyclic voltammograms were also recorded by initiating the sweep first in the negative direction, to check whether the peaks II_a and II_b are due to the reduction of the species formed in the oxidation reaction of peak I_a or are due to the independent reduction of sulfacetamide. The absence of reduction peaks clearly indicated that sulfacetamide does not undergo reduction and peaks II_a and II_b are related to the reduction of species generated in the peak I_a. The separation of peak potentials between $II_a/II_{a'}$ and $II_b/II_{b'}$ couples increased with increasing the sweep rate, indicating the quasi-reversible nature of these couples [229].

To find out the nature of the reaction, sweep rate studies were performed in the range 10 to 800 mV/s using SWCNT/p-DAN/EPPG sensor. The analyte peak current (i_p) was found to increase with increasing sweep rate and the plot of peak current versus scan rate showed straight line as shown in the inset of **Fig. 3.5.** The linear dependence of the peak current on scan rate can be represented by the relation:

$$i_p \ (\mu A) = 0.126 \ v \ (mVs^{-1}) + 7.029$$

having $R^2 = 0.987$. The linearity of above graph reveals that the oxidation reaction of SFA, occurring at the surface of modified EPPG, involves adsorption complications [229]. Further, to prove the electrode reaction mechanism, a graph was plotted between log i_p and log v. The equation arising from this plot is:

$$\log i_p = 0.970 \log v - 0.7363, \ (R^2 = 0.975)$$

The slope of this linear plot is larger than expected value 0.53 for purely diffusion controlled process confirming the electrode reaction as adsorption controlled [230]. A graph between peak current and square root of scan rate was also plotted and the equation can be represented as

$$i_p \ (\mu A) = 4.14 \ v^{1/2} + 18.32 \ (R^2 = 0.984)$$

It further confirms that the oxidation of sulfacetamide follows adsorption complications.
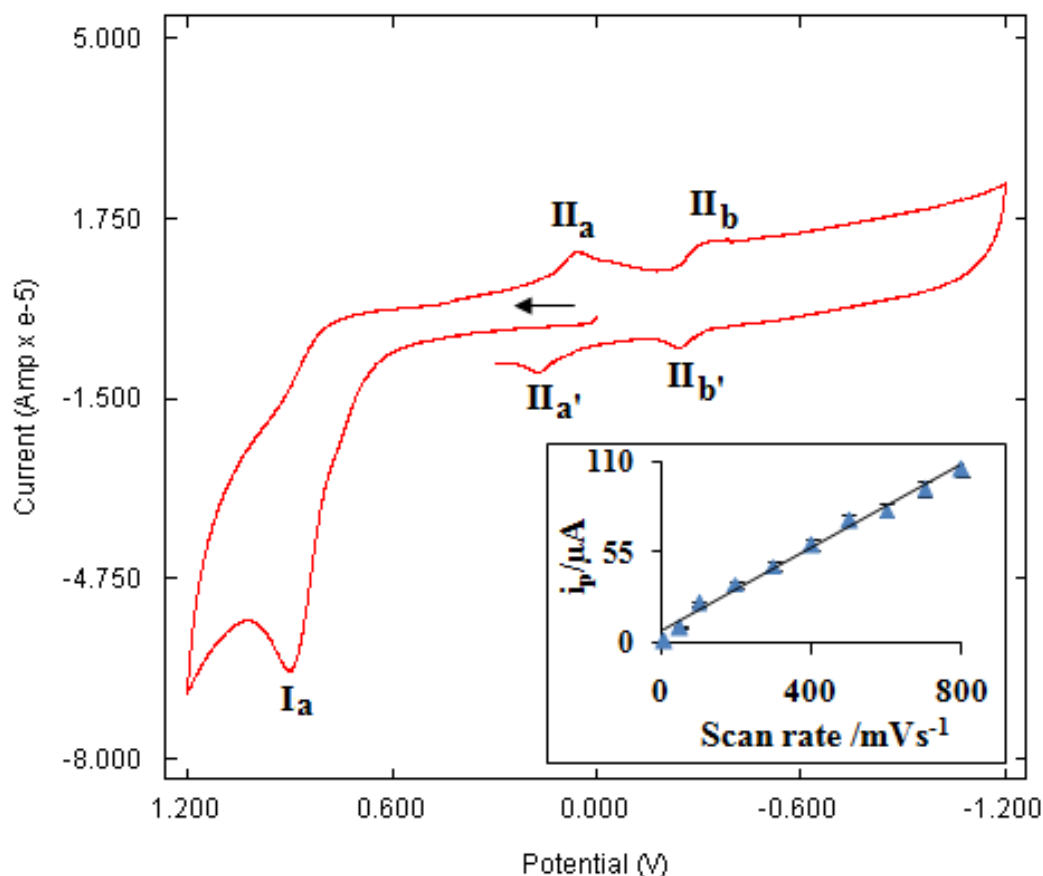
Fig. 3.5: Cyclic voltammogram observed for 1 mM SFA at scan rate 0.1 Vs^{-1} using SWCNT/p-DAN/EPPG; inset is showing a graph between i_p and v.

3.3.5 Square wave voltammetry

The electrocatalytic activity of the SWCNT/p-DAN modified pyrolytic graphite sensor was manifested by the comparison of the square-wave voltammograms of 0.5 mM SFA recorded at unmodified and modified EPPG. A well-defined sharp oxidation peak (peak b) with increased current response at peak potential ~850 mV was observed for SFA at SWCNT/p-DAN modified EPPG in comparison to the unmodified surface. Under similar conditions, a small peak (peak a) is obtained at E_p ~870 mV at unmodified EPPG **[Fig. 3.6]**. The remarkable increment of peak current together with shift in the E_p to a lower potential value clearly demonstrates that SWCNT/p-DAN modified EPPG acts as an efficient electron promoter to enhance the rate of the electrochemical reaction which can be assigned to the catalytic effects of SWCNT and p-DAN. As SWV is more sensitive analytical technique, hence, further voltammetric studies of SFA were carried out using this technique.
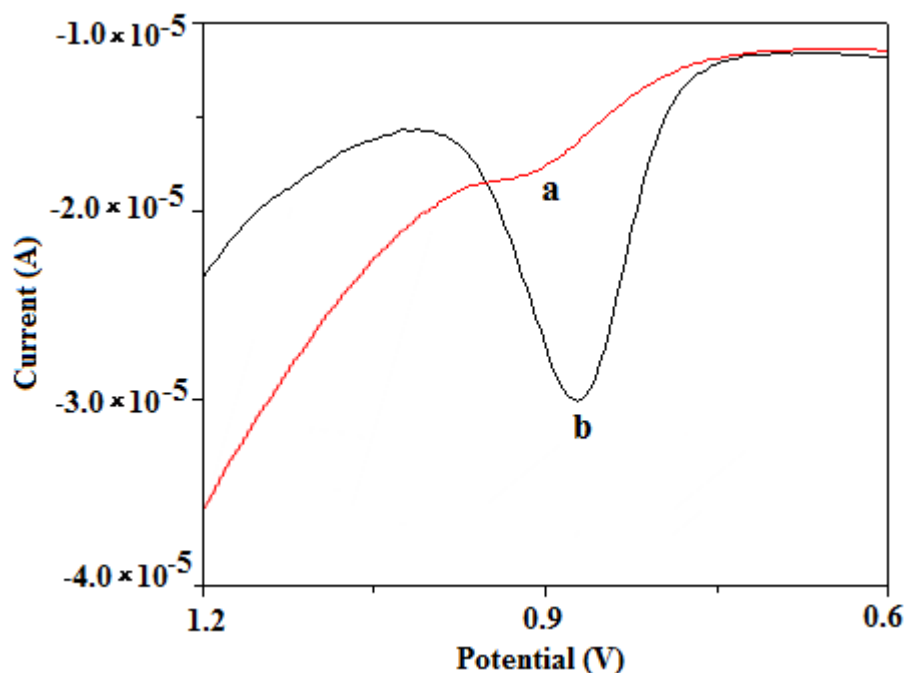
Fig. 3.6: Typical square wave voltammograms of 0.5 mM SFA observed at (a) unmodified and (b) SWCNT/p-DAN sensors at pH 7.2.

3.3.6 Effect of pH of supporting electrolyte

The pH of the supporting electrolyte plays an important role during any electrochemical reaction. In order to check the effect of pH on peak potential of SFA, pH of phosphate buffers was varied in the range 2.4–11.0 using unmodified and SWCNT/p-DAN modified EPPG. The peak potential of the SFA shifted towards less positive potentials with increase in pH (**Fig. 3.7**). The dependence of the peak potential on pH can be represented by the relations

E_p/mV (pH 2.4 - 11.0) = - 59.87 pH + 1302   at unmodified EPPG

E_p/mV (pH 2.4 - 11.0) = - 59.35 pH + 1261   at modified EPPG

with correlation coefficients of 0.994 and 0.997 for unmodified and modified EPPG, respectively. The identical value of the slope of these plots (0.059 V) indicates that equal number of protons and electrons are involved in the oxidation of sulfacetamide at unmodified and modified surfaces. SFA can undergo oxidation in two different ways: a single electron oxidation or a one electron process followed by subsequent electron transfer to form nitroso or azo products, respectively. Nitroso and azo compounds are found to be responsible for the formation of quasi reversible couples II_a-$II_{a'}$ and II_b-$II_{b'}$, respectively [231] and hence, it is concluded that oxidation of SFA occurs in 2e$^-$ oxidation at SWCNT/p-DAN modified EPPG.
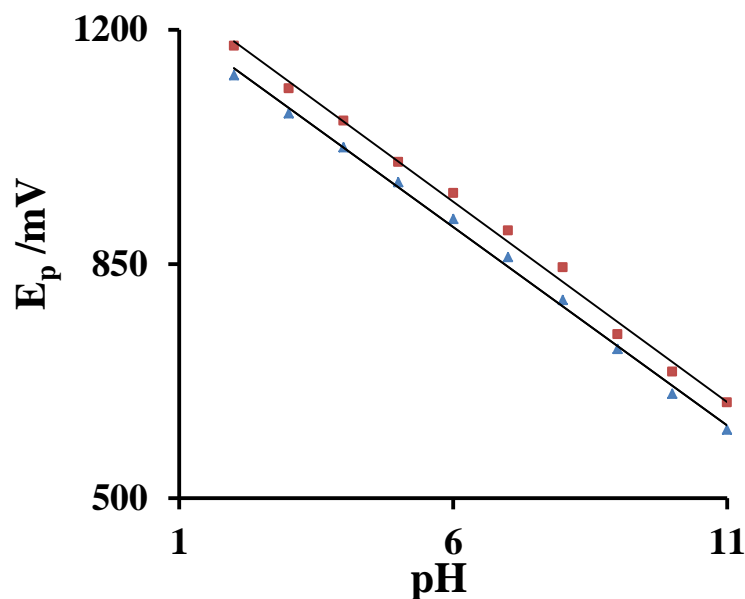
Fig. 3.7: Effect of pH of supporting electrolyte on peak potential of SFA at bare EPPG (■) and SWCNT/p-DAN/EPPG (▲).

3.3.7 Effect of square wave frequency

The dependence of peak current of 0.5 mM sulfacetamide on the square wave frequency (f) was studied in the range 5-35 Hz. The peak current was found to increase linearly with square wave frequency (**Fig. 3.8**) and the linear relation between i_p and f can be expressed by the following equations:

$i_p / \mu A = 0.053\,f + 0.975$ at unmodified EPPG

$i_p / \mu A = 0.420\,f + 7.751$ at modified EPPG

with R^2 of 0.996 and 0.988 for unmodified and SWCNT/p-DAN modified EPPG, respectively. These observations are in agreement with the results obtained from cyclic voltammetric analysis and confirm that electrochemical process involves adsorption complications.
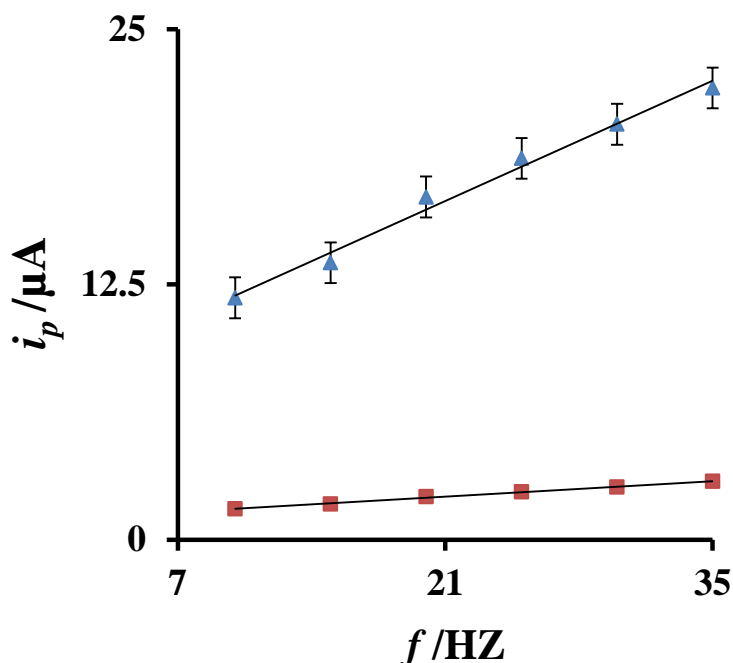
Fig. 3.8: Variation of peak current with square wave frequency at bare EPPG (■) and SWCNT/p-DAN/EPPG (▲).

3.3.8 Effect of concentration

The effect of concentration of SFA on peak current was studied at optimized parameters of SWV in the concentration range 0.005 to 1.5 mM using unmodified and SWCNT/p-DAN modified sensor (**Fig. 3.9A**). The peak current was found to increase with increase in concentration of SFA. The current values are reported as an average of at least three replicate determinations and are obtained by subtracting the background current. Linear calibration plots (i_p vs. concentration) for unmodified (0.3-1.5 mM) and modified EPPG (0.005-1.5 mM) are illustrated in **Fig. 3.9B**. The linear relation between i_p and concentration obeys the following regression equations:

$i_p/ (\mu A) = 3.4647\ C\ (mM) + 0.069$ at unmodified EPPG

$i_p/ (\mu A) = 23.977\ C\ (mM) + 3.353$ at modified EPPG

with R^2 of 0.992 and 0.993 for unmodified and modified EPPG, respectively, where C is the concentration of sulfacetamide. The sensitivity of SFA is found to be 3.4647 and 23.977 μA mM^{-1}, respectively. The detection limits were calculated using the formula 3σ/b, where σ is the standard deviation of blank solutions and b is the slope of calibration plots and were found to be 10.00 ± 0.02 and 0.11 ± 0.01 μM for unmodified and modified EPPG, respectively. The

calibration outputs obtained using unmodified and modified EPPG were validated using analytical parameters (**Table 3.1**) as per ICH guidelines [232, 233]. The results obtained using SWCNT/p-DAN modified EPPG indicate that the addition of SWCNT to polymer matrix enhances the electrochemical properties by promoting the charge transfer process. Low detection capability of SWCNT/p-DAN modified EPPG is found useful for the detection of SFA in pharmaceutical formulations up to low concentration.
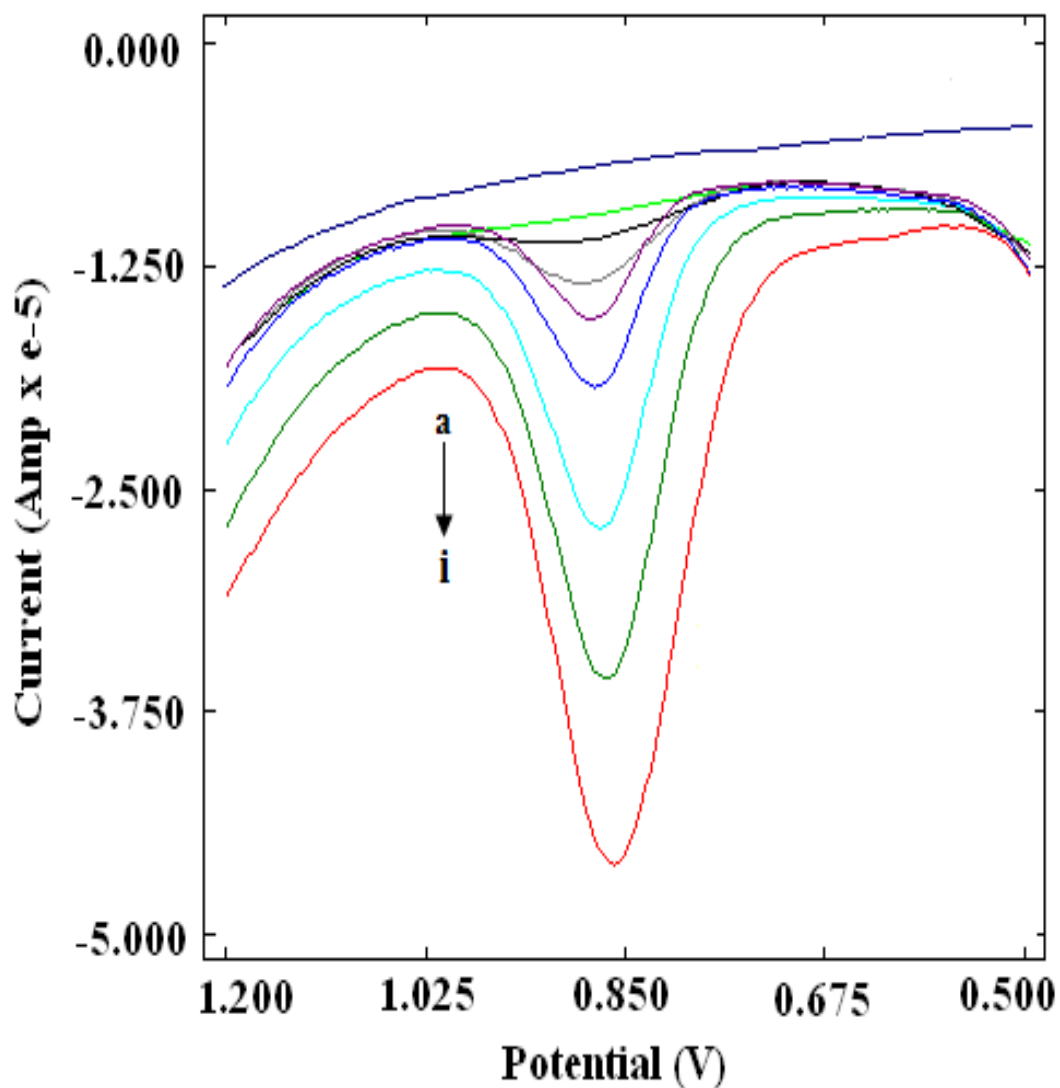
Fig. 3.9A: Square wave voltammograms observed for blank phosphate buffer (a) and increasing concentration of SFA at 0.005 mM (b), 0.05 mM (c), 0.1 mM (d), 0.3 mM (e), 0.5 mM (f), 0.75 mM (g), 1 mM (h) and 1.5 mM (i) using SWCNT/p-DAN/EPPG.
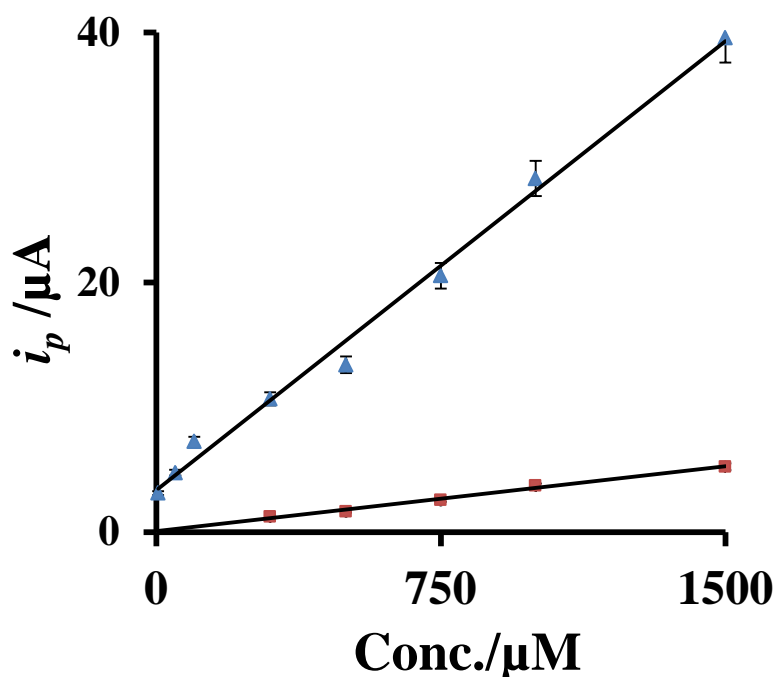
Fig. 3.9B: Calibration plot at bare EPPG (■) and SWCNT/p-DAN/EPPG (▲), with error bars of 5% value.

Table 3.1: The calibration characteristics for the determination of sulfacetamide using unmodified and modified EPPG.

Analytical Parameters	Unmodified	Modified
Concentration range (mM)	0.3 - 1.5	0.005 - 1.5
Correlation coefficient (R2)	0.992	0.993
Detection limit (μM)	0.993	0.11
Limit of quantification (μM)	33	0.37
RSD % of peak current	1.02%	1.97%
Bias % of peak current	0.48%	2.62%
Sensitivity (μA mM-1)	3.4647	23.977
Standard error of slope (α, 0.05)	± 0.343	± 2.64
Standard error of intercept (α, 0.05)	± 0.285	± 1.80
Precision of peak current	0.7	0.89
Accuracy in linearity (α, 0.1)	1.24 mM ± 0.0501	1.21 mM ± 0.0809

3.3.9 Stability and reproducibility

The long-term stability of the SWCNT/p-DAN modified EPPG was checked by measuring the peak current response of fixed concentration (0.1 mM) of SFA. Modified EPPG was stored for two weeks and response was checked again. There was no significant difference in current response even after two weeks. The peak current was slightly decreased with relative standard deviation (RSD) of 1.52%, which can be assigned to the excellent stability of the modified sensor. Furthermore, modified EPPG was stored for a period of one month and was found to exhibit good stability retaining ∼ 94% of its initial response to the oxidation of SFA.

To investigate the reproducibility of the modified electrode, repetitive determinations of SFA were carried out at fix concentration (0.1 mM). The intra-day precision of the method was evaluated by repeating six experiments in the same solution containing 0.1 mM of SFA using the modified EPPG. The RSD for oxidation peak was found to be 1.40%, indicating excellent intra-day reproducibility of the modified electrode. Inter-day precision was investigated by recording the peak current value of the modified electrode for eight consecutive days for the same concentration of SFA and the relative standard deviation was found to be 1.53% for oxidation of SFA, demonstrating the excellent reproducibility of modified EPPG.

3.3.10 Analytical utility

In order to evaluate the analytical applicability of the present methodology, the modified EPPG was applied for the determination of SFA in commercially available SFA containing eye drops viz. locula 20% and 30% (East India Pharmaceutical works ltd.) and albucid (Allergan India pvt. ltd.). Locula is the ophthalmic preparation of SFA which is the most prescribed eye drop for the treatment of common inflammatory disorders of eye. Prior to the determination of SFA in eye drops, the samples were dissolved in water and then diluted by required amount of the buffer solution of pH 7.2, so that the concentration of SFA was in the working range. Square wave voltammograms were recorded using SWCNT/p-DAN modified EPPG under exactly same conditions that were applied while recording the voltammogram during concentration study. Keeping dilution factor in consideration, the concentration of SFA was calculated using regression equation which was compared with the labeled amount printed on the eye drops. The results, as demonstrated in **Table 3.2** showed that the content of SFA in eye drops were within the claimed amount with error in the range 3.0 – 4.0%, revealing the good accuracy of proposed method.

3.3.11 Method validation with HPLC

To prove the validity of the developed method, the results obtained from pharmaceutical analysis of SFA, were compared with HPLC analysis. For this purpose different concentrations of SFA were analyzed using HPLC and a well-defined peak was obtained at R_t ~3.57 min in the standard solution of SFA (**Fig. 3.10**). A calibration curve was obtained by plotting the peak area of the analyte peaks against the analyte concentration. The resulting calibration plot was linear. Then the concentration of drug was determined in the pharmaceutical samples (eye drops). The samples were sufficiently diluted so that their concentration was in the working range of SFA. The HPLC chromatogram of SFA in pharmaceutical sample showed a peak at R_t ~3.57 min is due to SFA. However, no attempt was made to identify the rest of the peaks which are likely to be due to added components in the drug. In order to confirm that this peak is due to SFA, sample was then spiked with known concentration of standard solution of SFA. The chromatogram obtained for spiked sample indicates the increase in peak at R_t ~3.57 min, confirming that this peak corresponded to SFA. A comparison of the values, obtained by HPLC and the developed voltammetric method has been shown in **Table 3.2**, which indicates a good agreement in between the two methods with RSD values in the range 1.05 – 3.01 % for n = 5.

The values obtained for the determination of sulfacetamide in pharmaceutical tablets using electrochemical and HPLC methods were compared in terms of Student's t-test and F-test. It was found that in all samples the observed values of t and F were much smaller than their tabulated values and also the observed values of probability factor for t and F-test were lower than their significance levels. For example, the results obtained from the determination of sulfacetamide in pharmaceutical sample of Locula (3 mg) using electrochemical and HPLC methods for n = 3 measurements were compared by carrying out the Student's t-test and F-test. The calculated t and F values were 0.248 and 10.23, respectively which were lower than their tabulated values, showing that the results obtained by both the methods are not significantly different from each other. For t-test and F-test, the values of probability factors were 0.827 and 0.089, respectively, which were higher than the used significance level ($\alpha = 0.05$), confirming the high probability of acquiring these results.
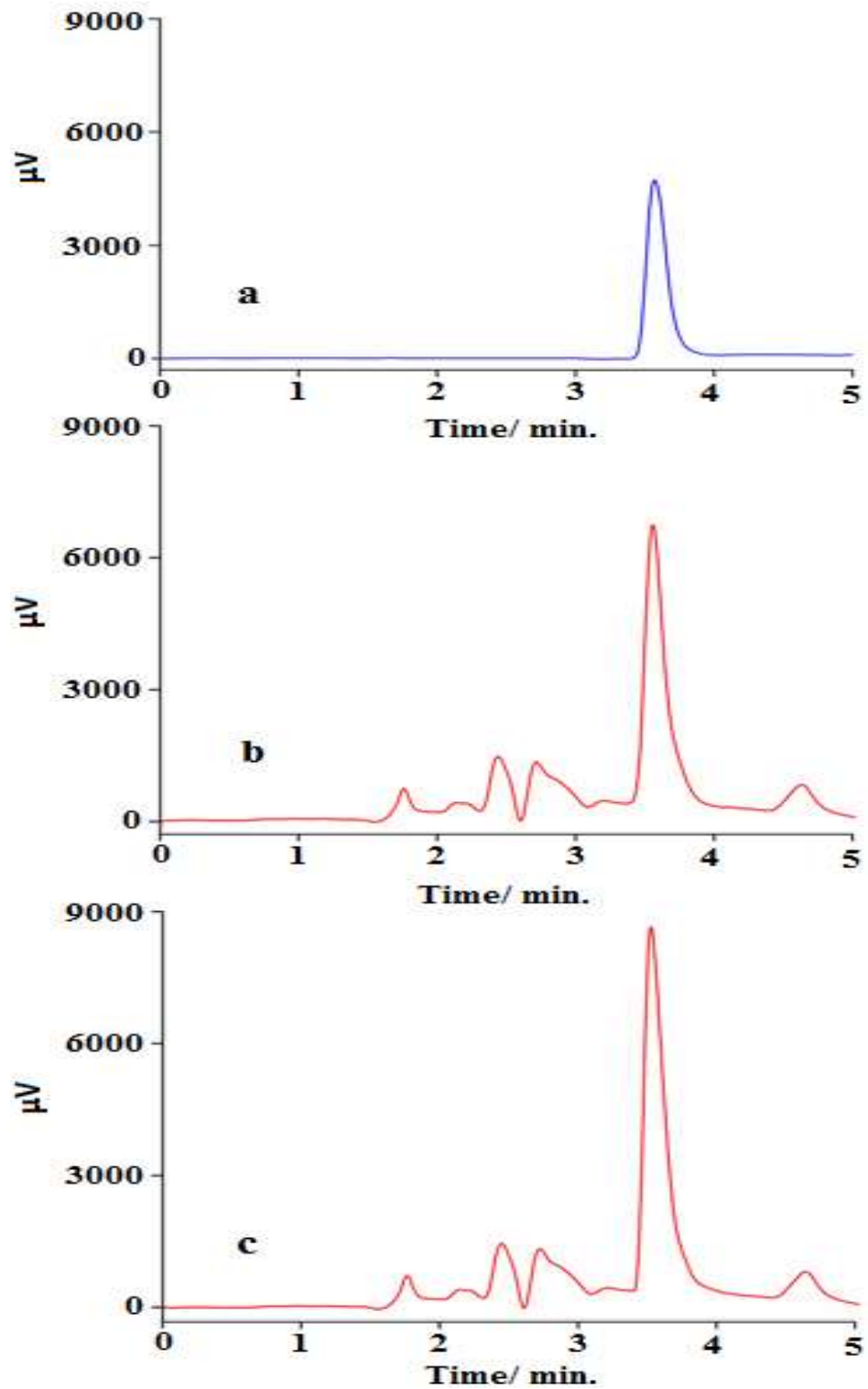
Fig. 3.10: HPLC chromatograms observed during analysis of SFA in (a) standard solution (b) pharmaceutical sample and (c) sample spiked with SFA standard solution.

Table 3.2: Determination of SFA in different pharmaceutical samples at SWCNT/p-DAN composite modified EPPG using SWV and validation of these voltammetric results with HPLC.

Sample	Stated content (/10ml)	Content determined by	
		SWV	HPLC
Locula	3 mg	2.91 mg (3.0%)	2.89 mg
Locula	2 mg	1.93 mg (3.5%)	1.94 mg
Albucid	2 mg	1.92 mg (4.0%)	1.90 mg

The RSD values were in the range 1.05-3.01% for n=5 determinations. The values in bracket denote the errors found during SWV observations.

3.4 CONCLUSIONS

In summary, this method provides a simple and quick tool for the direct anodic voltammetric determination of SFA using SWCNT/p-DAN modified EPPG. The conductivity of SWCNT/p-DAN modified EPPG was improved significantly in comparison to only p-DAN host owing to the excellent properties of carbon nanotubes [234], which were further reflected in the form of sensitivity of the sensor during voltammetric measurements. Modified EPPG exhibited ~ 8 times more sensitivity together with low detection capability in comparison to the unmodified EPPG. The high background current observed using conventional electrode causes a problem for electrochemical oxidation of sulfacetamide in achieving high sensitivity and reproducibility. The EPPG sensor with its excellent properties, modified with nanotube and polymer is observed to be a most suitable sensor for the detection of this drug. Low detection of SFA using proposed method indicates that this approach could be successfully applied to the trace analysis of SFA in pharmaceutical industries. The method was successfully employed for the determination of SFA in different pharmaceutical samples and the results obtained showed good accuracy with error in the range 3.0 – 4.0 %. The results were validated in term of HPLC showing a good agreement between the two methods. Furthermore, the SWCNT/p-DAN modified EPPG has long-term stability and good reproducibility with benefits of fast response time, ease of preparation and regeneration of the surface that makes the proposed platform very useful in many other sensing applications.

Chapter 4

Electrochemical determinaton of mometasone furoate, in micellar medium

4.1 INTRODUCTION

Mometasone furoate [MF, 9α, 21-dichloro-11β, 17α –dihydroxy-16α-methylpregna-1, 4-diene-3, 20-dione 17-(2-furoate) I] is a highly potent synthetic topical glucocorticosteroid which exhibits strong anti-inflammatory activities, rapid onset of action and low systematic bioavailability with a minimal potential for suppressing hypothalamic-pituitary-adrenocortical (HPA) axis [235, 236]. The clinical effectiveness of MF is related to its vasoconstrictive, anti-inflammatory, immunosuppressive and anti-proliferative effects [160]. Among various available corticosteroids, MF is well established topical nasal corticosteroid in children older than 2 years for chronic nasal obstruction and tonsils hypertrophy [237]. Several studies have reported that administration of MF-dry powder inhaler 200 μg improved lung function and reduce day time and night time asthma symptoms [238]. The clinical efficacy and safety of 0.1% MF ointment in the treatment of patients with moderate to severe plaque psoriasis symptoms such as erythema, indurations and scaling has also been reported [239]. It has been reported that overdose of MF absorbed into blood stream may cause a group of symptoms called Cushing's syndrome showing acne, depression, high blood pressure, muscle weakness and paranoia [161]. Therefore, various methods including high-performance liquid chromatography [240], liquid chromatography-mass spectrometry [241], supercritical fluid chromatography [242] and enzyme immunoassay [243] have been developed for the determination of MF in human body fluids. These methods require expensive instruments, time consuming complicated derivatization processes and extraction and purification of species prior to final analysis.

In this chapter, a simple and sensitive method has been developed for the detection of MF for the first time based on its voltammetric reduction. As surface active agents have been widely used in the electroanalysis for the electrocatalysis and protecting the surface from fouling [244, 245] and the use of surfactants in carbon paste or pyrolytic graphite has been found to enhance the performance in the determination of biomolecules [246, 247], an attempt is made to use surfactants to improve the sensitivity of determination. The importance of surfactants in simultaneous determination of various biomolecules has also been reported [248] and it is suggested that the interaction between surfactant aggregates and analytes in the solution phase is generally controlled by diffusion [249].

As surface modification by single walled carbon nanotube (SWCNT) has been found to enhance the electrochemical signal in a variety of compounds [250], a SWCNT modified pyrolytic graphite (MPG) in the presence of surface active agent is used in the present

investigations to get the synergetic effect of the SWCNT and surfactants. Although the use of SWCNT/MPG and CTAB/SWCNT/MPG for the determination of gluco-corticosteroids such as methylprednisolone [251] and betamethasone [252] in various pharmaceuticals formulation and human urine samples have been reported earlier and these sensors have been recognized to be very effective substrate to analyze the electrochemical activities of these drug. In CTAB/SWCNT/MPG sensor [252], the CTAB was casted at the surface of pyrolytic graphite by mixing with SWCNT. Still there is need to elaborate this kind of approach for further investigation of other molecules. In the present work CTAB was used by two methods, (i) casted with the SWCNT on pyrolytic graphite surface and (ii) used in the solution to monitor the effect of the method of CTAB used. As MF is clinically very important drug, determination of this drug is expected to be very helpful for further research studies. Therefore, we have tried to determine this corticosteroid using CTAB/SWCNT/MPG sensor and to the best of our concern no electro-analytical method for the investigation of MF has been reported till now. The effect of anionic, cationic and non-ionic surfactants on the reduction of MF has been studied in the present studies and the addition of CTAB has been found to catalyze the reduction of MF, whereas, SDS and Tween 60 show opposite effects. The MPG has further been used for the determination of MF in various pharmaceutical preparations and human urine samples. The product of reduction of MF was separated and site of reduction is confirmed by the characterization of the product using ^{1}H NMR and IR spectroscopic studies.

4.2 EXPERIMENTAL

4.2.1 Instrumentation

The voltammetric experiments were carried out using Bioanalytical system (BAS, West Lafayette, USA) CV-50W voltammetric analyzer. The voltammetric cell used was a single compartment glass cell equipped with MPG as a working, a platinum wire as counter and Ag/AgCl (3M NaCl) as the reference electrode (BAS Model MF-2052-5B) respectively. The pyrolytic graphite plates (6×1 cm^2) and pieces ($1 \times 0.2 \times 0.2$ cm^3) were obtained from Pfizer Inc. New York, USA. The pH of the phosphate buffers was measured using digital pH meter (model CP-901). The surface morphology of bare pyrolytic graphite (bare PG) and MPG was characterized by field emission scanning electron microscopy (FE-SEM) (JEOL JSM-7400) instrument.

Controlled potential electrolysis was performed in a three compartment electrolysis cell consisting of three electrode system using cylindrical platinum gauge as counter electrode,

Ag/AgCl as reference electrode and pyrolytic graphite plate as working electrode. Thin layer chromatography (TLC) on silica gel plates (8 cm × 2 cm, Merck) was performed for the identification of product of electroreduction of MF. UV-vis spectral studies were carried out using a Perkin-Elmer Lambda 35 UV-vis spectrophotometer. The FT-IR spectra were recorded using a Perkin-Elmer 1600 series spectrophotometer using KBr pallets. ^{1}H NMR spectra were recorded in appropriate deuteriated solvents (CDCl$_3$ and DMSO) with SiMe$_4$ as an internal standard using advance 500 digital NMR from Brucker. The chemical shift (δ) values have been reported in parts per million (ppm).

4.2.2   Reagents and materials

MF was purchased from Halcyon labs private Ltd. Ahmadabad, India. Single wall carbon nanotubes (SWCNTs) of purity >98% were purchased from Bucky, Houston, USA. The embedded metals Fe, Co, Ni in SWCNT were found as 0.819%, 0.412%, 0.207% respectively by Perkin Elmer Sciex ELAN DRC-e ICP-MS [253]. Cetyltrimethylammonium bromide was obtained from Sisco Research Labs Private Ltd. Mumbai, India. Phosphate buffers of ionic strength 0.5 M and pH (2.1-11.0) were prepared according to the method of Christian and Purdy [174]. MF containing creams and lotions of different companies, viz., Elocon (ZYG Pharm. Ltd., B. No. A511111), Momate (Glenmark Pharma, Ltd., B. No. 110617) and Momstar (Psychotropic India Ltd., B. No. W- 0062) were purchased from the local market of Roorkee. All other chemicals and reagents used were of analytical grade and double distilled water was used to prepare the solutions.

4.2.3   Preparation of MPG

A pyrolytic graphite electrode (PGE) with exposed edge plane site was prepared by the reported method [253]. Prior to modification, the PGE was cleaned by rubbing it on an emery paper (P-400) followed by washing it well with the double distilled water. A 0.5 mg mL^{-1} suspension of SWCNT was prepared by dispersing 0.5 mg SWCNT in 1 mL of N, N-dimethyl formamide using a sonicator to achieve well dispersed suspension. An optimized volume (40 µL) of this suspension was casted onto the surface of pyrolytic graphite (PG) and was allowed to evaporate at room temperature. The MPG having a well coated layer of SWCNT was then ready for voltammetric studies. The surface morphology of the bare PG and MPG was characterized by recording FE-SEM images. The SEM image of MPG surfaces clearly exhibit deposition of SWCNT at the surface of MPG (**Fig. 4.1**). Such a modification has been found to increase the effective surface area to ~0.225 cm^2 as compared to the bare PG area of 0.083 cm^2

as reported earlier [251]. The effective surface area of MPG was then calculated after full-monolayer adsorbed redox species (MF) for 90 second instead of the use of solution species and was found to be ~0.267 cm^2. Thus, the micro-structures of the sizes much smaller than the diffusion layer thickness also contribute to the effective surface area.
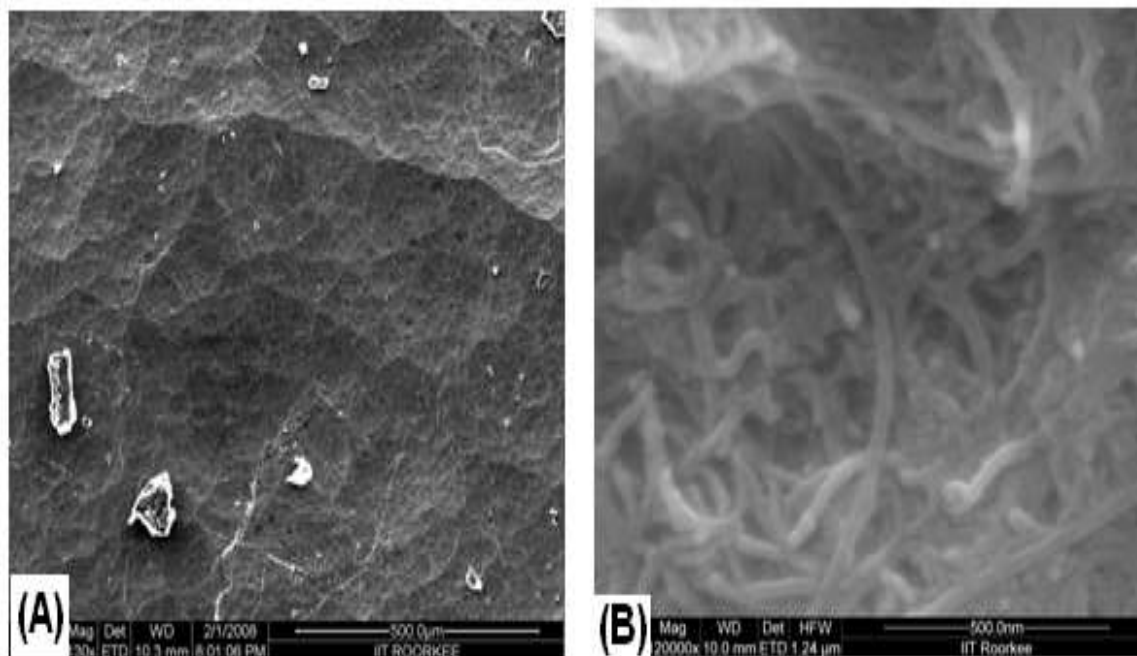
Fig. 4.1: Typical FE-SEM images of (a) unmodified and (b) MPG surfaces.

In another method of surface modification, CTAB (5 mg) was dissolved in 1 mL double distilled water and then 0.5 mg SWCNT was dispersed in 1 mL CTAB solution using ultrasonic bath. 30 µL of the well dispersed nanotubes suspension in CTAB solution was then casted onto the electrode surface of PGE and then dried at room temperature. The effective surface area in this case was found to increase by ~4 times as compared to bare PGE [20]. A comparison of the voltammetric behavior of MF was then studied using both the electrodes modified by different methods.

4.2.4   Voltammetric Procedure

MF is insoluble in water, hence, the stock solution of MF (2 mM) was prepared by dissolving the required amount in methanol. For voltammetric experiments, required volume of stock solution was added to the 1.8 mL of phosphate buffer solution and 0.2 mL of CTAB (3 mM) and the total volume was made to 4 mL with methanol. The percentage of methanol in the solutions was kept constant at 50%. The solution was degassed by bubbling pure nitrogen gas for 20 min before recording the voltammograms. The parameters of square wave voltammetry

(SWV) were optimized before recording the voltammograms and optimized parameters were: Initial (E): 0 mV, Final (*E*): -1800 mV, square wave frequency (*f*): 15Hz, square wave amplitude (E_{sw}): 25 mV, step (E): 4mV. All the potential were accounted with respect to Ag/AgCl reference electrode at an ambient temperature 25 ± 2 ℃.

4.2.5 Characterization of product

About 20 mg of MF was dissolved in 40 mL of 1:1 methanol - phosphate buffer (0.1M) solution of pH 7.2 and 1 mL of CTAB (6 mM) was added. The solution was electrolyzed by applying a constant potential ~ -1500 mV using potentiostat. The nitrogen gas was continuously bubbled in the solution at a slow rate. The progress of electrolysis was monitored by withdrawing a 2 mL solution from the cell at different time intervals and cyclic voltammogram and UV spectrum were recorded. When the absorption peak in the UV and reduction peak in CV disappeared (~24 h), the exhaustively electrolyzed solution was removed from the cell and lyophilized. The colorless material obtained after lyophilization was extracted with methanol and was used for further characterization.

4.2.6 Analytical procedure

MF is available as 0.1% w/w in cream/ointments. For the determination of MF in the cream/ointment, 1 g was weighed and dissolved in 10 ml of methanol by heating at water bath until the cream/ointment melts. The solution was then filtered by using whatman filter paper and the filtrate after suitable dilution was used for the voltammetric experiments.

4.3   RESULTS AND DISCUSSION

4.3.1   Cyclic voltammetry

Cyclic voltammograms for 0.5 mM MF were recorded using bare PG and MPG at a sweep rate of 100 mV/s in phosphate buffer of pH 7.2 ($\mu= 0.5$M). The sweep was initiated in the negative direction and MF was reduced irreversibly and exhibited reduction peak at - 1330 and - 1285 mV at bare PG and MPG respectively as shown in **Fig. 4.2**. The shifting of reduction peak potential of MF towards the less negative potentials and increase in peak current at MPG in comparison to the bare PG indicated that SWCNT modification facilitates the reduction of MF. This catalytic action may be assigned to several reasons such as increase in the effective surface area, embedded metals of SWCNT and increased diffusion due to thin layers [253, 254]. To determine the nature of the electrode reaction, scan rate studies were carried out in the range of 50-350 mV/s using MPG. It was observed that the peak current of

MF increased with increase in scan rate. The dependence of cathodic peak current on scan rate can be described by relationship;

$$i_p \, (\mu A) = 0.146 \, [v] + 3.214$$

where v is scan rate in mV/s and the relation has a correlation coefficient of 0.993. The linearity of graph of i_p vs v (**inset Fig. 4.2**) revealed that the reduction of MF is controlled by the adsorption process at the surface of MPG [229]. The plot of log i_p vs log v also exhibited a linear relation:

$$\log i_p = 0.850 \log v - 0.436$$

with correlation coefficient 0.991. The value of slope (>0.5) of log i_p versus log v plot further confirmed the adsorption of MF at the electrode surface [255].
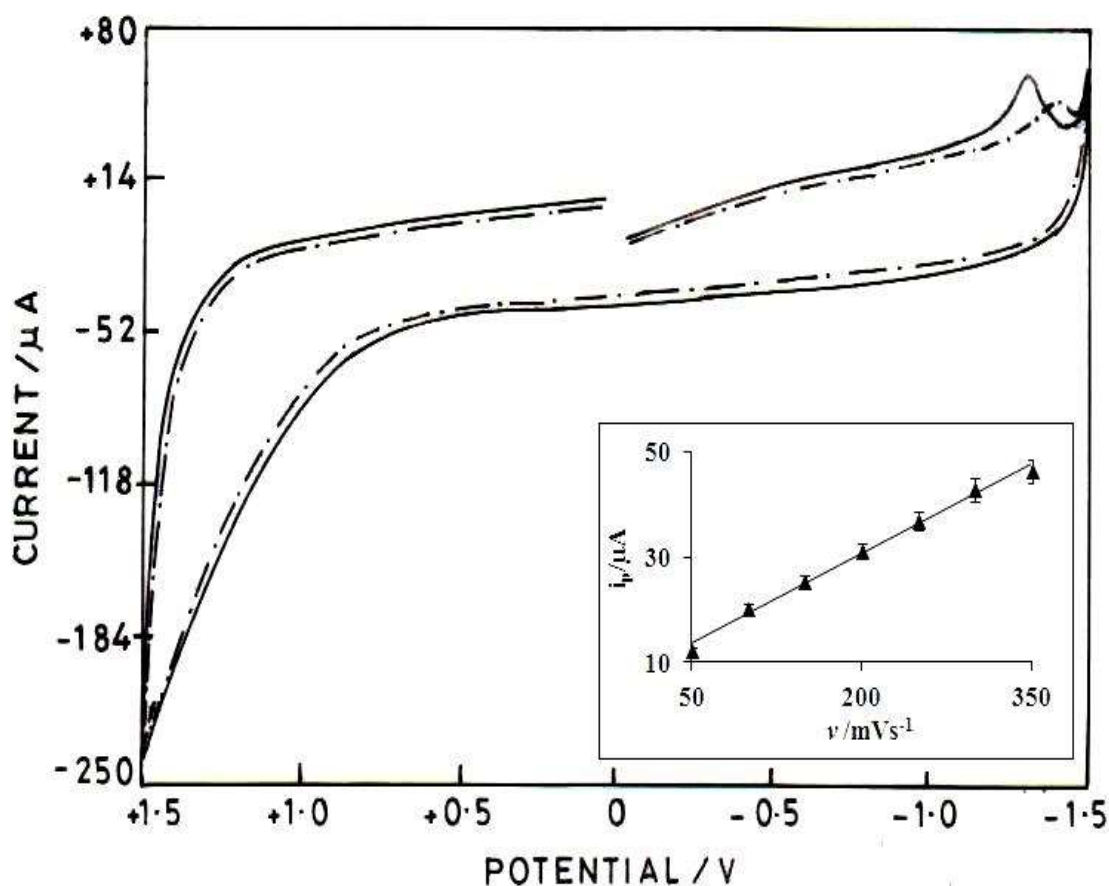
Fig. 4.2: Observed cyclic voltammograms of 0.5 mM MF using bare PG (—·—) and MPG (—) in phosphate buffer solution of pH 7.2 at a scan rate of 100 mVs^{-1}; inset is the plot showing variation of i_p with scan rate.

4.3.2 Effect of surfactants on the electrode response

The effect of different kinds of surfactants viz., cationic CTAB, anionic SDS and neutral Tween 80 was investigated on the electrochemical signal of MF. The change of reduction peak potential and peak current in absence and after the addition of different surfactants was studied and the observed results are summarized in **Table 4.1**. It can be seen from this Table that the addition of SDS and Tween 80 did not significantly affect the peak current and E_p of MF at concentrations below and above critical micelle concentrations. Therefore, it was concluded that anionic (SDS) and non-ionic (Tween 80) do not play any role in the reduction of MF.

Table 4.1: Observed changes in the peak potential and peak current of MF in absence and presence of different surfactants.

Surfactant	Concentration (M)	Peak potential (mV)	Peak current (µA)
-	-	1392	0.5
CTAB	0.15×10^{-3}	1254	9.3
SDS	2.50×10^{-4}	1396	0.3
	2.50×10^{-3}	1395	0.3
Tween-80	0.30×10^{-5}	1395	0.4
	0.30×10^{-4}	1392	0.3

CTAB having hydrophilic end on one side and a long hydrophobic tail on the other side is widely used in the electrochemical investigations. It affects the electrode processes either by adsorption at the electrode surface or by the solubilization of the compound in micelles [256, 257]. The amount of CTAB caused a significant effect towards the reduction of MF as shown in **Table 4.1**. The E_p shifted to less negative potentials and peak current of MF significantly increased. Further studies on CTAB addition were carried out by increasing the CTAB from 0.075 to 1.11 mML^{-1}. It was found that in the presence of 0.15 mM CTAB, the reduction peak current of MF increased and the peak potential decreased, however, further increase in CTAB volume up to 1.1 mM leads to the decrease in peak current and the E_p remained almost constant as shown in **Fig. 4.3**. Therefore, 0.15 mM CTAB was used as an optimum amount for further voltammetric determination of MF. This behavior can be explained on the basis of preferential adsorption of CTAB at the surface of electrode which facilitates the electron transfer between

MF and the electrode surface. After certain concentration of surfactant, micellization starts and MF encapsulates in micelles which decreases the value of diffusion coefficient followed by the lowering of peak current. A similar behavior has also been reported in dipyridamole in the presence of CTAB [258]. The concentration of CTAB at which the maximum current obtained was found to be 0.15 mM, well below the CMC (8×10^{-4} M) of CTAB in aqueous solutions [259] and (7×10^{-4} M) in presence of sodium salts [260]. Hence, it was concluded that the micelles did not play any significant role towards solubilization of MF and its adsorption on the surface of MPG plays a significant role. In addition adsorption of CTAB to the surface of MPG will occur through hydrophobic interaction to form positively charged film. The electron rich MF is then attracted to the electrode surface and cause an increase in the voltammetric signal.

(a)   (b)
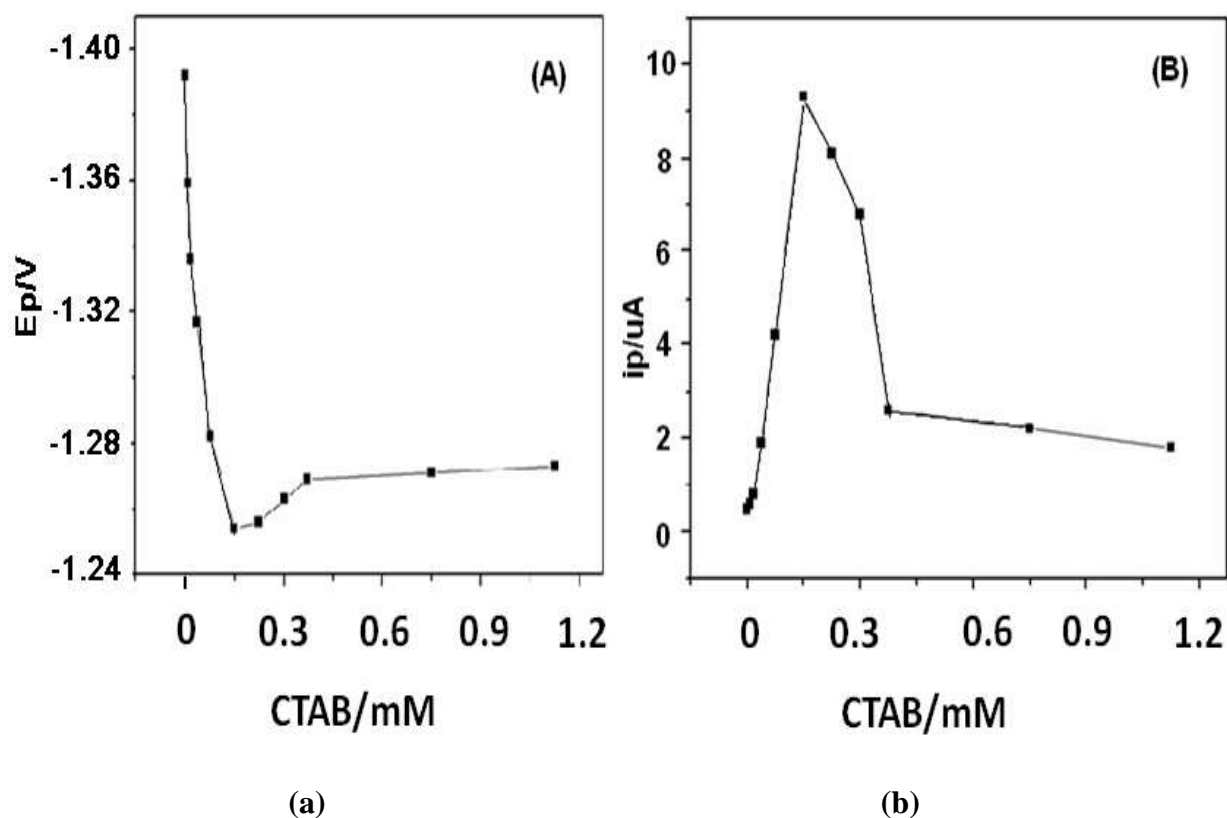
Fig. 4.3: Variation of peak potential E_p (A) and peak current i_p (B) of MF with increasing amount of CTAB at MPG.

4.3.3 Square wave voltammetry

Square wave voltammograms for 0.5 mM MF were recorded at bare PG and MPG in CTAB/phosphate buffer of pH 7.20. At MPG, the reduction of MF occurred in a well-defined peak (E_p -1265 mV), whereas, at bare PG the peak was observed at -1305 mV as shown in **Fig. 4.4.** In addition the peak current was found to be ~2.15 fold greater at MPG as compared to the

bare PG. This increase can be due to increase in adsorption or increase in reduction kinetics of MF or both. To confirm the reason for the increase, experiment was carried out by keeping the dipping time in solution for adsorption as constant (60 s) for bare PG and MPG and then voltammograms were recorded in buffer of pH 7.2. It was observed that the peak current at MPG was still greater by ~2.10 times, indicating thereby the catalytic activity of SWCNT towards the reduction of MF.
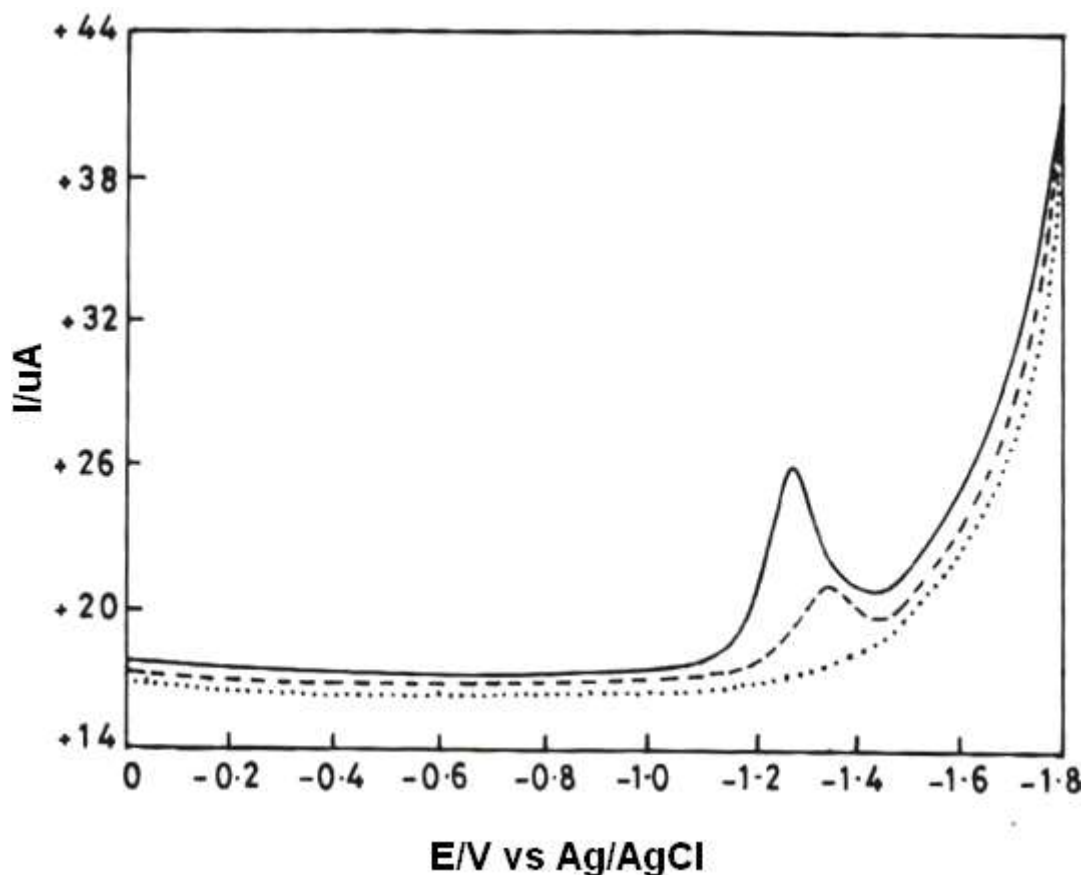
Fig. 4.4: A comparison of SWV recorded for 0.5 mM MF in CTAB/phosphate buffer of pH 7.2 at bare PG (---), MPG (—) and CTAB/phosphate buffer (…) using MPG.

4.3.3.1 Effect of concentration

The quantitative analysis of the MF is based on its concentration study. Dependence of the peak current on concentration of MF observed at MPG has been shown in **Fig. 4.5A**. It is observed that the peak current increases linearly with increase in the concentration of MF in the range 10 -1000 µM as presented in **Fig. 4.5A**. The peak current values are measured by subtracting the background current and are reported as an average of at least three replicate measurements. The plot of i_p vs [C] was linear at bare PG and MPG (**Fig 4.5B**) and the dependence of i_p on [C] can be represented by the relations:

$$i_p \, (\mu A) = 0.007 \, [C] + 1.170 \qquad\qquad \text{at bare PG}$$

$$i_p \, (\mu A) = 0.017 \, [C] + 0.934 \qquad\qquad \text{at MPG}$$

having correlation coefficients of 0.983 and 0.998, respectively and the term $[C]$ represents the concentration of MF in µM. The sensitivities were observed to be 0.007 and 0.017 µA/µM at, bare PG and MPG respectively indicating the catalytic behavior of MPG. The detection limit was calculated using the formula $3\sigma/b$, where σ is the standard deviation of the blank and b is the slope of the calibration curve and were found to be 9 µM and 1.23 µM, for bare PG and MPG respectively.
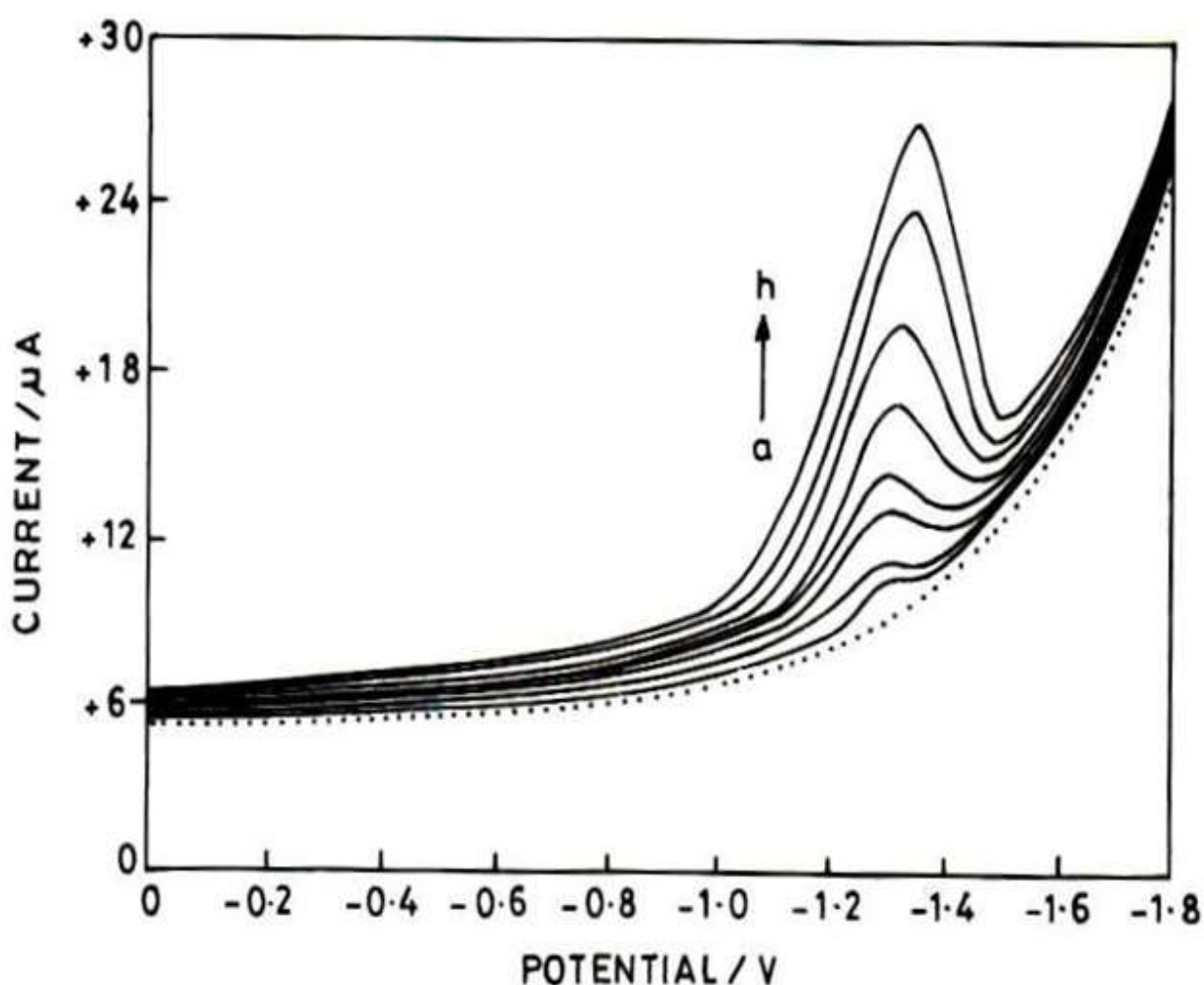
Fig. 4.5A: Observed SWV for (a) blank buffer (background) (…) and (ii) increasing concentration of MF; Curves were recorded at (a) = 10; (b) = 50; (c) = 200; (d) = 300; (e) = 400; (f) = 600, (g) = 800; (h) =1000 µM MF using MPG in CTAB/phosphate buffer of pH 7.2.
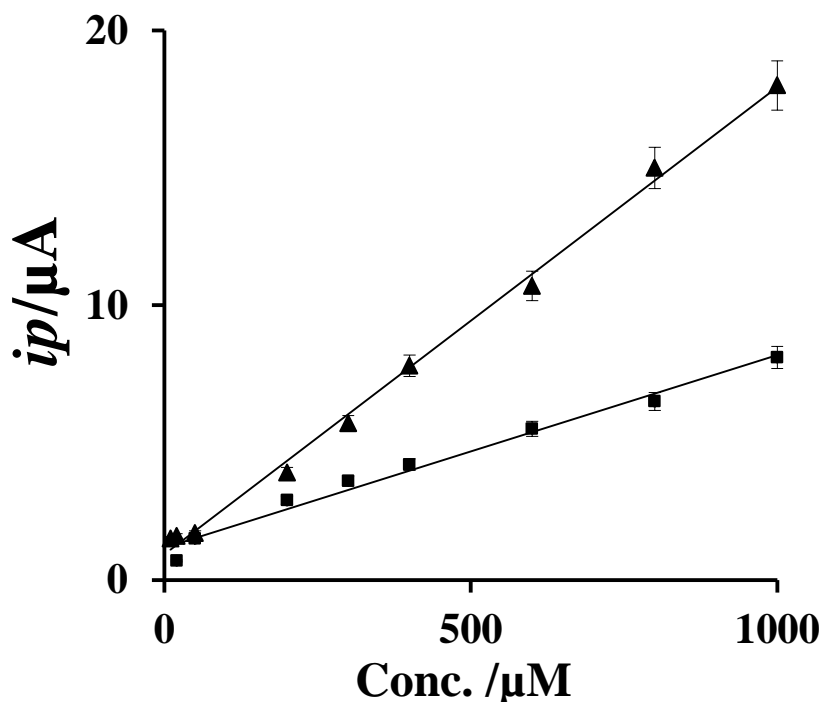
Fig. 4.5B: Calibration plot observed for MF at bare PG (■) and MPG (▲).

4.3.3.2 Effect of pH

The electrochemical behavior of MF at different pH was studied at bare PG and MPG. The voltammetric reduction of 0.5 mM MF was carried out by varying the pH of supporting electrolyte in the range 3.0-9.0 **(Fig. 4.6)**. The peak potential of MF was shifted towards more negative potentials with increase in the pH of supporting electrolyte. The linear relationship between E_p and pH can be expressed by the following equations:

$-E_p / mV = 58.61 \, pH + 879.07$ at bare PG

$-E_p / mV = 57.75 \, pH + 851.93$ at MPG

having correlation coefficients of 0.989 and 0.991, respectively. The slope values of E_p vs pH plot is close to ~59 mV in both the cases and indicates that equal numbers of electrons and protons participate in the reduction of MF [255].
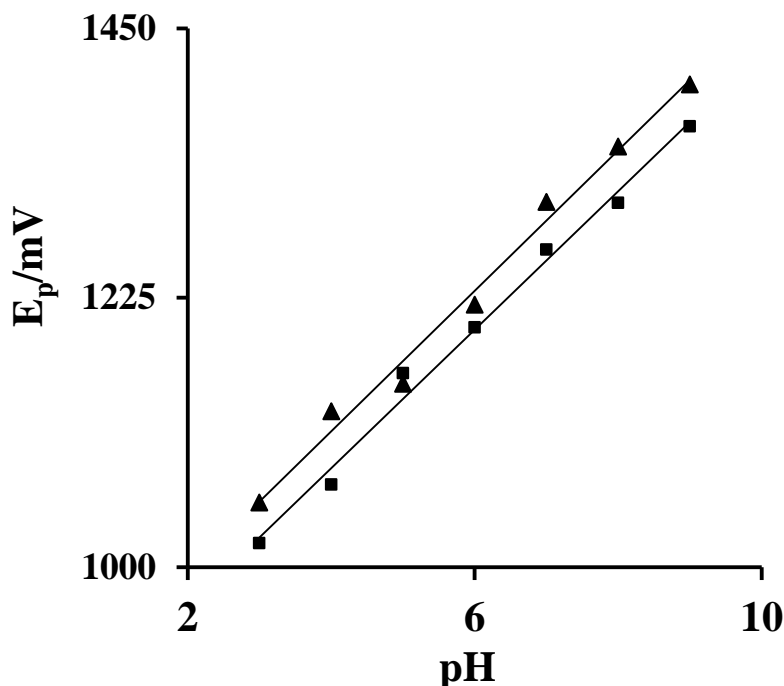
Fig. 4.6: Effect of pH of supporting electrolyte on E_p at bare EPPGE (■) and SWCNT/EPPGE (▲).

4.3.3.3 Square wave frequency study

The effect of square wave frequency on the reduction peak current of 0.5 mM MF was examined in the range 5-50 Hz in the phosphate buffer solution of pH 7.2 at bare PG and MPG **[Fig. 4.7]**. The peak of MF was found to increase with the increase in square wave frequency and the plot of i_p vs [f] was linear. The variation of peak current with square wave frequency observed at bare PG and MPG can be represented by the equations:

i_p (μA) = 0.450 [f] − 2.135   at bare PG

i_p (μA) = 1.077 [f] − 5.614   at MPG

having correlation coefficients of 0.999 and 0.997, respectively, where [f] is the square wave frequency in Hz. The linearity of i_p vs [f] plots and nature of CV as not history dependent, the reduction of MF is quite likely of thin layer diffusion behavior as reported earlier [7, 261].
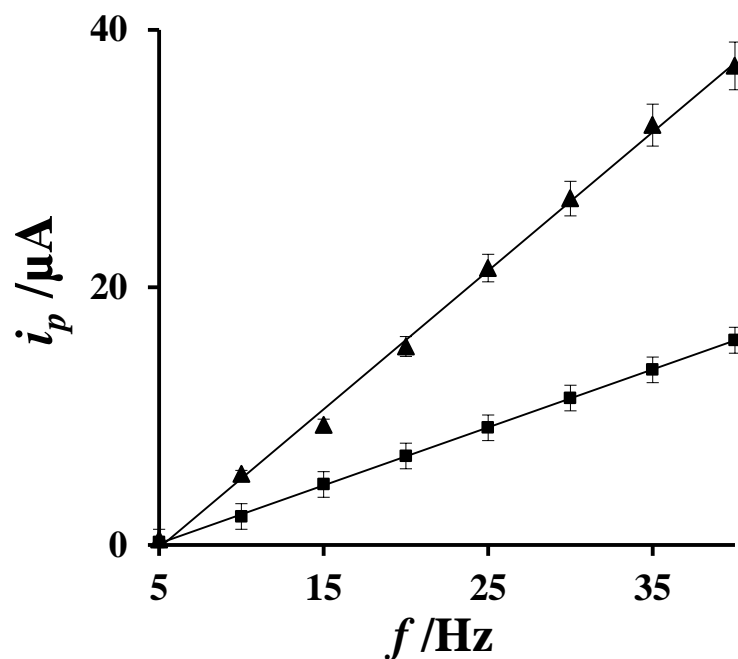
**Fig 4.7: Variation of peak current (i_p) with square wave frequency (f) at bare EPPGE (■)
and SWCNT/EPPGE (▲).**

4.3.4 Effect of method of CTAB casting

CTAB has also been used at the surface of electrode as CTAB-SWCNT composite to determine betamethasone [252]. To find out whether the method by which CTAB is used also affects determination, MF is also determined at CTAB-SWCNT composite modified PGE at pH 7.2. In cyclic voltammetry 0.5 mM MF exhibited well defined reduction peak at -1280 mV at composite modified electrode as compared to -1285 mV observed when CTAB was added in solution. Thus, the E_p values in both the cases were essentially similar. On the other hand, the peak current at composite modified electrode was 9.0 μA as compared to 7.5 μA. Thus, the peak current showed some increase, which can be assigned to enhanced surface area in the case of composite modification (~ 1.2 times more) as compared to CTAB added in solution [20]. Thus, it is concluded that the method of using CTAB does not affect the E_p and i_p of MF significantly.

Betamethasone has quite a bit similar molecular structure to MF. The structural differences include three substitutions of Cl to F, Cl to OH and phosphate ester group to 2-furoic acid ester at position 21. The reduction site in betamethasone and MF is C=O group present at position 3. The studies reported earlier [252] on betamethasone utilized a composite film of SWCNT-CTAB on EPPGE, in contrast to SWCNT film from the solution in the present

studies. CTAB solution was added separately in the present studies. This difference caused change in effective surface areas of the modified electrode. Also betamethasone was soluble in water (at 1 mM), whereas, MF was insoluble in water and hence, it's methanolic solution was used. Thus, the difference in the observed E_p (150 mV less negative for betamethasone as compared to MF) during voltammetric behavior of betamethasone can be accounted for to several parameters such as molecular charge (due to different substituents), different solvent and different effective surface areas.

4.3.5 Analytical utility

In order to establish the analytical applicability of the developed protocol, three pharmaceutical samples of MF cream were determined for their MF content. The solution obtained by dissolution of cream was subsequently diluted by the phosphate buffer of pH 7.2. For this purpose, 10 mL of the phosphate buffer was added to 10 mL of the filtered sample. Then 0.2 mL of CTAB was added to the 3.8 mL of this solution and square wave voltammograms were then recorded under exactly identical conditions that were employed while recording square wave voltammogram for calibration plot. The MF concentration after this dilution falls in the range of calibration plot. Concentration of MF in the samples was determined using calibration plot. The experimentally determined and reported MF in various creams indicates that the amount determined is within an error of ± 1%. Recovery experiments of MF were carried out in human urine in order to establish the accuracy of the proposed method. For this purpose methanolic solution of MF was added to 2 mL of human urine, 0.2 mL CTAB and 1.8 mL of phosphate buffer of pH 7.2 and the total volume was made to 4.0 mL by the addition of methanol. No further dilution was made. Under optimized parameters of SWV voltammograms were recorded at MPG at an ambient temperature 25±2˚C. A well-defined peak was noticed at peak potential -1268 mV corresponding to the reduction of MF as shown in **Fig. 4.8**. To confirm that this peak is due to the reduction of MF, urine sample was then spiked with known concentrations of standard solution of MF as depicted in **Table 4.2**. The peak current of the peak at E_p -1268 mV was increased with addition of MF and indicated that the peak at -1268 mV was due to the reduction of MF. The amount of MF was calculated using the regression equation and the recovery was found in the range 99.1 - 101.5%. The % bias was determined for $n=6$ and was found in the range 1.9 -3.6% as shown in **Table 4.2**. Thus, the method can be successfully applied for the determination of MF in human urine and different pharmaceutical formulation with acceptable level of accuracy and precession. No interference of common metabolites present in urine such as ascorbic acid, uric acid and

dopamine is observed because the analysis is based on reduction of MF and these interferents do not undergo reduction
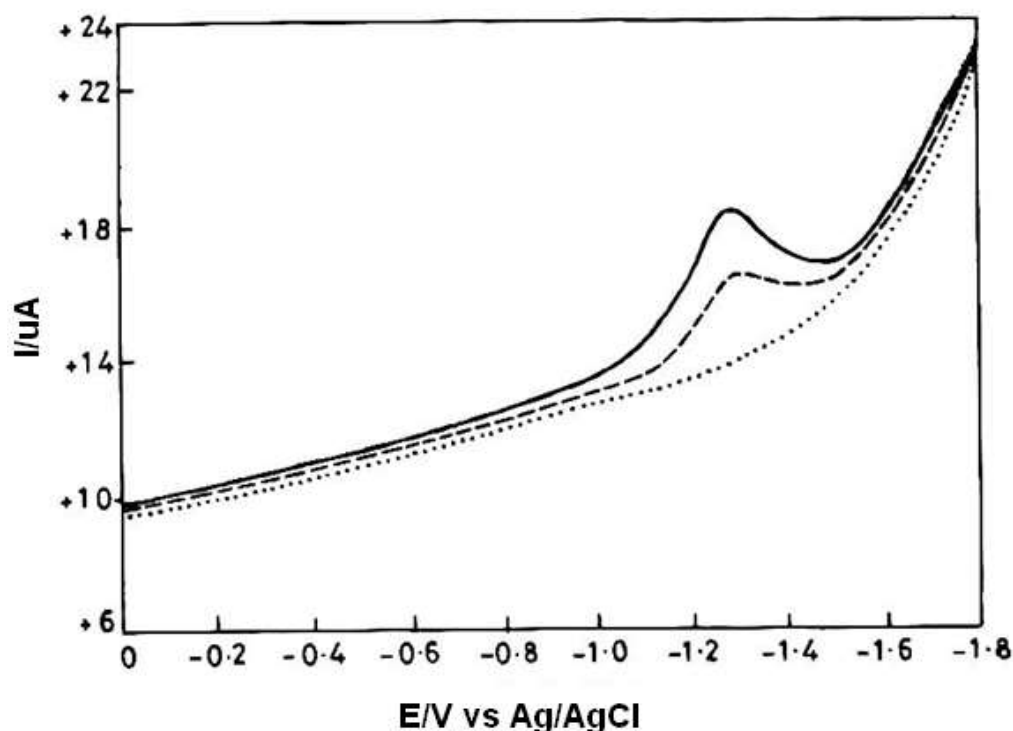
Fig. 4.8: Square wave voltammograms observed for blank buffer (background) (…..), urine sample (---) and sample spiked (—) with standard MF using MPG in CTAB/phosphate buffer of pH 7.2.

Table 4.2: Observed recovery of MF determined in human urine samples at MPG

	Amount spiked (mM)	Amount recovered (mM)	Recovery (%)	RSD[*] (%)	%B[**]
Sample 1[a]	0.01	0.01	100	2.3	3.6
	0.03	0.041	102.5	3	2.8
	0.055	0.094	98.9	2.7	2.5
Sample 2[a]	0.02	0.021	105	2.9	3.1
	0.05	0.068	97.1	2.1	2
	0.075	0.147	101.4	2.6	1.9

[a] The amount was spiked in the same solution

*The R.S.D. for the determination was for n=5

** % B is for n=5.

75

4.3.6   Stability and reproducibility of MPG

The stability and reproducibility of the MPG for the determination of MF was investigated. The long term stability of MPG was investigated by measuring the reduction peak current at a fixed MF concentration of 0.5 mM over a period of 15 days. The MPG was used daily and stored in the air. The experimental data showed that the inter-day precision and accuracy ($n = 15$) expressed as % RSD and % error were < 4.0 % and -1.3 - 3.0% respectively. After 15 days the MPG showed a decrease in peak current by ~5%, thus, it is recommended that after 15 days a new MPG should be prepared.

To ascertain the intra-day reproducibility of MPG, repetitive measurements for 0.5 mM MF were carried out at pH 7.2. The intra-day precision and accuracy (n = 10) expressed as % RSD and % error were <2.8 % and -2.5 - 2.0%, respectively.

4.3.7 Product characterization

The progress of electrolysis was monitored by recording UV spectrum and CV at different time intervals. The UV spectrum of MF exhibited a λ_{max} at 248 nm just before electrolysis. With the progress of electrolysis the absorbance at λ_{max} decreased and the maximum shifted to shorter wavelength (240 nm). Similarly in CV, the reduction peak current decreased with progress of electrolysis and finally disappeared after ~24 h. Thin layer chromatography of the lyophilized product exhibited a single spot in TLC (R_f ~ 0.36) and indicated the formation of single product. The product obtained after electrolysis of MF was characterized using FT-IR and ^{1}H NMR techniques.

MF contains three carbonyl groups viz., a cyclic (position 3) and other acyclic (**Scheme I**). To find out the site of reduction in MF, FT-IR spectra of reactant and product were recorded. The IR characteristic absorption bands for MF were observed at 3430 (O-H str.), 2938, 2886 (C-H str.), 1726 (C=O str. in ester), 1658 (cyclic C=O str.), 1610 (acyclic C=O str.), 1468, 1393 (C-H def.) and 1026 cm^{-1} (C-O str.). In the FT-IR spectrum of the product, absorption near 1658 cm^{-1} due to cyclic C=O str. did not appear rather an extra absorption band near 3130 cm^{-1}(O-H str.) was observed (**Fig. 4.9**). It is thus concluded that the reduction of MF occurs at cyclic >C=O group.
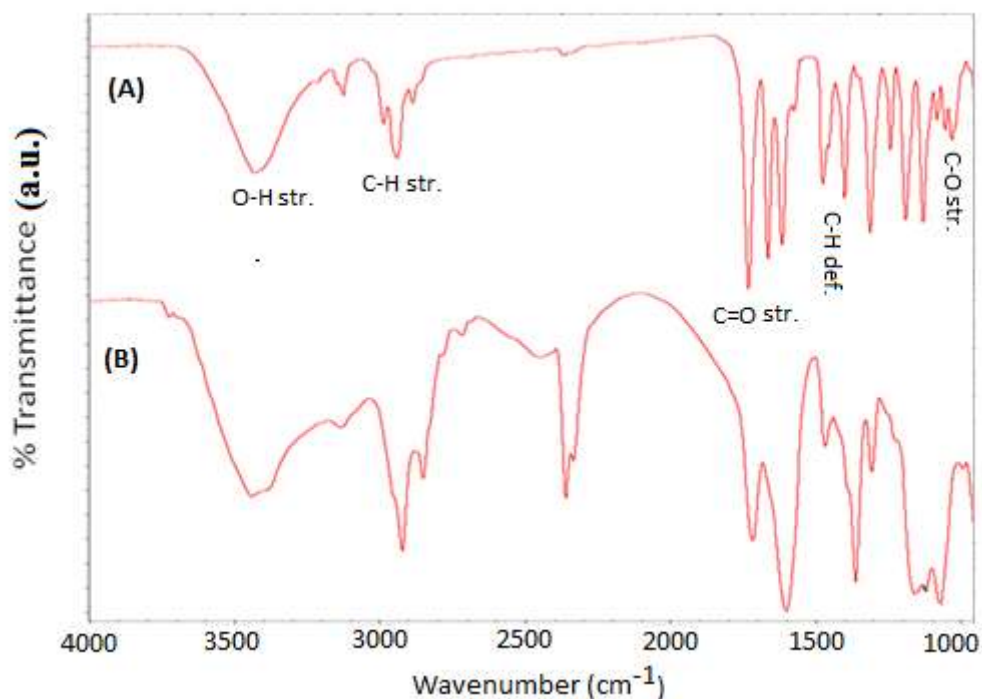
Fig 4.9: IR spectrum observed for the MF (A) and its reduction product (B).

^{1}H NMR spectra of the reactant and product of MF were recorded for further confirmation of reduction site and are presented in **Fig. 4.10**. It was found that MF showed the signals in NMR spectrum (**Fig. 4.10A**) which were essentially similar to the ones reported in literature [262, 225]. All chemical values of protons were found to be similar in the reactant and product, however, in the product an extra peak at δ 4.6 ppm (bs) was observed (**Fig. 4.10B**). This peak is assigned to the reduction of cyclic carbonyl group. In product, three of the olephenic –CH (cyclohexadienone moiety) were retained but they exhibited lower δ values than observed in the reactant because >C=O was converted to CH-OH and deshielding effect of >C=O had been removed in the product. Above results clearly indicate that conjugated cyclic carbonyl group at position 3 of MF undergoes electrochemical reduction and acyclic carbonyl groups remain unaffected during reduction of MF. It has also been reported earlier that conjugated carbonyl group undergoes easier reduction in the steroids than the isolated one [263, 264]. Thus, the reduction in MF occurs at C-3 position and the keto group is converted to hydroxyl group by $2e^-$, $2H^+$ process as shown in **Scheme1.**
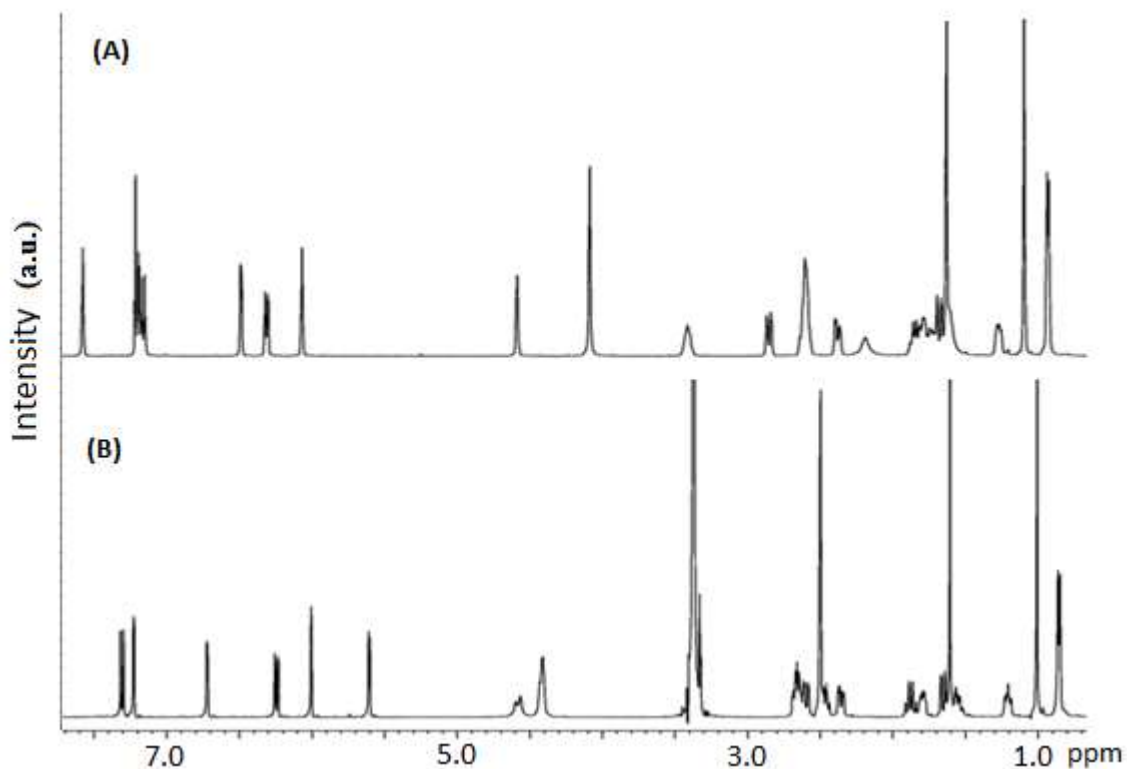
Fig. 4.10: ^{1}HNMR spectrum observed for the MF (A, CDCl$_3$ solvent peak 7.22 ppm) and its reduction product (B, DMSO solvent peak 2.54 ppm).
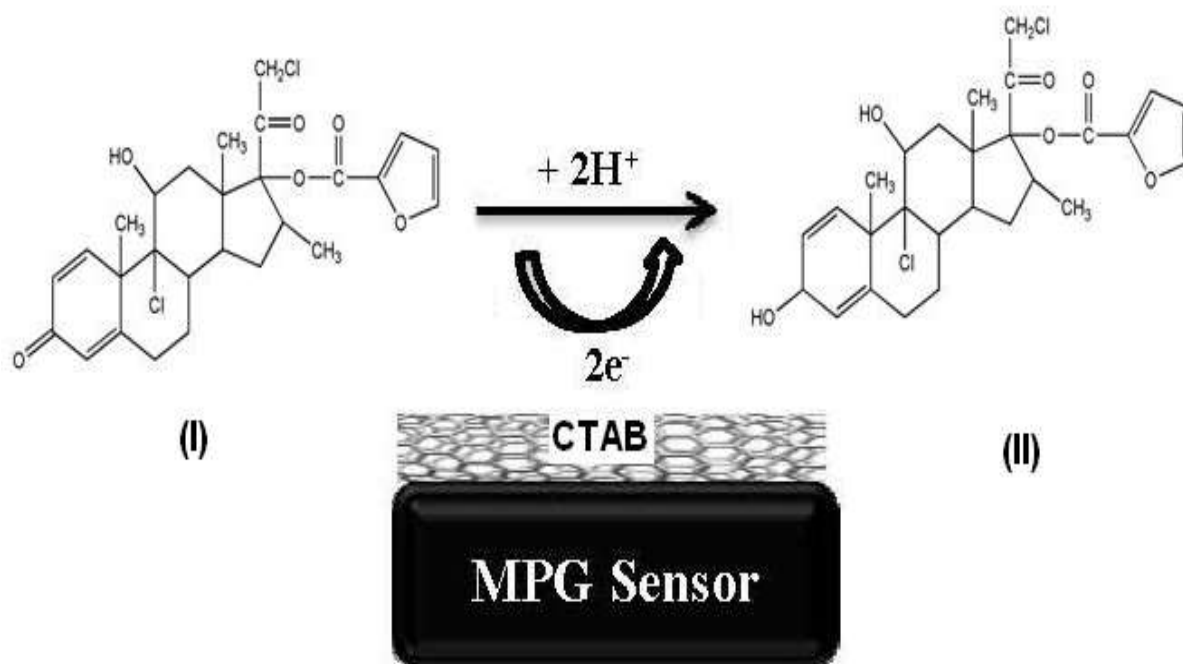
Scheme 1: Tentative mechanism proposed for the reduction of MF.

4.4   CONCLUSIONS

The proposed method provides an extremely sensitive and selective means for MF analysis based on its reduction utilizing MPG in presence of CTAB. The SWCNT modified electrode not only shifted the peak potential of MF towards the less negative potentials but also increased the peak current values significantly in comparison to the bare PG. The electro-catalytic activity of the carbon nano tube has been attributed to their large surface area, presence of edge plane like sites which occur at the end of nano tubes and some kind of metal impurities, which have been documented to result in low detection limit, high sensitivity, reduction of over potential and resistance to surface fouling [71]. The presence of cationic surfactant CTAB increased the peak current due to surfactant aggregation at the surface of MPG in the form of bilayers, surface micelles or cylinders. The charge transfer can take place either by the displacement of adsorbed surfactant by the MF or by the approach of MF between the spaces of one or two head groups of CTAB as reported earlier for isoniazid, an antituberculosis drug [265]. The adsorption of MF on the surface of MPG appears to increase the rate of electron transfer. Moreover, the results obtained from the application of the proposed method for determining MF in pharmaceutical samples confirmed the good accuracy and precision of proposed method. There is no literature concerning the electrochemical behavior of MF and its determination, hence the present study with a low detection limit is a very useful tool for selective analysis of MF without any interference from the common metabolites present in the blood and urine. The IR and NMR studies confirmed that the reduction of MF occurs at acyclic $>C=O$ group to give $>CH-OH$ in a $2e^-$, $2H^+$ process. As electrode fabrication is easy and low cost, MPG is of great utility for the detection of MF.

CHAPTER 5

AuNPs-poly-DAN modified pyrolytic graphite sensor for the determination of Cefpodoxime Proxetil in biological fluids
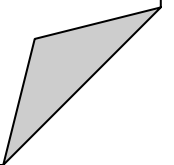
5.1 INTRODUCTION

Cefpodoxime Proxetil (CP, (6R, 7R)-7-{[(2Z)-2-(2-amino-1,3-thiazol-4-yl)-2-methoxy imino-acetyl]amino}-3-(methoxymethyl)-8-oxo-5-thia-1-azabicyclo[4.2.0]oct-2-ene-2 carboxylic acid, is a semi-synthetic beta-lactam antibiotic belonging to the third generation of cephalosporin group [266, 267]. CP is a prodrug and it is hydrolyzed into its parent moiety cefpodoxime acid (CA) by specific cholinesterase enzyme in the intestinal wall/plasma to exhibit its antibiotic activity [268]. It shows broad spectrum antimicrobial activity against several microorganisms and its antibacterial action is suggested by binding to specific penicillin-binding proteins located inside bacterial cell wall [269]. It is used orally for the treatment of mild to moderate respiratory tract infections, gonorrhoea and urinary tract infections and also in the treatment of skin infections, acute media otitis, pharyngitis and tonsillitis [154, 155]. CP is absorbed orally throughout the gastro-intestinal wall and shows about 50% bioavailability after the administration of CP as a 132 mg tablet (equivalent to 100 mg of cefpodoxime). The low bioavailability of CP is attributed to its poor water solubility and pre-absorption luminal metabolism into CA by the action of digestive enzymes [270-272]. It has been observed that CP is a well-tolerated antibiotic but it is not suitable for patients allergic to metabolites of CP. Adverse effects of this drug include maculopapular rash, bronchospasm, exfoliative dermatitis, Steven Johnson syndrome and anaphylaxis. Overdose of CP is associated with nausea, vomiting, flatulence, oral candidiasis, epigastric distress and diarrhoea [273]. The chemical structure of CP and 1, 5-DAN is presented in **Scheme 1**.

[CP]

[1, 5-DAN]
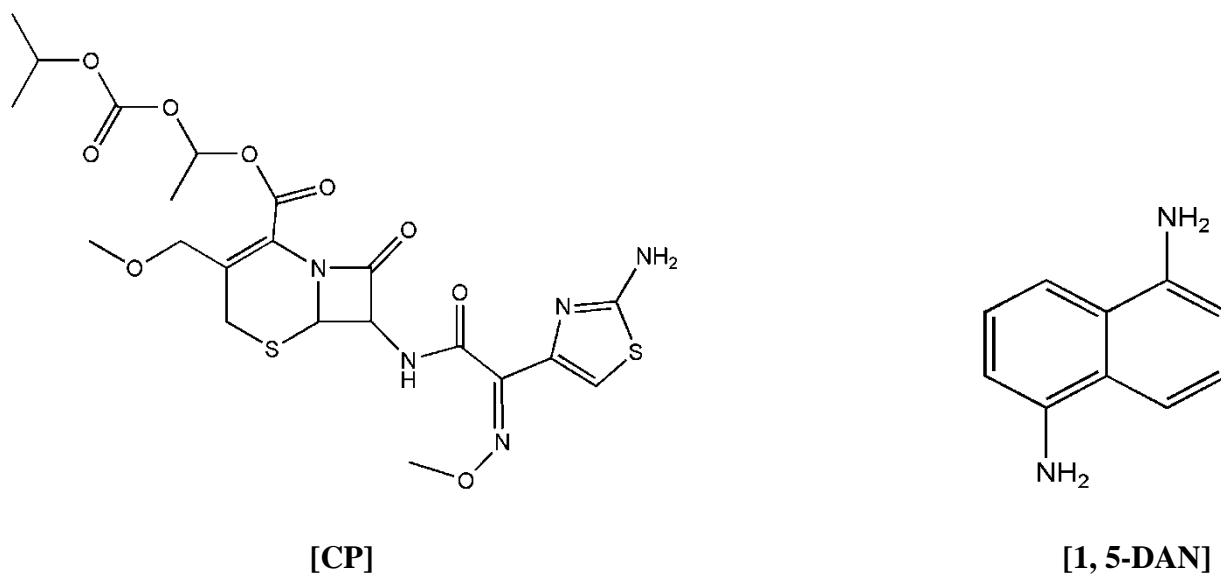
Scheme 1

The broad spectrum clinical use of CP triggered our interest to develop a sensitive and rapid method for CP determination in pharmaceutical samples and human biological samples. Various techniques have been developed for the evaluation of cephalosporins in body fluids and dosage forms, which include spectrophotometric [274, 275], fluorometric [276] and chromatographic techniques [277-279]. Although sensitivity and detection limit of CP determination have been improved in these techniques, these are rather expensive and require time consuming methods prior to analysis. Therefore, a simple and easy determination of CP in drug dosage forms, human urine and serum is desirable without time consuming extraction and separation steps with ease of analysis. In recent years, electroanalytical methods have attracted much attention of researchers towards the determination of drugs and various cephalosporins in dosage forms and biological fluids due to their high sensitivity and selectivity [280, 281]. Many electrochemical methods have been described in literature concerning the reduction behaviour of CP using dropping mercury or hanging drop electrodes [282-284]. As mercury is toxic and causes environmental threat, solid electrodes have also been used to study the oxidation of cephalosporin group antibiotics [285-287]. Till date, no oxidation studies on the determination of CP have been reported at solid electrodes. Therefore, the aim of this study is to develop a simple electroanalytical method for the determination of this drug in pharmaceutical dosage forms and biological fluids.

Conductive polymers have continued to be the major concerns during the past decade due to their potential applications in battery electrodes, electrochromic devices and electroluminescent devices [288]. Application of conductive polymers in electrochemical sensors has been extensively increased due to their advantages, such as possibility of one step synthesis on different substrates with good stability, reproducibility and low cost. Recently, organic conductive polymers have been used to prepare chemically modified electrodes for highly sensitive and selective analysis of tetracycline and β-lactam antibiotic, amoxicillin [289, 290]. Among organic compounds, aromatic amino compounds have gained a particular attention for their capability to provide polymer coating on metallic or carbon electrode by electrooxidative polymerization. As poly-1,5-diaminonaphthalene (p-DAN) is found to have versatile applications in the construction of chemically modified sensors, it has been confirmed as a promising candidate to form polymer-drug conjugate for drug delivery purposes [226, 133]. In the present chapter we report the electropolymerization of 1,5-diaminonapthalene (1,5-DAN) at the edge plane surface of pyrolytic graphite (EPPG). As gold nanoparticles (AuNPs) have attracted substantial interest in electrode modification due to their capability of enhancing the electrode conductivity, which improves sensitivity and selectivity, hence incorporation of

AuNPs onto p-DAN has also been carried out to fabricate the sensor [121, 291-292]. To the best of our knowledge, electrochemical oxidation of CP is reported for the first time involving low cost conducting polymer modified sensor. The electrochemical method presented in this chapter is a promising substitute to the frequently reported chromatographic, photometric and other analytical methods due to its simplicity, rapidity, reliability and low cost of analysis. The application of the proposed method has been demonstrated by the determination of CP in biological samples and pharmacological formulations and results have been successfully validated.

5.2 EXPERIMENTAL

5.2.1 Instrumentation

All the voltammetric experiments were performed with a computerized bioanalytical system (BAS, West Lafayette, USA) CV-50W voltammetric analyzer. A conventional single compartment three electrode glass cell equipped with EPPG/p-DAN/AuNPs sensor as the working electrode, Ag/AgCl (3M NaCl) reference electrode (BAS Model MF-2052 RB-5B) and a platinum wire as the counter electrode was used. The pH of the phosphate buffers was measured using digital pH metre (model CP-901). Pyrolytic graphite pieces were received as a gift from Pfizer Inc., New York, USA. Field Emission Scanning Electron Microscopy instrument (FE-SEM) (JEOL, JSM-7400) was used to characterize the surface of sensor. X-ray Photoelectron Spectroscopy (XPS) measurements were carried out using a VG scientific ESCA lab 250 XPS spectrometer coupled with a monochromated Al K-source having charge compensation, at Pusan National University, Busan (S. Korea). HPLC studies were carried on Shimadzu (LC-2010 HT) equipped with C-18 reverse phase column. Mobile phase used was a mixture of 20 mM phosphate buffer (pH 7.2) and acetonitrile in the ratio of 62:38 at a flow rate of 1 ml min^{-1} and the absorbance of the eluent was monitored at 235 nm.

5.2.2 Chemicals and reagents

CP was purchased as a gift from Alkum Drugs and Pharmaceuticals Ltd., Haridwar (India). Phosphate buffers of different pH were prepared according to Christian and Purdy [174]. 1,5-DAN and hydrogen tetrachloroaurate (HAuCl$_4$) were purchased from Sigma-Aldrich. Perchloric acid (HClO$_4$) was purchased from Rankem Chemicals, Delhi. CP containing tablets manufactured by different companies were purchased from the local market of Roorkee. All other solvents and reagents used in the experiment were of analytical grade. Double distilled water was used throughout the experiments.

5.2.3 Fabrication of p-DAN/AuNPs- on the surface of EPPG

Prior to modification of edge plane surface of pyrolytic graphite (area 3 mm^2), it was rubbed on an emery paper (P-400) and then rinsed thoroughly with double distilled water and dried. p-DAN film was then grown in solution of 1M HClO$_4$ containing 10 mM 1,5-DAN. Polymerization was carried out by cycling the potential between - 0.1 and + 1.0 V vs. Ag/AgCl (in saturated NaCl) at a scan rate of 100 mVs^{-1} for 50 scans. After the stable polymer film was prepared on the surface, it was rinsed with distilled water carefully in order to remove soluble products as well as monomer of 1,5-DAN before it was subjected to further experiments.

Fig. 5.1 presents a comparison of the XPS survey spectrum of unmodified and p-DAN modified surface of pyrolytic graphite. Two sharp peaks were noticed in the unmodified surface at 299.1 and 540.3 eV corresponding to carbon and oxygen. After polymerization of DAN, a sharp peak at about 398.9 eV appeared, which was absent in the unmodified surface (**Fig. 5.1**), due to the NH$_2$ group present in the polymer backbone. This confirmed that p-DAN has been successfully deposited at the surface of pyrolytic graphite. Incorporation of gold nanoparticles on the surface of polymer coated pyrolytic graphite was then made by using cyclic voltammetry. For this, the potential from -0.8 to +0.4 V was scanned at a scan rate of 50 mVs^{-1} for 20 cycles in 1 mM HAuCl$_4$ solution as described in literature [115]. The electrode was then taken out, washed well with distilled water and dried under the flow of nitrogen. The XPS spectrum after AuNPs deposition on p-DAN modified pyrolytic graphite exhibited two additional peaks at 83.4 and 86.8 eV corresponding to Au4f as shown in **Fig. 5.1**. FE-SEM images of unmodified pyrolytic graphite surface (PGS), p-DAN modified PGS and AuNPs/p-DAN modified PGS are presented in **Fig. 5.2**, and clearly show the deposition of polymer and nanogold clusters at the EPPG surface. The polymer coated gold nano particles modified sensor was then ready for use and denoted as EPPG/p-DAN/AuNPs.
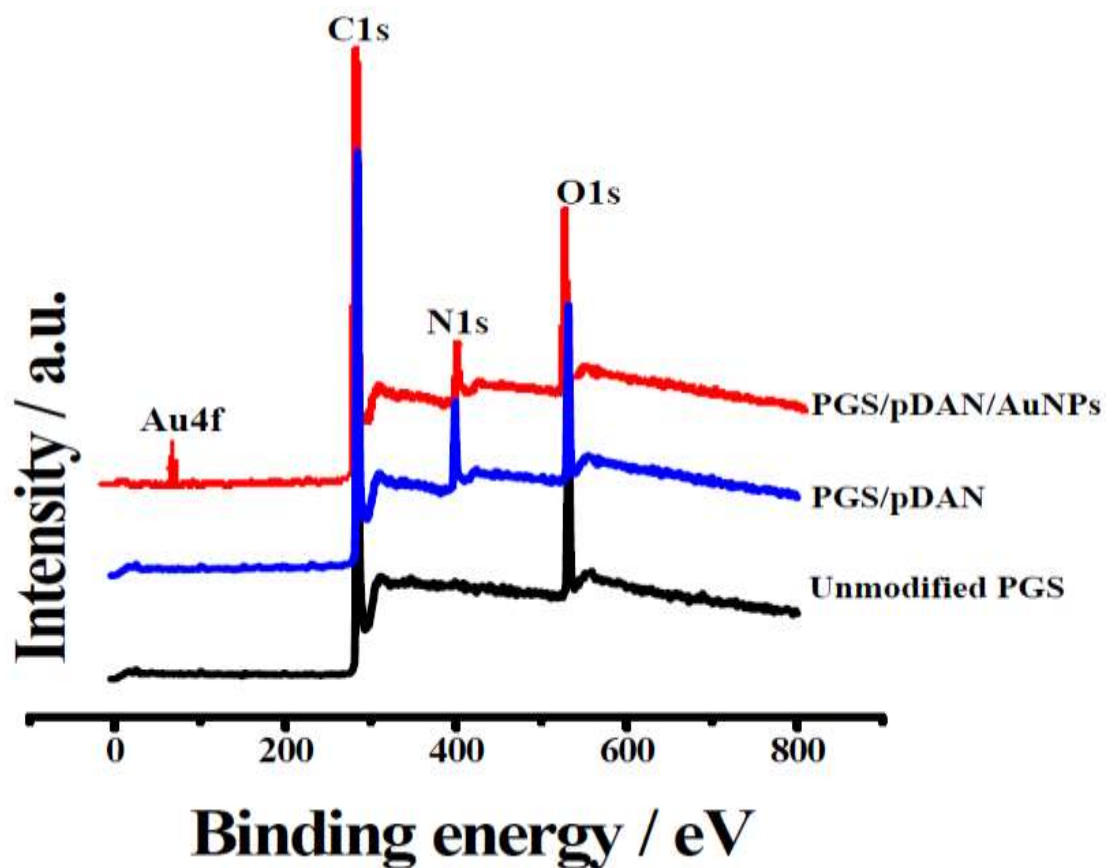
Fig. 5.1: Observed XPS survey spectrum of unmodified PGS, PGS/pDAN and PGS/p-DAN/AuNPs.
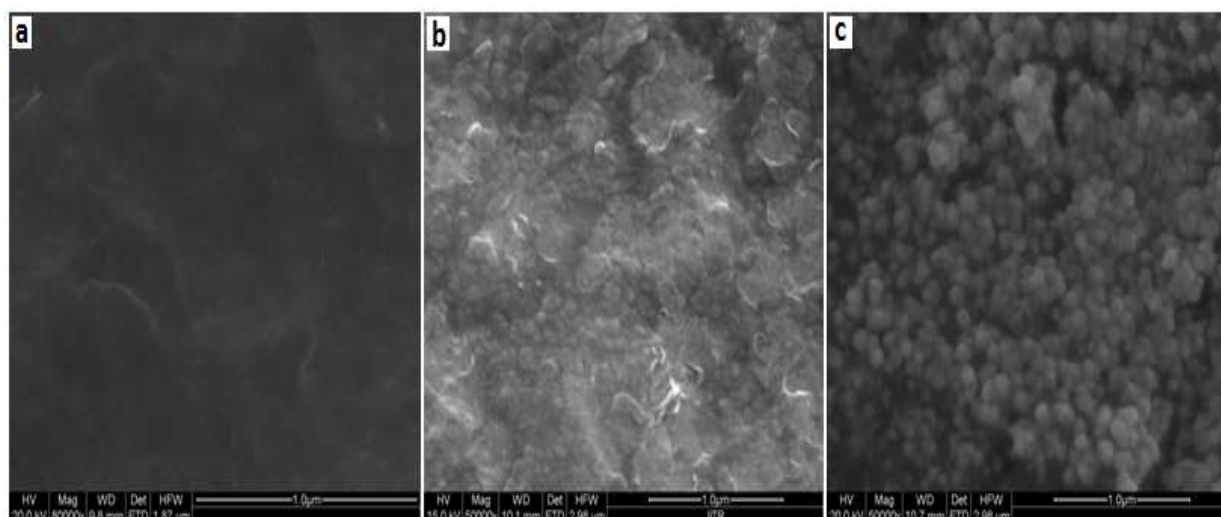
Fig. 5.2: Typical FE-SEM images of (a) unmodified EPPG (b) EPPG/p-DAN and (c) EPPG/p-DAN/AuNPs

5.2.4 Analytical Procedure

CP is insoluble in water; hence, stock solution of CP (1 mM) was prepared by dissolving the required amount of CP in a mixture of methanol and water (1:4) using a stirrer for 30 min. For recording voltammograms, aliquots of the stock solution of CP were diluted with 2 ml of phosphate buffer of pH 7.20 (μ=1M) and total volume was made to 4 mL. The optimized instrumental parameters for square wave voltammetry (SWV) were initial potential (E): 0 mV, final (E): 1200 mV, square wave amplitude (Esw): 25 mV, step potential (E): 4 mV and square wave frequency (f): 15 Hz. All the potentials are reported with respect to Ag/AgCl reference electrode at an ambient temperature of 25±2 ^{o}C. Some other experimental parameters such as deposition time and stripping potentials were also optimized using 6 μM CP at EPPG/p-DAN/AuNPs sensor. For this purpose modified sensor was dipped in CP solution for the time period varying from 10 s to 200 s in the same solution. Variation of deposition time showed that peak current increased with deposition time and reached a plateau after a period longer than 120 s; hence, deposition time 120 s was chosen as an optimum time. Using optimum deposition time, a potential was applied in the range 0.0-1.0 V, which indicated that maximum value of peak current was observed at 0.660 V. Stripping potential of 0.660 V was selected as an optimum for further experiments.

The surface of the EPPG/p-DAN/AuNPs was cleaned after each run using time base technique by applying a constant potential (-100 mV) for 60 s in buffer.

The human urine samples of patients undergoing treatment with CP were obtained from the institute hospital after the clearance from ethics committee of Indian Institute of Technology, Roorkee. The samples were obtained after 6 h of administration of CP tablet (50 mg). Urine sample of normal person received from the laboratory personnel was used as control. Urine samples were diluted two times with phosphate buffer of pH 7.2 prior to analysis.

5.3   RESULTS AND DISCUSSION

5.3.1   Fabrication of p-DAN/AuNPs film

Fig. 5.3 shows consecutive cyclic voltammograms recorded during the growth of p-DAN layer at the surface of pyrolytic graphite. In the first sweep towards positive potentials, the 1,5- DAN was oxidized exhibiting well-defined anodic peak (Ep ~0.66 V) corresponding to the oxidation of DAN monomer into cationic radical which is suppressed in subsequent potential cycles. A cathodic peak at 0.48 V was observed in the reverse sweep. During the early stage of growth two polymer anodic peaks at 0.32 V and 0.51 V and cathodic peaks at 0.15 and 0.47 V along with monomer oxidation peak at 0.68 V are observed due to the polymer film formation. The peak current of new peaks increased with increase in the number of potential scans, whereas peak current of peak at 0.68 V decreased with increase in the cycles. In later stage of polymerization two anodic CV peaks merged into one at about 0.52 V and finally in the 50th cycle two well-defined anodic and cathodic peaks were observed at 0.53 V and 0.45 V, respectively, related to the subsequent growth of polymer film and a uniform adherent polymer film was developed on the pyrolytic graphite surface. The CV results observed showed good agreement with the earlier reported electropolymerization studies of 1,5-DAN at gold disc electrode [293]. Electrochemical deposition of AuNPs on polymer coated EPPG surface provided nano structured surface which exhibited excellent catalytic activity due to the unique properties of AuNPs such as increased surface area, good conductivity and biocompatibility [294].
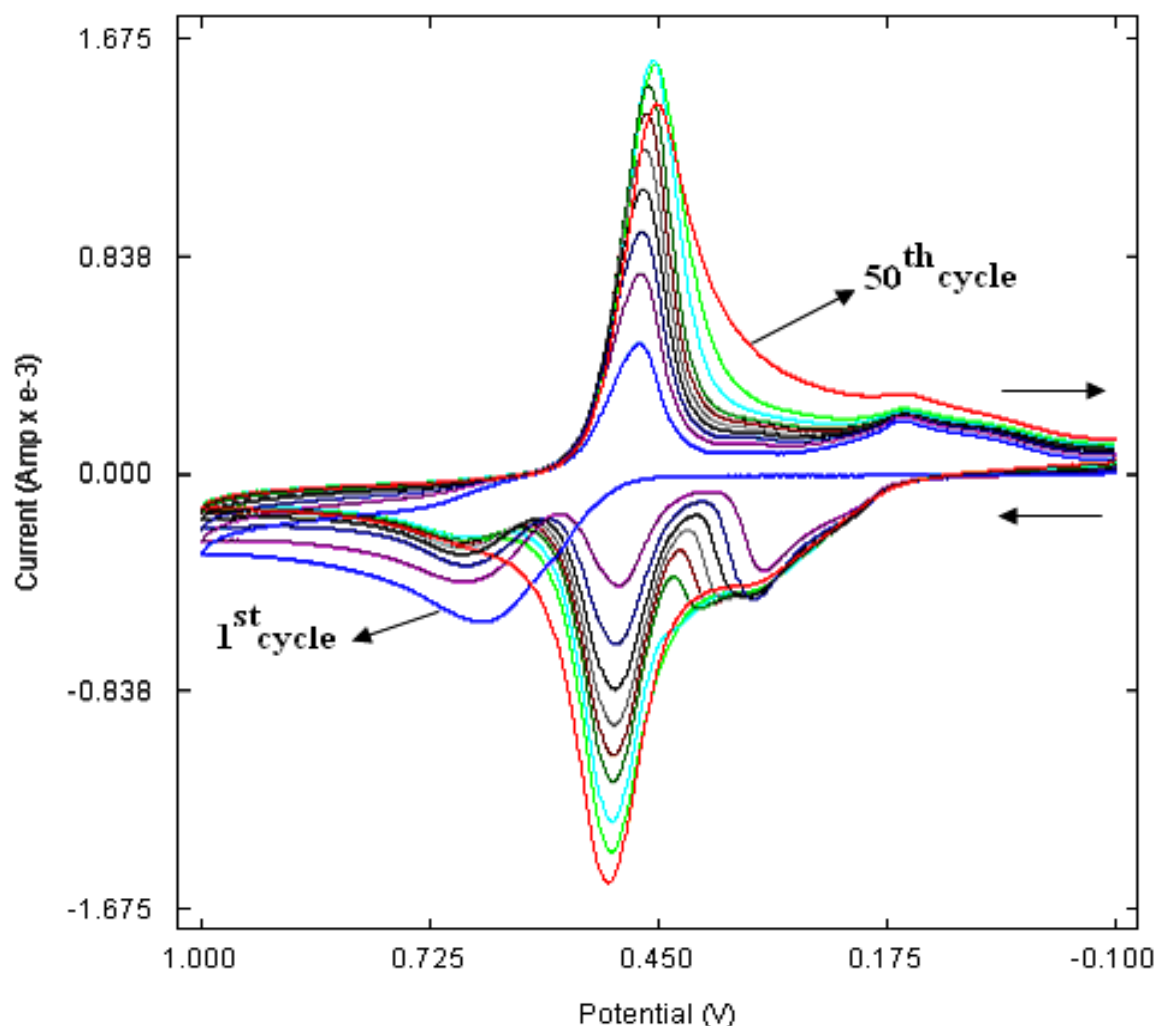
Fig. 5.3: A series of cyclic voltammograms recorded during fifty consecutive potential cycles between -0.1 to 1.0 V in 10 mM 1,5-diaminonaphthalene and 1 M HClO$_4$ at a scan rate 100 mVs^{-1} using EPPGE

5.3.2   Electrochemical response of p-DAN/AuNPs film

Electrochemical response of unmodified EPPG, EPGE/p-DAN and EPPG/p-DAN/AuNPs surfaces is examined by recording CV of K$_3$[Fe(CN)$_6$] and a comparison of three surfaces is presented in **Fig. 5.4**. A well-defined redox couple for Fe^{3+}/Fe^{2+} was observed at all the three surfaces. However, the peak currents for the redox couple increased in the case of EPPG/p-DAN/AuNPs **(Fig. 5.4c)** and the ΔEp value decreased to 0.65 V showing more reversible nature of the redox couple at the modified surface. The effective surface areas after modification was also determined by recording cyclic voltammograms of 1 mM K$_3$[Fe(CN)$_6$] at different scan rates using 0.1 M KCl as supporting electrolyte. The surface area was calculated

from the slopes of i_p vs. $v^{1/2}$ plots using Randles-Sevcik equation and found as 0.081, 0.102 and 0.174 cm^2 for unmodified EPPG, EPPG/p-DAN and EPPG/p-DAN/AuNPs surfaces, respectively. Thus, the EPPG/p-DAN/AuNPs sensor had an area more than double of unmodified EPPG surface.
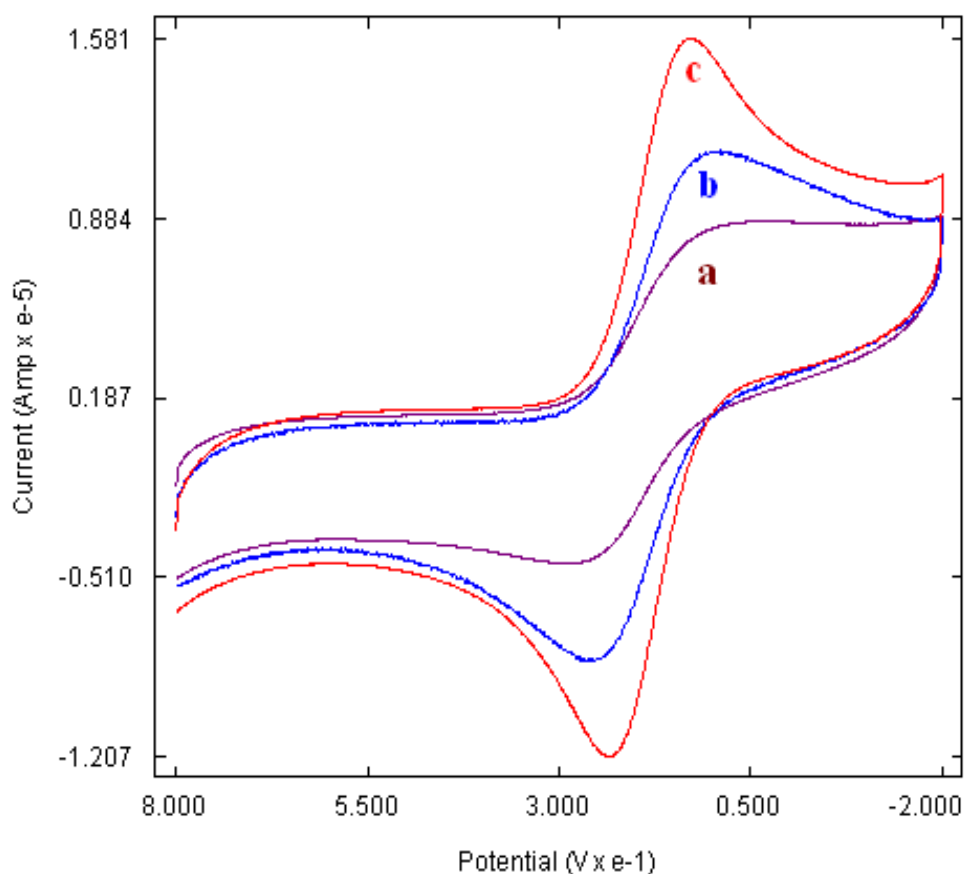
Fig. 5.4: Comparative cyclic voltammograms of 1mM K$_3$[Fe(CN)$_6$] in 0.1 M KCl at (a) unmodified EPPG, (b) EPPG/p-DAN and (c) EPPG/p-DAN/AuNPs.

5.3.3 Cyclic voltammetry

The cathodic behaviour of CP has been reported at mercury electrodes earlier [20], however, no information is available concerning the electrooxidative behaviour of CP. Therefore, to study the anodic voltammetric behaviour of CP, first it was subjected to cyclic voltammetric study. **Fig. 5.5** presents a cyclic voltammogram was recorded for 6 μM CP using EPPG/p-DAN/AuNPs sensor at pH 7.2 at a scan rate of 100 mVs^{-1}. CP is irreversibly oxidized giving rise to a well-defined oxidation peak (I) at E$_p$ (725 mV) when sweep is initiated in the positive direction and two reduction peaks at - 950 mV (II$_a$) and - 1110 mV (II$_b$) are observed

in the reverse sweep. To confirm whether the reduction peaks are related to oxidation peak or are due to independent reduction of CP, CV was also recorded by initiating the sweep in the negative direction. In this case two reduction peaks were observed at - 950 mV and - 1110 mV and an oxidation peak was observed in the reverse sweep. Thus, it is concluded that CP can undergo oxidation as well as reduction. The anodic peak at 725 mV can be assigned to the oxidation of 2-amino group located on the thiazole ring in the side chain on C-7. Similar oxidation of amino group has been reported for cefixime, cefepime and related compounds [285, 295]. As p-DAN layer exhibits two significant peaks at 0.53 V and 0.45 V in acidic medium and no peaks are observed while recording voltammograms in phosphate buffer of pH 7.20, it is concluded that p-DAN layer shows redox behaviour only in acidic medium.

To ascertain the nature of the electrode reaction scan rate studies were performed in the range of 50-350 mVs^{-1}. The peak current of CP was found to increase with increase in the sweep rate and dependence of the anodic peak current on scan rate can be expressed by following linear relationship:

$$i_p = 0.22 \ [v] + 3.71$$

with correlation coefficient of 0.995, where v is scan rate in mVs^{-1} and i_p is peak current in μA. The linearity of i_p versus scan rate plot (inset of **Fig. 5.5**) indicated that oxidation of CP is adsorption controlled which was further confirmed by linearity of $i_p/v^{1/2}$ vs. log v and log i_p vs. log v plot. Following relation was observed for log i_p vs. log v plot:

$$\log i_p = 0.859 \log v - 0.293$$

with a correlation coefficient 0.993. The slope value (> 0.5) of log i_p versus log v plot further confirmed that oxidation of CP is followed by adsorption of CP at the electrode surface [279, 296].
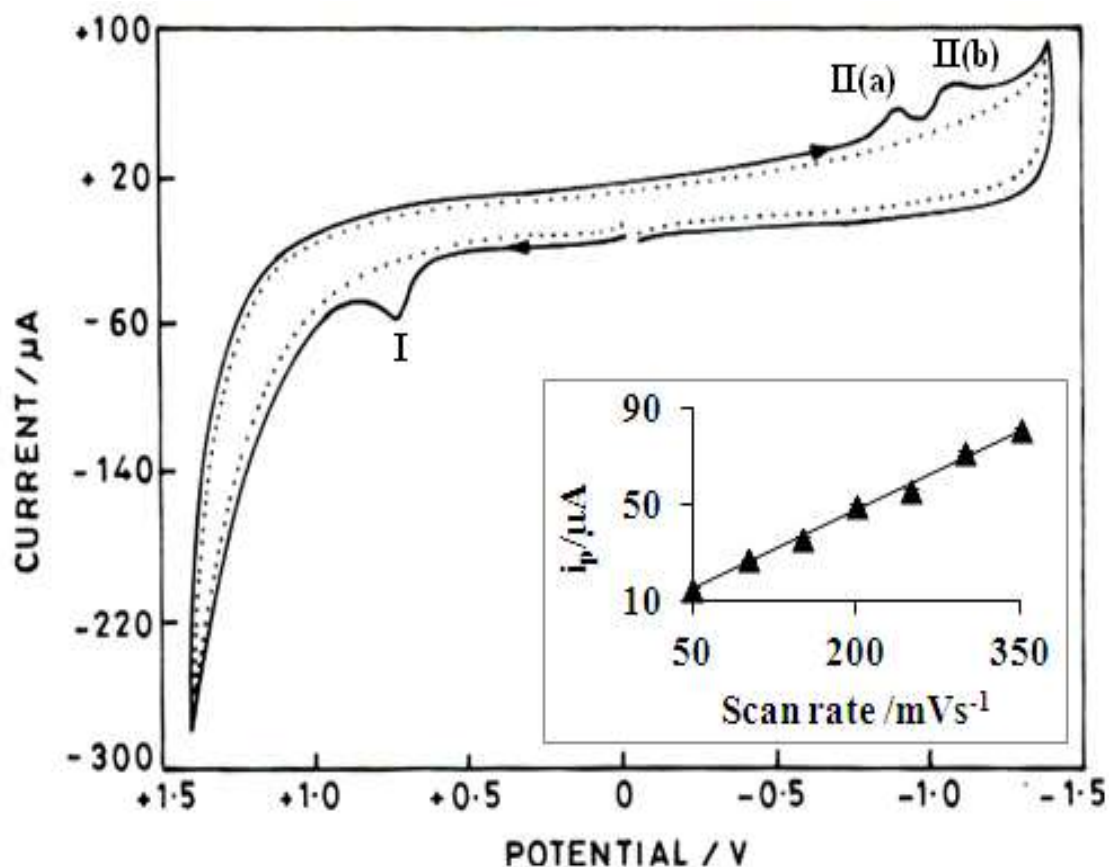
Fig. 5.5: Observed cyclic voltammogram for 6 μM CP at scan rate 100 mVs^{-1} at EPPG/p-DAN/AuNPs (—) and background phosphate buffer (....) at pH 7.20; inset is graph between i_p and scan rate (v)..

5.3.4 Square wave voltammetry

As square wave voltammetry (SWV) is considered to be a more sensitive technique than cyclic voltammetry, hence, further studies are carried out using SWV. Square wave voltammograms were recorded for 6 μM CP at unmodified EPPG, EPPG/p-DAN and EPPG/p-DAN/AuNPs surfaces in phosphate buffer solution of pH 7.2 using the optimized parameters of SWV. On scanning the potential 0-1200 mV, a well-defined oxidation peak is obtained at potential 660 mV at EPPG/p-DAN/AuNPs. Under the similar condition, small bumps were observed at potential 720 mV and 733 mV at EPPG/p-DAN and unmodified EPPG, respectively (**Fig. 5.6**). The remarkable increment in peak current and decrement in oxidation potential proved that EPPG/p-DAN/AuNPs sensor has excellent electrocatalytic properties to enhance the rate of electrochemical process towards the oxidation of CP. Hence, EPPG/p-DAN/AuNPs sensor was used for further analytical studies of CP.
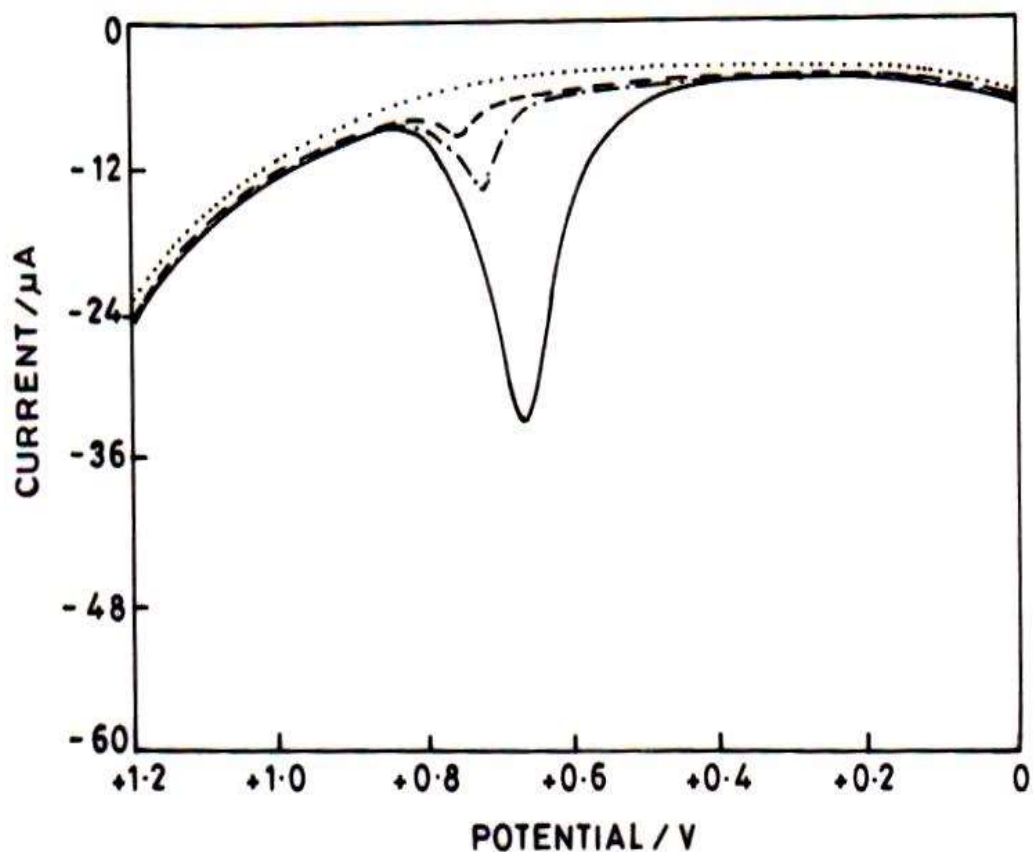
Fig. 5.6: Comparison of square wave voltammogram for 6 μM CP at bare EPPGE (---), EPPG/p-DAN ($-\cdot-$), EPPG/p-DAN/AuNPs (—) and back ground phosphate buffer (...) at pH 7.20.

5.3.5 pH study

The pH of supporting electrolyte has a remarkable effect on the peak potential of the electrochemical species. The effect of pH of phosphate buffers was studied in the range 2.4-11.0 and it was found that the value of peak potential of CP shifted to less positive potential with increase in pH (**Fig. 5.7**). The sharpness of peak and peak current value did not significantly change in the pH range 2.4 to 7.2, but the peak current decreased at pH > 7.2, probably due to the poor availability of protons. Hence, pH of the supporting electrolyte was kept constant at physiological pH 7.2 and all experiments were carried out using this pH. The E_p of CP shifted to less positive potential with increase in pH and the dependence of the E_p on pH of supporting electrolyte at EPPG/p-DAN/AuNPs sensor can be described by the equation:

E_p (pH 2.4 – 11.0) = [-57.62 pH + 1053] V vs. Ag/AgCl

with correlation coefficient of 0.991. The observed value of the slope of dE_p/dpH indicated that equal number of protons and electrons takes part in the electrochemical oxidation of CP. This

behaviour suggests that the oxidation mechanism of CP is closely related to the mechanism of other similar cephalosporin antibiotics [285, 286].
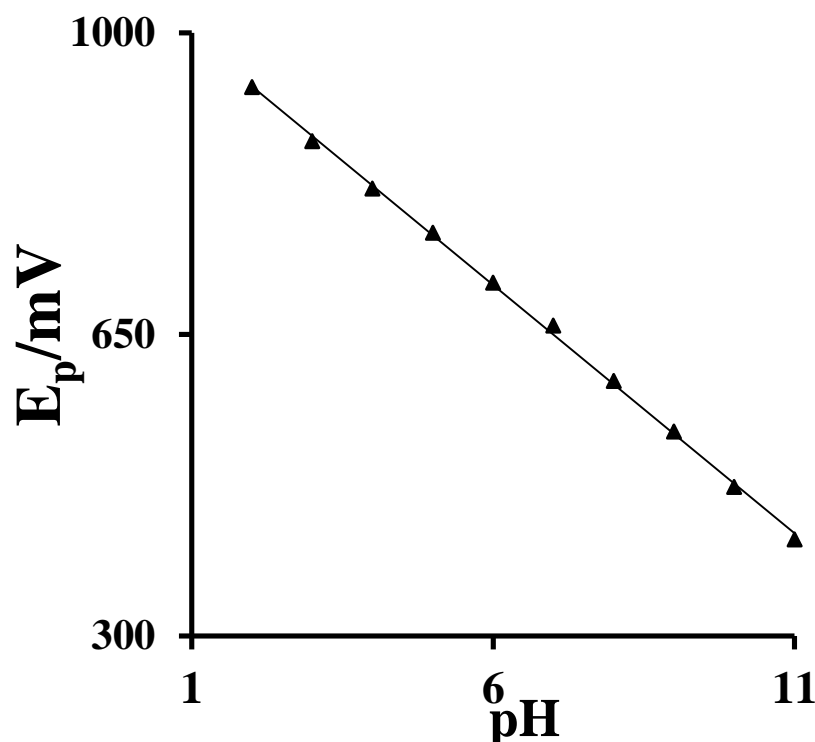
Fig. 5.7: Effect of pH of supporting electrolyte on E_p of CP at EPPG/p-DAN/AuNPs.

5.3.6 Frequency study

The dependence of the anodic peak current of CP on the square wave frequency was studied in range 5-40 Hz using EPPG/p-DAN/AuNPs sensor. The anodic peak current of CP was found to increase linearly with increasing square wave frequency in the range 5-40 Hz (**Fig. 5.8**). The linear relationship between peak current and square wave frequency can be described by the equation:

$i_p = 1.319\,[f] + 9.49$

having R^2 of 0.994, where i_p is peak current in µA and $[f]$ is square wave frequency in Hz. The above voltammtric response further confirmed that the nature of electrode reaction is adsorption controlled [297].
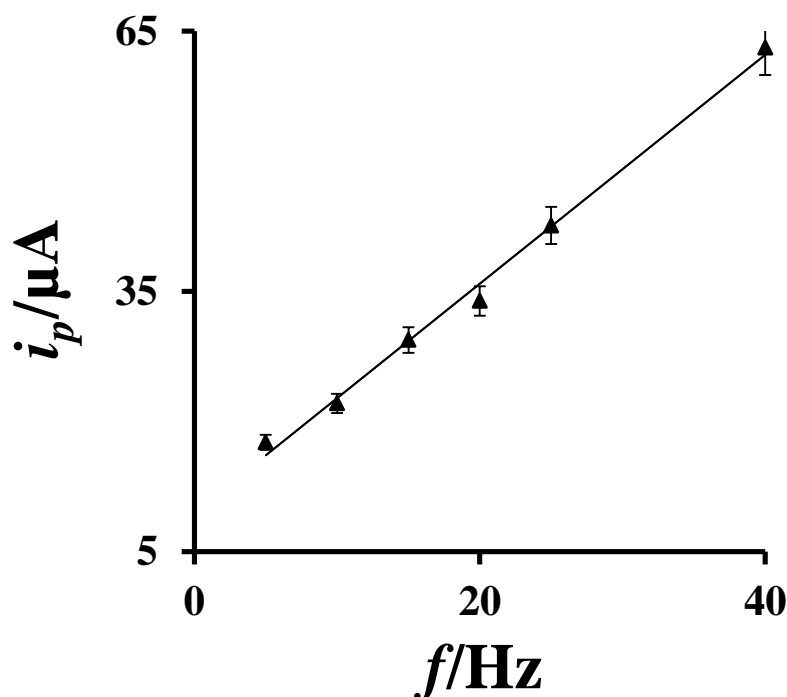
Fig. 5.8: Variation of peak current (i_p) with square wave frequency (f) at EPPG/p-DAN/AuNPs.

5.3.7   Concentration study

The quantitative determination of CP is based on the dependence of the anodic peak current on the concentration of CP. Therefore, square wave volltammograms were recorded at different concentration of CP in the range 0.1 - 20 µM using EPPG/p-DAN/AuNPs surface as shown in **Fig. 5.9A**. The values of the anodic peak current are obtained by subtracting the background current and reported as an average of three replicate determinations. The peaks currents were found to increase with increase in the concentration range 0.1-12 µM of CP and become constant at higher concentrations. The plot of concentration vs. i_p was linear in the range 0.1-12 µM (**Fig. 5.9B**). The linear relationship in anodic peak current and concentration of CP can be expressed by the following regression equation:

$$i_p = 4.621 \ [C] + 3.050$$

with correlation coefficient of 0.990, where i_p is peak current in µA and C is concentration of CP in µM. The sensitivity of the proposed method is found to be 4.621 µA µM^{-1} and the detection limit was found to be 39 nM using the formula 3σ/b where σ is the standard deviation of blank solution and b is the slope of calibration plot. These results indicate that using EPPG/p-DAN/AuNPs sensor CP can be determined in biological fluids.
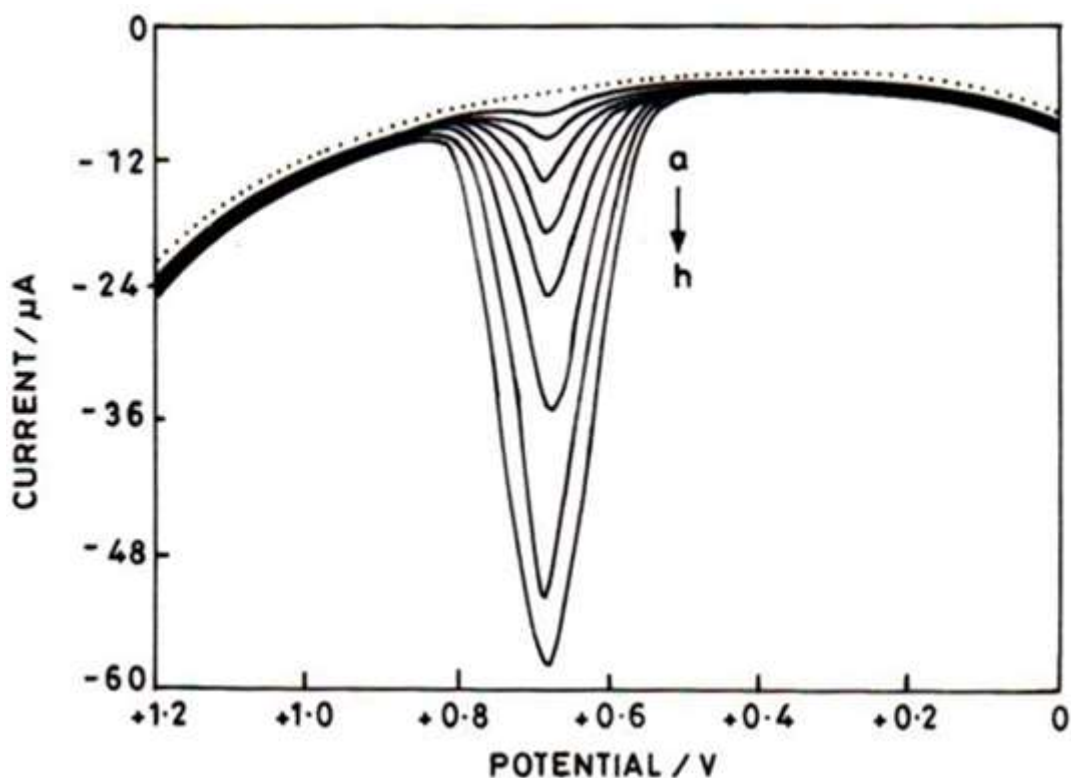
Fig. 5.9A: Observed square wave voltammograms for background phosphate buffer (...) and increasing concentration of CP. Curves were recorded at (a) = 0.1; (b) = 0.5; (c) = 1.0; (d) = 2.0; (e) = 4.0; (f) = 6.0; (g) 9.0 and (h) 12.0 μM concentrations using EPPG/p-DAN/AuNPs in phosphate buffer of pH 7.2.
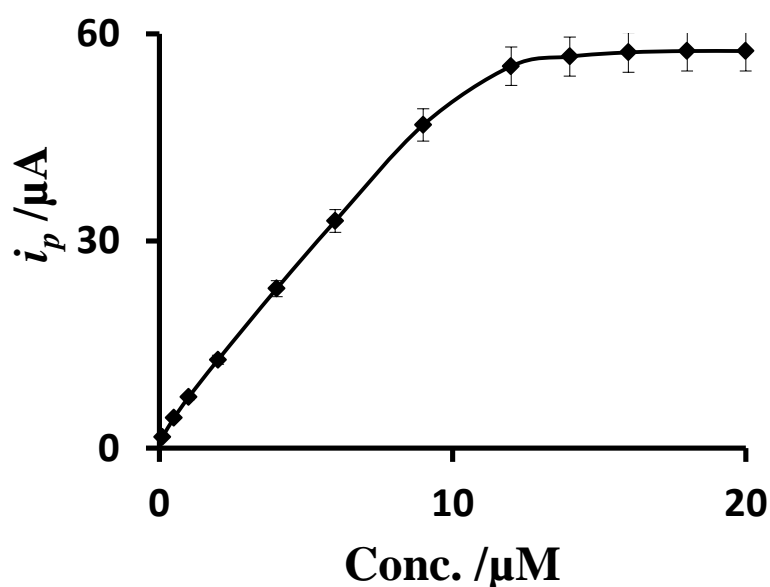
Fig. 5.9B: Calibration curve of peak current versus CP concentration observed at EPPG/p-DAN/AuNPs sensor.

5.3.8 Stability and reproducibility of EPPG/p-DAN/AuNPs sensor

The long-term stability of the EPPG/p-DAN/AuNPs sensor was investigated by measuring the anodic current response for fixed concentration of 1 µM CP over a period of 15 days. The modified sensor was used daily and stored in air. The experimental results revealed that current response of CP deviated interday by ±2.1%, suggesting thereby, that EPPG/p-DAN/AuNPs sensor possessed excellent stability for the determination of CP.

To establish the intraday reproducibility of EPPG/p-DAN/AuNPs, consecutive repetitive determinations (n=10) of 1 µM CP were carried out at the same time and several measurements (n=6) were also made at an interval of 1 h each. The results indicated that the current response deviated during repetitive measurements by ±1.2% and intraday by ±1.9 % exhibiting the excellent reproducibility of EPPG/p-DAN/AuNPs sensor for CP detection.

5.3.9. Interference study

Several metabolites present in urine or blood may alter the electrochemical signal of the sensor and consequently affect the selectivity of developed method. Uric acid, ascorbic acid, xanthine and hypoxanthine are common metabolites present in biological systems, which can interfere in the electrochemical response of CP. Hence, interference study was carried out at pH 7.2 by keeping the concentration of CP fixed at 1 µM and varying the amount of interferents up to 100-fold excess. In all these voltammograms, CP exhibited an anodic peak at 660 mV and some additional peaks were also observed at - 10, 280, 790 and 970 mV corresponding to the oxidation of ascorbic acid, uric acid, xanthine and hypoxanthine, respectively (**Fig. 5.10**). It was found that there was no significant change in the anodic peak current response of CP up to 100-fold excess of each of the interferents. This proved that the developed method can be successfully applied for the determination of CP in human body fluids as well as in pharmaceutical preparations without facing any complexity due to the interferents.
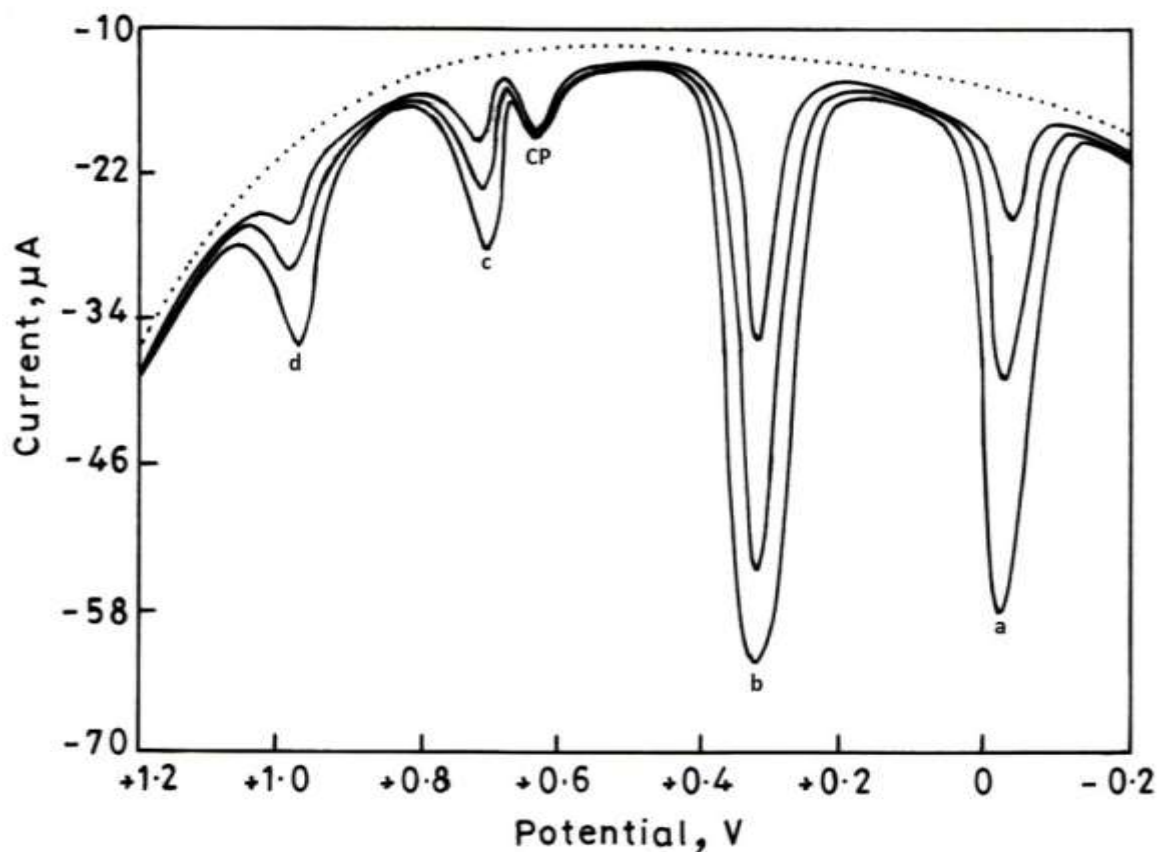
Fig. 5.10: **Square wave voltammograms showing interference of ascorbic acid (peak a), uric acid (peak b), xanthine (peak c) and hypoxanthine (peak d) at fixed CP concentration (1 μM); dotted line shows background current of phosphate buffer.**

5.3.10 Analytical utility

5.3.10.1 Pharmaceutical samples analysis

To demonstrate the applicability of the proposed method in drugs, three commercially available CP containing pharmaceutical samples, viz. Switch-50 (Alkem Lab Ltd., Baddi Himanchal Pradesh), Monocef (Aristo pharma pvt. Ltd., Daman, U.T.), Switch-200 (Alkem Lab Ltd., Baddi, Himanchal Pradesh), were purchased from the local market of Roorkee. Solution was obtained by the dissolution of pharmaceutical samples in methanol and water (1:4) and the samples were subsequently diluted with buffer (pH 7.2) so that concentration of CP lies in the range of calibration plot. Square wave voltammograms were then recorded under identical conditions that were used for the concentration study. Keeping dilution factor in consideration concentration of CP in pharmaceutical samples was determined and the results were in good agreement with the labeled amount as shown in **Table 5.1**. The CP content for all

the pharmaceutical samples were within an error range of -0.7 % to -0.9% demonstrating the good accuracy of the developed method.

Table 5.1: Determination of CP in pharmaceutical samples using EPPG/p-DAN/AuNPs Sensor.

Sample	Stated content (mg)	Determined content[a] (mg)	Error (%)
Switch-50	50	49.62	-0.76
Monocef	100	99.14	-0.86
Switch-200	200	198.04	-0.98

[a] RSD for the determination was $< \pm 2.1\%$ for n=5.

5.3.10.2 Real samples analysis

In order to examine the stability of CP in biological samples and establish the utility of the proposed method, the EPPG/p-DAN/AuNPs sensor was applied for the determination of CP in human urine samples of the patients undergoing treatment with CP. Prior to analysis, the urine samples were diluted 2 times with phosphate buffer to reduce the matrix complexity. Square wave volltammogram of patient urine sample is presented by curve a in **Fig. 5.11A** and a well-defined peak of CP is observed at ~662 mV in addition to peak at 280 mV corresponding to the oxidation of uric acid . To confirm that the peak at 662 mV is due to the oxidation of CP, the sample was spiked with known amount of CP and the peak current increased (**Fig. 5.11A curves b and c**). It was found that peak current of CP increased on spiking CP, while uric acid peak current (at potential ~280 mV) remained constant. The concentration of CP in urine samples of patients before and after spiking was calculated by preparing standard addition plot as shown in **Fig. 5.11B**. The absolute value of x-intercept represents the concentration of CP in urine sample of patient undergoing treatment with CP and is found to be 3.32 μM. These results were validated in form of statistical terms such as precision, RSD% and Bias%, which were found to be 0.054, 1.62% and 0.60%, respectively for n=5, proving the validity of the proposed method.

The recovery experiments were also carried out to check the stability of CP in human body fluids using EPPG/p-DAN/AuNPs. Square wave voltammogram of urine sample of two healthy persons were recorded. The standard addition method was used for recovery experiments. Drug free urine samples were spiked with known concentration of standard

solution of CP. Standard addition plot was used to calculate the concentration of CP and results obtained are summarized in **Table 5.2.** CP showed recovery in the range 101-99%, with relative standard deviation of ±3.4% indicating good stability of CP in human biological samples.
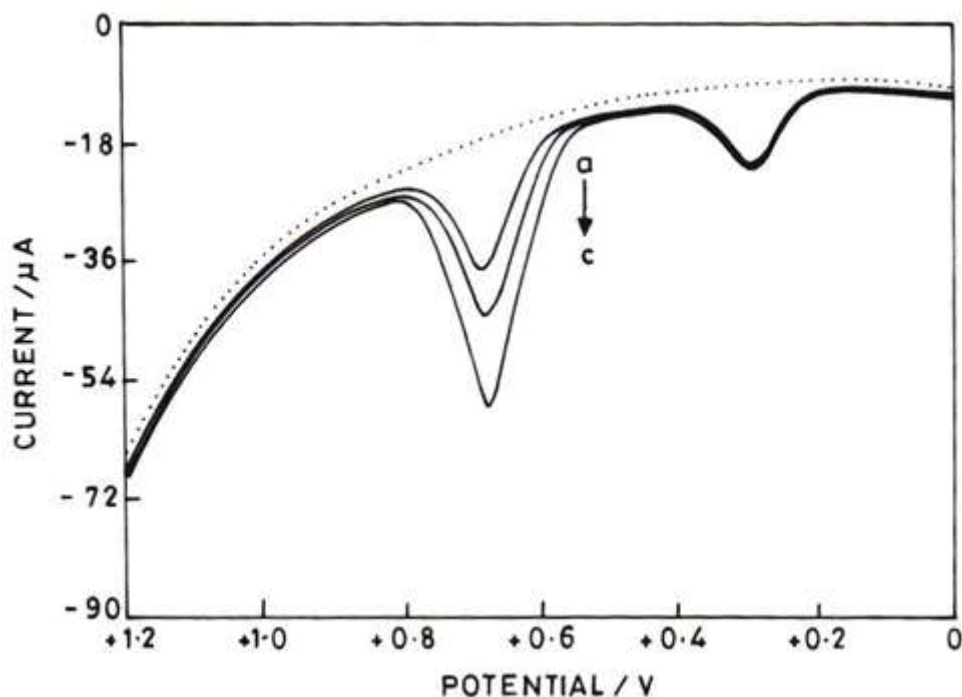
Fig. 5.11A: Square wave voltammograms observed for determination of CP in urine sample of patient (peak a) and after spiking (peaks b and c) with standard CP; dotted line shows blank at pH 7.20.
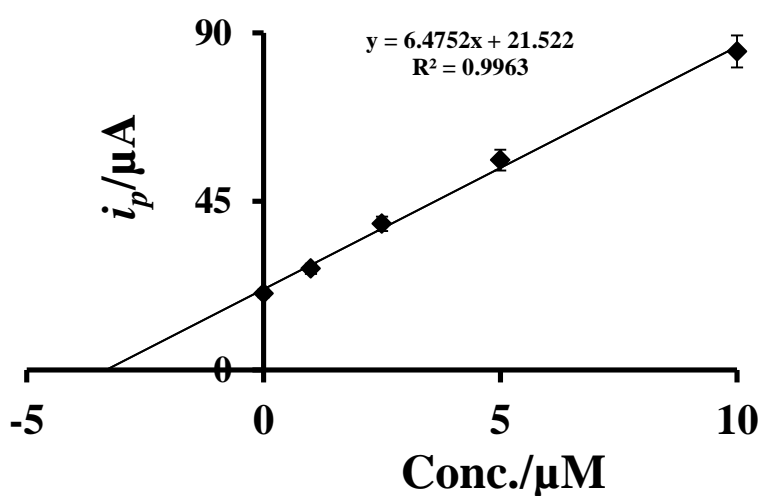
Fig. 5.11B: The observed standard addition plot of CP.

Table 5.2: Recovery analysis of CP in urine samples of healthy person at EPPG/p-DAN/AuNPs sensor.

	Spiked amount (µM)	Detected amount[a] (µM)	Recovery (%)
	0.5	0.49	98
Sample 1	1	0.97	97
	1.5	1.48	98.67
	0.5	0.48	96
Sample 2	1	0.98	98
	1.5	1.49	99.33

[a] The R.S.D. value for CP determination was less than ± 3.4 % for $n=3$.

5.3.11 Validation with HPLC

In order to prove the reliability of data obtained and validate the result of voltammetric determination of CP, HPLC method was used. For this purpose different concentrations of standard CP were analyzed using HPLC and a well-defined peak was obtained at retention time (R_t) ~2.869 min. The peak area under the peak was calculated and a calibration curve was obtained by plotting the peak area of the CP peaks against concentration. We obtained a linear calibration plot and finally the concentration of CP was determined in urine samples. Typical HPLC chromatograms observed for human urine sample of patients undergoing treatment with CP exhibited five peaks at R_t ~ 1.400, 1.549, 1.940, 2.068 and 2.869 min (**Fig. 5.12**). The peak at R_t ~2.869 is found to be due to CP, whereas, other peaks are due to the common metabolites present in urine samples. Concentration of CP in urine sample was calculated using calibration plot of standard CP obtained from HPLC analysis. These results were compared with the results obtained from real sample analysis (**Table 5.3**). The results clearly indicated that the results obtained by the two methods are in good agreement confirming the accuracy of the present protocol. In addition, HPLC method and electrochemical method were compared by performing student's t-test and F-test at significance level of 0.05. The t-values and F-values were observed as 0.012 and 1.091, respectively, which were smaller than the critical values of these observation, indicating strong evidence towards the null hypothesis (i.e. results of both treatments do not differ from one another). Values of probability factor for t and F tests were 0.991 and 0.479, respectively, which were much higher than that of significance level, further confirming the high probability of getting these results. These observations provide a big support to claim the accuracy of both methods.
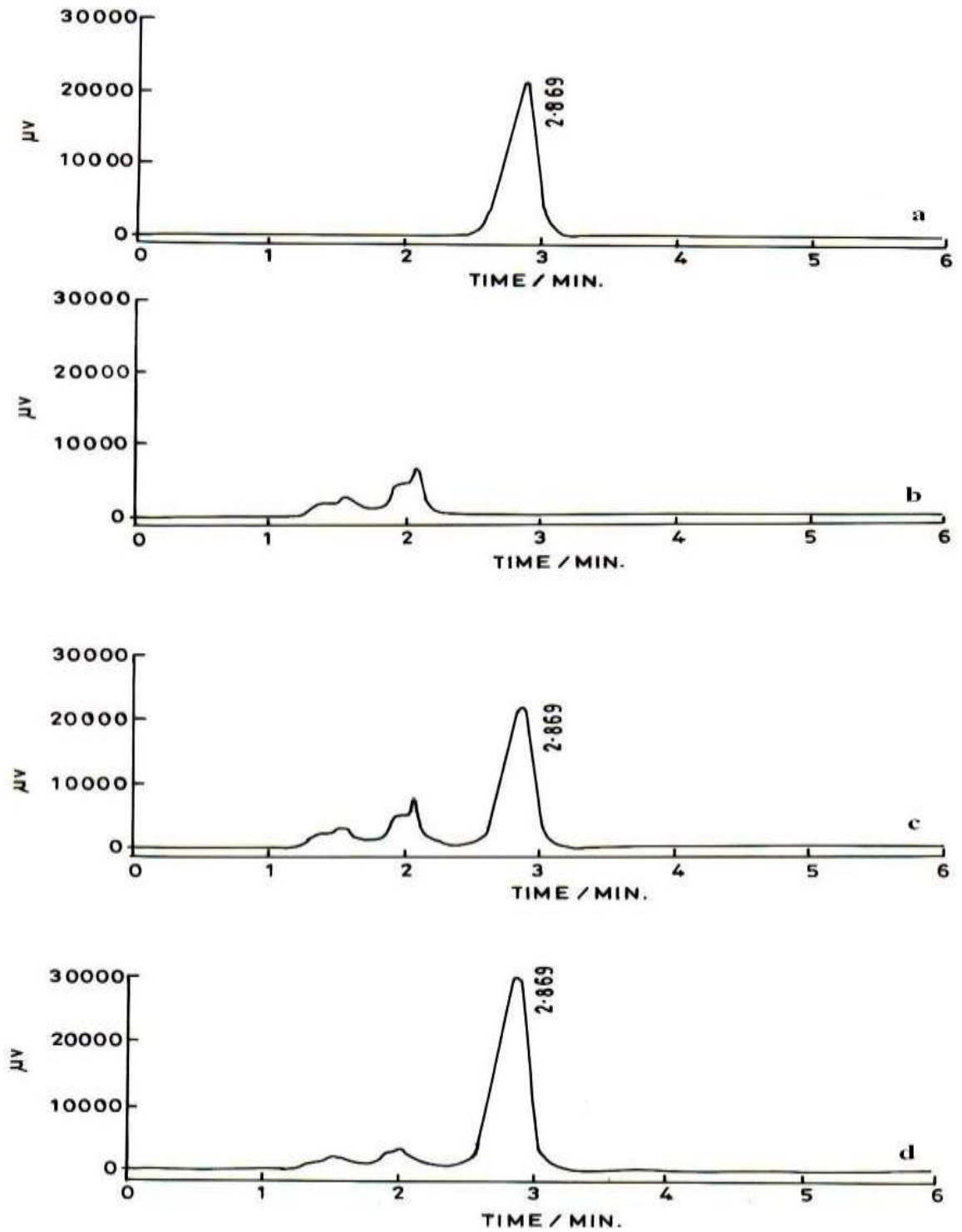
Fig. 5.12: Observed HPLC chromatograms of (a) standard CP (b) control urine (c) patient urine sample 1 treated with CP (d) patient urine sample 1 after spiking with CP.

101

Table 5.3: HPLC validation of the results obtained for the determination of CP in human urine samples at EPPG/p-DAN/AuNPs sensor after 6 h of oral administration of CP.

Sample	Observed CP concentration (µM) determined by	
	EPPG/p-DAN/AuNPs	HPLC
1	3.32 (1.01%)	3.34 (1.21%)
2	3.34 (2.13%)	3.33 (1.76%)
3	3.92 (1.87%)	3.90 (3.76%)
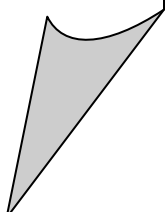
The values in brackets represents the relative standard deviation for *n*=3 determination.

5.4 CONCLUSIONS

The proposed work provides an extremely sensitive and selective electroanalytical method for the determination of CP in pharmaceutical samples as well as in biological fluids using EPPG/p-DAN/AuNPs sensor. The fabricated sensor was characterized by XPS and SEM studies. p-DAN modified pyrolytic graphite having AuNPs not only significantly increased the anodic peak current but also shifted the peak potential of CP to lower potentials as compared to the unmodified EPPG. The enhanced eletrocatalytic activity is attributed to the conductivity of polymer coated electrode and increased surface area due to gold nano-particles. Unique properties of AuNPs, such as stability, sensitivity and ability of electrocatalysis, have been shown to be a versatile tool to construct sensors due to which AuNPs have been used by several earlier researchers [139, 298]. The combination of conductive polymer and AuNPs allowed the successful determination of CP with a detection limit of 32 nM. This detection limit is much lower than reported in literature in which determination of CP is based on reduction [282, 283]. The selectivity of the present method was also investigated in the presence of other substances present in complex matrix. The application of the developed method for the determination of CP in urine of patients undergoing treatment with CP has also been carried out and the results are compared with HPLC. An excellent correlation between the two techniques is observed indicating thereby that the proposed work is sensitive and selective for the determination of CP.

CHAPTER 6

In vitro chloramphenicol detection in a Haemophilus influenza model using an aptamer-polymer based electrochemical biosensor

6.1 INTRODUCTION

Chloramphenicol (CAP) is a broad spectrum antibiotic, which inhibits the activity of both Gram-positive and Gram-negative bacteria [299]. It is an antimicrobial drug which was first obtained from the culture of a soil bacterium Streptomyces venezuelae and was chemically synthesized in 1948 [300]. It is the drug of first choice for the treatment of vancomycin-resistant enterococcus, tetracycline-resistant vibrio cholera and the patients having severe penicillin or cephalosporin allergy. Although CAP is clinically important, it has some serious harmful effects which form the basis of CAP detection in various clinical, environmental, and pharmaceutical samples. Many countries such as USA, Canada, and China have banned the use of CAP in food producing animals. The United States food and drug administration has decided the "minimum required performance limit" (MRPL) of CAP as 0.3 $\mu g\ kg^{-1}$ for the detection of its residues in food products [301, 302]. Thus, it is interesting and extremely important to develop a simple, sensitive, and selective method for CAP detection in the *in vitro* and real sample.

CAP has been detected using various techniques such as; gas chromatography-mass spectrometry [303], liquid chromatography-tandem mass spectrometry [304], capillary electrophoresis with amperometric detection [305], enzyme immunoassay [306] and electrochemical sensors using variety of unmodified and modified electrodes [307-309]. An aptasensor has also been reported in literature for the determination of chloramphenicol [310]. A short review dealing with electrochemical and immunosensing strategies for the detection of CAP has also appeared in the literature [311]. Recently single wall carbon nanohorns –TiO2 – porphyrin modified electrode has also been used for the determination of CAP and sandwich nano structure of the electrode has been found to exhibit good analytical performance [312]. Although these methods can be used to detect CAP but they require multiple steps fabrication and long analysis time, thus limited in their real applications. Also, the reported immunosensors for the detection of CAP require animal models for the antibody production, hence are expensive. Additionally, antibodies can be easily denatured, and hence affect the long term storage of the immunosensor. It is, therefore, desirable to develop a single step, sensitive, selective, quick, less expensive, and easily fabricable biosensor for CAP detection. To achieve a robust and simple detection method for CAP, an aptamer is one of the candidate probe materials because it has been widely used to detect important clinical molecules with different fabrication approaches [313].

A polymer modified sensor is the class of chemically modified electrodes which comprise a novel approach to electrode system and are very useful in basic electrochemical investigations [288, 314-317]. Compared to the other electrodes, edge plane surface of pyrolytic graphite (EPPG) has been widely used due to its wide potential window and minimum possibility to show deteriorated response as a result of surface fouling. Hence, we used a poly-(4-amino-3-hydroxynapthalene sulphonic acid) (p-AHNSA) coated EPPG for the quantitative detection of CAP.

The resistance of CAP in different bacterial species has a significant impact on the public health and clinical implications, particularly in the areas of the world where these bacterial strains are endemic. The availability of rapid and sensitive screening methods for the detection of CAP resistance is extremely important. In the present study, we fabricated a simple and efficient aptamer based biosensor for the direct *in vitro* determination of CAP. Electro-polymerization of AHNSA onto the EPPG was carried out to increase the surface area for the aptamer interaction due to the electrostatic interaction between sulphonic acid group and amino group, providing significant signal amplification, for the CAP detection. *H. influenza* was used to investigate the *in vitro* CAP detection ability of the biosensor. The experimental parameters affecting the CAP detection in standard solution and in *in vitro* detection were optimized and the detection limit of CAP was determined. The drug resistant and sensitive *H. influenza* strain was identified using the fabricated biosensor based on the CAP accumulation.

6.2 EXPERIMENTAL

6.2.1 Instrumentation

The electrochemical measurements were carried out using a BAS (West Lafayette, USA) CV-50W voltammetric analyzer. Voltammetric cell used was a single compartment glass cell containing aptamer immobilized polymer modified edge plane pyrolytic graphite sensor, Ag/AgCl (3 M NaCl) as reference electrode (model BAS MF-2050 RB-5B) and a platinum wire as counter electrode. The pH of buffer solutions was measured using pH meter (model Eutech pH 700). The pyrolytic graphite piece was obtained from Pfizer Inc., USA as a gift. The micro structure of working electrode surface was characterized using field emission scanning electron microscopy (Quanta 200 FE-SEM).

6.2.2 Chemicals and reagents

The aptamer sequence used in the present study was procured from Genxbio Health Sciences, India, and had the sequence: (5′-NH2-ACTTCAGTGAGTTGTCCCACGGTCGGCGAGTCGGTGGTAG-3′) [318]. CAP and 4-amino-3-hydroxynaphthalene sulfonic acid were obtained from Sigma–Aldrich Inc., USA and used as received without further purification. Phosphate buffers of different pH and ionic strength (μ = 1.0 M) were prepared by the reported method using analytical grade chemicals. The double distilled water was used to prepare the solutions [174].

6.2.3 Fabrication of aptamer/p-AHNSA/EPPG biosensor

Prior to modification, the edge surface of pyrolytic graphite was cleaned by rubbing it on an emery paper (P-400), washed with double distilled water and then dried. The electrochemical polymerization of AHNSA on the EPPG was carried out using CV in a solution containing 2 mM of AHNSA in 0.1 M HNO_3 solution. The cyclic voltammograms were recorded by scanning the potentials between - 0.8 V and + 2.0 V at a scan rate of 0.1 Vs^{-1} for 15 scans. The film obtained was rinsed with double distilled water. In the next step electrode was cycled between - 1.0 and + 1.0 V at a scan rate of 0.1 Vs^{-1} in 0.5 M H_2SO_4 until a stable voltammogram is obtained. The polymer modified sensor was then rinsed with water, and dried under nitrogen. Next, the immobilization of aptamer on to the polymer modified EPPG was carried out by the spin coating technique. The appropriate aptamer concentration prepared in tris EDTA buffer (pH 8.0) was coated on the polymer film and left over night. Thereafter, the modified electrode was washed with the same buffer followed by 0.1 M mercaptoethanol for 2 min to remove any unbound aptamer. The final fabricated electrode is termed as aptamer/p-AHNSA/EPPG biosensor. Further, the cyclic voltammetric response of the aptamer/p-AHNSA/EPPG biosensor was studied in phosphate buffer of pH 7.2. No oxidation or reduction peak was observed in this case and hence, it was concluded that the polymeric layer was not electroactive in the neutral medium. Similar observation is also reported in the literature [317].

6.2.4 Voltammetric procedure

The stock solution of 50 μM of CAP was prepared by dissolving the required amount in double distilled water. For electrochemical experiments, a required amount of the stock solution was further diluted. For the detection of CAP, the aptamer/p-AHNSA/EPPG was dipped in CAP solutions of various concentrations for appropriate time at room temperature

and the electrochemical response of the biosensor was checked in a deoxygenated phosphate buffer to avoid the oxygen interference. The optimized square wave voltammetric conditions to record square wave voltammograms were as follows: initial (E): - 400 mV, final (E): - 1000 mV, square wave amplitude (E_{sw}): 25 mV, potential step (E): 4 mV, square wave frequency (*f*): 15 Hz. The surface of aptamer/p-AHNSA/EPPG was cleaned after each run by applying a potential of -100 mV for 120 s to remove the adsorbed CAP from the surface.

6.2.5 Preparation and processing of *H. influenza* bacterial cultures

Various strains of *H. influenzae* were cultured in the laboratory on a chocolate agar medium with added X(Hemin) & V(NAD) factors at 37°C in an enriched CO_2 incubator. The broth cultures were prepared in supplemented brain-heart infusion (sBHI) broth. The bacterial cultures were stored frozen in skim milk at - 80°C when not in use and inoculated onto solid media prior to each experiment. The bacterial cultures were grown to mid-log phase in sBHI and after centrifugation cells were treated with 10 μM CAP for different time intervals. After this step cells were centrifuged and CAP was assayed in the supernatant using the developed aptamer sensor. Before each experiment bacterial cells were counted using a hemocytometer under optical microscope.

6.3 RESULTS AND DISCUSSION

6.3.1 Characterization of aptamer/p-AHNSA/EPPG biosensor

The developed biosensor was characterized using electrochemical techniques and quartz crystal microbalance studies. **Fig. 6.1A** shows the repetitive cyclic voltammograms of 2 mM AHNSA in a 0.1 M HNO_3 at bare EPPG. In the first scan AHNSA monomer shows two anodic peaks ($E_p \sim +146$ and $\sim +415$ mV) and three cathodic peaks ($E_p \sim +44.5$, $\sim +331.9$ and ~ 1384 mV). In the consecutive scans an additional anodic peak began to appear at 1706 mV. Upon continuous scanning, the peak current of these peaks increases indicating the formation of the conducting electrode surface. The peaks having peak potential 1384 and 1706 mV did not increase much as compared to other peaks as they were not related to the oxidation of 4-amino-3-hydroxynapthalene sulphonic acid [317].

After the polymerization step, the electrode was cycled in 0.5 M H_2SO_4 until a stable voltammogram was obtained. A typical cyclic voltammogram of p-AHNSA/EPPG observed in 0.5 M H_2SO_4 is presented in **Fig. 6.1B** and shows three redox couples a-a', b-b' and c-c', which confirms the successful formation of the polymer film at the electrode surface. The polymer

modified surface was then characterized by FE-SEM to confirm the formation of polymer film. A comparison of FE-SEM images of bare and polymer modified EPPG is presented in the **Fig. 6.2**. The morphology of the polymer modified EPPG surface shows layer of polymer and was completely different as compared to the bare EPPG surface. This was due to the coverage of the electrode surface by polymer film. These results clearly indicate that p-AHNSA has been successfully coated on the electrode surface.
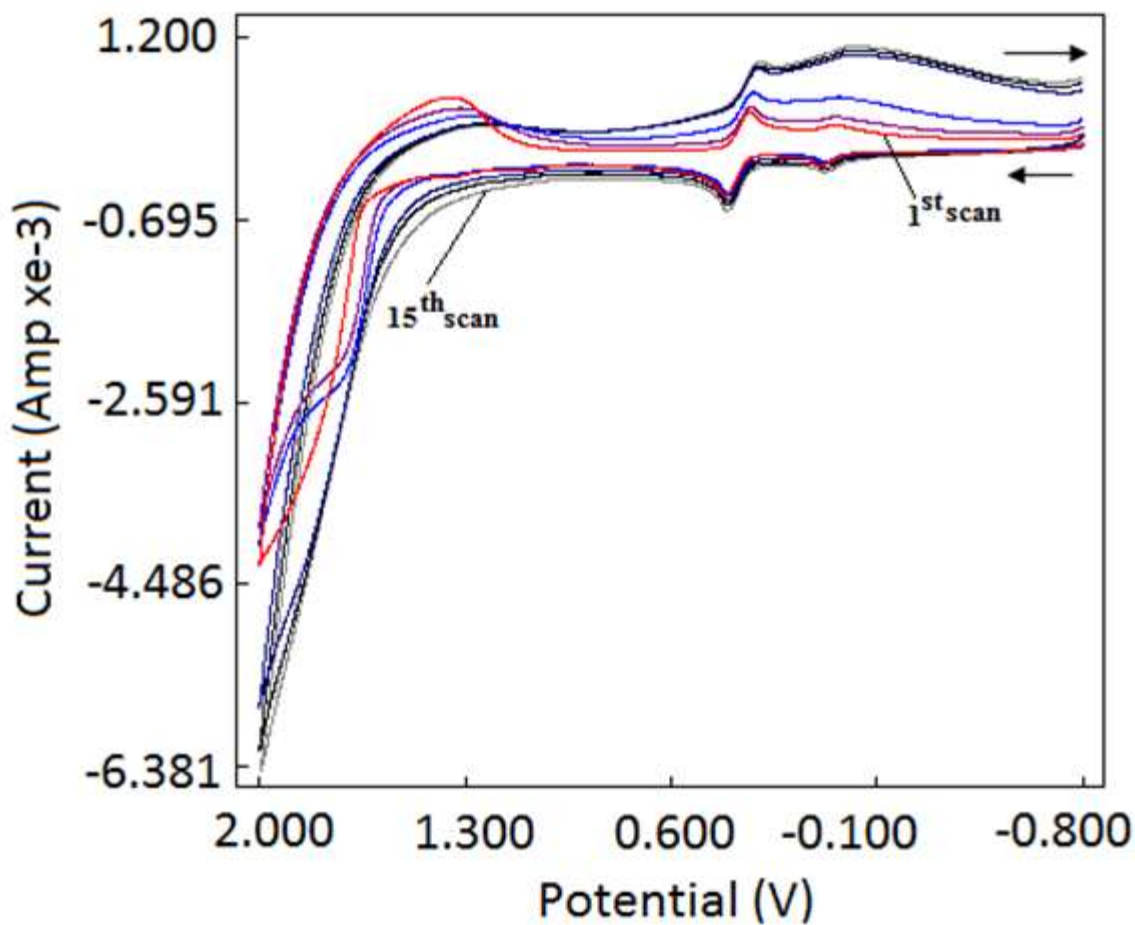
Fig. 6.1A: Cyclic voltammograms observed during electro polymerization of AHNSA in 0.1 M HNO₃ at scan rate of 0.1 Vs⁻¹.
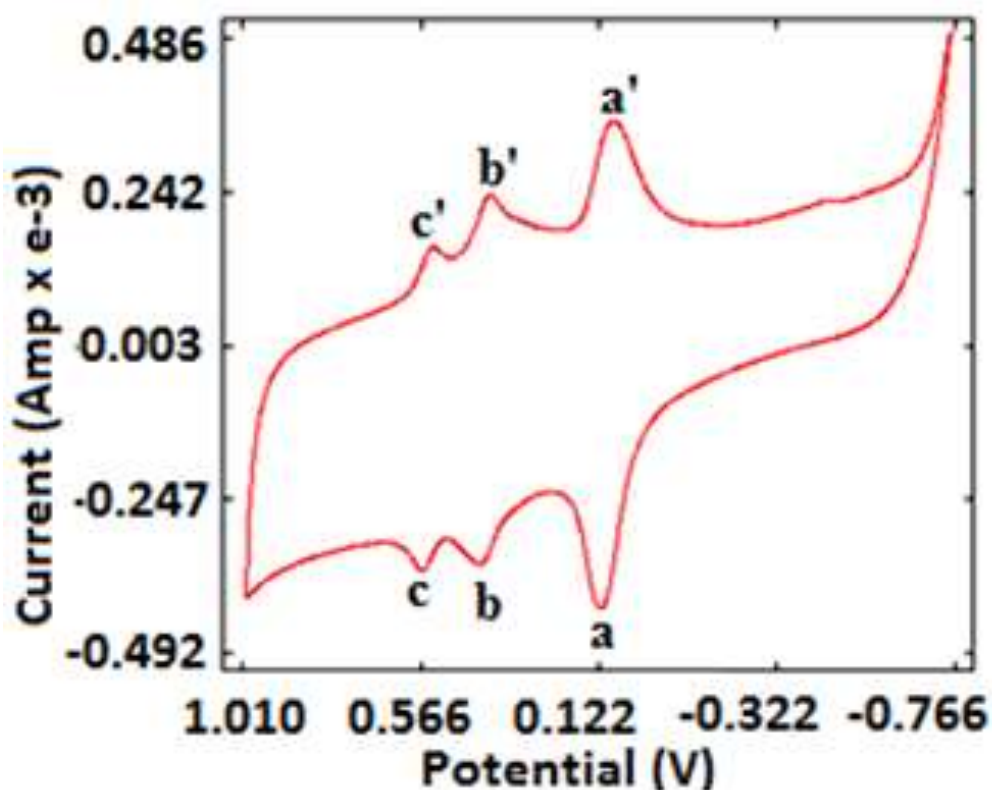
Fig. 6.1B: An enlarged view of cyclic voltammogram of polymer film in 0.5 M H_2SO_4.
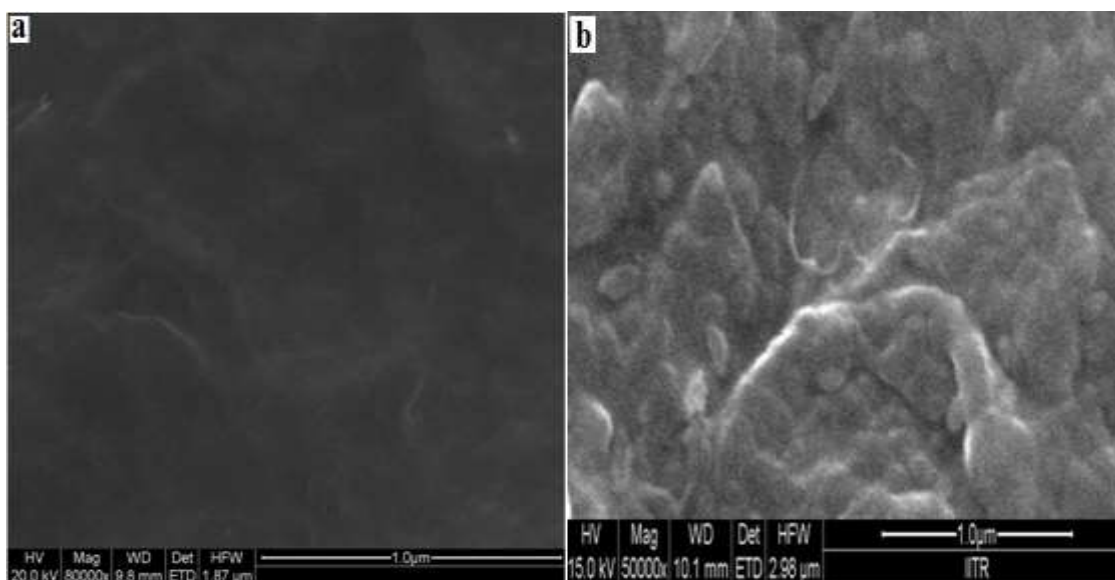
Fig. 6.2: FE-SEM images of (a) bare EPPGE (b) p-AHNSA/EPPGE.

Further studies were performed through QCM experiments to confirm the interaction between aptamer and p-AHNSA/EPPG surface based on the frequency change. The plot observed for change in Δf with time is presented in **Fig. 6.3**. In this case, the decrease in frequency reaches a complete steady state after about 45 min, with an overall frequency change

(Δf) of 0.76 Hz, corresponding to a mass change (Δm) of $8.34 \pm 0.31 \times 10^{-10}$ g based on the following equation $\Delta m = \Delta f \times 5.608$ (ng/cm^2) / Hz $\times 0.196$ cm^2. In this equation, Δf is the change in frequency, 5.608 (ng/cm^2)/ Hz is the sensitivity factor calculated from the physical constant for quartz, and 0.196 cm^2 is the electrode area [319]. The number of molecules per area for the aptamer on the surface was determined to be 1.8×10^{-10} mol cm^{-2}. These results confirm that the aptamer has successfully interacted with the p-AHNSA/EPPG surface.
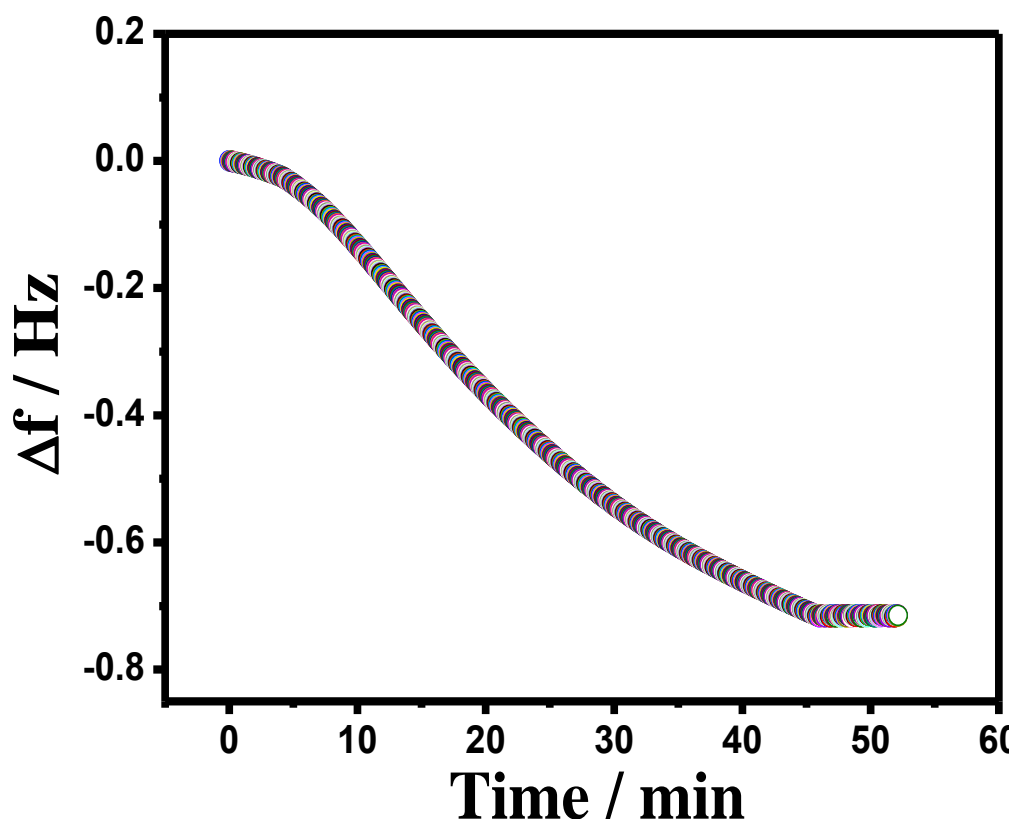
Fig. 6.3: Observed plot for change in Δf with time.

6.3.2 Electrochemical characterization of CAP at aptamer/p-AHNSA/EPPG

The cyclic voltammetric response of the aptamer/p-AHNSA/EPPG biosensor was studied in phosphate buffer of pH 7.2. No oxidation or reduction peak was observed in this case and hence, it was concluded that the polymeric layer was not electroactive in the neutral medium. Similar observation is also reported in the literature [317]. The voltammetric studies of CAP were carried out by dipping the aptamer/p-AHNSA/EPPG electrode in CAP solutions. The fabrication of sensor, chemical structure of AHNSA and CAP and mechanism of biosensing of CAP by the sensor is shown in **Fig. 6.4**. Initially the polymeric layer is formed at the surface of EPPG as shown in **Fig. 6.4 (A)**. The aptamer is then attached to the polymer

modified surface of EPPG, which then captures CAP. The reduction of CAP then occurs to give voltammetric signal. The chemical structures of CAP and the monomer 4-amino-5-hydroxynaphthalene sulfonic acid are presented in **Fig. 6. 4 (B)** and **(C)** respectively. The *in vitro* sensing mechanism of CAP resistant and CAP sensitive H. influenza is shown in **(D)**. In the case of CAP resistant *H. influenza*, the concentration of CAP in the supernatant is much higher than CAP sensitive *H. influenza*. Cyclic voltammetry (CV) is the most effective and versatile electroanalytical technique available for the mechanistic study of redox systems, hence, initially, cyclic voltammograms were recorded for CAP using aptamer/p-AHNSA/EPPG at pH 7.2. **Fig. 6.5** shows the CV of 2 μM CAP solution at aptamer/p-AHNSA/EPPG. In the first negative scan only one reduction peak I_c is appeared at 660 mV, which corresponds to the electrochemical reduction of NO_2 group of CAP to hydroxyl amine [300, 320]. In the reverse scan an oxidation peak (II_a) is observed at 62 mV which formed a quasi-reversible couple with peak II_b (112 mV) observed in the cathodic scan. To confirm the quasireversible nature of the redox couple (II_a/II_b), effect of sweep rate was studied. It was found that in the low sweep rate range (10–150 mV s^{-1}), the peak potentials were practically constant with ratio of peak currents as 1.0. However, at higher sweep rates, the ΔE_p value increased indicating quasi-reversible nature of the redox couple. To confirm that peak II_a is not due to the oxidation of CAP, voltammogram was also recorded by initiating the sweep in the positive direction. No oxidation peak was noticed in this case, it was necessary to record peak I_c to see other peaks (II_a and I_b). When number of cycles increased, peak current of peaks II_a and II_b increased, whereas peak current of irreversible peak (I_c) decreased indicating that product of irreversible reduction is responsible for the formation of redox couple (II_a and II_b). The 4e, 4H$^+$ reduction of the nitro group of CAP to hydroxylamine has been well documented at the mercury electrode in literature [321]. Further oxidation of hydroxyl amine derivative in 2e, 2H$^+$ reaction has been found to give nitroso derivative. The detailed mechanism for the reduction of CAP has already been reported in literature [300].
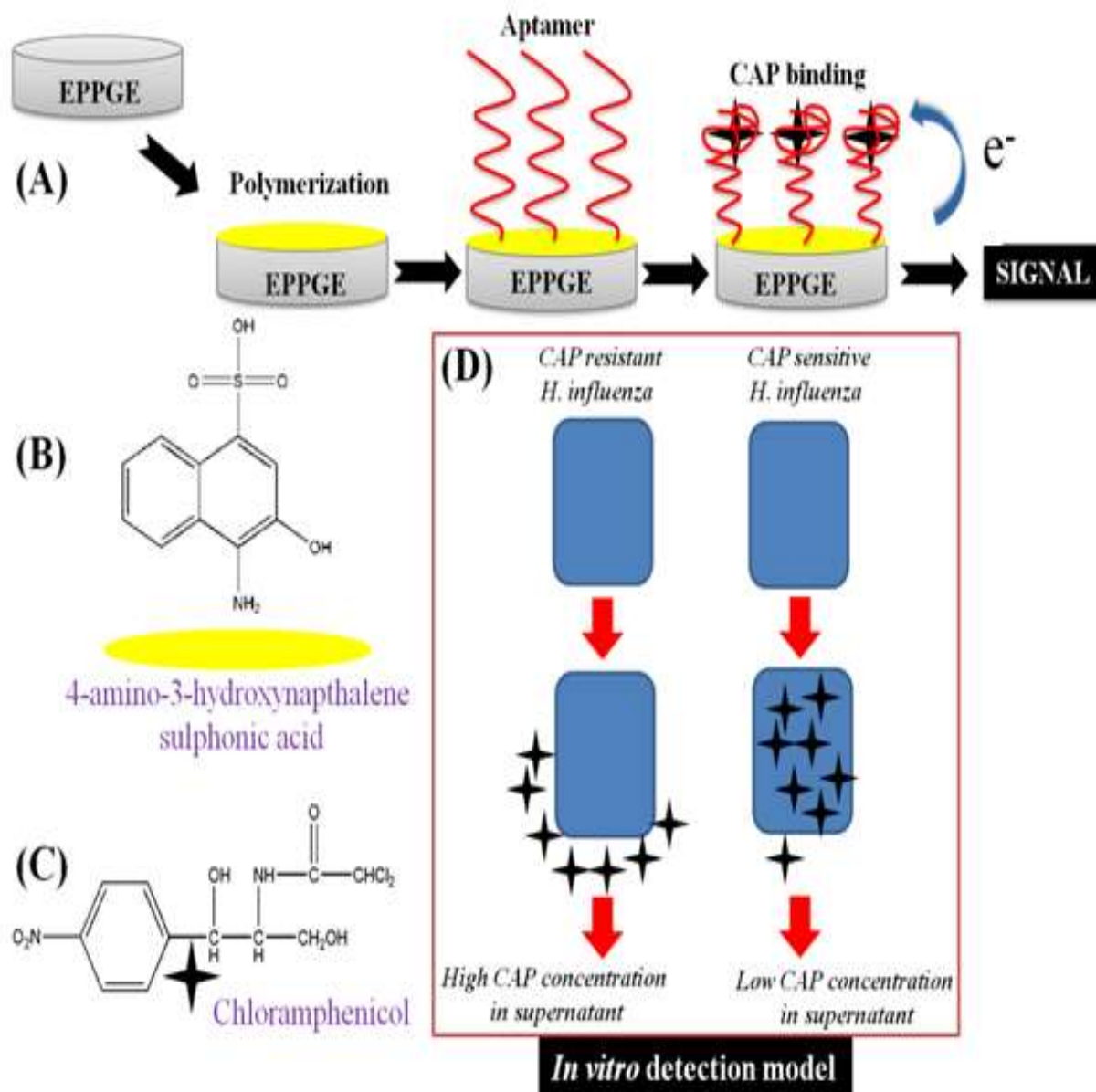
Fig. 6.4: (A) Schematic representation of the biosensor fabrication, (B) chemical structure of 4-amino-3-hydroxynapthalene sulphonic acid monomer, (C), chemical structure of chloramphenicol, (D) *in vitro* **detection model for CAP detection using** *H. influenza.*

To determine the nature of the electrode reaction, sweep rate studies were performed in the range 25 - 250 mVs^{-1}. The peak current was found to increase linearly with increasing sweep rate as shown in inset of **Fig. 6.5.** The dependence of scan rate on peak current of CAP is expressed by the equation:

i_p /μA = 1.766 [v] − 16.63

with the correlation coefficient of 0.979, where i_p is the peak current and v is scan rate in mVs^{-1}. To further confirm the mechanism of electrode reaction, a graph was plotted between log i_p and log v. The slope of this graph was found to be ~ 1.07 confirming that the electrode process is adsorption controlled [230, 229]. A similar experiment was performed at bare EPPG and p-AHNSA/EPPG surfaces for 2.0 µM CAP, where the current signal observed was substantially lower as compared to the aptamer/p-AHNSA/EPPG modified surface (11.8, 24 and 120 µA respectively). The E_p of main reduction peak (I_c) of CAP at these surfaces was -585, -450 and -660 mV respectively. This was due to the successful capturing of CAP due to the aptamer present on the sensing surface. Hence, a stable and higher signal was observed at aptamer/p-AHNSA/EPPG modified surface.
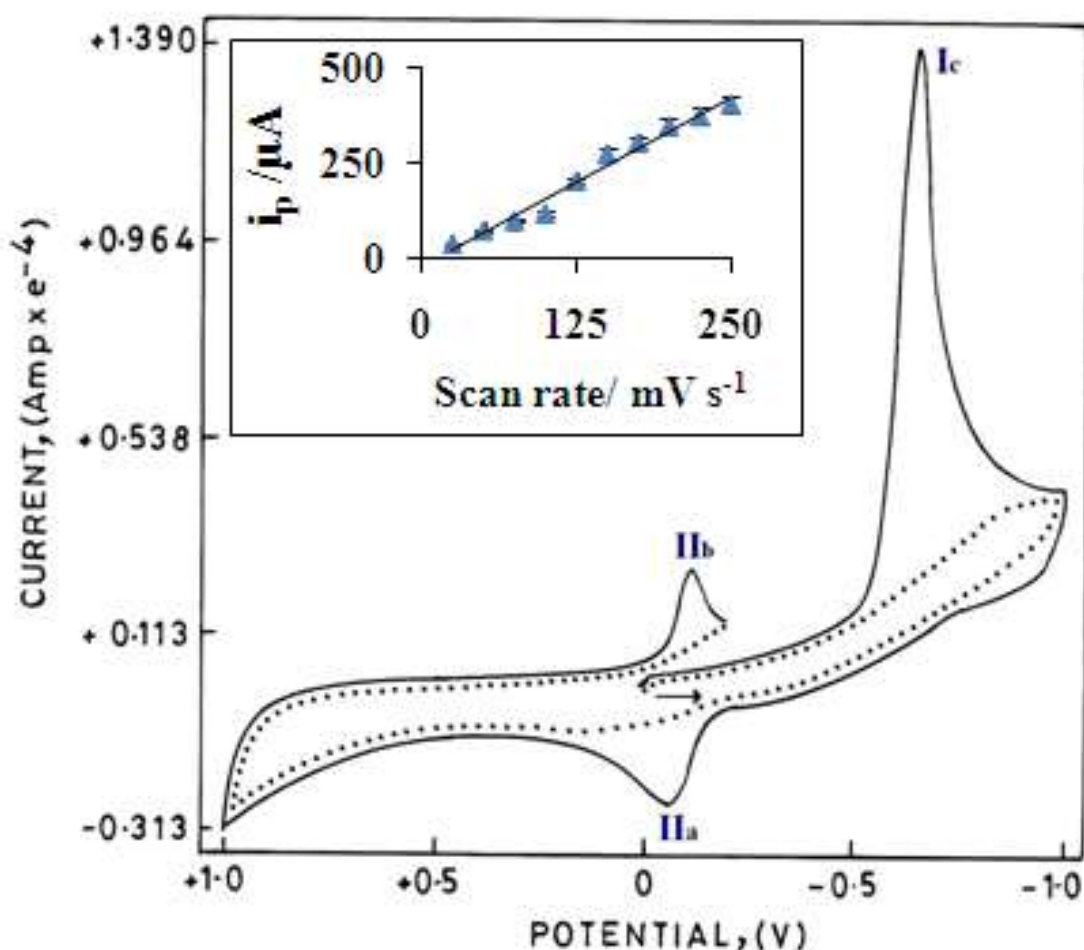
Fig. 6.5: A typical cyclic voltammogram of 2 µM CAP at aptamer/p-AHNSA/EPPG in phosphate buffer of pH 7.2 at a scan rate of 0.1 Vs^{-1}. The background buffer is shown by dotted line. Inset is the graph between peak current and scan rate for peak I_c

The experimental parameters for the analysis of CAP with the aptamer/p-AHNSA/EPPG were optimized for the concentration of immobilized aptamer, temperature, and

reaction times, where the CAP concentration was kept constant and were used throughout the studies.

6.3.3 Optimization of experimental parameters

Several parameters were optimized systematically for the detection of CAP, including the amount aptamer immobilized, incubation time and dipping time in CAP solution. The optimum amount of aptamer immobilized was decided by varying the amount from 0.5 to 10 µL which was dropped onto the active surface of polymer coated EPPG. The effect of aptamer amount on the electrochemical response of 10 nM CAP is shown in **Fig. 6.6 (a)**. It was found that on increasing the amount of aptamer from 0.5 to 5 µL, reduction current of CAP is increased and it goes to maximum when amount is reached to 6 µL, however, further increase in aptamer amount up to 10 µL leads to no significant response in peak current, due to the saturation of the active sites of aptamer. Therefore, 6µL was selected as an optimum amount.

The incubation time plays an important role in the interaction between aptamer and polymer. The results showed that the interaction between aptamer and polymer increased with increasing the incubation time from 1 h to 10 h as shown in **Fig. 6.6 (b)**. It was found that maximum interaction is observed at 5 h, therefore this time was chosen as an optimum incubation time.

Another important parameter is the dipping time of aptamer/p-AHNSA/EPPG in CAP solution. Electrode was dipped in CAP solution and time was varied from 5 to 30 min at fixed concentration (10 nM) of CAP and response was checked by recording voltammogram. It is observed that maximum binding in between aptamer and CAP takes place when electrode is dipped for 20 min. Effect of dipping time on electrochemical response of CAP can be seen in **Fig. 6.6 (c)**. After optimizing the various parameters voltammetric studies of CAP were carried out.
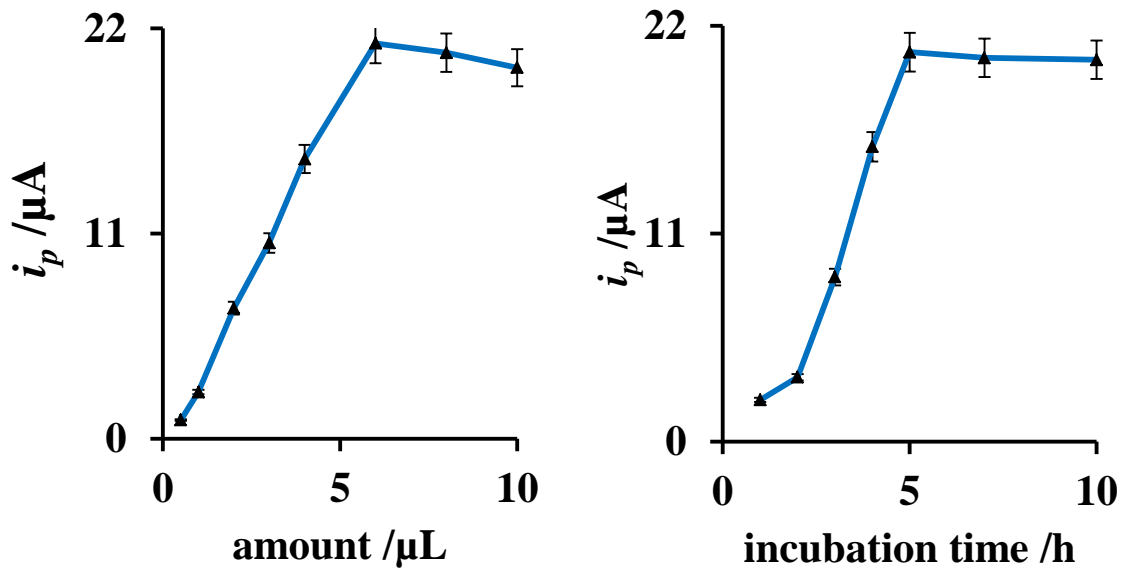
(a)

(b)
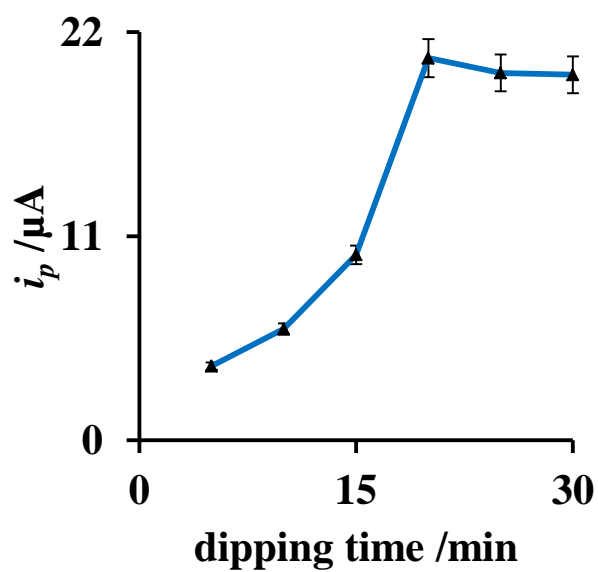
(c)

Fig. 6.6: Optimization of experimental parameters; effect of (a) aptamer amount (b) incubation time (c) dipping time in CAP solution, on the peak current of CAP.

6.3.4 Analytical performance of aptamer/p-AHNSA/EPPG

To quantitatively assess the detection limit and dynamic range of CAP aptasensor, square wave voltammetry (SWV) was employed to determine the dependence of the peak current on the concentration of CAP. The sensor probe was dipped into the buffer (blank/no CAP) and square wave voltammogram was recorded. No reduction peak was observed because no CAP was captured by the aptamer/p-AHNSA/EPPG. Thereafter, the aptamer/p-AHNSA/EPPG was reacted with different concentrations of CAP and then square wave voltammograms were recorded, where a well defined reduction peak at peak potential ~ -590 mV was observed. **Fig. 6.7A** shows the square wave voltammograms, recorded using aptamer/p-AHNSA/EPPG sensor after capturing various concentrations of CAP. A calibration plot **(Fig. 6.7B)** was obtained with the dynamic range between 0.1 – 2500 nM. The linear regression equation is expressed as follows:

i_p /μA = 0.102 [C] + 19.15

with a correlation coefficient of 0.995. The detection limit for CAP was determined to be 0.02 nM. (R.S.D. < 5%) based on the measurements performed five times for the standard deviation of the blank solution (95% confidence level, k=3, n=5). This detection limit is 80 times lower as compared to the method recently reported for CAP detection using apta sensing [307]. The detection limits of recently reported methods for CAP determination at other electrodes were, 1μM at gold electrode [301], 0.29 nM at aptasensor based electrode [308], 0.59 mM at nitrogen doped graphene nanosheets [309], 0.34 nM at screen printed electrode [322], and 2 nM at molecularly imprinted polymer modified carbon paste electrode [323]. These detection values clearly indicate that the present sensor is more sensitive in comparison to recently reported sensors. The impact of other parameters such as pH of the supporting electrolyte and square wave frequency on the electrochemical response of aptamer/p-AHNSA/EPPG was also studied for the detection of CAP.
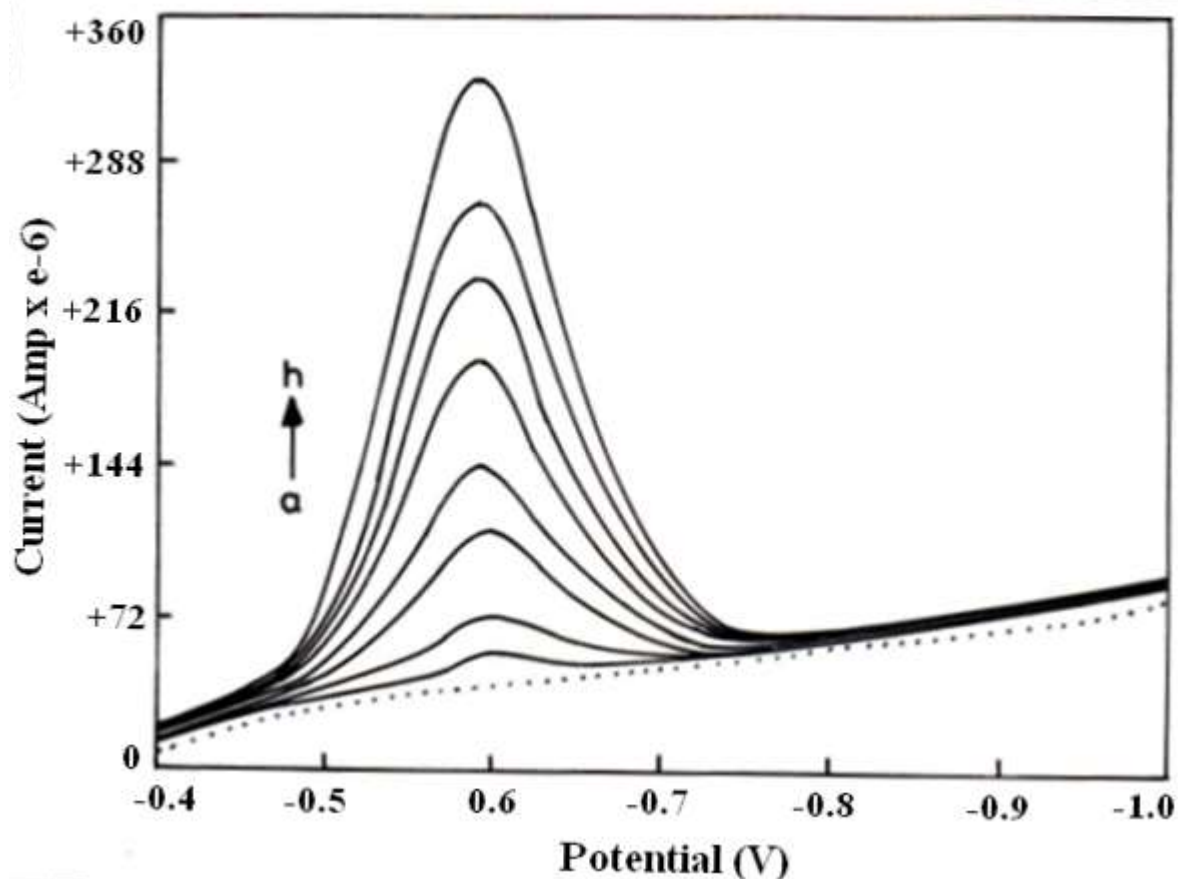
Fig. 6.7A: Square wave voltammograms observed for background phosphate buffer (…) and on increasing the concentration of CAP. Curves were recorded at (a) 0.1, (b) 5, (c) 80, (d) 400, (e) 700, (f) 1600 (g) 2000 and (h) 2500 nM concentrations using aptamer/p-AHNSA/EPPG in phosphate buffer of pH 7.2.
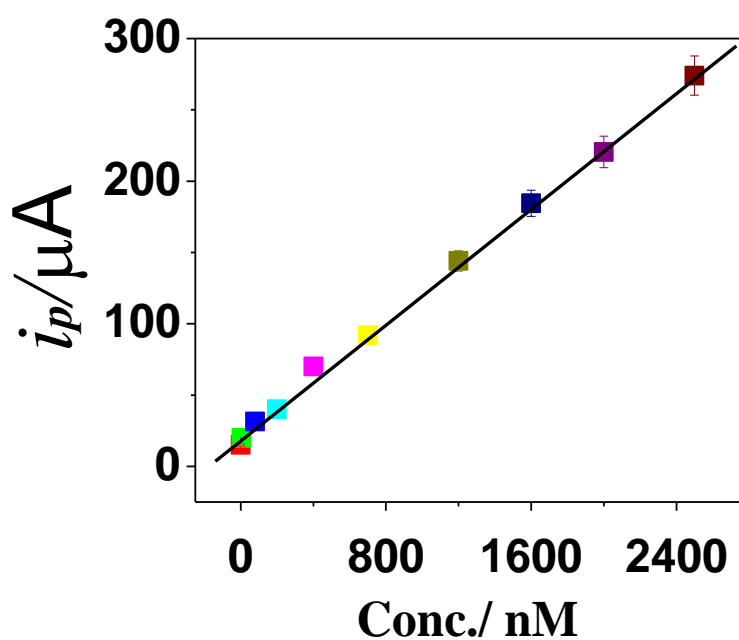
Fig. 6.7B: Calibration curve of peak current versus CAP concentration.

6.3.5 Effect of pH and square wave frequency

The pH of the solution has a significant influence on the peak potential (E_p) of CAP. The electrochemical behaviour of CAP at different pH was then studied using aptamer/p-AHNSA/EPPG. The voltammetric reduction of 250 nM CAP was studied in the pH range 2.0 - 11. The peak potential was shifted towards more negative potentials with increase in pH as depicted in **Fig. 6.8 (a)**. The dependence of peak potential on pH can be expressed by the following equation:

$$-E_p /mV = 57.93 \, [pH] + 173.9$$

having correlation coefficient of 0.99. The slope of $dE_p/dpH \sim 59$ mV/pH indicates that the number of protons and electrons involved in the reduction process of CAP is equal.

The dependence of peak current of 400 nM CAP on the square wave frequency was studied in the range 5–50 Hz. The peak current was found to increase linearly with square wave frequency (as shown in **Fig. 6.8 (b)** and the relation between peak current and frequency can be expressed by the following relation:

$$i_p /\mu A = 1.432 \, [f] + 48.78$$

having correlation coefficient of 0.987, where f is the square wave frequency. This result is in agreement with that obtained from cyclic voltammetric study confirming the electrode process as adsorption controlled.

(a)   (b)
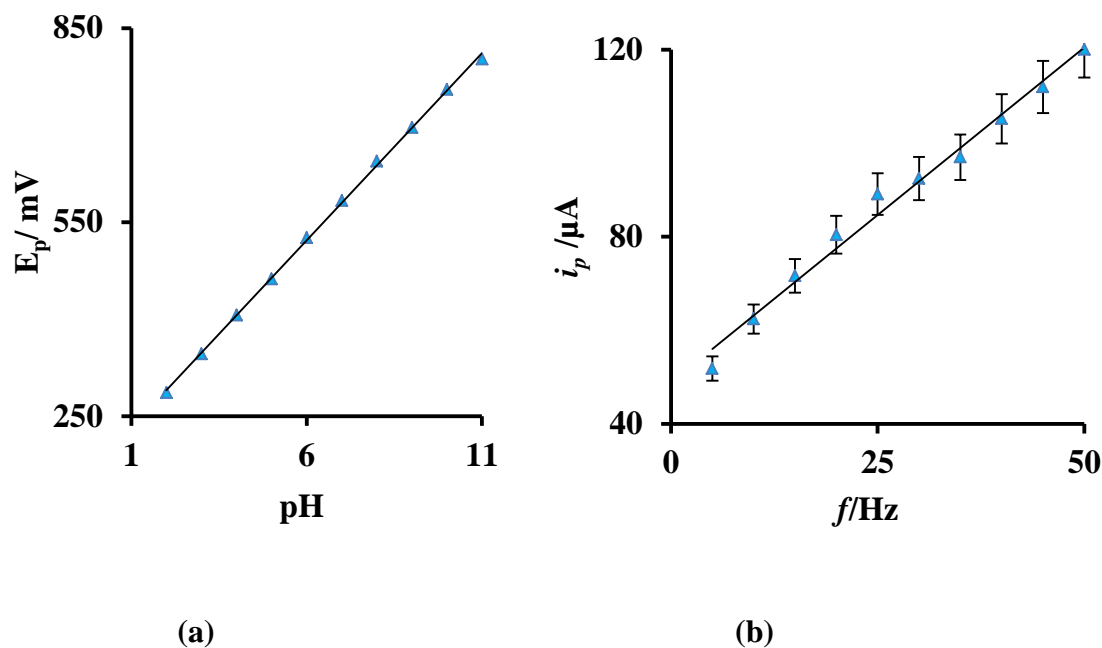
Fig. 6.8: (a) dependence of peak potential of CAP on pH of supporting electrolyte (b) dependence of peak current of CAP on square wave frequency.

6.3.6   Real sample analysis

In order to evaluate the practical applicability of the proposed method, three commercial medicinal samples containing CAP were examined. The CAP containing commercial medicinal tablets, viz. paraxin-250 (Piramal Healthcare Ltd. Baddi, Himanchal Pradesh), chloromycetin 250 mg and 500 mg capsules (Pfizer Ltd., Navi, Mumbai), were purchased from the local market of Roorkee. **Table 6.1** shows that the aptamer/p-AHNSA/EPPG sensor can detect CAP in various pharmaceutical samples irrespective of the type and formulation. We also analysed the CAP detection in the urine samples after spike and recovery method. For this purpose, the biosensor was used to detect the CAP concentration in 10-fold diluted urine sample. Under the optimized conditions, CAP was detected in the similar dynamic range as in the blank buffer. The linear regression equation for CAP detection in urine is expressed as follows:

i_p /µA = 0.097 [C] +18.01

with a correlation coefficient of 0.987. The recovery in all the cases was more than 96.4 % and the relative standard deviations were less than 5 %. The results based on the recovery obtained clearly indicate that the developed sensor can detect CAP from the complex urine matrix. Interestingly, in medicinal as well as in the urine samples no foreign peak was observed which

clearly indicated that other chemical and biomolecules do not interfere in CAP detection. One of the reasons for such non-interference can be explained on the basis of the fact that most of the compounds present in urine matrix are non-reducible in nature. A 3.9 % decrease in the CAP signal, however, was observed which was possibly due to the negligible electrode fouling by protein contents present in the urine sample.

Table 6.1: Determination of CAP using aptamer/p-AHNSA/EPPG in different pharmaceutical tablets.

Sample	Stated content (mg)	Detected content* (mg)	Error (%)
Paraxin-250	250	248.7	-0.52
Chloromycetin-250	250	248.3	-0.68
Chloromycetin-500	500	502.8	0.56

* RSD for the determination was $< \pm 3.1\%$ for n=5.

6.3.7 *In vitro* CAP detection *H. influenza* model

The *in vitro* detection of CAP was performed in the CAP treated *H. influenza* cells supernatant (CAP-s). In a control experiment CAP untreated supernatant was tested, where no CAP reduction peak was observed. This was due to the absence of CAP in the sample solution. In another experiment 30 min incubated CAP-s was analysed using the biosensor, where a clear CAP reduction peak was observed. Interestingly, the peak current was lower as compared to the only 5 min incubated CAP-s. The lower current signal in 30 min can be assigned to the higher CAP uptake with increase in the incubation time. Further, to confirm the CAP uptake, *H. influenza* cells were treated with CAP with different incubation time from 5 min to 90 min and subsequently the supernatant was analyzed as mentioned above. During this experiment, the number of *H. influenza* cells, the CAP concentration, and the reaction time (between sensor probe and supernatant) were kept constant. The CAP reduction peak current gradually decreased with increase in the incubation time indicating thereby that the *H. influenza* strain under investigation was CAP sensitive **(Fig. 6. 9 (a))**. When another strain was examined under the similar experimental conditions the CAP concentration did not decrease with time **(Fig. 6. 9(b))**. This was because the *H. influenza* was resistant to CAP and hence no CAP uptake was observed in this case. These results are extremely important in diagnosis and therapeutics due to their uniqueness in terms of simultaneous *in vitro* CAP detection and bacterial susceptibility

/ resistant diagnosis. To the best of our knowledge this is the first report, where CAP detection has been done in an *in vitro* model using an electrochemical biosensor.
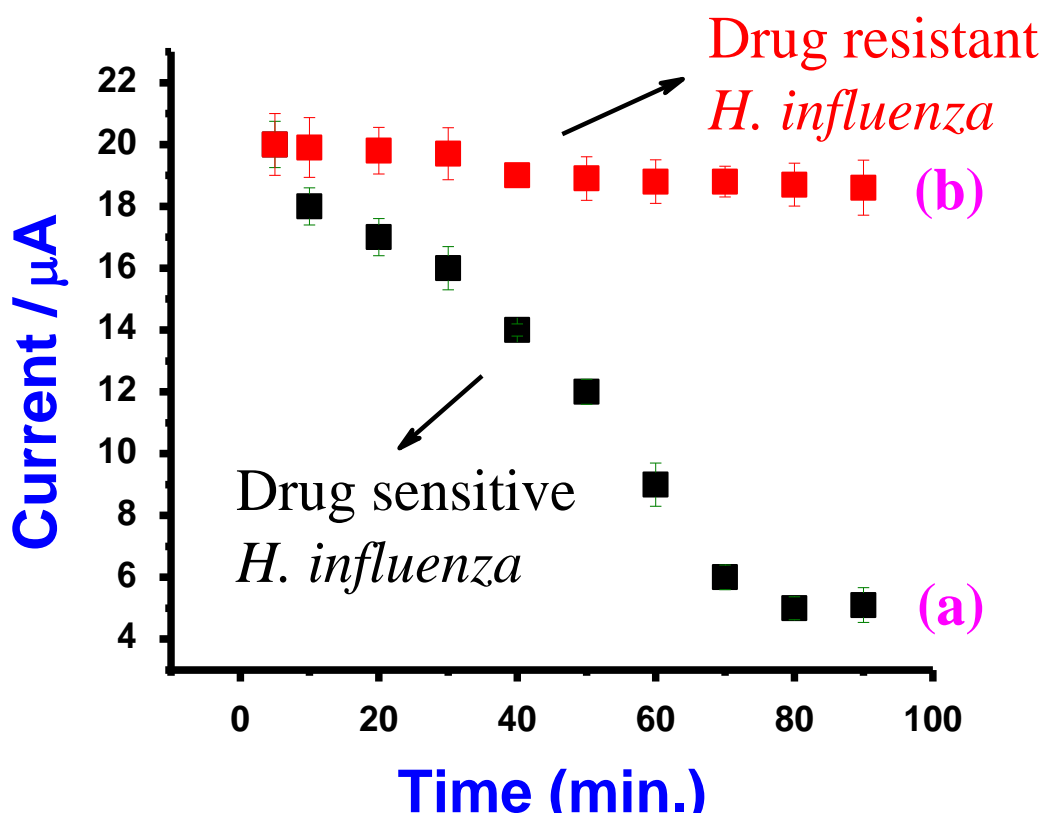
Fig. 6.9: *In vitro* **analysis of CAP in drug sensitive (a) and drug resistant (b) *H. Influenza* isolates. CAP concentration was 5 nM. SWV signals were obtained at different incubation times using the biosensor.**

6.3.8   Specificity, reproducibility, and stability of aptamer/p-AHNSA/EPPG

To assess the possibility of interference, the SWV response of the aptamer/p-AHNSA/EPPG was measured for tetracycline, kanamycin, chloramphenicol, neomycin and anthraquinone at 100.0 nM. These drugs did not interfere because the CAP selective aptamer could not interact with these drugs and aptamer–drug complex was not observed for these drugs. Also, no foreign peaks appeared in the real sample experiment indicating that other components present in the real sample matrix do not interfere with the sensor probe. These results indicate that proposed aptasensor has an excellent specificity for CAP detection.

The reproducibility of the method was determined by observing the current response at four prepared sensors for the replicate measurements. The good reproducible results were observed with relative standard deviation of only ~ 3.5 % which revealed acceptable

reproducibility of the method. Stability of aptamer/p-AHNSA/EPPG is a major issue due to its application in several pharmacological operations. In order to check the stability of aptamer/p-AHNSA/EPPG, the sensor was stored in pH 7.2 solution. The sensor is found to retain 97 % of its initial current upto 30 days indicating thereby, that the aptamer/p-AHNSA/EPPG sensor has very good stability and life length.

6.4   CONCLUSIONS

A facile, highly sensitive, selective, and stable biosensor for CAP detection using aptamer has been developed. The biosensor surface was successfully characterized using FE-SEM, QCM, and electrochemical techniques. The detection limit of the proposed biosensor was 0.02 nM, which is lower than the previously reported results. A comparison of detection limit of the present sensor with recently reported methods for CAP determination at other electrodes clearly indicate that the present sensor is much more sensitive in comparison to other recently reported sensors. Also, the present biosensor exhibited long term stability up to 30 days and was successfully used to detect CAP in pharmaceutical and urine samples. The CAP biosensor was also successfully applied to detect CAP concentrations in *in vitro H. influenza* models to monitor the CAP uptake by the various strains of *H. influenza*.The CAP sensitive *H. influenza* strains were identified by this method and differentiated from the resistant *H. influenza* strains very effectively using an electrochemical biosensor. The strategy described here has many attractive features: simplicity, rapidity, low cost, and no requirement for a specific label (i.e., a fluorescent or reactive moiety), all of which indicate that this could be a useful method for diagnosis of CAP resistant *H. influenza* and other important CAP resistant bacterial isolates.

BIBLIOGRAPHY
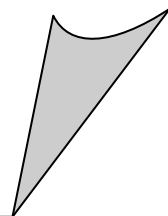
Bibliography

[1]   A.J. Bard, L.R. Faulkner; "Electrochemical methods, fundamental and applications", Second Ed., Wiley: New York, (1980).

[2]   C. Brett, A.M.O. Brett; "Electroanalysis", Oxford University Press, Oxford, (1998) 96.

[3]   J.O.M. Bockris, R.E. White (eds.); "Modern aspects of electrochemistry", Kluwer Plenum Publisher, New York, 34 (2001) 283.

[4]   J.T. Stock; "Electrochemistry in retrospect", ACS Symposium Series, January 1, 1989, doi: 10.1021/bk-1989-0390.ch001.

[5]   R.W. Murray, C.N. Reilley; "Electroanalytical principals", Wiley: New York, (1963).

[6]   L. Meites; "Hand book of analytical chemistry", Mcgrahill book company, (1963).

[7]   J.R. Stetter, W.R. Penrose, S. Yao, "Sensors, chemical sensors, electrochemical sensors and ECS", J. Electrochem. Soc., 150 (2003) S11.

[8]   A. Abbott; "Focus on electrochemistry: bringing electrochemistry to life", Chem. Soc. Rev. iii, (1997) 26.

[9]   P.A. Christensen, A. Hamnet; "Techniques and mechanisms in electrochemistry", Chapman & Hall: New York, (1994).

[10] T.D. Chung; "Electrochemistry and sensor and life phenomena", Hwahak Sekye, 43 (2003) 70.

[11] U. Krast; "Analytical methods: electrochemistry/mass spectrometry (EC/MS) – a new tool to study drug metabolism and reaction mechanism", Angew. Chem., 43 (2004) 2476.

[12] A.M. Bond; "Electrochemistry", J.A. McCleverty, T.J. Meyer (Eds.), Elsevier Ltd, (2004).

[13] W.U. Malik, R.N. Goyal; "Nanomaterial and electrochemistry – a review on some less familiar aspects", Indian J. Chem. Sect. A: Inorg. Bioinorg. Phys. Theor. Anal. Chem., 44A (2005) 861.

[14] Y.R. Kim, R.K. Mahajan, J.S. Kim, H. Kim; "Highly sensitive gold nanoparticle-based colorimetric sensing of mercury (ii) through simple ligand exchange reaction in aqueousmedia", ACS Appl. Mater. Interfaces,2 (2010) 292.

[15] S.K. Guin, H.S. Sharma, S.K. Aggarwal; "Electrosynthesis of lead nanoparticles on template free gold surface bypotentiostatic triple pulse technique", Electrochim. Acta,55 (2010) 1245.

[16] S.K. Guin, R. Phatak, J.S. Pillai, A. Sarkar, S.K. Aggarwal; "A mechanistic study on the effect of a surface protecting agent on electrocrystallization of silvernanoparticles", RSC Adv., 4 (2014) 599927.

Bibliography

[17] S.K. Guin, S.K. Aggarwal; "Prospective use of the potentiostatic triple pulsestrategy for the template-free electrosynthesis of metal nanoparticles", RSC Adv., 4 (2014) 55349.

[18] A. Merkoci; "Electrochemical biosensing with nanoparticles", FEBS J.I. 274 (2007) 310.

[19] X. Luo, A. Morrin. A.J. Killard, M.R. Symth; "Application of nanoparticles in electrochemical sensors and biosensors", Electroanalysis, 18 (2006) 319.

[20] F. Gao, M.S.E. Deab, T. Oshaka; "Electrodeposition of gold nanorods with a unidirectional crystal growth and lower Au (111) facets area", Indian J. Chem. Sect. A: Inorg. Bioinorg. Phys. Theor. Anal. Chem., 44A (2005) 932.

[21] D.T. Mcquade, A.E. Pullen,T.M. Swager; "Conjugated polymer-based chemical sensors", Chem. Rev., 100 (2000) 2537.

[22] U. Lange, N.V. Roznyatovskaya, V.M. Mirsky; "Conducting polymers in chemical sensors and arrays", Anal. Chim. Acta, 614 (2008) 1.

[23] R. Stella, G. Serra, D.D. Rossi, J.N. Barisci, G.G. Wallace, P.D. Harris, M.K. Andrews, A.C. Partridge; "Conducting polymer based device for odour detection", Ad. Sc. Tech., 26 (1999) 363.

[24] Y. Xiang, M. Xie, R. Bash, J.J.L. Chen, J. Wang; "Ultrasensitive lable-free aptamer-based electronic detection", Angew. Chem. Int. Ed., 46 (2007) 9054.

[25] Q. Cai, M. He, H. Shi; "Apllication of immunosensor for the environmental monitoring", Chu. Jis. Xueb, 17 (2004) 526.

[26] C.M.A. Brett, A.M.O. Brett, "Electrochemistry: principles, methods and applications", Oxford University Press: Oxford, (1993).

[27] R.S. Nicholson; "Theory and application of cyclic voltammetry for measurement of electrode reaction kinetics", Anal. Chem., 37 (1965) 1351.

[28] R. Talwar, R.K. Mahajan; "Electrochemical measurements of phenothiazine drugs in the presenceof surface active ionic liquids", Key Eng. Mater., 605 (2014) 581.

[29] L. Ramaley, M.S. Krause; "Theory of square wave voltammetry", Anal. Chem., 41 (1969) 1362.

[30] R.A. Osteryoung, J. Osteryoung; "Pulse voltammetric methods of analysis", Phil. Trans. R. Lond. A, 302 (1981) 315.

[31] J. Osteryoung, J.J.O. Dea; "In Electroanalytical chemistry", Marcel Dekker, NY, USA, 14 (1986) 209.

[32] J.J. Odea, J. Osteryoung, R.A. Osteryoung; "Theory of square wave voltammetry for kinetic systems", Anal. Chem., 53 (1981) 695.

[33] J.J. Lingane; "Some analytical applications of controlled potential electrolysis", Electrochem. Soc., 92 (1947) 505.

[34] P.T. Kissinger, W.R. Heineman (Eds.); "Laboratory techniques in electroanalytical chemistry", Marcel Dekker, (1984).

[35] A.J. Bard, K.S.V. Santhanam; "Electroanalytical chemistry", Marcel Dekker, New York, 4 (1970) 215.

[36] J.J. Lingane; "Recent applications of controlled potential electrolysis", Discuss. Faraday Soc., 1 (1947) 203.

[37] J.H. Kennedy, F. Adamo; "Controlled potential electrolysis: An experiment for elementary quantitative analysis", J. Chem. Educ., 47 (1970) 461.

[38] R.P.W. Scott; "Contemporary liquid chromatography", John Wiley, New York, 11 (1976).

[39] V.G. Berezkin; "On the determination of the chromatography", Zh. Anal. Khim., 48 (1993) 1242.

[40] V.A. Davankov; "What is chromatography, and can it be a single-phase process", J. Anal. Chem., 56 (2001) 1061.

[41] L.R. Snyder, J.J. Kirkland, J.W. Dolan; "Introduction to modern liquid chromatography", John Wiley & Sons, New York (2009).

[42] L.V. Tsakanika, M.T. Ochsenkuhn-Petropoulou, L.N. Mendrinos; "Investigation of the separation of scandium and rare earth elements from red mud by use of reversed-phase HPLC", Anal. Bioanal., Chem, 379 (2004) 796.

[43] N.M. Raut, P.G. Jaison, S.K. Aggarwal; "Comparative evaluation of three alpha-hydroxycarboxylic acids for the separation of lanthanides by dynamically modified reversed-phase high-performance liquid chromatography', J. Chromatogr. A, 959 (2002) 163.

[44] Y. Liu, S. Mou; "Nano high performance liquid chromatographic system and its application in biochemical analysis", Fenxi Yiqi, (2001) 40.

[45] R.L. Moritz, A.B. Clippingdale, E.A. Kapp, J.S. Eddes, H. Ji, S. Gilbert, L.M. Connolly, R.J. Simpson; "Application of 2-D free-flow electrophoresis/RP-HPLC for proteomic analysis of human plasma depleted of multi high-abundance proteins", Protemics, 5 (2005) 3402.

[46] T. Isobe, M. Taoke, F. Shinkai, M. Ishikura, M. Maeda, M. Fukuda, N. Kobayashi, H. Fukuda, K. Seta; "Mapping and structural analysis of biomolecules using an off-line multidimensional HPLC-MALDI/TOFMS system", Chromatography, 18 (1997) 148.

[47] M. Kanai, H. Xu, M. Yamaguchi, K. Seta, H. Nakayama, F. Shinkai, T. Isobe, T. Okuyama; "HPLC-ESI/ion trapmass spectrometer system for structural analysis of biomolecules", Kuromatogurafi, 17 (1996) 162.

[48] J. Zagrodzka; "Application of HPLC in studies of pharmaceutical substances: A review", Przem.Chem., 85 (2006) 363.

[49] J. Matthey; "Palladium in temporary and permanently implantable medical devices", Platinum Metals Rev., 56 (2012) 213.

[50] A. Changotra, R. Gupta, S. Paul; "Selective Oxidation of Benzyl Alcohol Over Hydroxyapatite–Supported Au-Pd Nanoparticles", J. Appl. Chem., 3 (2014) 653.

[51] X. Chen; "Palladium as electrode in DNA sequencing", Appl. Phys. Lett., 103 (2013) 063306.

[52] A. Changotra, R. Gupta, S. Paul; "Reduction of carbon–carbon double bond in α,β-unsaturated ketones over bimetallic Pd and Au nanoparticles immobilized on amine-functionalizedmagnetite nanoparticles: A novel and highly active bimetallic catalyst", Der. Pharma.Chemica., 6 (2014) 385.

[53] E.A. Khudaish, M.R.A. Birikei; "The role of bromine adlayer at palladium electrode in the electrochemical oxidation of dopamine in alkaline solution", J. Electroanal. Chem., 650 (2010) 68.

[54] E. Sosa, G. Carreno, C.P.D. Leon, M. T. Oropeza, M. Morales, I. Gonzalez, N. Batina; "Lead deposition onto fractured vitreous carbon: influence of electrochemical pretreated electrode", Appl. Surf. Sci, 153 (2000) 245.

[55] K. Gu, J. Zhu, Y. Zhu, J. Xu, H.Y. Chen; "Voltammetric determination of mifepristone at a DNA-modified carbon paste electrode", Fresenius J. Anal. Chem., 368 (2000) 832.

[56] Y. Sallez, P. Bianco, E. Lojou; "Electrochemical behavior of c-type cytochromes at clay-modified carbon electrodes: A model for the interaction between proteins and soils", J. Electroanal. Chem., 493 (2000) 37.

[57] M. Niculescu, T. Ruzgas, C. Nistor, I. Frebort, M. Sebela, P. Pec, E. Csoregi, "Electrooxidation mechanism of biogenic amines at amine oxidase modified graphite electrode", Anal. Chem., 72 (2000) 5988.

[58] Z. Wang, D. Liu, S. Dong; "Study on adsorption and oxidation of calf thymus DNA at glassy carbon electrode", Electroanalysis, 12 (2000) 1419.

[59] Q. Fulian, R.G. Compton; "Laser activated voltammetry: Application to the determination of phenol in aqueous solution at a glassy carbon electrode", Analyst, 125 (2000) 531.

[60] M.H.P. Azar, R. Ojani; "Electrochemistry and electrocatalytic activity of polypyrrole/ferrocyanide films on a glassy carbon electrode", J. Solid State Electrochem, 4 (2000) 75.

[61] A.J. Downard, A.D. Roddick; "Protein adsorption at glassy carbon electrodes: The effect of covalently bound surface groups", Electroanalysis, 7 (1995) 376.

[62] P.K. Brahman, R.A. Dar, K.S. Pitre; "Voltammetric study of ds-DNA–flutamide interactionat carbon paste electrode", Arabian J. Chem., (2012), http://dx.doi.org/10.1016/j.arabjc.2012.08.007.

[63] K. Kinoshita; "Electrochemical and physicochemical properties", Carbon, Wiley-Interscience, New York, (1988)..

[64] I. Gustavsson, K. Lundstrom; "A pyrolytic carbon film electrode for voltammetry-III application to anodic-stripping voltammetry", Talanta, 30 (1983) 959..

[65] E. Csoregi, L. Gorton, G.M. Varga; "Carbon fibers as electrode materials for the construction of peroxidase-modified amperometric biosensors", Anal. Chim. Acta., 273 (1993) 59.

[66] S.Tiwari, K.S. Pitre; "Anticancer drug modified GCFE, for the study of its in-vivointeraction mechanism", J. Chinese Chem. Soc., 55 (2008) 1166.

[67] R.S. Kelly, D.J. Weiss, S.H. Chong, T. Kuwana; "Charge-selective electrochemistry at high-surface-area carbon fibers", Anal. Chem., 71 (1999) 413.

[68] W.C. Yang, A.M. Yu, Y.Q. Dai, H.Y. Chen; "Determination of hydrazine compounds by capillary electrophoresis with a poly (Glutamic Acid) modified microdisk carbon fiber electrode", Anal. Lett., 33 (2000) 3343.

[69] F. Cespedes, F. Valero, E.M. Fabregas, S. Alegret; "Fermentation monitoring using a glucose biosensor based on an electrocatalytically bulk-modified epoxy-graphite biocomposite integrated in a flow system", Analyst, 120 (1995) 2255.

[70] M. Pedrero, P. Mateo, C. Parrado, J.M. Pingarron; "Metallized graphite ethylene/propylene/diene tetra polymer composte electrodes as electrocatalytic amperometric detectors in flowing systems", Quim. Anal., 19 (2000) 171.

[71] C.E. Banks, A. Crossley, C. Salter, S.J. Wilkins, R.G. Compton; "Carbon nanotubes contain metal impurities which are responsible for the "electrocatalysis" seen at some nanotubes-modified electrodes", Angew Chemie. Intl. Ed., 45 (2006) 2533.

[72] F. Wantz, C.E. Banks, R.G. Compton; "Edge plane pyrolytic graphite electrodes for stripping voltammetry: a comparison with other carbon based electrodes", Electroanalysis, 17 (2005) 655.

[73] C.E. Banks, R.G.Compton; "Exploring the electrocatalytic sites of carbon nanotubes for NADH detection: an edge plane pyrolytic graphite electrode study", Analyst, 130 (2005) 1232.

[74] C.E. Banks, A. Goodwin, C.G.R. Heald, R.G. Compton; "Exploration of gas sensing possibilities with edge plane pyrolytic graphite electrodes: Nitrogen dioxide detection", Analyst, 130 (2005) 280.

[75] E.R. Lowe, C.E. Banks, R.G. Compton; "Gas sensing using edge-plane pyrolytic-graphite electrodes: Electrochemical reduction of chlorine", Anal. Bioanal. Chem., 382 (2005) 1169.

[76] E.V. Ivanova, E. Magner; "Direct electron transfer of haemoglobin and myoglobin in methanol and ethanol at didodecyldimethylammonium bromide modified pyrolytic graphite electrodes", Electrochem. Commun., 7 (2005) 323.

[77] D. Johnson, S. Norman, R.C. Tuckey, L.L. Martin; "Electrochemical behaviour of human adrenodoxin on a pyrolytic graphite electrode", Bioelectrochemistry, 59 (2003) 41.

[78] L.L. Wu, J.Z. Zhou, J. Luo; "Oxidation and adsorption of deoxyribonucleic acid at highly ordered pyrolytic graphite electrode", Electrochim. Acta, 45 (2000) 2923.

[79] A. Salimi, C.E. Banks, R.G. Compton; "Abrasive immobilization of carbon nanotubes on a basal plane pyrolytic graphite electrode: Application to the detection of epinephrine", Analyst, 129 (2004) 225.

[80] S. Zhu, W. Qu, H. Chen; "Electroanalytical chemistry of small biological molecules: molecular orientation and surface interaction of guanine, adenine and hypoxanthine on rough pyrolytic graphite electrode", Huaxue Xuebao, 51 (1993) 594.

[81] A. Salimi, R.G. Compton, R. Hallaj; "Glucose biosensor prepared by glucose oxidase encapsulated sol-gel and carbon-nanotube-modified basal plane pyrolytic graphite electrode", Anal. Biochem., 333 (2004) 49.

[82] L. Shang, X. Liu, C. Fan, G. Li; "A nitric oxide biosensor based on horseradish peroxidase/kieselguhr co-modified pyrolytic graphite electrode", Annali di Chimica., 94 (2004) 457.

[83] K.A. Hirasawa, T. Sato, H. Asaniha, S. Yamaguchi, S. Mori; "In situ electrochemical atomic force microscope study on graphite electrodes", J. Electrochem. Soc., 144 (1997) L81.

[84] T. Sagara, H. Nomaguhi, N. Nakashima; "Surface anisotropic electroreflectance response at an edge-plane pyrolytic graphite electrode", J. Phys. Chem., 100 (1996) 6393.

[85] X. Jiang, X. Lin; "Atomic force microscopy of DNA self-assembled on a highly oriented pyrolytic graphite electrode surface", Electrochem. Commun., 6 (2004) 873.

[86] A.M.O. Brett, A.M. Chiorcea; "Atomic force microscopy of DNA immobilized onto a highly oriented pyrolytic graphite electrode surface", Langmuir, 19 (2003) 3830.

[87] M.C. Daniel, D. Astruc; "Gold nanoparticles: assembly, supramolecular chemistry, quantum-size related properties, and applications towards biology, catalysis and nanotechnology",Chem. Rev., 104 (2004) 293.

[88] A. Yu, Z. Liang, J. Cho, F. Caruso; "Electrochemical nanoreactors based on dense gold nanoparticle films", Nano Lett., 3 (2003) 1203.

[89] W. Cheng, S. Dong, E. Wang; "Gold nanoparticles as fine tuners of electrochemical properties of electrode/solution interface", Langmuir, 18 (2002) 9947.

[90] M.S.E. Deab, T. Ohsaka; "An extraordinary electrocatalytic reduction of oxygen on gold nanoparticles-electrodeposited gold electrodes", Electrochem. Commun.,4 (2002) 288.

[91] N.B. Ibrahim, K. Lawrence, T.D. James, F. J. Xia, M. Pan, J.M. Mitchels, M. Marken; "Surface-dopylated carbon nanoparticles sense gas-induced pH changes", Sensor Actuat. B-Chem., 161 (2012) 184.

[92] D.S. Su, S. Perathoner, G. Centi; "Nanocarbons for the development of advanced catalysts", Chem. Rev., 113 (2013) 5782.

[93] G.P. Lopinski, V.I. Merkulov, J.S. Lannin; "Semimetal to semiconductor transition in carbon nanoparticles", Phys. Rev. Lett., 80 (1998) 4241.

[94] A.J. Amaratunga, M. Chhowalla, C.J. Kiely, I. Alexandrou, R. Aharonov, R.M. Devenish; "Hard elastic carbon thin films from linking of carbon nanoparticles", Nature 383 (1996) 321.

[95] R.H. Baughman, A.A. Zakhidov, W.A.D. Heer; "Carbon nanotubes-the route toward applications", Science 297 (2002) 787.

[96] G.A. Rivas, M.D. Rubianes, M.C. Rodriguez, N.F. Ferreyra, G.L. Luque, M.L. Pedano, S.A. Miscoria, C. Parrado; "Carbon nanotubes for electrochemical biosensing", Talanta, 74 (2007) 291.

[97] S. Kurbanoglu, C.C.M. Martinez, M.M. Sanchez, L. Rivas, S.A. Ozkan, A. Merkoçi; "Antithyroid drug detection using an enzyme cascade blocking in ananoparticle-based lab-on-a-chip system", Biosens. Bioelectron., 67 (2015) 670.

[98] M.L. Pedano, G.A. Rivas; "Adsorption and electrooxidation of nucleic acids at carbon nanotubes paste electrodes", Electrochem. Commun., 6 (2004) 10.

[99] W. Liang, Y. Zhuobin; "Direct electrochemistry of glucose oxidase at a gold electrode modified with single-walled carbon nanotubes", Sensors, 3 (2003) 544.

[100] H. Zhao, H. Ju; "Multilayer membranes for glucose biosensing via layer-by-layer assembly of multiwall carbon nanotubes and glucose oxidase", Anal. Biochem., 350 (2006) 138.

[101] Z.D. Gao, Y. Qu, T. Li, N.K. Shrestha, Y.Y. Song; "Development of amperometric glucose biosensor based on prussian blue functionlized tio2 nanotube arrays", Scientific Reports, 4 (2014) 6891.

[102] L.Y. Heng, A. Chou, J. Yu, Y. Chen, J.J. Gooding; "Demonstration of the advantages of using bamboo-like nanaotubes for electrochemical biosensor applications compared with single walled carbon nanotubes", Electrochem. Commun., 7 (2005) 1457.

[103] B.D. Malhotra, A. Chaubey, S.P. Singh; "Prospects of conducting polymers in biosensors", Anal. Chim. Acta, 578 (2006) 59.

[104] M. Atesa, A.S. Sarac; "Conducting polymer coated carbon surfaces and biosensor applications", Prog. Org. Coat., 66 (2009) 337.

[105] C. Janáky, C. Visy; "Conducting polymer-based hybrid assemblies for electrochemical sensing: a materials science perspective", Anal. Bioanal. Chem., 405 (2013) 3489.

[106] M. Pumera, A. Merkoci, S. Alegret; "Carbon nanotube-epoxy composites for electrochemical sensing", Sens. Actuat. B, 113 (2006) 617.

[107] Y.H. Yun, V. Shanov, M.J. Schulz, Z. Dong, A. Jazieh, W.R. Heineman, H.B. Halsall, D.K.Y. Wong, A. Bange, Y. Tu, S. Subramaniam; "High selective carbon nanotube tower electrodes", Sens. Actuat. B, 120 (2006) 298.

[108] B. Zeng, S. Wei, F. Xiao, F. Zhao; "Voltammetric behavior and determination of rutin at a single-walled carbon nanotubes modified gold electrode", Sens. Actuat. B, 115 (2006) 240.

[109] K. Murakoshi, K. Okazaki; "Electrochemical potential control of isolated single-walled carbon nanotubes on gold electrode", Electrochim. Acta, 50 (2005) 3069.

[110] P.B. Luppa, L.J. Sokoll, D.W. Chan; "Immunosensors--principles and applications to clinical chemistry", Clin. Chem., 314 (2001) 1.

[111] I. Ojeda, J.L. Montero, M.M. Guzman, B.C. Janegitz, A.G. Cortes, P.Y. Sedeno, J.M. Pingarron; "Electrochemical immunosensor for rapid and sensitive determination of estradiol", Anal. Chim. Acta, 743 (2012) 117.

[112] M. Guzman, A.G. Cortis, P.Y. Sedeno, J.M. Pingarron; "Multiplexed ultrasensitive determination of adrenocorticotropin and cortisol hormones at a dual electrochemical immunosensor", Electroanalysis, 24 (2012) 1100.

[113] M.J. Monerris, F.J. Arevalo, H. Fernandez, M.A. Zon, P.G. Molina; "Integrated electrochemical immunosensor with gold nanoparticles for the determination of progesterone", Sens. Actuat. B, 166 (2012) 586.

[114] J. Zhang, M. Oyama; "A hydrogen peroxide sensor based on the peroxidase activity of hemoglobin immobilized on gold nanoparticles-modified ITO electrode", Electrochim.Acta, 50 (2004) 85.

[115] E.V. Milsom, J. Novak, M. Oyama, F. Marken; "Electrocatalytic oxidation of nitric oxide at TiO_2–Au nanocomposite film electrodes", Electrochem. Commun.,9 (2007) 436.

[116] J. Li, L. Zhou, X. Han, H. Liu; "Direct electrochemistry of hemoglobin based on Gemini surfactant protected gold nanoparticles modified glassy carbon electrode", Sensor Actuat. B, 135 (2008) 322.

[117] S. Frasca, O. Rojas, J. Salewski, B. Neumann, K. Stiba, I.M. Weidinger, B. Tiersch, S. Leimkühler, J. Koetz, U. Wollenberger; "Human sulfite oxidase electrochemistry on gold nanoparticles modified electrode", Bioelectrochem., 87 (2012) 33.

[118] M.A. Augelli,R.A.A. Munoz,E.M. Richter,A.G. Junior, L. Angnes; "Chronopotentiometric stripping analysis using gold electrodes, an efficient technique for mercury quantification in naturalwaters", 17 (2005) 755.

[119] X. Zhu, C. Li, X. Zhu, M. Xu; "Nonenzymatic glucose sensor based on Pt-Au-SWCNT nanocomposites", Int. J. Electrochem. Sci., 7 (2012) 8522.

[120] R.N. Goyal, V.K. Gupta, M. Oyama, N. Bachheti; "Gold nanoparticles modified indium tin oxide electrode for the simultaneous determination of dopamine and serotonin: Application in pharmaceutical formulations and biological fluids", Talanta, 72 (2007) 976.

[121] R.N. Goyal, M.A. Aziz, M. Oyama, S. Chatterjee, A.R.S. Rana; "Nanogold based electrochemical sensor for determination of norepinephrine in biological fluids", Sensor Actuat. B 153 (2011) 232.

[122] L. Wang, J. Bai, P. Huang, H. Wang, L. Zhang, Y. Zhao; "Self-assembly of gold nanoparticles for the voltammetric sensing of epinephrine", Electrochem. Commun., 8 (2006) 1035.

[123] R.N. Goyal, A. Aliumar, M. Oyama; "Comparison of spherical nanogold particles and nanogold plates for the oxidation of dopamine and ascorbic acid", J. Electroanal. Chem., 631 (2009) 58.

[124] C.N.R. Rao, B.C.S. Kumar, A. Govindraj, M. Nath; "Nanotubes", Chem. Phys. Chem., 2 (2001) 78.

[125] S. Ijima; "Helical microtubules of graphitic carbon", Nature, 354 (1991) 56.

[126] S. Iijima, T. Ichihashi; "Singled-shell carbon nanotubes of 1-nm diameter", Nature, 363 (1993) 603.

[127] P.J. Britto, K.S.V. Santhanam, P.M. Ajayan, "Carbon nanotubes electrode for oxidation of dopamine", Bioelectrochem. Bioener., 41 (1996) 121.

[128] S.A. Ozkan;"Principles and techniques of electroanalytical stripping methods for pharmaceutically active compounds in dosage forms and biologicalsamples", Curr. Pharm. Anal., 5 (2009) 127.

[129] N. Karadas, S.A. Ozkan; "Electrochemical preparation of sodium dodecylsulfate doped over-oxidized polypyrrole/multi-walled carbon nanotube composite on glassy carbon electrode and its application on sensitive and selective determination of anticancer drug: pemetrexed", Talanta 119 (2014) 248.

[130] M. Ates; "A review study of (bio)sensor systems based on conducting polymers", Mater. Sci. Eng. C, 33 (2013) 1853.

[131] Q.G. Silva, N.V. Barbosa, E.P. Troiani, R.C. Faria; "Electrochemical Determination of Norepinephrine on Cathodically Pretreated Poly(1,5-diaminonaphthalene) Modified Electrode", Electroanalysis, 23 (2011) 1359.

[132] J.B. Raoof, R. Ojani, S.R. Hosseini; "Electrocatalytic oxidation of methanol onto platinum particles decorated nanostructured poly (1,5-diaminonaphthalene) film", J. Solid State Electrochem., 16 (2012) 2699.

[133] A.A. Abdelwahab, H.M. Lee, Y.B. Shim; "Selective determination of dopamine with a cibacron blue/poly-1,5-diaminonaphthalene composite film", Anal. Chim. Acta, 650 (2009) 247.

[134] A. Missio, C. Marchioro, T. Rossi, M. Panunzio, S. Selva, P. Seneci; "Polymer-supported silyl cyanide and silyl azide: useful reagents for solid-phase applications", Biotechnol. Bioeng., 71 (2000) 38.

[135] R.A. Dar, G.A. Naikoo, K.S. Pitre; "Electrocatalytic oxidative determination of reserpine at electrochemically functionalized single walled carbonnanotube withpolyaniline", Electrochim. Acta, 111 (2213) 526.

[136] P.M. Ajayan, J.M. Tour, "Nanotube composites", Nature, 2 (2007) 1066.

[137] A. Kausar, S.T. Hussain; "Synthesis and properties of poly(thiourea-azo-naphthyl)/multi-walled carbonnanotube composites", J. Plast. Film Sheeting, 0 (0) 1.

[138] P.R. Martins, L.M.C. Ferreira, K. Araki, L. Angnes; "Influence of cobalt content on nanostructured alpha-phase-nickel hydroxide modified electrodes for electrocatalytic oxidation of isoniazid", Sensor Actuat. B chem., 192 (2014) 601.

[139] P. Kannan, S. A. John; "Fabrication of conducting polymer-gold nanoparticles film on electrodes using monolayer protected gold nanoparticles and its electrocatalytic application", Electrochim. Acta, 56 (2011) 7029.

[140] A.D. Ellington, J.W. Szostak; "In vitro selection of RNA molecules that bind specific ligands", Nature, 346 (1990) 818.

[141] Y.S. Kim, H.S. Jung, T. Matsuura, H.Y. Lee, T. Kawai, M.B. Gu; "Electrochemical detection of 17beta-estradiol using DNA aptamer immobilized gold electrode chip", Biosens. Bioelectron., 22 (2007) 2525.

[142] B.K. Kim, J. Li, J.E. Im, K.S. Ahn, T.S. Park, S.I. Cho, Y.R. Kim, W.Y. Lee; "Impedometric estrogen biosensor based on estrogen receptor alpha-immobilized gold electrode", J. Electroanal. Chem., 671 (2012) 106.

[143] T.Y. Lee, Y.B. Shim; "Direct DNA hybridization detection based on the oligonucleotide-functionalized conductive polymer", Anal. Chem., 73 (2001) 5629.

[144] Y. Zhu, P. Chandar, K.M. Song, C. Ban, Y.B. Shim; "Label-free detection of kanamycin based on the aptamer-functionalized conducting polymer/gold nanocomposite", Biosens. Bioelectron., 36 (2012) 29.

[145] P. Chandra, H.B. Noh, M.S. Won, Y.B. Shim; "Detection of daunomycin using phosphatidylserine and aptamer co-immobilized on Au nanoparticles deposited conducting polymer", Biosens. Bioelectron., 26 (2011) 4442.

[146] P. Damier, E.C. Hirsch, Y. Agid and A.M. Graybiel; "The substantia nigra of the human brain II. patterns of loss of dopamine-containing neurons in Parkinson's disease" Brain, 122 (1999) 1437.

[147] K. Anderson, A. Kuruvilla, N. Uretsky, D.D. Miller; "Synthesis and Pharmacological Evaluation of Sulfonium Analogues of Dopamine: Nonclassical Dopamine Agonists", J. Med. Chem., 24 (1981) 683.

Bibliography

[148] L.L. Iversen; "Dopamine handbook", oxford university press, Newyork (2010).

[149] M.S.M. Quintino, M.Yamashita, L. Angnes; "Voltammetric studies and determination of levodopa and carbidopa in pharmaceutical products" 18 (2006) 655.

[150] C.A. Hull, S.M. Johnson; "A double-blind comparative study of sulfacetamide lotion 10% versus selenium sulfide lotion 2.5% in the treatment of pityriasis (tinea) versicolor", Cutis, 73 (2004) 425.

[151] J.Q.D. Rosso; "Evaluating the role of topical therapies in the management of rosacea: a focus on combination Sulfacetamide and sulfur formulations", Cutis, 73 (2004) 29.

[152] S.M. Fuchs, P. Elsner; "Sulfonamides in dermatology", Clin Dermatol., 21 (2003) 7.

[153] W.M. Todd; "Cefpodoxime proxetil: a comprehensive review", Int. J. Antimicrob. Ag., 4 (1994) 37.

[154] C. Senthilkumar, G. Rameshkumar, S. Subathra, T. Sureshkumar, S. Arunkumar; "Enhancement of solubility and dissolution rate of drug cefpodoxime proxetil", Int. Res. J. Pharm., 3 (2012) 384.

[155] J.C. Rodriguez, R. Hernandez, M. Gonzalez, Z. Rodriguez, B. Tolon, H. Velez, B. Valdes, M.A. Lopez, A. Fini; "An improved method for preparation of cefpodoxime proxetil", IL Farmaco, 58 (2003) 363.

[156] K. Chugh, S. Agrawal; "Cefpodoxime: pharmacokinetics andtherapeutic uses", Int. J. Pediatr., 70 (2003) 227.

[157] M.E. Falagas, A.P. Grammatikos, A. Michalopoulos; "Potential of old-generation antibiotics to address current need for new antibiotics", Expert Rev. Anti-Infect. Ther., 6 (2008) 593.

[158] M.L. Rich, R.J. Ritterhoff, R.J. Hoffmann; "A fatal case of aplastic anemia followingchloramphenicol (chloromycetin) therapy", Ann. Intern. Med. 33 (1950) 1459.

[159] J. Bousquet; "Mometasone furoate: an effective anti-inflammatory with a well-defined safety and tolerability profile in the treatment of asthma", Int. J. Clin. Pract., 63 (2009) 806.

[160] S. Wiedersberg, C.S. Leopold, R.H. Guy; "Bioavailability and bioequivalence of topical glucocorticoids", Eur. J. Pharm. Biopharm., 68 (2008) 453.

[161] S.P.K. Durmazlar, B. Oktay, C. Eren, F. Eskioglu; "Cushing's syndrome caused by short-term topical glucocorticoid use for erythrodermic psoriasis and development of adrenal insuf", Eur. J. Dermatol., 19 (2009) 169.

[162] J. Huang, Y. Liu, H. Hou, T. You; "Simultaneous electrochemical determination of dopamine, uric acid and ascorbic acid using palladium nanoparticle-loaded carbon nanofibers modified electrode", Biosens. Bioelectron., 24 (2008) 632.

[163] S. Guo, E. Wang; "Synthesis and electrochemical applications of gold nanoparticles", Anal. Chim. Acta, 598 (2007) 181.

[164] C.M. Welch, R.G. Compton; "The use of nanoparticles in electroanalysis: a review", Anal. Bioanal. Chem., 384 (2006) 601.

[165] B. Uslu, S.A. Ozkan; "Solid electrodes in electroanalytical chemistry: present applications and prospects for high throughput screening of drug compounds", Ombinatorial Chemistry & High Throughput Screening, 10 (2007) 495.

[166] M. Panunzio, E. Tamanini, Y.S. Denis, F.M. Sabbatini, R. Di Fabio, Z. Xia; "Palladium-catalyzed heteroaromatic couplings mediated by microwave irradiation" Synth. Commun., 37 (2007) 4239.

[167] M.J.N. Pourbaix, J. Van Muylder, N. de Zoubov; "Electrochemical properties of the platinum metals", Platinum Metals Rev., 3 (1959) 3.

[168] J.D. Fernstrom, M.H.J. Fernstrom; "Tyrosine, phenylalanine, and catecholamine synthesis and function in the brain", Nutrition, 137 (2007) 1539S.

[169] Y.R. Kim, S. Bong, Y.J. Kang, Y. Yang, R.K. Mahajan, J.S. Kim, H. Kim; "Electrochemical detection of dopamine in the presence of ascorbic acidusing graphene modified electrodes", Biosens. Bioelectron.,25 (2010) 2366.

[170] M. Heien, A. Khan, J. Ariansen, J. Cheer, P. Phillips, K. Wassum, M. Wightman; "Real-time measurement of dopamine fluctuations after cocaine in the brain of behaving rats", Proc. Natl. Acad. Sci., USA 102 (2005) 10023.

[171] L.G. Shaidarova, I.A. Chelnokova, A.V. Gedmina, G.K. Budnikov; "Simultaneous voltammetric determination of dopamine and ascorbic acid at an electrode modified with the gold–palladium binary system", J. Anal. Chem., 64 (2009) 36.

[172] B. Zhang, D. Huang, X. Xu, G. Alemu, Y. Zhang, F. Zhan, Y. Shen, M. Wan; "Simultaneous electrochemical determination of ascorbic acid, dopamine and uric acid with helical carbon nanotubes", Electrochim. Acta, 91 (2013) 261.

[173] Q. Huang, S. Hu, H. Zhang, J. Chen, Y. He, F. Li, W. Weng, J. Ni, X. Bao, Y. Lin; "Carbon dots and chitosan composite film based biosensor for the sensitive and selective determination of dopamine", Analyst, 138 (2013) 5417.

[174] G.D. Christian, W.C. Purdy; "Residual current in orthophosphate medium", J. Electroanal. Chem., 3 (1962) 363.

[175] N.R. Jana, L. Gearheart, C.J. Murphy; "Wet chemical synthesis of high aspect ratio cylindrical gold nanorods", J. Phys. Chem. B, 105 (2001) 4065.

[176] Y. Nakayama, M. Oyama; "Electrocatalytic oxidation of water observed on a nano-gold/palladium electrode", Chem. Commun., 49 (2013) 5228.

[177] B.A. Feinberg, L. Petro, G. Hock, W. Qin, E. Margoliash; "Using entropies of reaction to predict changes in protein stability: tyrosine-67-phenylalanine variants of rat cytochrome c and yeast Iso-1 cytochromes c", J. Pharm. Biomed. Anal., 19 (1999) 115.

[178] M.L. Yola, N. Ozaltin; "Square-wave voltammetric determination of ezetimibe", Rev. Chim. (Bucharest), 62 (2011) 420.

[179] L. Lin, J. Chen, H. Yao, Y. Chen, Y. Zheng, X. Lin; "Simultaneous determination of dopamine, ascorbic acid and uric acid at poly(Evans Blue) modified glassy carbon electrode", Bioelectrochemistry, 73 (2008) 11.

[180] L. Lin, J. Chen, H. Yao, Y. Chen, Y. Zheng, X. Lin; "Simultaneous determination of dopamine, ascorbic acid and uric acid at poly (Evans Blue) modified glassy carbon electrode", Bioelectrochemistry, 73 (2008) 11.

[181] D. J. Guoz, M. Jin; "Electrocatalytic oxidation and the mechanism of dopamine on a MWNT-modified glassy carbon electrode", J. Russ. Electrochem., 49 (2013) 200.

[182] I. Eichler, H.G. Eichler, M. Rotter, P.A. Kyrle, S. Gasic, A. Korn; "Plasma concentrations of free and sulfoconjugated dopamine, epinephrine, and norepinephrine in healthy infants and children", Kiln. Wochenschr, 67 (1989) 672.

[183] Y. Tong, Z. Li, X. Lu, L. Yang, W. Sun, G. Nie, Z. Wang, C. Wang; "Electrochemical determination of dopamine based on electrospun CeO_2/Au composite nanofibers", Electrochim. Acta, 95 (2013) 12.

[184] S. Reddy, B.E.K. Swamy, H. Jayadevappa; "ZnO nanoparticle/carbon paste electrode as an electrochemical sensor for the detection of dopamine", Int. J. Science Res., 1 (2012)96.

[185] C.X. Xu, K.J. Huang, Y. Fan, Z.W. Wu, J. Li, T. Gan;"Simultaneous electrochemical determination of dopamine and tryptophan using a TiO_2-graphene/poly(4-aminobenzenesulfonic acid) compositefilm based platform",Mat. Sci. Eng. C, 32 (2012) 969.

[186] R. Salgado, R.D. Rio, M.A.D. Valle, F. Armijo; "Selective electrochemical determination of dopamine, using a poly(3,4-ethylenedioxythiophene)/polydopamine hybrid film modified electrode", J. Electroanal. Chem., 704 (2013) 130.

[187] G.P. Keeley, N. McEvoy, H. Nolan, S. Kumar, E. Rezvani, M. Holzinger, S. Cosnier, G.S. Duesberg; "Simultaneous electrochemical determination of dopamine and paracetamol based on thin pyrolytic carbon films", Anal. Methods, 4 (2012) 2048.

[188] J. Li, J. Yang, Z. Yang, Y. Li, S. Yu, Q. Xu, X. Hu; "Graphene–Au nanoparticles nanocomposite film for selective electrochemical determination of dopamine", Anal. Methods, 4 (2012) 1725.

[189] A. Dirany, I. Sires, N. Oturan, M.A. Oturan; "Electrochemical abatement of the antibiotic sulfamethoxazole from water", Chemosphere, 81 (2010) 594.

[190] C.D. Souza, O.C. Braga, I.C. Vieira, A. Spinelli; "Electroanalytical determination of sulfadiazine and sulfamethoxazole in pharmaceuticals using a boron-doped diamond electrode", Sensor Actuat. B chem., 135 (2008) 66.

[191] D. Sensoy, E. Cevher, A. Sarici, M. Yilmaz, A. Ozdamar, N. Bergisadi; "Bioadhesive sulfacetamide sodium microspheres: Evaluation of their effectiveness in the treatment of bacterial keratitis caused by staphylococcus aureus and pseudomonas aeruginosa in a rabbit model", Eur. J. Pharm. Biopharm., 72 (2009) 487.

[192] C.A Hull, S.M. Johnson; "A double-blind comparative study of sodium sulfacetamide lotion 10% versus selenium sulfide lotion 2.5% in the treatment of pityriasis (tinea) versicolor", Cutis., 73 (2004) 425.

[193] W.P. Bowe, A.R. Shalita; "Effective over-the-counter acne treatments", Semin. Cutan. Med. Surg., 27 (2008) 170.

[194] R. Mohammadpour, S. Safarian, N. Sheibani, S. Norouzi, A. Razazan; "Death inducing and cytoprotective autophagy in T-47D cells by two common antibacterial drugs: sulphathiazole and sulphacetamide", Cell Biol. Int., 24 (2013) 348.

[195] L. Byrom, T. Zappala, J. Muir; "Toxic epidermal necrolysis caused by over the counter eyedrops", Australas. J. Dermatol., 54 (2013) 144.

[196] J.F. Jen, H.L. Lee, B.N. Lee; "Simultaneous determination of seven sulfonamide residues in swine wastewater by high-performance liquid chromatography",J. Chromatogr. A, 793 (1998) 378.

[197] K. Takatsuki, T. Kikuchi; "Gas chromatographic-mass spectrometric determination of six sulfonamide residues in egg and animal tissues", J. Assoc. Off. Anal. Chem., 73 (1990) 886.

[198] A.S. Amin, M.M. Zareh; "Mikrochim acetylacetone-formaldehyde reagent for the spectrophotometric determination of some sulfa drugs in pure and dosage forms", Mikrochim. Acta, 124 (1996) 227.

[199] F.H. Salami, M.E.C. Queiroz; "Microextraction in packed sorbent for determination of sulfonamides in egg samples by liquid chromatography and spectrophotometric detection", J. Braz. Chem. Soc., 22 (2011) 1656.

[200] M.S. Pena, A.M.D.L. Pena, F. Salinas, M.C. Mahedero, J.J. Aaron; "Determination of binary mixtures of sulfonamides by photochemically induced fluorescence using partial least squares multivariate calibration", Analyst, 119 (1994) 1177.

[201] M.C. Mahedero, J.J. Aaron; "Flow-injection determination of sulphonamides with fluorimetric or photochemical-fluorimetric detection", Anal. Chim. Acta, 269 (1992) 193.

[202] H. Pasekova, M. Polasek, J.F. Cigarro, J. Dolejsova; "Determination of some sulphonamides by sequential injection analysis with chemiluminescence detection", Anal. Chim. Acta, 438 (2001) 165.

[203] M.A. Khorassani, M.T. Combs, L.T. Taylor, J. Willis, X. Liu, C.R. Frey; "Separation and identification of sulfonamide drugs via SFC/FT-IR mobile-phase elimination interface", Appl. Spectrosc., 51 (1997) 1791.

[204] A. Wang, F. Gong, H. Li, Y. Fang; "Separation and determination of the active ingredients intablets of composite sulphonamides by capillary zone electrophoresis with amperometric detection", Anal. Chim. Acta, 386 (1999) 265.

[205] C.E. Lin, W.C. Lin, Y.C. Chen, S.W. Wang; "Migration behavior and selectivity of sulfonamides in capillary electrophoresis", J. Chromatogr. A, 792 (1997) 37.

[206] R.F. Cross, J. Cao; "Salt effects in capillary zone electrophoresis IV. Resolution versus time and the effect of potassium phosphate and its concentration in the high ionic strength separation of sulphonamides", J. Chromatogr. A, 849 (1999) 575.

[207] J.M.L. Gallego, J.P. Arroyo; "Determination of prednisolone acetate, sulfacetamide phenylefrine in local pharmaceutical preparations by micellar electrokinetic chromatography", J. Pharm. Biomed. Anal., 31 (2003) 873.

[208] J.J.B. Nevado, G.C. Penalvo, F.J.G. Bernardo; "Micellar electrokinetic capillary chromatography as an alternative method for the determination of sulfonamides and their associated compounds", J. Liq. Chrom. Rel. Technol., 22 (1999) 1975.

[209] B. Chiavarino, M.E. Crestoni, A.D. Marzio, S. Fornarini; "Determination of sulfonamide antibiotics by gas chromatography coupled with atomic emission detection", J. Chromatogr. B: Biomed. Appl., 706 (1998) 269.

[210] R.N. Goyal, D. Kaur, B. Agrawal, S.K. Yadav; "Electrochemical investigations of mometasone furoate, a topical corticosteroid, in micellar medium", J. Electroanal. Chem., 695 (2013) 17.

[211] V.A. Momberg, B.M.E. Carrera, D.V. Baer, F.C. Bruhn, M.R. Smyth; "The oxidative voltammetric behaviour of some sulphonamides at the glassy carbon electrode", Anal. Chim. Acta, Volume 159 (1984) 119.

[212] J.M.P. Carrazon, A.D. Recio, L.M.P. Diez; "Electroanalytical study of sulphamerazine at a glassy-carbon electrode and its determination in pharmaceutical preparations by HPLC with amperometric detection", Talanta, 39 (1992) 631.

[213] J.D. Voorhies, R.N. Adams; "Voltammetry at solid electrodes: Anodic polarography of sulfa drugs", Anal. Chem., 30 (1958) 346.

[214] T.N. Rao, B.V. Sarada, D.A. Tryk, A. Fujishima; "Electroanalytical study of sulfa drugs at diamond electrodes and their determination by HPLC with amperometric detection", J. Electroanal. Chem., 491 (2000) 175.

[215] I. Campestrini, O.C. Braga, I.C. Vieira, A. Spinelli; "Application of bismuth-film electrode for cathodic electroanalytical determination of sulfadiazine", Electrochim. Acta, 55 (2010) 4970.

[216] A.E. Ghenymy, P.L. Cabot, F. Centellas, J.A. Garrido, R.M. Rodriguez, C. Arias, E. Brillas; "Electrochemical incineration of the antimicrobial sulfamethazine at a boron-doped diamond anode", Electrochim. Acta, 90 (2013) 254.

[217] A.G. Fogg, A.R.H.M. Yusoff, J.C. Moreira, R. Zhao; "Cathodic stripping voltammetric determination of sulfonamides as copper(I) complexes at a hanging mercury drop electrode", Anal. Proc., 32 (1995) 95.

[218] X. Zhang, J. Zhang, Z. Liu; "Conducting polymer/carbon nanotube composite films made by in situ electropolymerization using an ionic surfactant as the supporting electrolyte", Carbon, 43 (2005) 2186.

[219] Z. Spitalsky, D. Tasis, K. Papagelis, C. Galiotis; "Carbon nanotube–polymer composites: Chemistry, processing, mechanical and electrical properties", Prog. Polym. Sci., 35 (2010) 357.

[220] R. Andrews, M.C. Weisenberger; "Carbon nanotube polymer composites", Curr. Opin. Solid St. M., 8 (2004) 31.

[221] M. Pumera, A. Merkoc, S. Alegret; "Carbon nanotube-epoxy composites for electrochemical sensing", Sensor. Actuat. B-Chem., 113 (2006) 617.

[222] B.F. Jogi, M. Sawant, M. Kulkarni, P.K. Brahmankar; "Dispersion and performance properties of carbon nanotubes (cnts) based polymer composites: a review", J. Encapsul. Ads. Sci., 2 (2012) 69.

[223] A. Kausar, S.T. Hussain; "Synthesis and properties of poly(thiourea-azonaphthyl)/ multi-walled carbon nanotube composites", J. of Plast. Film and Sheeting, 0 (0) 1.

[224] S. Bal, S.S. Samal; "Carbon nanotube reinforced polymer composites–A state of the art", Bull. Mater. Sci., 30 (2007) 379.

[225] R.N. Goyal, B. Agrawal; "Carbon nanotube-based electrochemical sensor for the determination of halobetasol propionate, a topical corticosteroid", J. Appl. Electrochem., (2012) 31.

[226] Q.G. Silva, N.V. Barbosa, E.P. Troiani, R.C. Faria; "Electrochemical determination of norepinephrine on cathodically pretreated poly(1,5-diaminonaphthalene) modified electrode", Electroanal., 23 (2011) 1359.

[227] S.K. Yadav, B. Agrawal, R.N. Goyal; "AuNPs-poly-DAN modified pyrolytic graphite sensor for the determination of Cefpodoxime Proxetil in biological fluids", Talanta, 108 (2013) 30.

[228] E. Tamburri, S. Orlanducci, M.L. Terranova, F. Valentini, G. Palleschi, A. Curulli, F. Brunetti, D. Passeri, A. Alippi, M. Rossi; "Modulation of electrical properties in single-walled carbon nanotube/conducting polymer composites", Carbon, 43 (2005) 1213.

[229] R.H. Wopschall, I. Shain; "Adsorption characteristics of the methylene blue system using stationary electrode", Polarography, 39 (1967) 13.

[230] O. Gilbert, B.E.K. Swamy, U. Chandra, B.S. Sherigara; "Electrocatalytic oxidation of dopamine and ascorbic acid at poly (eriochrome black-t) modified carbon paste electrode", Int. J. Electrochem. Sci., 4 (2009) 582.

[231] R.N. Goyal, N.C. Mathur, S. Bhargava; "Electrochemical oxidation of sulphacetamide", J. Electroanal. Chem. Interfac. Electrochem., 247 (1988) 229.

[232] International Conference on Harmonisation of Technical Requirements for Registration of Pharmaceuticals for Human Use (ICH), Q2 (R1): Validation of Analytical Procedures: Text and Methodology. 2001, http://www.ich.org/LOB/media/MEDIA417.pdf.

[233] DIN 38402 part 51st, "Calibration of Analytical Procedures", Beuth Verlag, Berlin,1986.

[234] A. Liu, I. Honma, H. Zhou; "Simultaneous voltammetric detection of dopamine and uric acid at their physiological level in the presence of ascorbic acid using poly(acrylic acid)-multiwalled carbon-nanotube composite-covered glassy-carbon electrode", Biosens. Bioelectron., 23 (2007) 74.

[235] M.S. Puar, P.A. Thompson, M. Ruggeri, D. Beiner, A.T. McPhailt; "An unusual rearrangement product formed during production of mometasone furoate", Steroids, 60 (1995) 612.

[236] Rajnikant, V.K. Gupta, J. Firoj, Shafiullah, R. Gupta; "3β-acetoxy-5α-cholestan-6-one: a steroid",Cryst. Res. Technol., 2 (36) 215.

[237] R.M. Rezende, F. Silveira, A.P. Barbosa, U.P. Menezes, V.P.L. Ferriani, P.H.C. Rezende, W.T.A. Lima, F.C.P. Valera; "Objective reduction in adenoid tissue after mometasone furoate treatment", Int. J. Pediatr. Otorhi., 76 (2012) 829.

[238] O. Zetterstroma, R. Dahl, A. Lindqvist, P. Olsson; "Comparable morning versus evening administration of once-daily mometasone furoate dry powder inhaler", Res. Med., 102 (2008) 1406.

[239] R.S. Medansky, C.A. Cuffie, D.J. Tanner; "Mometasone furaote 0.1% -salicylic acid 5% ointmenttwice daily fluocinonide 0.05% ointment twice daily in management of patients with psoriasis", Clinical Therapeutics, 19 (1997) 701.

[240] X.W. Teng, K. Foe, K.F. Brown, D.J. Cutler, N.M. Davies; "High-performance liquid chromatographic analysis of mometasone furoate and its degradation products application to in vitro degradation studies" J. Pharm. Biomed. Anal., 26 (2001) 313.

[241] S. Sahasranaman, Y. Tang, D. Biniasz, G. Hochhau; "A sensitive liquid chromatography–tandem mass spectrometry method for the quantification of mometasone furoate in human plasma", J. Chromatogr. B, 819 (2005) 175.

[242] Z. Wang, H. Zhang, O. Liu, B. Donovan; "Development of an orthogonal method for mometasone furoate impurity analysis using supercritical fluid chromatography", J. Chromatogr. A, 1218 (2011) 2311.

[243] C.J. Wang, Z. Tian, K. Byrnes, C.C. Lin; "A competitive enzyme immunoassay for the direct determinationof mometasonefuroate in human plasma", J. Pharm. Biomed. Anal., 10 (1992) 473.

[244] C.G. Caridade, R. Pauliukaite, M.A. Brett; "Influence of nafion coatings and surfactant on the stripping voltammetry of heavy metals at bismuth-film modified carbon film electrodes", Electroanal., 18 (2006) 854.

[245] R. Vittal, H. Gomathi, K.J. Kim; "Beneficial role of surfactants in electrochemistry and in the modification of electrodes", Adv. Colloid Interface Sci., 119 (2006) 55.

[246] N. Chowdappa, B.E.K. Swamy, E. Niranjana, B.S. Sherigara; "Cyclic voltammetric studies of serotonin at sodium dodecyl sulfate modified carbon paste electrode", Int. J. Electrochem. Sci., 4 (2009) 425.

[247] D.S. Shishmarev, N.V. Rees, R.G. Compton; "Enhanced performance of edge-plane pyrolytic graphite (eppg) electrodes over glassy carbon (gc) electrodes in the presence of surfactants: application to the stripping voltammetry of copper", Electroanal., 22 (2010) 31.

[248] A.P. Dos Reis, C.R.T. Tarley, N. Maniasso, L.T. Kubota; "Exploiting micellar environment for simultaneous electrochemical determination of ascorbic acid and dopamine", Talanta, 67 (2005) 829.

[249] A. Diaz, A.E. Kaifer; "Self-assembled surfactant monolayers on electrode surfaces: The formation of surfactant viologen monolayers on gold and platinum", J. Electroanal. Chem. Interfac. Chem., 249 (1988) 333.

[250] R.N. Goyal, S. Bishnoi; "Surface modification in electroanalysis: Past, present and future", Indian J. Chem., 51 (2012) 205.

[251] R.N. Goyal, S. Chatterjee, A.R.S. Rana; "A single-wall carbon nanotubes modified edge plane pyrolytic graphite sensor for determination of methylprednisolone in biological fluids", Talanta, 80 (2009) 586.

[252] R.N. Goyal, S. Bishnoi; "Effect of single walled carbon nanotube–cetyltrimethyl ammonium bromide nanocomposite film modified pyrolytic graphite on the determination of betamethasone in human urine", Coll. Surf. B, 77 (2010) 200.

[253] R.N. Goyal, S. Chatterjee, A.R.S. Rana; "The effect of modifying an edge-plane pyrolytic graphite electrode with single-wall carbon nanotubes on its use for sensing diclofenac", Carbon, 48 (2010) 4136.

[254] I. Streeter, G.G. Wildgoose, L. Shao, R.G. Compton; "Cyclic voltammetry on electrode surfaces covered with porous layers: An analysis of electron transfer kinetics at single-walled carbon nanotube modified electrodes", Sens. Actuators B: Chem., 133 (2008) 462.

[255] E.R. Brown, R.F. Large;"Physical Methods Chemistry", (Ed. A. Weissberger, B.W. Rossiter) Wiley Interscience, Rochester, N.Y. 1964.

[256] X. Yang, F. Wang, S. Hu; "High sensitivity voltammetric determination of sodium nitroprusside at acetylene black electrode in the presence of CTAB", Colloid Surf. B, 54 (2007) 60.

[257] X.L. Wen, Y.H. Jia, Z.L. Liu; "Micellar effects on the electrochemistry of dopamine and its selective detection in the presence of ascorbic acid", Talanta, 50 (1999) 1027.

[258] C.Li; "Electrochemical determination of dipyridamole at a carbon paste electrode using cetyltrimethyl ammonium bromide as enhancing element", Colloid Surfaces B, 55 (2007) 77.

[259] R. Zana, S. Yiv, C. Straziella, P. Lianos; "Effect of alcohol on the properties of micellar systems", J. Colloid Interface Sci., 80 (1981) 208.

[260] M. Halder; "Determination of the critical micellar concentration (cmc) of a cationic micelle from stokes shift data", The Chemical Educator, 12 (2007) 33.

[261] J.S. Yu, C. Yang, H.Q. Fang; "Variable thickness thin-layer cell for electrochemistry and in-situ UV–VIS absorption, luminescence and surface-enhanced Raman spectroelectrochemistry", Anal. Chim. Acta, 420 (2000) 45.

[262] G. Cravottoa, G.B. Giovenzanab, N. Masciocchic, G. Palmisanoc, P. Volanted; "A degradation product of halobetasol propionate-Characterization and structure", Steroids, 72 (2007) 787.

[263] C. Vedhi, R. Eswar, H.G. Prabu, P. Manisankar; "Determination of triamcinolone acetonide steroid on glassy carbon electrode by stripping voltammetric methods", Int. J. Electrochem. Sci., 3 (2008) 509.

[264] A. E. Leontjev, L. L. Vasiljeva, K. K. Pivnitsky; "Reduction of steroidal ketones with amine-boranes", Russian Chem. Bull., 53 (2004) 703.

[265] N.F. Atta, A. Galal, F.M.A. Attia, S.M. Azab; "Characterization and electrochemical investigations of micellar/drug interactions", Electrochim. Acta, 56 (2011) 2510.

[266] S. Bhandari, N. Khisti; "Development and validation of a densitometric HPTLC method for quantitative analysis of cefpodoxime proxetil in human plasma", Int. J. Pharm. Pharm. Sci., 4 (2012) 100.

[267] A.K. Gupta, S. Sharma; "Formulation of fast dissolving tablets of cefpodoxime proxetil by effervescent technique", J. Pharm. Res., 5 (2012) 1902.

[268] U.A. Nimbalkar, M.V. Dhoka, P.A. Sonawane; "Formulation and optimization of cefpodoxime proxetil loaded solid lipid nano particles by box-behnken design", Int. J. Res. Ayur. Pharm., 2 (2011) 1779.

[269] S. Biondi, S. Long, M. Panunzio,W.L. Qin; "Current trends in β-lactam based β-lactamases inhibitors", Curr. Med. Chem., 18 (2011) 4223.

[270] V.K. Kakumanua, V. Arora, A.K. Bansal; "Investigation of factors responsible for low oral bioavailability of cefpodoxime proxetil", Int. J. Pharm., 317 (2006) 155.

[271] J. Chu, G. Li, K.H. Row, H. Kim, Y.W. Lee; "Preparation of cefpodoxime proxetil fine particles using supercritical fluids", Int. J. Pharm., 369 (2009) 85.

[272] G. Nicolaos, S.C. Manciet, R. Farinotti, D. Brossard; "Improvement of cefpodoxime proxetil oral absorption in rats by an oil-in-water submicron emulsion", Int. J. Pharm., 263 (2003) 165.

[273] K. Chugh, S. Agrawal; "Cefpodoime: Pharmacokinetics and therapeutic uses", Int. J. Pediatr., 70 (2003) 227.

[274] G. Jigar, K. Jagdish, S. Nehal; "Development and validation of dual wavelength UV spectrophotometric method for simultaneous estimation of ambroxol hydtochloride and cefpodoxime proxetil in their combined tablet dosage form", Int. Res. J. Pharm., 3 (2012) 330.

[275] A.V. Subbayamma, C. Rambabu; "Spectrophotmetric determination of cefpodoxime proxetil in tablets", Asian J. Chem., 22 (2010) 3345.

[276] A.B.C. Yu, C.H. Nightingale, D.R. Flanagan; "Rapid sensitive fluorometric analysis of cephalosporin antibiotics", J. Pharm. Sci., 66 (1977) 213.

[277] N. Fukutsu, T. Kawasaki, K. Satio, H. Nakazawa; "Application of high-performance liquid chromatography hyphenated techniques for identification of degradation products of cefpodoxime proxetil", J. Chromatogr. A, 1129 (2006) 153.

[278] V. Prakash, G. Suresh; "Method development and validation of cefpodoxime proxetil by UV-spectrophotometric method in bulk drug and formulation", Int. J. Pharm. Res. Dev., 4 (2012) 276.

[279] A.S. Patel, A.S. Patel; "Development and validation of RP-HPLC method for simultaneous estimation of cefpodoxime proxetil and ofloxacin in tablet dosage form", Int. J. Inst. Pharm. Life Sci., 2 (2012) 535.

[280] O.A. Farghaly1, O.A. Hazzazi, E.M. Rabie, M. Khodari; "Determination of some cephalosporins by adsorptive stripping voltammetry", Int. J. Electrochem. Sci., 3 (2008) 1055.

[281] M.M. Aleksic, V. Kapetanovic; "Application of adsorptive stripping voltammetry for determination of selected methoxyimino cephalosporins in urine samples", Comb. Chem. High Throughput Screen, 13 (2010) 758.

[282] T.M. Reddy, M. Sreedhar, S.J. Reddy; "Voltammetric behavior of cefixime and cefpodoxime proxetil and determination in pharmaceutical formulations and urine", J. Pharm. Biomed. Anal., 31 (2003) 811.

[283] R. Jain, R. Mishra; "Voltammetri behavior of an antibiotic drug and its enhancement determination in the presence of cetyltrimethylammonium bromide", J. Sci. Ind. Res., 68 (2009) 945.

[284] M. Aleksic, M. Ilic, V. Kapetanovic; "Adsorptive properties of cefpodoxime proxetil as a tool for a new method of its determination in urine", J. Pharm. Biomed. Anal., 36 (2004) 899.

[285] A.E. Golcu, B. Dogan, S.A. Ozkan; "Anodic voltammetric behavior and determination of cefixime in pharmaceutical dosage forms and biological fluids", Talanta, 67 (2005) 703.

[286] P. Nigam, S. Mohan, S. Kundu, R. Prakash; "Trace analysis of cefpodoxime at carbon paste electrode modifiedwith novel Schiff base Zn(II) complex", Talanta, 77 (2009) 1426.

[287] N. Yilmaz, I. Biryol; "Anodic voltammetry of cefpodoxime", J. Pharm. Biomed. Anal., 17 (1998) 1335.

[288] M. Kanungo, A. Kumar, A.Q. Contractor, "Studies on electropolymerization of aniline in the presence of sodiumdodecyl sulfate and its application in sensing urea", J. Electroanal. Chem., 528 (2002) 46.

[289] H. Wang, H. Zhao, X. Quan, S. Chen; "Electrochemical determination of tetracycline using molecularly imprinted polymer modified carbon nanotube-gold nanoparticles electrode", Electroanalysis, 23 (2011) 1863.

[290] D.P. Santos, M.F. Bergamini, M.V.B. Zanoni; "Voltammetric sensor for amoxicillin determination in human urine using polyglutamic acid/glutaraldehyde film", Sensors Actuat. B, 133 (2008) 398.

[291] H. Chen, Y. Cuia, B. Zhang, B. Liua, G. Chena, D. Tanga; "Poly(o-phenylenediamine)-carried nanogold particles as signal tags for sensitive electrochemical immunoassay of prolactin", Anal. Chim. Acta, 728 (2012) 18.

[292] C.E. Banks, R.G. Compton; "Edge plane pyrolytic graphite electrodes in electroanalysis: An overview", Anal. Sci., 21 (2005) 1263.

[293] S.Y. Honga, S.M. Park; "Electrochemistry of conductive polymers", J. Electrochem. Soc., 150 (2003) E360.

[294] R.N. Goyal, V.K. Gupta, M. Oyama, N. Bachheti; "Differential pulse voltammetric determination of atenolol in pharmaceutical formulations and urine using nanogold modified indium tin oxide electrode", Electrochem. Commun., 8 (2006) 65.

[295] S.A. Ozkan, N. Erk, B. Uslu, N. Ilmaz, I. Biryol; "Study on electrooxidation of cefadroxil monohydrate and its determination by differential pulse voltammetry", J. Pharm. Biomed. Anal., 23 (2000) 263.

[296] E. Laviron; "A multilayer model for the study of space distributed redox modified electrodes: Part I. Description and discussion of the model", J. Electroanal. Chem., 112 (1980) 1.

[297] S. Yilmaz; "Adsorptive stripping voltammetric determination of zopiclone in tablet dosage forms and human urine", Colloids Surf. B, 71 (2009) 79.

[298] S. Tuncagil, C. Ozdemir, D.O. Demirkol, S. Timur, L. Toppare; "Gold nanoparticle modified conducting polymer of 4-(2,5-di(thiophen-2-yl)-1Hpyrrole-1-l) benzenamine for potential use as a biosensing material", Food Chem., 127 (2011) 1317.

[299] A. Wang, L. Zhang, Y. Fang; "Determination and separation of chloramphenicol and its hydrolysate in eye-drops by capillary zone electrophoresis with amperometric detection", Anal. Chim. Acta, 394 (1999) 309.

[300] H. Alemu, L. Hlalele; "Voltammetric determination of chloramphenicol at electrochemically pretreated glassy carbon electrode", Bull. Chem. Soc. Ethiop., 21 (2007) 1.

[301] S. Pilehvar, F. Dardenne, R. Blust, K.D. Wael; "Electrochemical sensing of phenicol antibiotics at gold", Int. J. Electrochem. Sci., 7 (2012) 5000.

[302] N.A. Karaseva, T.N. Ermolaeva; "A piezoelectric immunosensor for chloramphenicol detection in food", Talanta, 93 (2012) 44.

[303] P. Li, Y. Qiu, H. Cai, Y. Kong, Y. Tang, D. Wang, M. Xie; "Simultaneous determination of chloramphenicol, thiamphenicol, and tlorfenicol residues in animal tissues by gas chromatography/mass spectrometry", Chin. J. Chromatogr., 24 (2006) 14.

[304] A.F. Forti, G. Campana, A. Simonella, M. Multari, G. Scortichini; "Determination of chloramphenicol in honey by liquid chromatography–tandem mass spectrometry", Anal. Chim. Acta, 529 (2005) 257.

[305] W. Jin, X. Ye, D. Yu, Q. Dong; "Measurement of chloramphenicol by capillary zone electrophoresis following end-column amperometric detection at a carbon fiber micro-disk array electrode", J. Chromatogr. B, 741 (2000) 155.

[306] J. Xu, W. Yin, Y. Zhang, J. Yi, M. Meng, Y. Wang, H. Xue, T. Zhang, R. Xi; "Establishment of magnetic beads-based enzyme immunoassay for detection of chloramphenicol in milk", Food Chem., 134 (2012) 2526.

[307] S. Pilehvar, J. Mehta, F. Dardenne, J. Robbens, R. Blust, K.D. Wael; "Aptasensing of chloramphenicol in the presence of its analogues: reaching the maximum residue limit", Anal. Chem., 84 (2012) 6753.

[308] M. Yuan, W. Sheng, Y. Zhang, J. Wanga, Y. Yang, S. Zhang, I.Y. Goryachevab, S. Wan; "A gel-based visual immunoassay for non-instrumental detection of chloramphenicol in food samples", Anal. Chim. Acta, 751 (2012) 128.

[309] J. Borowiec, R. Wang, L. Zhu, J. Zhang; "Synthesis of nitrogen-doped graphene nanosheets decorated with gold nanoparticles as an improved sensor for electrochemical determination of chloramphenicol", Electrochim. Acta, 99 (2013) 138.

[310] L. Yan, C. Luo, W. Cheng, W. Mao, D. Zhang, S. Ding; "A simple and sensitive electrochemical aptasensor for determination of chloramphenicol in honey based on target-induced strand release", J. Electroanal. Chem., 687 (2012) 89.

[311] S.A. Zaidi; "Recent advancement in various electrochemical and immunosensing strategies for detection of chloramphenicol", Int. J. Electrochem. Sci., 8 (2013) 9936.

[312] W. Tu, J. Lei, L. Ding, H. Ju; "Sandwich nanohybrid of single-walled carbon nanohorns–TiO_2–porphyrin for electrocatalysis and amperometric biosensing towards chloramphenicol", Chem. Commun., 9 (2009) 4227.

[313] P. Chandra, H.B. Noh, Y.B. Shim; "Cancer cell detection based on the interaction between an anticancer drug and cell membrane components", Chem. Commun., 49 (2013) 1900.

[314] K. Krishnamoorthy, M. Kanungo, A.Q. Contractor; "Electrochromic polymer based on a rigid cyanobiphenyl substituted 3, 4-ethylenedioxythiophene", Synth. Met., 124 (2001) 471.

[315] A. Geto, M. Amare, M. Tessema, S. Admassie; "Voltammetric determination of nicotine at poly(4-Amino-3-Hydroxynaphthalene Sulfonic Acid)-modified glassy carbon electrode", Electroanalysis, 24 (2012) 659.

[316] R.B. Dabke, A. Dhanabalan, S. Major, S.S. Talwar, R. Lal, A.Q. Contractor; "Electrochemistry of polyaniline Langmuir-Blodgett films", Thin Solid Films, 335 (1998) 203.

[317] M. Amare, W. Lakew, S. Admassie; "Poly (4-amino-3-hydroxynaphthalene sulfonic acid)-modified glassy carbon electrode for electrochemical detection of ephedrine in human urine", Anal. Bioanal. Electrochem. 3 (2011) 365.

[318] J. Mehta, B.V. Dorst, E.R. Martin, W. Herrebout, M.L. Scippo, R. Blust, J. Robbens; "In vitro selection and characterization of DNA aptamers recognizing chloramphenicol", J. Biotechnol., 155 (2011) 361.

[319] K.S. Lee, M.S. Wonb, H.B. Noha, Y.B. Shim; "Triggering the redox reaction of cytochrome-C on a biomimetic layer and elimination of interferences for NADH detection",Biomaterials, 31 (2010) 7827.

[320] C. Zhang, J. Yang, Z. Wu; "Electroreduction of nitrobenzene on titanium electrode implanted with platinum", Mater. Sci. Eng. B, 68 (2000) 138.

[321] K. Fossdal, E. Jacobson; "Polarographic determination of chloramphenicol", Anal. Chim. Acta, 56 (1971) 105.

[322] X.Yang, N. Gang, N.X. Luo, N.X. Xie, W.G. Wen; "A disposable and magnetic nano-particles composite membrane modified amperometric immunosensor for determination of chloramphenicol", In: Proceedings of the 2nd International Conference Biomedical Engineering and Informatics, BMEI 09, 1.

[323] T. Alizadeh, M.R. Ganjali, M. Zare, P. Norouzi; "Selective determination of chloramphenicol at trace level in milk samples by the electrode modified with molecularly imprinted polymer", Food Chem., 130 (2012) 1108.